ABSTRACT

Title of Thesis: **A FIELD DEMONSTRATION OF A QUANTITATIVE FRAMEWORK FOR DEFINING THE LIMITS ON IN SITU BIOREMEDIATION**

Matthew York Wheaton, Master of Science, 2006

Thesis Directed By: **Associate Professor, Eric A. Seagren, Department of Civil and Environmental Engineering**

Historic *cis*-dichloroethene (cDCE) groundwater concentrations leaving the Russell Road landfill were greater than Virginia groundwater protection standards. In response, a pilot-scale system was implemented to stimulate reductive dechlorination. In support of this program, this study investigated the utility of a quantitative framework analysis to determine the overall rate-limiting step for *in situ* bioremediation at the site, based on a set of dimensionless parameters estimated from site-specific, scale-dependent processes. Sorption was determined not to be limiting due to the small magnitude and relatively rapid rate. However, either the biokinetics and/or the horizontal transverse dispersion, D_T, processes were predicted to be the rate-limiting step(s) due to the apparently slow biokinetics and low D_T value. These conclusions were consistent with the pilot-scale data, which indicated no enhancement of cDCE reduction or injected electron donor in many downgradient wells, demonstrating the potential utility of the dimensionless quantitative decision making framework applied in this work.

A FIELD DEMONSTRATION OF A QUANTITATIVE FRAMEWORK FOR DEFINING THE LIMITS ON IN SITU BIOREMEDIATION

By

Matthew York Wheaton

Thesis submitted to the Faculty of the Graduate School of the
University of Maryland, College Park, in partial fulfillment
of the requirements for the degree of
Master of Science
2006

Advisory Committee:
Associate Professor Eric A. Seagren, Chair
Associate Professor Alba Torrents
Professor Allen P. Davis

Dedication

For Monica and Tristen

Acknowledgements

First, I would like the thank Dr. Eric Seagren for initially taking me into the environmental engineering program as a transfer, and working with me to incorporate his ongoing research into this rather difficult site, Russell Road Landfill. I would especially like to thank Dr. Seagren for his diligence on this project, even when I chose to work 2,600 miles from campus.

I must also thank my wife, Monica, for supporting me through every step of this work. Without her I would have never had the drive or the patience to finish.

Table of Contents

List of Tables

List of Figures

1.0 INTRODUCTION

1.1 Chlorinated Solvents in the Environment

The chlorinated aliphatic hydrocarbons (CAHs) tetra- or per-chloroethene (PCE) and trichloroethene (TCE) are widely used as mechanical degreasers, and as solvents in the dry-cleaning industry (Shimotori and Arnold, 2002). During the production of highly chlorinated solvents, such as PCE, lesser chlorinated intermediates can also be generated. Examples of these lesser chlorinated aliphatics include the isomers 1,2-*trans*-dichlorothene (tDCE), and 1,2-*cis*-dichloroethene (cDCE). Similar to PCE and TCE, the DCE isomers are commonly found as a mixture, and are also used as mechanical degreasers and as refrigerants, as well as for the production of pharmaceuticals (EPA, 2006a). A third DCE isomer, 1,1-Dichloroethene (1,1-DCE), is primarily used in the production of copolymers with vinyl chloride (EPA, 2006c). The degradation daughter compound of the DCE isomers, vinyl chloride (VC), is a compound widely used in the production of numerous products, such as electrical wire insulation and cables, piping, and as a refrigerant (EPA, 2006d). Although VC has many uses in the industrial world that result in frequent releases to the environment, the standards for permissible limits in soils and groundwater for this compound are the most rigorous compared to the other CAHs listed above.

Two key factors have contributed to large volumes of CAHs released to the environment. One, the huge quantities of chlorinated solvents that were generated since the 1950's subsequently increased the total mass released to the environment. For example, the US EPA Toxic Release Index for 1988 listed the U.S. on- and off-

site releases for 1,2-DCE (including both isomers) as approximately 2 x 10^5 lbs. Two, strict regulations did not exist for treatment and disposal of such organic chemicals prior to and during the 1980's. As a result, according to Hunkeler (2000), enormous volumes of chlorinated solvents were released to the environment either deliberately or accidentally, due in part to the general ignorance regarding the environmental fate of these chemicals. Unfortunately, due to the high solvent densities relative to water, improper disposal of the chlorinated solvents has resulted in the migration of these compounds into groundwater aquifers at hundreds of locations across the United States.

These chlorinated solvents are highly volatile and it was originally believed that the bulk of the CAHs discarded into landfills other waste disposal areas were volatilizing to the atmosphere. Nonetheless, although a large volume of such solvents could potentially enter the atmosphere, a significant portion of the contaminant mass partitioned to the aqueous phase as infiltrating water percolated through the soil. Furthermore, these chemicals were found to be very persistent and remained in the subsurface for years, migrating with local groundwater flow patterns. Due to their environmental persistence and the subsequent identification of the health risks associated with exposure to such chemicals, many chlorinated alkanes and alkenes were regulated by the US EPA's National Primary Drinking Water Regulations, which were established under The Safe Drinking Water Act (SDWA), as passed in 1974 and amended in 1986 and 1996. Under this act the EPA established federally mandated Maximum Contaminant Levels (MCLs) for several of the chlorinated solvents in drinking water (Table 1.1).

Table 1.1. Maximum contaminant levels for chlorinated ethenes. (EPA, 2003)

Contaminant	MCL (mg/L)
PCE	0.005
TCE	0.005
cDCE	0.07
tDCE	0.1
1,1-DCE	0.007
VC	0.002

The MCLs are defined as the levels that may be achieved with the use of the best available technology, treatment techniques, and other means that EPA finds are appropriate (after examination for efficiency under field conditions and not solely under laboratory conditions), taking cost into consideration, as well as health effects (EPA, 2006b). For example, based on such considerations, VC, a known carcinogen, has the most stringent cleanup levels compared to the less (known) toxic DCE isomers.

1.2 Field Site, Marine Corps Base Quantico

1.2.1 Site Background

The chlorinated-solvent contaminated site that was the focus of this study is the Russell Road landfill (RRL), which is located in the northeast corner of the Marine Corps Base Quantico (MCBQ) in northern Virginia. This site became of concern because groundwater from the RRL site was found to be contaminated with CAHs (Battelle, 2003). The landfill is situated on the northwest corner of Interstate 95 and Russell Road (see Figure 1.1), and has a total aerial extent of approximately 28 acres. RRL was operated from 1971 to June 1983 as the base's primary sanitary

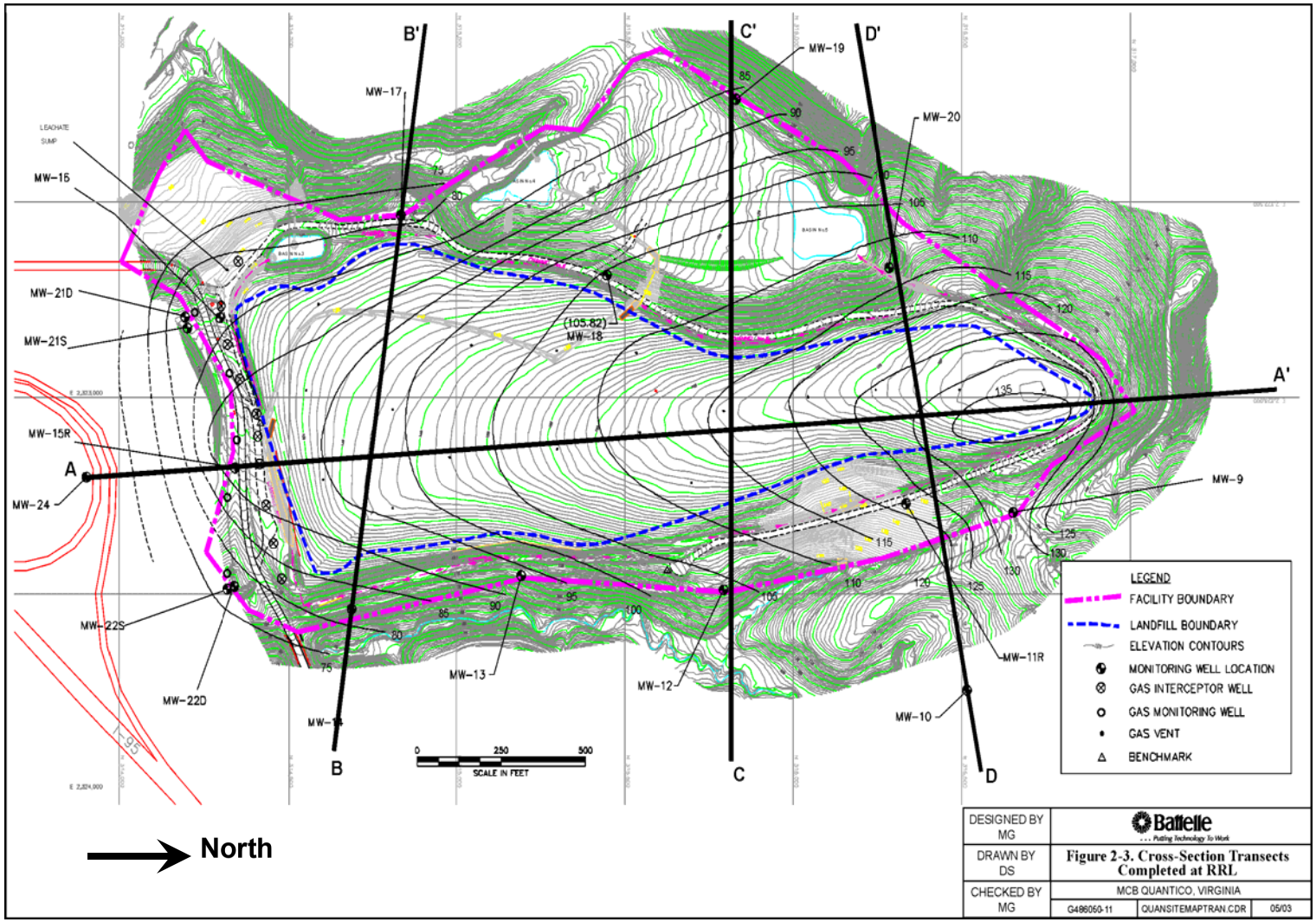

Figure 1.1. Russell Road Landfill site plan. (Battelle, 2003)

landfill, during which time undocumented materials, generated from numerous activities on base (e.g., vehicle and building maintenance, cleaning operations, laboratory operations) were disposed of in the unlined landfill (Tetra Tech, 2002).

Closure of RRL, which was initiated in April 1995 and completed in September 1996 was implemented with the installation of a Resource Conservation and Recovery Act (RCRA) multilayer cap, a subsurface leachate collection system, and a methane gas management system, as depicted in Figure 1.1. The leachate collection system, which encircles the entire landfill, was designed to only capture lateral leachate seepage. There was no control set in place to intercept leachate emanating from beneath the landfill. Included in the methane gas management system are eighteen passive gas vents located across the landfill, and four gas monitoring probes located along the southern boundary to the landfill. The latter have, in the past, detected methane levels above the 5% trigger level (Tetra Tech, 2002). Additionally, seventeen monitoring wells (MWs), also shown in Figure 1.1, were installed around the perimeter of the landfill, at intervals of approximately 500 feet. In compliance with RCRA closure requirements these wells were installed to monitor for leachate migrating from beneath the landfill. Post-closure activities at RRL are being conducted as per a Hazardous Waste Management Post-Closure Permit, effective October 29, 2000.

Chlorinated solvent concentrations in groundwater at RRL were found to exceed the Virginia groundwater protection standards (GPSs), which are set equal to MCLs (see Table 1.1), in two of the 17 monitoring wells surrounding the RRL. Specifically, groundwater samples from MW-9, located in the northeast corner of the landfill, and

MW-15R, located at the southern boundary of the landfill, both contained elevated levels of PCE, TCE and cDCE. Accordingly, the area in the vicinity of MW-15R was the focus of this study. Historic concentrations of cDCE in the area of MW-15R, henceforth referred to as RRL-South, were consistently greater than the concentrations of PCE and TCE. For example, baseline sampling concentrations measured in wells near MW-15R (e.g., TMW-26S) have produced average cDCE, PCE, and TCE concentrations of approximately 0.4, 0.05, and 0.02 mg/L, respectively, as discussed further in Section 1.4.1.

1.2.2 Site Geology

Waste disposal activities at the RRL consisted primarily of trench-and-fill disposal operations, which began at the southern end and progressed northward (Tetra Tech, 2000). It is unclear as to the depth of the debris, or at what location within the landfill the source of the chlorinated solvent plume is located. Records were not kept during the construction and operation of the landfill with regards to geologic setting, and only after completion of RCRA closure activities were underlying geologic profiles created.

RRL lies on the eastern edge of the Virginia Piedmont. Based on soil excavation logs generated during the installation of the leachate collection system, described previously, some insight can be obtained into the geology underlying the landfill. The soils data from the excavations, coupled with monitoring well boring logs, were used by the consultant, Tetra Tech, to create rough cross sections through the landfill (See Figure 1.1 for cross section locations). Cross sections A-A' and B-B', provided in Figures 1.2 and 1.3, depict geologic profiles near RRL-South. These

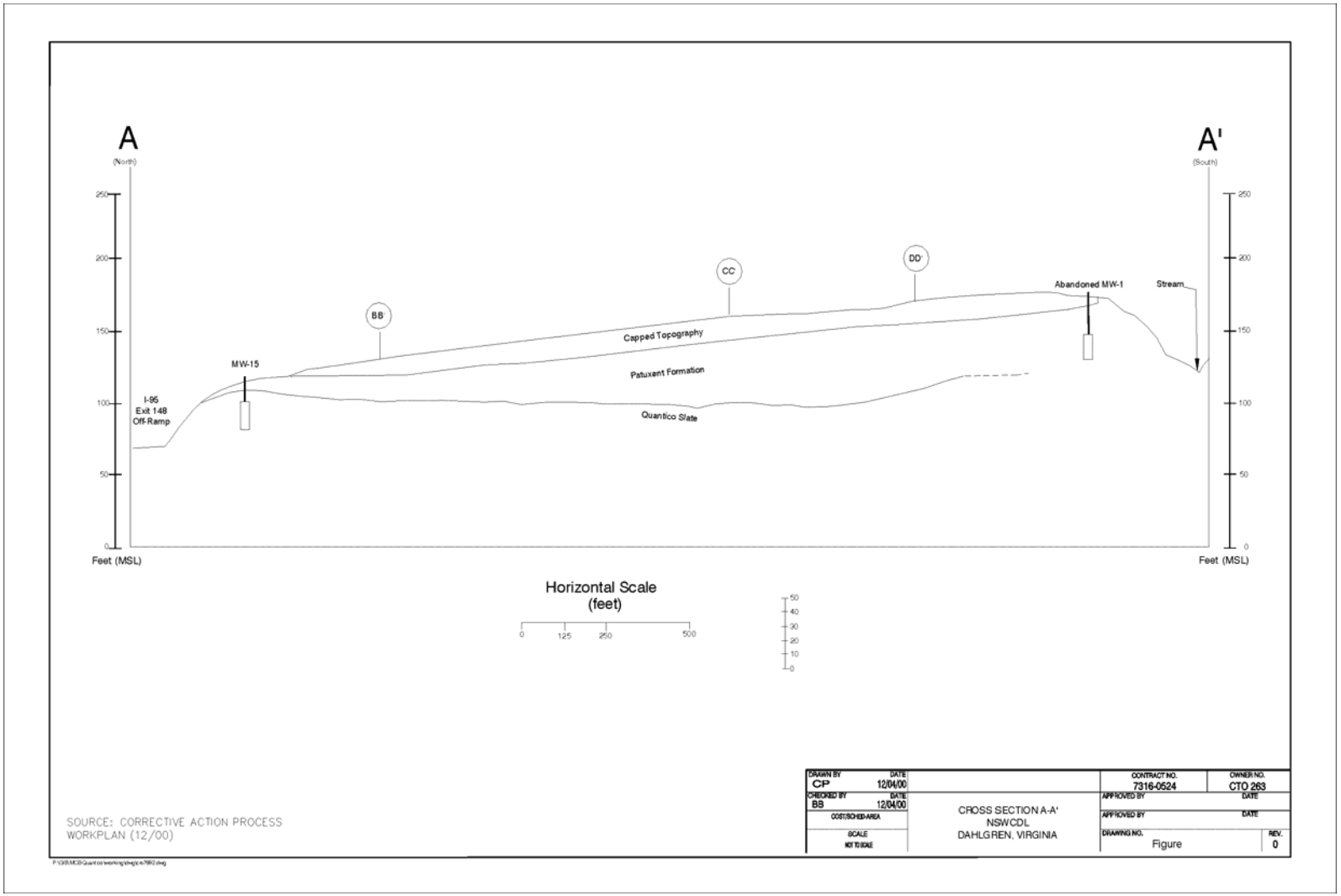

Figure 1.2. Cross section A-A' of Russell Road Landfill (see Figure 1.1 for locations). (Battelle, 2003)

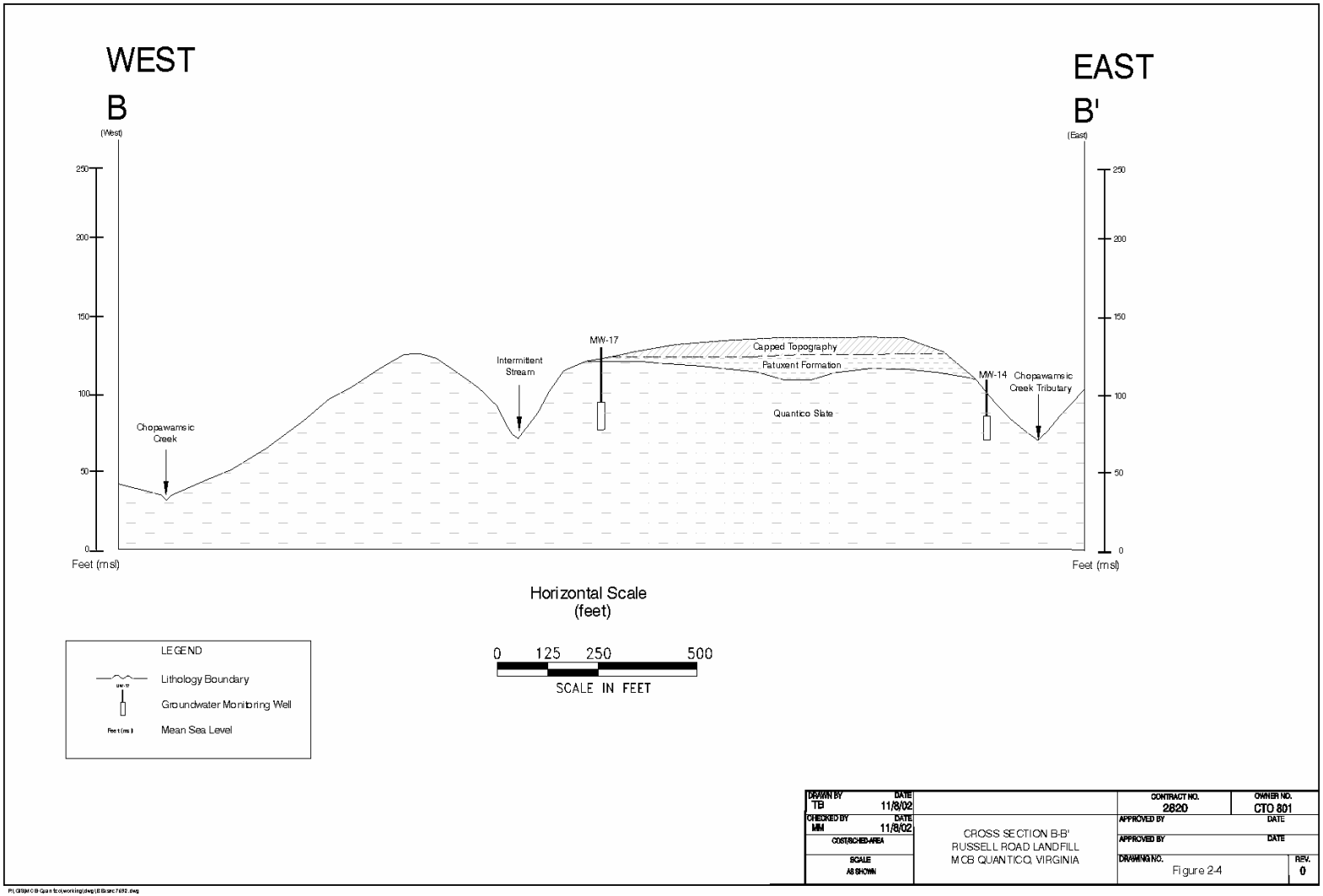

Figure 1.3. Cross section B-B' of Russell Road Landfill (see Figure 1.1 for locations). (Battelle, 2003)

geologic profiles indicate that the landfill has been constructed on, and perhaps dug into, the Patuxent formation, which overlies the Quantico slate. As noted in Figure 1.2, cross section A-A', the Patuxent formation narrows to the south, possibly indicating that the landfill had been excavated into the Quantico slate north of RRL-South. Therefore, in the area of RRL-South the underlying geology consists of three lithologic units: Fill material, the Cretaceous age Patuxent Formation, and the Quantico Formation (also referred to as the Quantico Slate) (Battelle, 2003). The fill material is a mixture of Patuxent soils, fill cover, and weathered Quantico Slate.

The thickness of the fill material varies across RRL, and is difficult to distinguish from the Patuxent Formation. The Patuxent Formation is a saprolite, defined as a soft, partially decomposed rock rich in clay and remaining in its original place. This 2 – 20 m thick saprolite can be found covering most rock groups within the Virginia Piedmont. The Patuxent Formation is composed of gray to brown, fine to coarse-grained arkosic sands and gray to brown clay containing varying amounts of sand and silt. In addition, gravel is periodically encountered in this unit as separate beds or dispersed throughout the sand and clay units. There is an erosional boundary between the Patuxent Formation and the underlying Quantico Slate, the lowest characterized geologic formation in the landfill's vicinity. The Quantico Slate is a poorly metamorphosed graphitic slate composed of dark-gray to black, thinly foliated slate and chlorite-actinolite green schist. The foliation generally strikes north-northeast, with a nearly vertical dip. An out crop of Quantico Slate is present in the vicinity of the I-95 off ramp, which is located approximately 30 feet south of MW-15R. Figures 1.4 and 1.5 are photographs of the Quantico Slate near the off ramp.

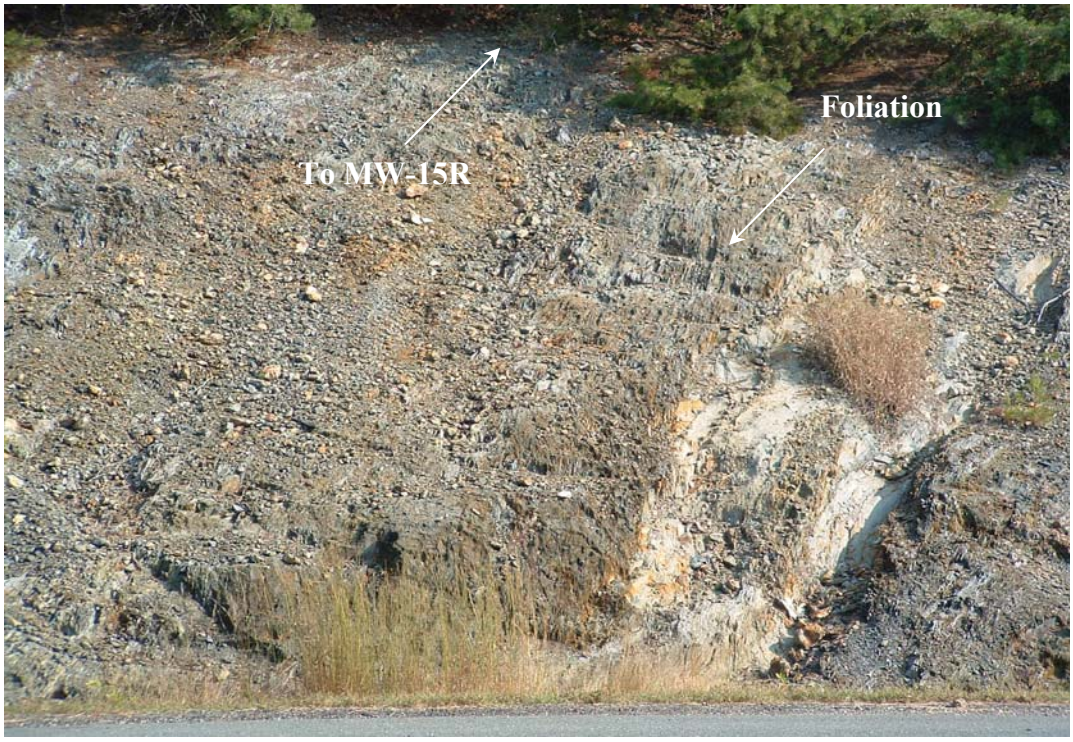

Figure 1.4. View of Quantico slate in I-95 off ramp road cut facing north. Note vertical foliation in center of the photograph. TMW-15R is located approximately 30 feet north of road cut, as indicated.

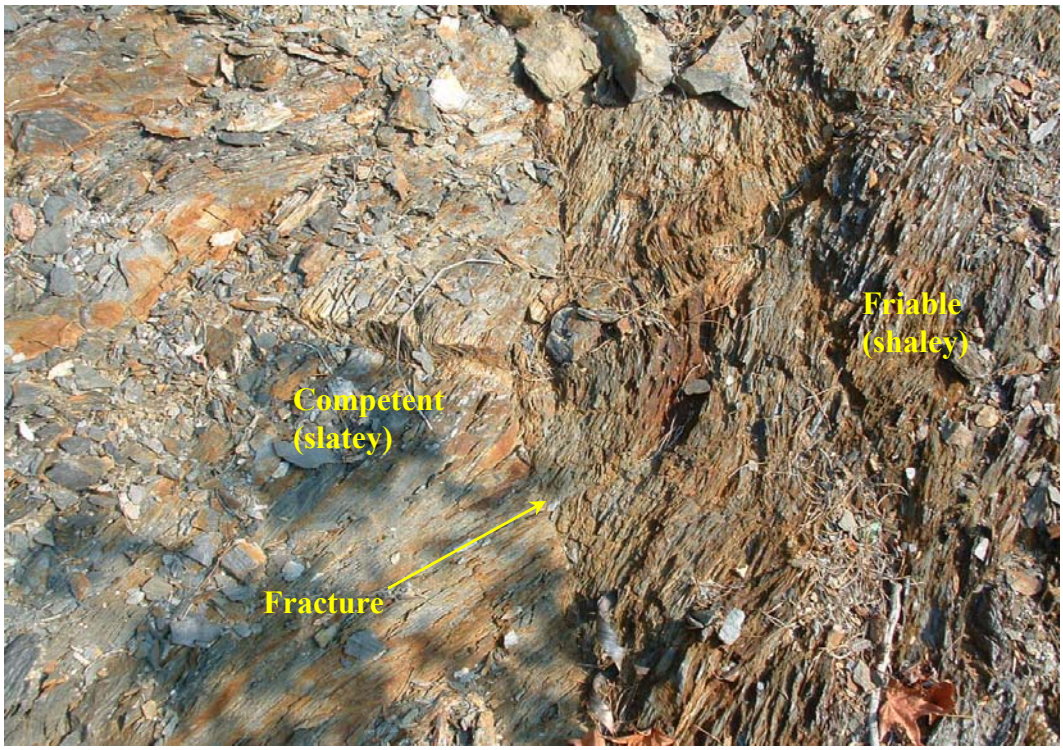

Figure 1.5. Map view of Quantico slate foliation in I-95 road cut. Note fracture.

As described previously, the Quantico Slate is poorly metamorphosed, which The near vertical foliation is apparent in both photographs, as well as evidence of minor fracturing. means that a shale has undergone minimal heat and pressure to form slate, therefore, characteristics of a shale are still present. In certain areas across the landfill, as visible in the road-cut (see Figure 1.5), the slate is extremely friable and is better defined as a shale, while adjacent zones are more competent and characteristic of slate. Based on the presence of friable slates adjacent to competent bedrock, and the observed fracturing in the road-cut, it is possible that the slates in the area of RRL-South have been altered due to localized faults and fracturing, although no literature is available to support this hypothesis. Additionally, shale depositional environments are typically marine or transitional marine (e.g., estuaries) in which organic rich sediments are deposited under anaerobic conditions (Friedman et al., 1992). Such conditions also contribute to the formation and accumulation of sulfidic minerals, such as pyrite (Friedman et al., 1992). When exposed to water and oxygen, the sulfides in sulfidic rich deposits, such as the Quantico formation, are oxidized to form sulfuric acid, which in turn dissolves surrounding minerals, creating a very acidic metalliferous leachate referred to as acid rock drainage (Orndorff and Danniels, 2004). The resulting acidic conditions will not support vegetation, as illustrated in the photograph of the road cut in Figures 1.4 and 1.5. Orndorff and Daniels (2004) analyzed geologic materials and road drainage at acid road cuts in the pyretic phyllite and slate of the Quantico formation along I-95 and Mine Road (Route 610), near Stafford, VA. Surface samples had potential peroxide acidity (PPA) values ranging from 6 – 22 mg $CaCO_3$/1000 Mg material and Sulfide (S) ranging from 0.24 – 1.00%,

while a relatively unweathered sample had higher PPA (99 mg $CaCO_3$/1000 Mg material) and S (3.8%) levels. Based on these data and previous analyses, Orndorff and Daniels (2004) concluded that sulfide levels were variable in the Quantico formation. Drainage samples collected in the same study generally had very low conductivity (0.37 – 3.27 S/cm) and metal concentrations.

1.2.3 Site Hydrology

Based on quarterly groundwater monitoring data, groundwater flow at RRL is essentially radial, and controlled by the surface topography and two adjacent streams (Battelle, 2003). The groundwater is generally unconfined, with depths to groundwater ranging from approximately 15 to 30 ft. below ground surface. Historic quarterly groundwater monitoring indicates that water levels at RRL, in general, stabilized relatively quickly following the installation of the landfill cap, with the exception of the south end. This may indicate that the addition of a cap reduced recharge to this area. As a result, monitoring Well 15 (MW-15), located in RRL-South, was replaced with the deeper (40 ft with a 15 ft screen interval) MW-15R (see Figure 1.1) in 2001 due to continued declining groundwater levels. MW-15 has since been abandoned.

Groundwater contour lines at the site are shown in Figure 1.1 as the dark lines. The hydraulic gradient in RRL-South indicates that flow in the area of MW-15R is generally toward the south and, based on an absence of a confining layer, can generally be classified as unconfined. Depths to groundwater average between 15 and 17 fbg. At these depths based on the cross sections discussed previously (see Figures 1.2 and 1.3), the water table surface is in the shallow Quantico Slate. After

significant precipitation events groundwater can be observed seeping from the Quantico Slate at the I-95 road cut in the vicinity of RRL-South. Hydraulic conductivity was previously reported to be approximately 0.91 to 6.7 m/day (3 to 22 ft/day), and coupled with the steep hydraulic gradients between wells MW-15R and MW-24 (0.0625 ft/ft), it was estimated that groundwater velocities were in the range of hundreds of feet per year (Battelle, 200). However, this large hydraulic gradient between MW-15R and MW-24 is due to the road cut between these two locations and the actual groundwater velocities in the vicinity of MW-15R may be significantly less.

1.2.4 RRL Site Characterization

At the time of the Final Corrective Action Plan for groundwater remediation at RRL (Battelle, 2003), the lateral and vertical extent of chlorinated solvent contamination was unknown, aside from the groundwater monitoring data for MW-15R which confirmed µg/L levels of cDCE, PCE, and TCE in the groundwater since quarterly monitoring activities began. Early monitoring data for MW-15, and -15R, indicated PCE and TCE were present at concentrations greater than the GPS (0.005 mg/L for both), however, by the 28th quarterly monitoring event PCE and TCE concentrations had declined and only cDCE was observed at levels exceeding the GPS (0.07 mg/L) (Battelle, 2003). The quarterly monitoring PCE, TCE and cDCE trends are provided in Appendix A. Based on the available data, four alternatives for remedial action at RRL-South were proposed in the Draft Final Corrective Action Plan for groundwater at the RRL, subject to additional study and analysis (Battelle, 2003): (1) groundwater compliance monitoring; (2) administration controls and

monitored natural attenuation; (3) enhanced natural attenuation, e.g., using Hydrogen Release Compound (HRC®); and (4) placement of an *in situ* permeable reactive barrier, e.g., using zero-valent iron.

Based on the historic CAH groundwater levels observed in RRL-South, specifically, the increasing cDCE concentrations, the Virginia Department of Environmental Quality deemed that the chlorinated solvents in the area were not being removed by existing mechanisms at a rate that was sufficiently protective of human health and the environment. Therefore, it was decided to implement a pilot-scale remedial program to evaluate the potential efficacy of proposed remedial alternative 3; "enhanced" natural attenuation using HRC®. The principal components of this approach include long-term monitoring and periodic reviews to assess attenuation of cDCE, along with the initial introduction of the HRC® compound into the area of MW-15R. The first step in implementing the pilot-scale test was to determine the location for the study through further site characterization activities, as described in the following paragraphs.

Given the uncertainty regarding the extent, fate, and transportation mechanisms of CAH contamination at RRL-South, defining the plume boundaries, both horizontal and vertical, was the first step required to proceed with remedial activities. This plume delineation was carried out by installing monitoring wells in key areas, with all activities centered around TMW-15R. Additional information, such as soil and bedrock types and groundwater elevations, were also collected during monitoring well installation in order to enhance existing geologic and hydrologic site

descriptions. All wells were installed by a subcontractor between July and September 2003, using a CME 55 ATV drill rig equipped with 8 inch hollow stem auger.

The first additional wells to be installed at RRL-South were TMW-26S and TMW-26D, which were located approximately 15 feet northwest of MW-15R (Figure 1.6). TMW-26S and TMW-26D are nested wells, meaning they were set within the same borehole at staggered intervals, and extend to approximately 33.5 and 44 feet below grade (fbg), respectively. Screened intervals for both wells are 2.5 ft. These nested wells, TMW-26S and -26D, were installed to further define the vertical extent of the plume. Two additional monitor wells, TMW-31 and TMW-32, were installed to 35 fbg approximately 50 feet to the west and east of TMW-26S, respectively, with screened intervals of 15 ft (Figure 1.6). Depths and screened intervals for these two wells were chosen to mimic the screen interval of MW-15R (25 to 40 fbg), based on the assumption that the contaminant plume would be detected in these similarly constructed wells.

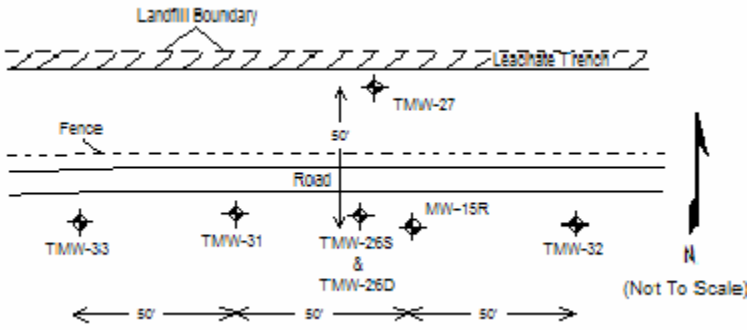

Figure 1.6. Site plan of RRL-South area centered around MW-15R.

Finally, to confirm that the contaminant source was originating from the up gradient landfill (relative to MW-15R), monitoring well TMW-27 was installed

approximately 50 feet up gradient of TMW-26S and -26D (Figure 1.6). This well was also set to 35 fbg with a 15 ft screened interval, the same as TMW-31 and -32.

Soil grab samples were collected from cuttings derived from the bottoms of all additional bore holes, prior to well installation, to confirm the presence of chlorinated solvents. Additionally, upon completion, the monitoring wells were developed by purging approximately 10 gallons from each well. Groundwater samples were collected from the purge water and submitted to an independent lab for analyses (Accura Analytical Lab, Norcross Georgia). All soil and groundwater samples were analyzed for PCE, TCE, cDCE, tDCE, and VC. The analytical results are presented in Table 1.2. cDCE, PCE and TCE were present at concentrations in the groundwater in excess of the GPS at TMW-26S and TMW-31, while groundwater in TMW-27 contained only cDCE concentrations greater than the GPS. Very little tDCE or VC was detected at any of the sampling locations (e.g., <0.1 and 0.002 mg/L). Trends in the soils concentrations were consistent with the groundwater data.

Table 1.2. Groundwater and soil (grab) sample results.

Well/Sample ID	Groundwater Concentrations (mg/L)				
	PCE	***TCE***	***cDCE***	***tDCE***	***VC***
GPS	0.005	0.007	0.07	0.1	0.002
TMW-26S	0.01	0.009	0.37	0.001	0.003
TMW-26D	0.001	0.0004	0.062	BRL*	BRL
TMW-27	0.002	0.005	0.27	0.0004	0.001
TMW-31	0.008	0.039	0.11	0.001	BRL
TMW-32	BRL	BRL	0.001	BRL	BRL
	Soil Concentrations (mg/kg)				
TMW-26S	0.005	0.006	0.17	0.0004	BRL
TMW-26D	BRL	BRL	37	BRL	BRL

***BRL = Below Reporting Limit**

Based on these data, plus the historical quarterly contaminant trends (Appendix A), several general comments may be made. One, the currently high cDCE and low PCE and TCE levels, coupled with the historical declines in PCE and TCE and increase in cDCE at MW-15 and -15R, suggest that anaerobic biodegradation of PCE and TCE via reductive dechlorination to cDCE may be occurring, possibly as a result of anaerobic conditions created during the capping of the landfill. Two, the accumulation of cDCE with little VC is a common observation during anaerobic biodegradation of PCE, indicating that conversion of cDCE is the rate-limiting step (e.g., Harkness, 1999; Lenczewski et al., 2003; Aulenta et al., 2005). Three, the observation of cDCE but little tDCE is consistent with previous observations that, although all three DCE isomers (tDCE, cDCE, and 1,1-DCE) can be produced via reductive dechlorination of PCE or TCE, cDCE is the most commonly observed intermediate (Bouwer, 1994). Finally, the presence of a dense NAPL source in the vicinity of RRL-South is unlikely because of the relative magnitude of the chlorinated solvents compared with their aqueous solubility (e.g., cDCE solubility is approximately 3,500 mg/L) (Battelle, 2003).

The contaminant levels in TMW-31 indicated that plume boundaries were further west than TMW-31. Therefore, an additional well, TMW-33, was installed approximately 50 feet west of TMW-31 with identical well characteristics (i.e., well depth and screen length). Groundwater samples from the well development purge water were submitted for analysis, and all chlorinated solvent contaminant levels were below reporting limits for this well (data not shown). Subsequently, the approximate plume boundaries were loosely defined, and illustrated in Figure 1.7.

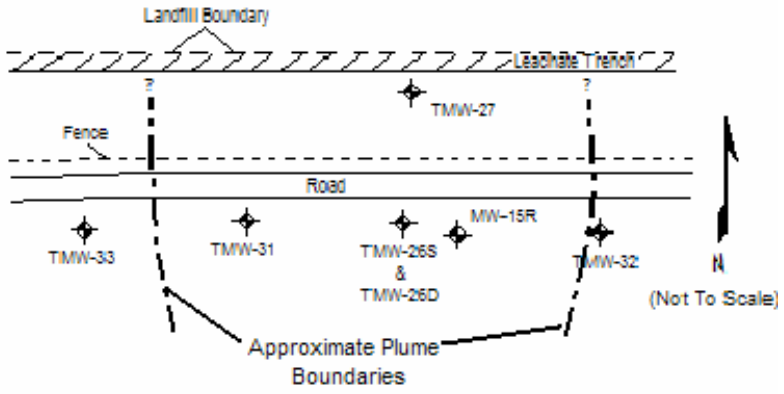

Figure 1.7. Approximate plume boundaries in RRL-South.

1.3 Pilot Remediation Program

Based on the approximate CAH plume boundaries (Figure 1.7) determined during the site characterization, it was decided that the pilot-scale tests would be centered around the nested wells TMW-26S and -26D. HRC® and its implementation in the pilot study are described in the following sub sections.

1.3.1 Hydrogen Release Compound

As discussed above, the primary contaminant of concern at RRL-South is cDCE due to the historic accumulation of cDCE, apparently as a result of the reduction of PCE and TCE occurring naturally in the RRL-South aquifer. Biodegradation of cDCE is possible under both aerobic and anaerobic conditions, with the choice of remedial method, therefore, depending on the site specific groundwater conditions, primarily dissolved oxygen concentrations. Many field sites have shown complete degradation of PCE to ethene after creating an aerobic environment conducive to cDCE oxidation downgradient of anaerobic conditions

appropriate for reductive dechlorination of PCE to cDCE (e.g., Ellis, 2000; Morkin et al, 2000). However, this process may be costly due to the necessity of establishing two redox zones.

Another option is to try to create conditions in the subsurface appropriate for promoting the microbially mediated reductive dechlorination of cDCE to ethene, e.g., by adding an electron-donor substrate. Such an approach could potentially be an effective treatment of cDCE at RRL-South, given current anaerobic groundwater conditions, assuming the presence of dehalorespirers such as *Dehalococcoides ethenogenes* at the site. Although it is unclear which microorganism is responsible for the degradation of PCE and TCE at RRL-South, the historic accumulation of cDCE suggests the possibility of a dehalorespiring population. As reviewed further in Chapter 3, ***D. ethenogenes,*** a species which has been found at numerous field sites (e.g. Murray et al, 2001; North et al, 2001), are capable of degrading PCE to ethene by using the chlorinated ethenes as terminal electron acceptors (Maymó-Gatell et al, 1997, 2001), and the hydrogen (and in some cases acetate) as the electron donors.

One option currently available for increasing the supply of electron donors in the subsurface in order to stimulate the naturally occurring bacteria and bring about rapid reductive dechlorination rates is to inject HRC®. HRC® is a proprietary (Regenesis of San Clemente, CA), food-grade compound, glycerolpolylactate, which slowly releases lactic acid into the groundwater through hydration. The lactic acid in turn acts as a substrate for fermentative anaerobic microbes that metabolize the lactic acid, producing hydrogen and acetate (see Figure 1.8). If the rate-limiting factor controlling biodegradation is the lack of an electron donor, which is the presumed

condition at RRL-South, the injection of HRC® could possibly eliminate this rate-limiting step under ideal conditions. Importantly, the success of a substrate injection program requires that a useful mass of substrate is able to migrate through the subsurface to where the contaminants of concern (e.g., cDCE) and the microbial populations of interest are

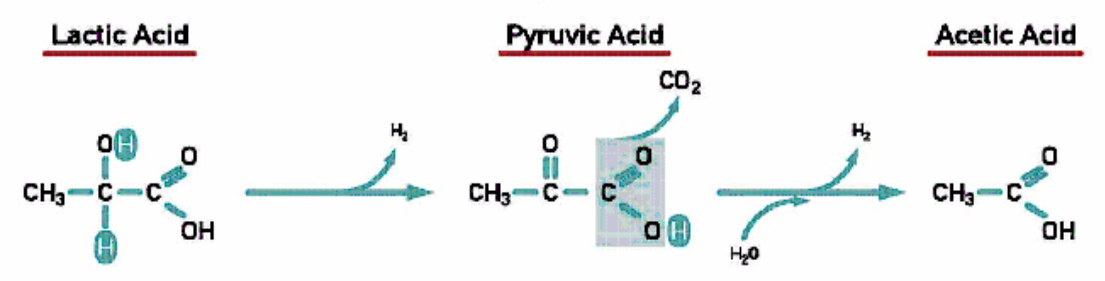

Figure 1.8. Breakdown of lactic acid yielding H_2. (Regenesis, 2006)

located (e.g., micropores), thereby allowing for the possibility of accelerated degradation. In the case of HRC®, stimulated degradation should result in the cDCE being reduced to VC, which may be further reduced to ethene.

The advantage in using HRC®, as opposed to other complex organics, is the slow release of hydrogen and acetate, which favors dehalorespirers. As described in Rittman and McCarty (2001) the hydrogen threshold for dehalorespirers is lower than other hydrogenotropic organisms commonly found in the same environments, such as methanogens and homoacetogens. Therefore, dehalorespirers will out-compete methanogens and homoacetogens for low H_2 concentrations. For example, methanogens and homoacetogens will couple hydrogen oxidation with the reduction of CO_2 to either methane, or acetate, respectively. The redox potentials for the reduction of CO_2 to methane and acetate are -0.24 (E_H°') and -0.29 (E_H°'),

respectively, while the redox potential for PCE to TCE is +0.58 (E_Hº'). Based on free energy considerations, the greater the redox potential of the electron acceptor, the lower the H_2 concentration at which that organism can function. This represents a hydrogen threshold level, i.e., the lowest H_2 level at which an organism can effectively couple hydrogen oxidation with reduction of its respective electron acceptor. Therefore, at sufficiently low hydrogen concentrations threshold levels required by methanogens and homoacetogens to utilize CO_2 as an electron donor, the dehalorespirers will be able to outcompete these organisms for H_2.

1.3.1.1 Regenesis Benchscale Study

One soil sample from the area of RRL-South (the specific bore hole location unknown) was submitted to Regenesis and the treatability tests were conducted on August 8, 2003 (Regenesis, 2003). To verify the use of HRC® as an effective treatment option for clients, Regenesis conducts bench scale studies on the potential for bioremediation of TCE. Although TCE is not the primary contaminant of concern at RRL-South, useful information could still be obtained on the reductive dechlorination of CAHs in the native soil. During this study bacterial plate counts were also performed.

To conduct the treatability test, a total of fifteen 200 ml test tubes were prepared, with each containing 10 grams of soil (innoculum) and 150 ml of distilled water containing approximately 15 mg/L of TCE, a concentration much higher than present at RRL-South. In addition, 1.5 grams of HRC® was added to each test tube. Triplicate test tubes were then sampled every 7 days, for five weeks, with baseline samples taken on the first day. The initial addition of TCE resulted in a measured

average aqueous concentration in the test tubes at time zero of 10.87 ppm of TCE, suggesting the possibility of some sorption; however, The sorption capacity of the soil, with respect to chlorinated solvents, was not determined during this experiment. At the tests conclusion, TCE was reduced to an average concentration of 8.84 ppm (see Table 1.3). Chlorinated ethene daughter products were also generated during the experiment. The final total concentration of DCE was, on average, 1.35 ppm, which includes t-DCE, c-DCE and 1,1-DCE, and the final VC concentration was 0.61 ppm. Interestingly, the amount of cDCE formed was the lowest of all the DCE isomers. Based on these results it was concluded that reductive dechlorination may be taking place within the test tubes.

Table 1.3. Regenesis treatability study results (values are the average of triplicate concentrations in mg/L). (Regenesis, 2003)

Sample ID	Time (days)				
	0	***7***	***14***	***21***	***28***
TCE	10.87	9.47	8.84	8.16	8.84
cDCE	0.0	0.0	0.0	0.0	0.056
tDCE	0.0	0.15	0.10	0.15	0.90
1,1-DCE	0.0	0.25	0.10	0.18	0.39
VC	0.0	0.29	0.30	0.49	0.61

From the results of the bench-scale study the half life of TCE can be calculated. The half-life is a useful parameter because it can be utilized to aid in predicting cleanup durations in the field setting. The first step in calculating this parameter is to assume a reaction rate. For the batch data from Regenesis, a first order reaction rate was found to be reasonable:

$$\frac{dC}{dt} = -kC \qquad (1.1)$$

Eq. 1.1 indicates that the change in concentration with respect to time (dC/dt) is equal to the product of the first order degradation rate constant (*k*) and the aqueous concentration (C). Integration of Eq. 1.1 gives the following linear equations with a slope of *k*:

$$\ln\left(\frac{C_O}{C}\right) = kt \qquad (1.2)$$

Data from the Regenesis batch tests were fit to Eq. 1.2, where t is equal to time (days), and C_O and C are the initial concentration of TCE and the concentration of TCE at any time, *t*, respectively. A plot of the data is presented in Figure 1.9.

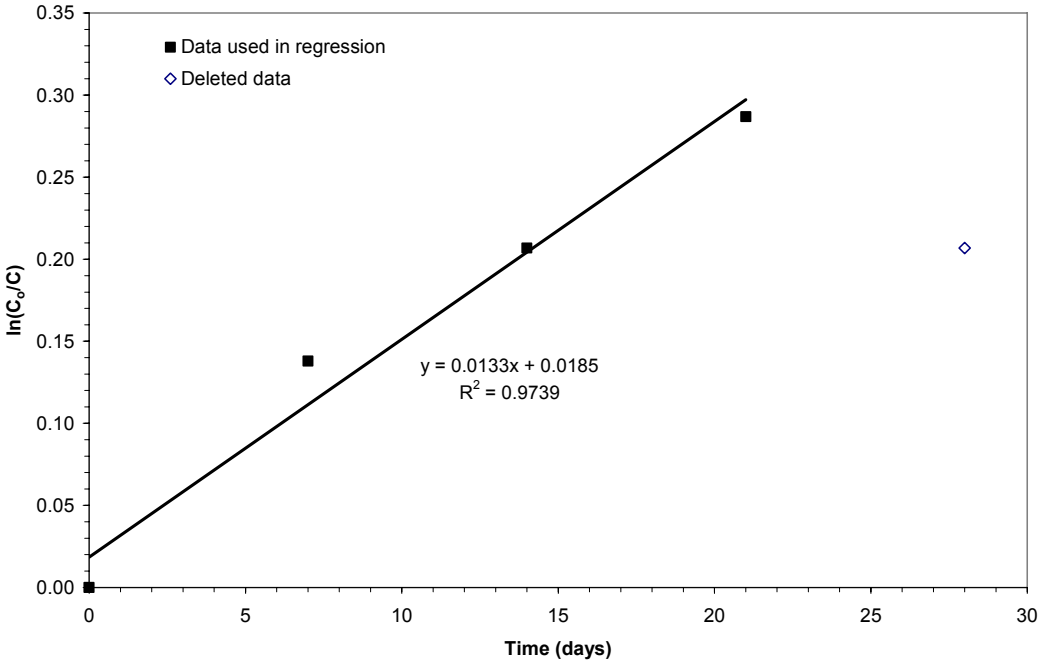

Figure 1.9. Regenesis (2003) TCE bench-scale degradation rate constant (k) determination.

As illustrated in Figure 1.9, the final point that was recorded at 28 days was dropped from the *k* estimate. It is unknown why the final Regenesis reported concentration

increased, but in order to calculate a best fit trend line this point could not be included. However, given that four points prior to this measurement yield a trend line with an R-squared value of 0.97, the slope is considered to be representative of the data. Therefore, based on the least squares linear regression equation, the TCE first-order degradation rate constant in the batch test was equal to 0.013 day^{-1}.

From the best fit *k* value, a bench-scale TCE half life can be calculated using Eq. 1.2, where $k = 0.013\ d^{-1}$, and setting $(C_O/C) = (1/0.5)$. These results indicate that the laboratory half-life of TCE in RRL-South soil is equal to approximately 53 days. Unfortunately, the total batch test time did not allow for a significant mass of DCE to accumulate and degrade, therefore, half-lives could not be calculated for any of the DCE isomers.

Following the conclusion of the HRC® treatability study, the last set of triplicate test tubes were analyzed for microbial populations using plate count techniques. Based on the results, Regenesis (2003) reported "higher than normal numbers" of anaerobic and aerobic microbes. Additionally, sulfate reducing bacteria (SRB) counts were described as "in the expected range" for this site. Regenesis (2003) concluded that the presence of SRB may indicate the possible presence of other beneficial halorespirers, as the SRB prefer similar redox environments.

Overall, Regenesis (2003) concluded that the above normal anaerobic microbial counts, coupled with the TCE reduction in the bench study may support the potential of successful field application of HRC for reductive dechlorination, and it was on this basis that the HRC® injection pilot study was initiated. Nevertheless, it was also noted that the high microbial counts should have reduced TCE

concentrations far more than those observed in the study. The complete Regenesis Bench Scale Treatability Study is provided in Appendix B.

1.3.2 Well Configuration Design

Given that the greatest concentrations of chlorinated solvents were detected in TMW-26S the addition of the HRC® remedial amendment was focused at a depth of approximately 20 to 35 fbg, approximately the same depth as the well screen interval for TMW-26S. A total of three additional monitoring wells (TMW-S1, -S2, and -S3) and two HRC injection wells (IP-S1 and –S2) were installed north of TMW-26S. All of these wells, including the injection wells, were installed to a depth of 35 fbg with 15 foot screen intervals. The approximate configuration of all the monitoring wells within the RRL-South pilot program area is illustrated in Figure 1.10, and the boring logs for wells shown are provided in Appendix B.

With the addition of five new wells to RRL-South as part of the pilot program, the existing geologic profile was further clarified. According to the well logs, the contact between the Patuxent formation and the underlying Quantico slate was generally between 10 and 12 fbg. While the shallow geologic setting was described by the logs, groundwater elevations could not be determined due to low recharge conditions. Therefore, only during monitor well sampling activities could accurate water table elevations be recorded.

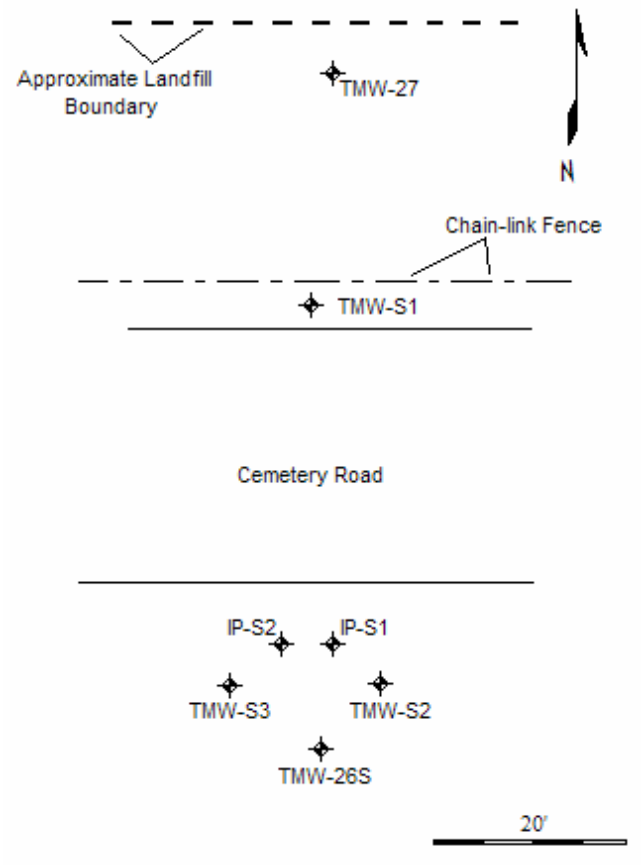

Figure 1.10. RRL-South pilot well configuration.

1.3.3 Low Flow Groundwater Sampling

Due to slow groundwater recharge rate encountered during the monitoring well installation, and to mimic quarterly sampling practices, low-flow sampling was used during the pilot remediation study. A QED Sample Pro Portable MicroPurge® Pump (The Groundwater Specialists, Ann Arbor, MI), was used for all sampling at RRL. Following EPA guidelines for low flow sampling as set forth by Puls and Barcelona (1996), it was attempted to maintain water drawdown levels during sampling at approximately 0.3 ft below the original groundwater surface elevation. To achieve this drawdown, sampling flow rates were typically in the range of 0.05 to 0.15 L/min. During all sampling events the following groundwater "field

parameters" were collected: pH, temperature (°C), dissolved oxygen (DO) (mg/L), specific conductivity (S/cm), oxidation-reduction potential (ORP) (mV), turbidity (NTU), and flow rate (using a graduated cylinder). These samples were collected approximately every five minutes until stabilization was achieved between three consecutive readings. Stabilization was defined by using pH, DO, ORP, and turbidity as the controlling parameters, with changes in consecutive readings not to vary greater than ± 0.1 pH units, ± 10%, ± 10 mV, and ± 10 NTUs (when turbidity is greater than 10 NTU).

1.3.4 Baseline Groundwater Conditions

Prior to the HRC® injections, baseline sampling was conducted by the author on October 28 & 29, 2003, using the low flow sampling procedures described above. The resulting stabilized "field parameters" for RRL-South are presented in Table 1.4. In addition to these parameters, other groundwater characteristics were collected from the wells within the vicinity of the HRC® injection wells (e.g., TMW-S1, TMW-S2, TMW-S3, and TMW-26S) during baseline sampling activities, including the chlorinated ethene groundwater concentrations (see Table 1.5) and other key groundwater characteristics (see Table 1.6). The analyses for the value presented in Tables 1.5 and 1.6 were performed by Accura Analytical Lab (Norcross, Georgia).

The results in Table 1.5 indicate that, in general, all CAH concentrations are higher than those recorded in September 2003. However, the relative magnitude of chlorinated solvent concentrations are identical to those previously observed. Additionally, ethene concentrations (see Table 1.6) are also low, which, combined with the low VC levels, further support the idea that reductive dechlorination was

stopping at cDCE. Chloride concentrations (Table 1.6) can be useful for demonstrating the occurrence of reductive dechlorination, given that one chloride ion is produced during each step in the sequential dechlorination of chlorinated ethenes. Unfortunately, the chloride concentrations in the baseline study are not helpful in this case because chloride values outside of the contaminant plume boundaries are unknown, although the concentration within the plume boundaries may result from reductive dechlorination of PCE and TCE.

The other groundwater characteristics suggest that the aquifer conditions are probably not conducive to reductive dechlorination. The average DO concentrations of 1.49 mg/L, coupled with the relatively low methane and high sulfate concentrations, suggest aerobic conditions in the aquifer (Cookson, 1995), not a reduced environment where reductive dechlorination would occur. The ORP values are lower than one would expect for oxidized environments, but are subject to a number of well-known shortcomings. The relatively high concentrations of dissolved Fe and Mn are generally not associated with oxidizing environments, but can be explained by other site conditions, as described below.

The aquifer characteristics do appear to be consistent with the occurrence of sulfide oxidation (sulfuricization). As summarized by Orndorff and Daniels (2004), pyrite oxidation is a complex biogeochemical process that is affected by a variety of parameters (e.g., temperature, pH, sulfide surface area, DO concentrations, water saturation, chemical activity of Fe^{3+}, and sulfur-oxidizing bacteria) and can be

Table 1.4. RRL-South baseline stabilized "field parameters".

Well ID	pH	Temp (°C)	Conductivity (S/cm)	DO (mgL)	Turbidity (NTU)	ORP (mV)	Purge Flow Rate (L/min)
TMW-S1	5.66	15.72	0.326	1.02	--*	247	0.10
TMW-S2	4.91	15.06	0.171	1.50	--	263	0.10
TMW-S3	6.05	15.15	0.316	0.89	--	196	0.13
TMW-26S	5.99	14.96	0.533	0.95	--	198	0.08
TMW-26D	5.93	14.95	0.268	2.79	--	212	0.10
MW-15R	4.22	15.23	0.940	0.86	--	378	0.13
TMW-27	5.75	15.53	0.343	1.34	--	224	0.10
TMW-31	5.47	15.02	0.382	2.20	9.8	257	0.08
TMW-32	NOT SAMPLED						
TMW-33	5.27	16.29	0.616	1.83	9.1	272	90
Average	5.47	15.32	0.433	1.49	9.5	249.7	98.9

*No readings due to broken turbidimeter

Table 1.5. Baseline chlorinated ethene concentrations (mg/L).

Well ID	PCE	TCE	cDCE	tDCE	VC
TMW-S1	0.059	0.031	0.520	0.002	0.006
TMW-S2	0.075	0.027	0.510	0.002	0.005
TMW-S3	0.043	0.020	0.250	0.001	0.003
TMW-26S	0.025	0.010	0.250	0.001	0.003

Table 1.6. Baseline groundwater parameters (mg/L).

Well ID	Chloride	Total Fe	Dissolved Fe	Total Mn	Dissolved Mn	Nitrate	Sulfate	Sulfide	Methane	Ethane	Ethene
TMW-S1	60	27.3	26.2	5.42	5.80	0.005*	7.7	1	1.9	0.0205*	0.0035*
TMW-S2	19	13.8	15.6	4.78	5.58	0.9	4.3	1.6	0.55	0.012	0.0035*
TMW-S3	28	42.1	41.7	5.69	6.05	0.005*	18	1.4	0.64	0.017	0.0035*
TMW-26S	29	35.3	32.2	5.16	5.27	0.005*	99	1.8	0.91	0.008	0.0035*

*The compound was analyzed for but not detected, therefore, the 1/2 reporting limit was used.

described by the following series of reactions. First, the pyrite is oxidized by O_2 and water, producing dissolved ferrous iron, sulfate and acidity:

$$FeS_{2(S)} + 7/2\,O_2 + H_2O \Rightarrow Fe^{2+} + 2SO_4^{2-} + 2H^+ \qquad (1.3)$$

The ferrous iron can be further oxidized to ferric iron,

$$Fe^{2+} + 1/4\,O_2 + H^+ \Rightarrow Fe^{3+} + 1/2\,H_2O \qquad (1.4)$$

which may be hydrolyzed, producing iron hydroxide precipitates and acidity,

$$Fe^{3+} + 3H_2O \Rightarrow Fe(OH_3) + 3H^+$$

(1.5)Alternatively, the ferric iron may react with pyrite and water:

$$FeS_2 + 14Fe^{3+} + 8H_2O \Rightarrow 15Fe^{2+} + 2SO_4^{2-} + 16H^+ \qquad (1.6)$$

The latter reaction is pH dependent because Fe^{3+} becomes increasingly soluble and less likely to precipitate (Eq. 1.5), as the pH is reduced. Eq. 1.4 is slow under abiotic conditions, while Eq. 1.6 is very fast. However, acidophilic iron-oxidizing bacteria can greatly accelerate Eq. 1.4, creating a rapid, self-perpetuating pyrite oxidation process. This bacterial activity has an optimum temperature of 30°C and pH 3.2. It ceases in the absence of O_2, but occurs at even low levels of O_2, with a maximum at approximately 1% partial pressure O_2 (i.e., 0.42 mg/L). The pH and DO at the RRL-South site (see Table 1.4) are both higher than these optimum values, but the low pH, high dissolved iron, high sulfate, and low sulfide levels are consistent with the occurrence of pyrite oxidation in the formation at RRL-South (Table 1.4).

Orndorff and Daniels (2004) reported that the Quantico Slate contained large quantities of sulfur and frequently exhibited acidic conditions in numerous road cuts across Virginia. The high levels of sulfate, coupled with the low levels of sulfide also

support these findings, and may indicate that H_2S is being oxidized to sulfate, thus, increasing the acidity within the RRL-South aquifer.

1.4 Post-injection Results

Approximately 30 days after the first round of HRC® injections into IP-S1, and IP-S2 the first set of groundwater samples were collected by the author from TMW-S1, -S2, -S3, and -26S, as described previously. All data analyses on the samples were performed by Accura Analytical Lab (Norcross, Georgia). Included in Appendix D are the data for post injection results sampling events.

The initial approach for analyzing the post injection data involved a visual inspection of the chlorinated solvent concentrations to determine if there were any trends that could be attributed to the biodegradation of CAHs. In general, the cDCE concentration in all monitoring wells, with the exception of TMW-S1, tended to increase with time (see Figure 1.11). However, the concentrations of TCE and PCE did not show the expected corresponding decrease in concentrations (see Figures 1.12 and 1.13). In fact, PCE concentrations in TMW-S3 and -26S increased with time. Furthermore, the concentrations of VC (see Figure 1.14) remained relatively constant, or declined, indicating that no formation of VC has occurred due to the degradation of cDCE. A comparison of CAH concentrations with respect to time for all monitoring wells can be made using Figures 1.15 and 1.16. When comparing the CAH concentrations in each well, the similarities in the trends for all of the CAHs suggest

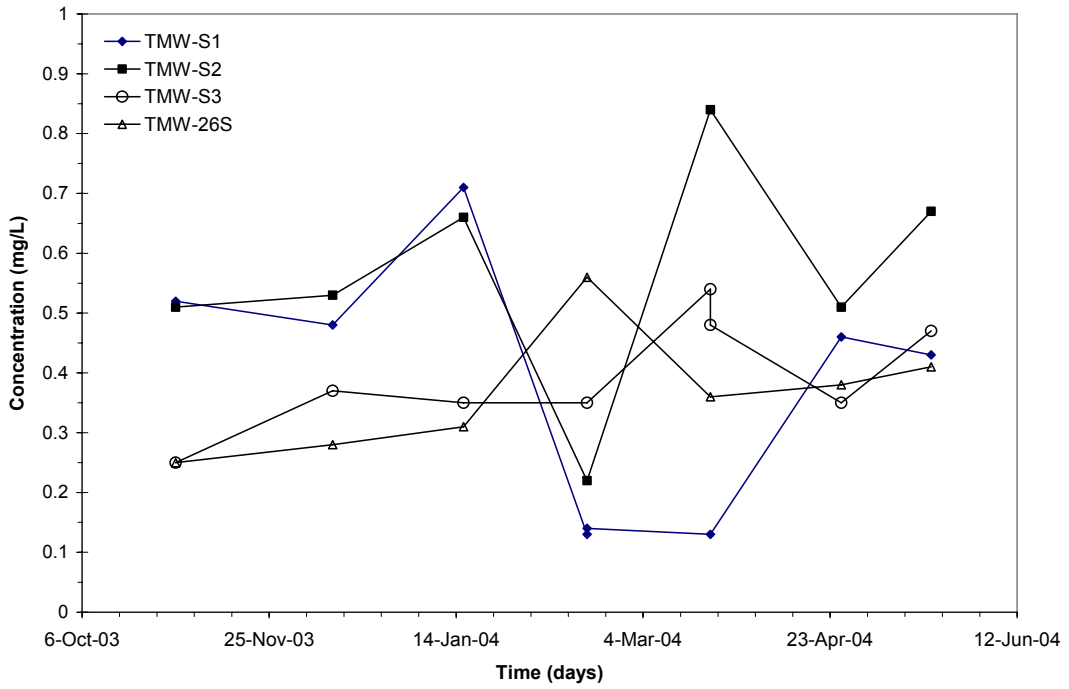

Figure 1.11. RRL-South cDCE concentration trends. Each point represents one sampling event.

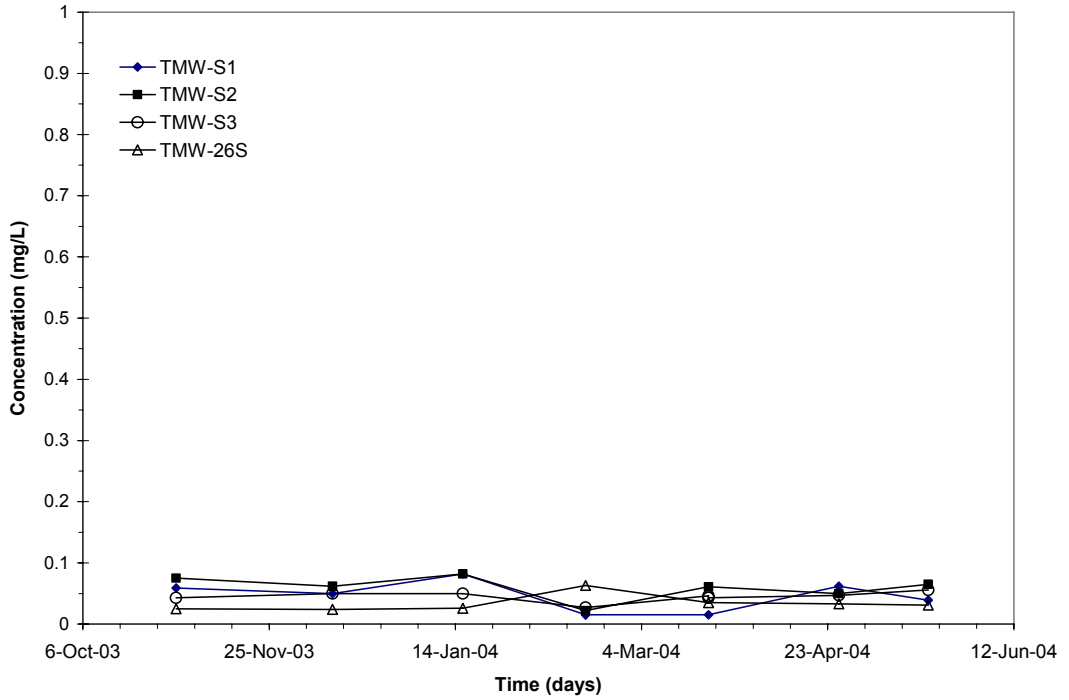

Figure 1.12. RRL-South PCE concentration trends. Each point represents one sampling event.

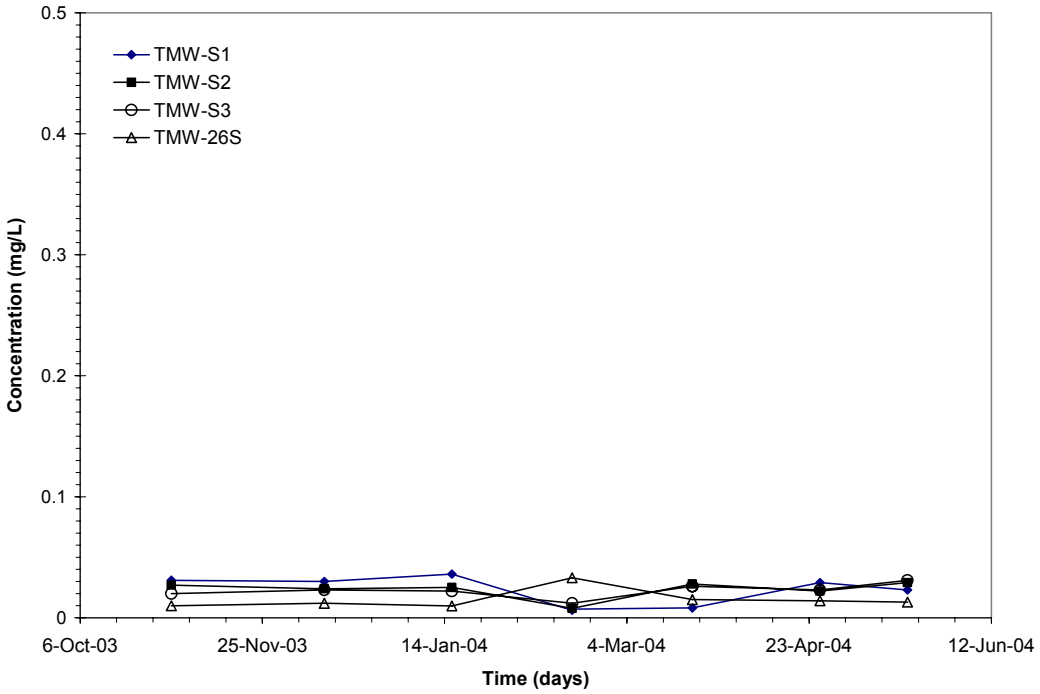

Figure 1.13. RRL-South TCE concentration trends. Each point represents one sampling event.

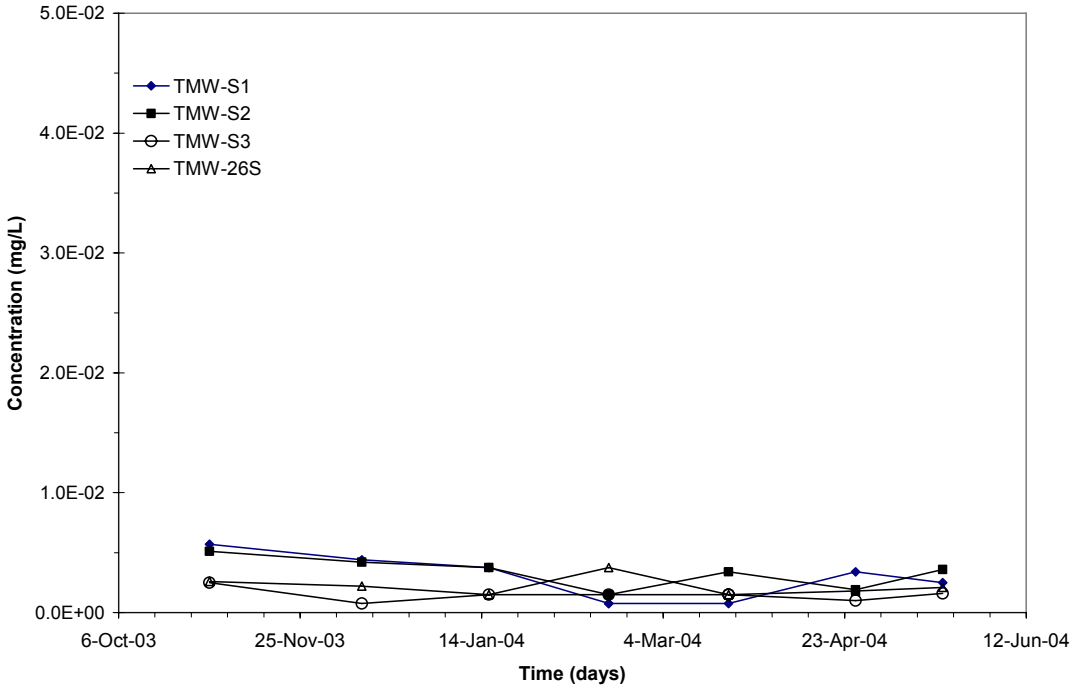

Figure 1.14. RRL-South VC concentration trends. Each point represents one sampling event.

that concentrations were fluctuating due to fluctuations in source concentrations rather than from biodegradation. For example, in Figure 1.15 the concentrations of all of the CAHs in TMW-26S increased during the February sampling event, suggesting that an overall increase in CAH concentrations occurred. Similarly, the data in Figure 1.16 show that all of the CAH concentrations in TMW-S1 decreased during the February and March sampling events, but returned to near-baseline concentrations in the later events. Because TMW-S1 is out of the expected zone of influence for the HRC® effects, it is assumed that the similar fluctuations in concentrations observed in the pilot injection area were also caused by source area concentration fluctuations.

A visual inspection of RRL-South water quality parameters was also conducted to determine if the addition of HRC® had any of the expected impacts on

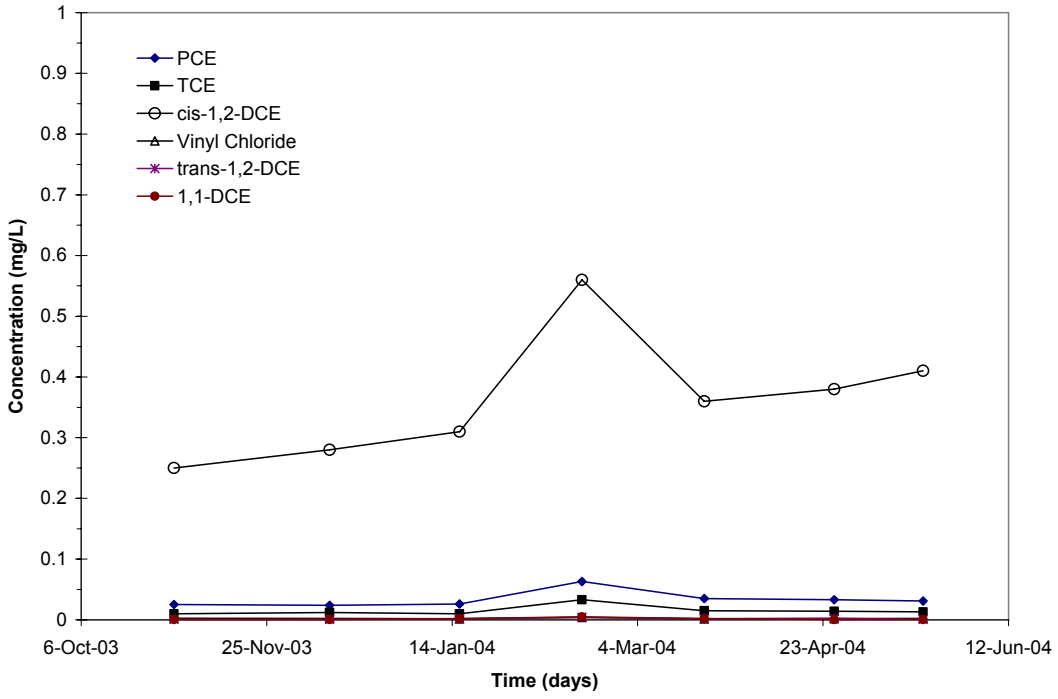

Figure 1.15. TMW-26S CAH trends. Each point represents one sampling event.

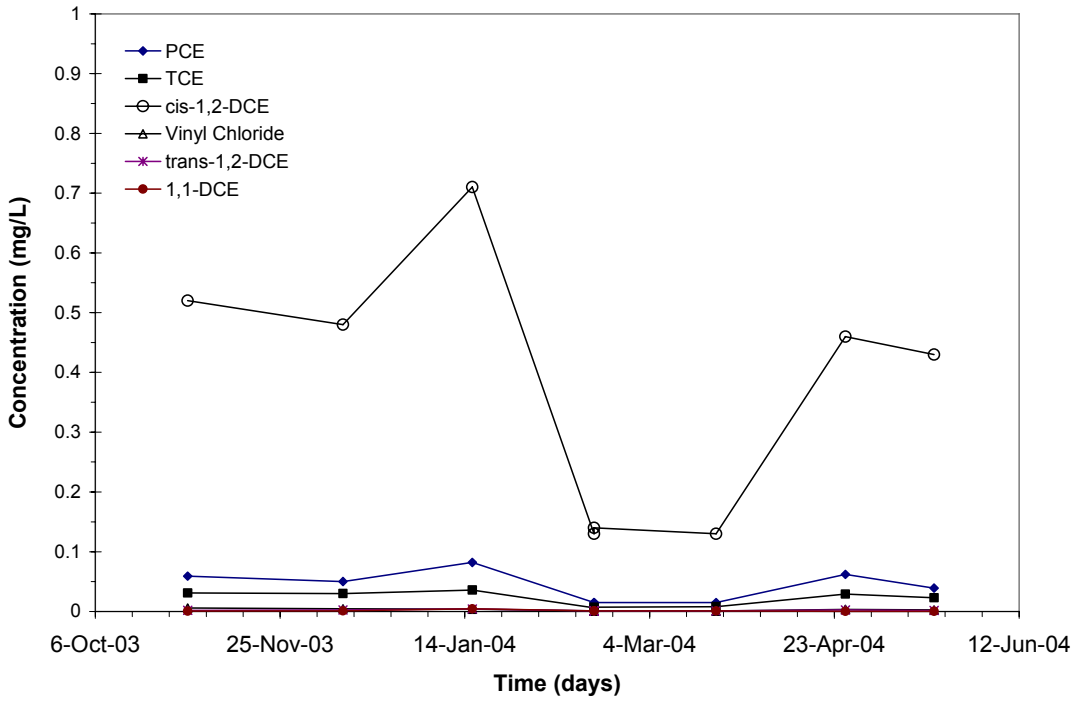

Figure 1.16. TMW-S1 CAH trends. Each point represents one sampling event.

the levels of dissolved oxygen, oxidation-reduction potential (ORP), pH, or conductivity. For simplification, the water quality parameter results (provided in Appendix D) were normalized by dividing the values by the baseline results in order to highlight any variation from the recorded levels discussed in Section 1.3. Upon inspection of the normalized data presented in Figures 1.17a, b, c, and d, the only parameters that varied significantly from the baseline were oxygen and ORP levels, while conductivity and pH remained relatively close to baseline concentrations throughout the duration of post-injection monitoring. A decrease in ORP was observed in all wells, and may indicate that the addition of HRC® to the subsurface has created reducing conditions as expected. However, the oxygen levels fluctuated, whereas they would be expected to decrease when the ORP levels decrease, as

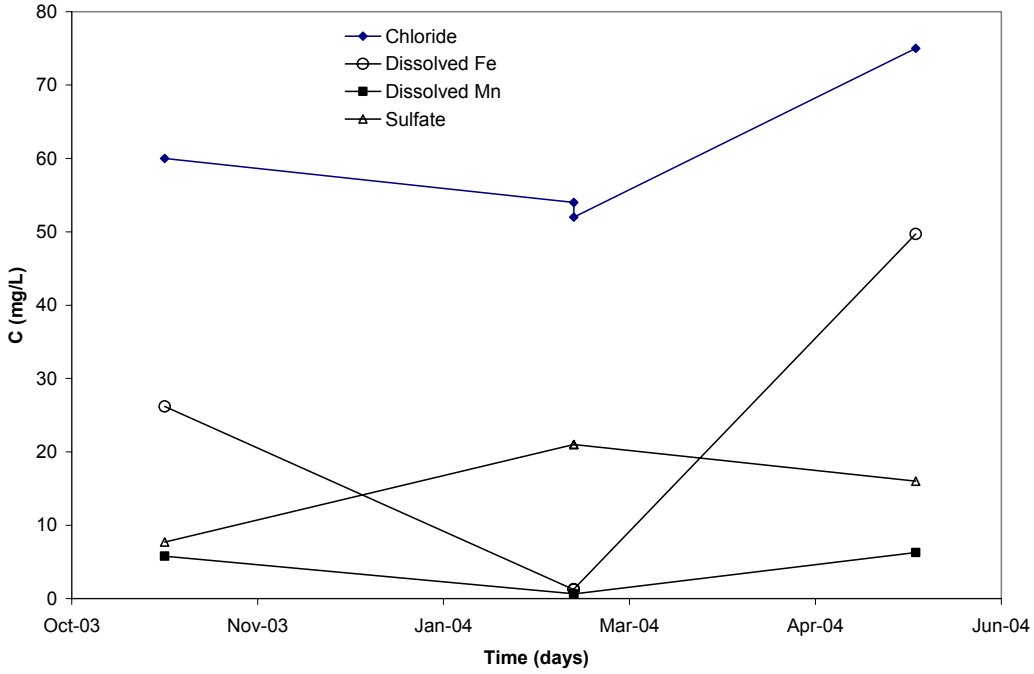

Figure 1.17a. TMW-S1 normalized groundwater parameters.

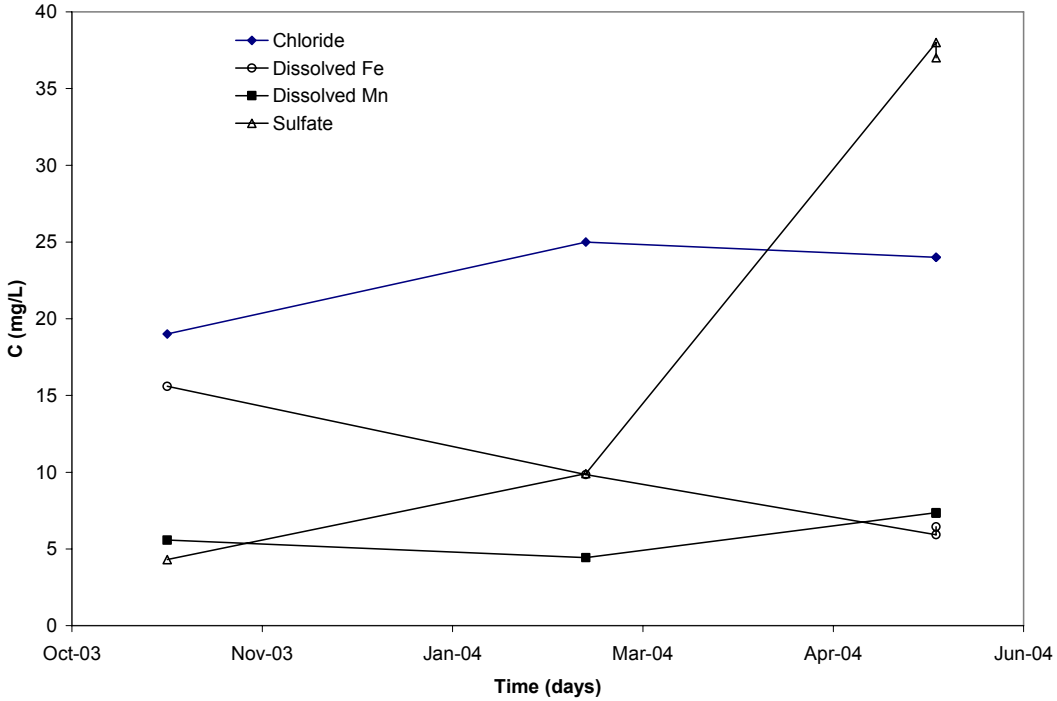

Figure 1.17b. TMW-S2 normalized groundwater parameters.

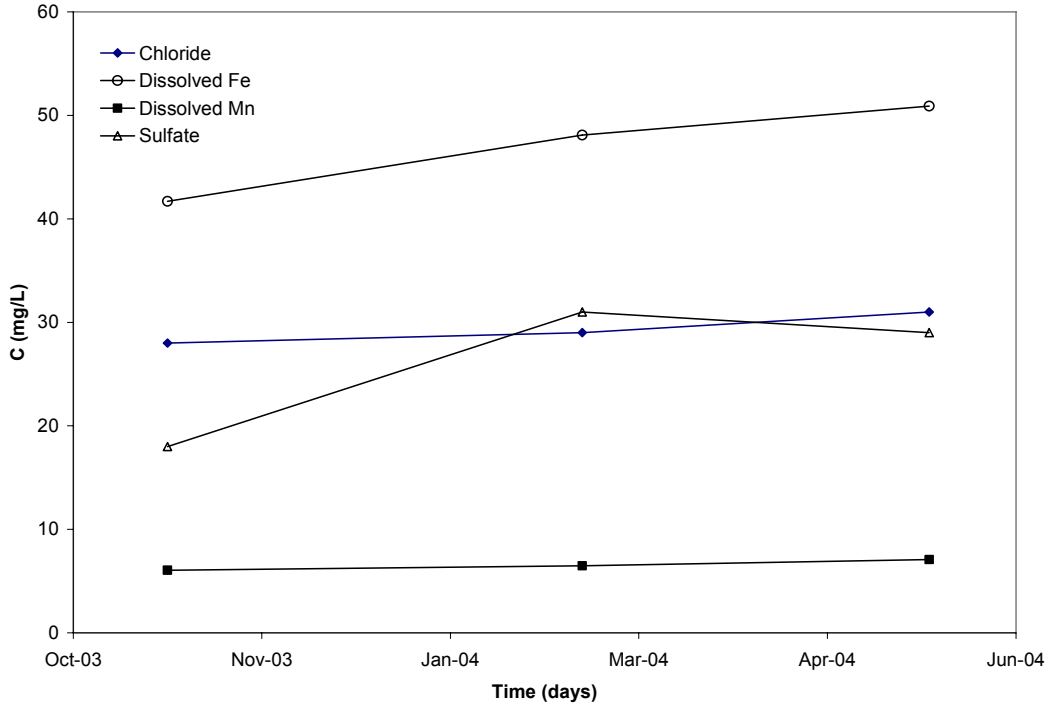

Figure 1.17c. TMW-S3 normalized groundwater parameters.

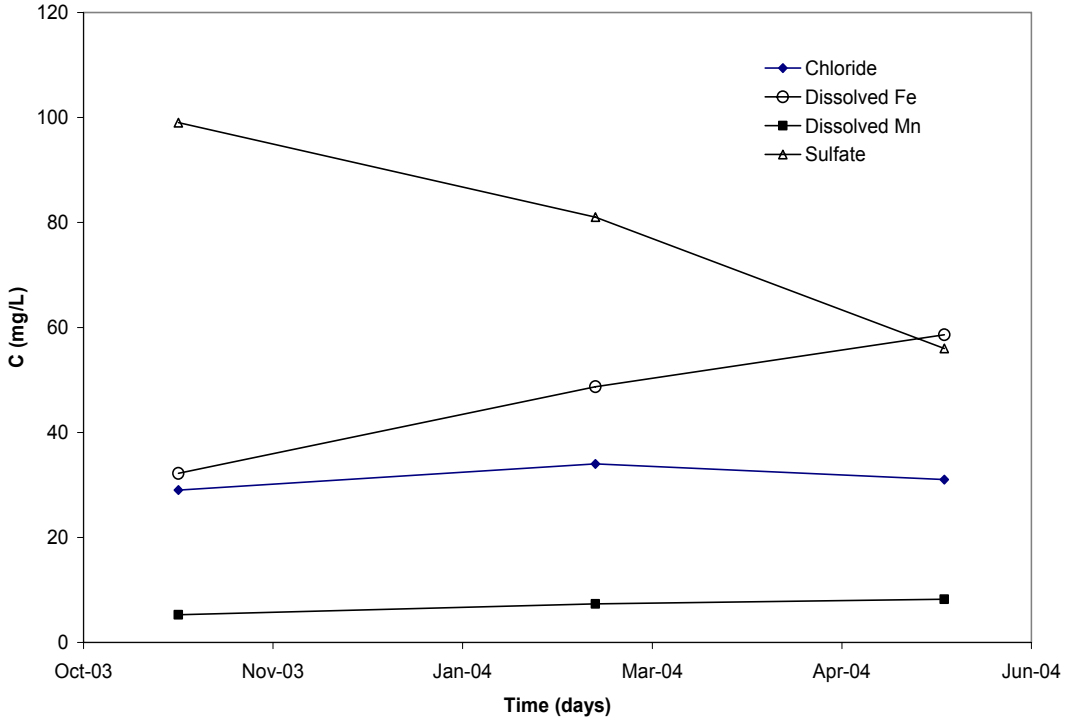

Figure 1.17d. TMW-26S normalized groundwater parameters.

oxygen is consumed and the system changes to a more reducing environment. This trend is only observed in TMW-S2 (see Figure 1.18) while in the other wells the oxygen levels fluctuate. Nevertheless, these O_2 data should not be given too much weight, because one explanation for these wide fluctuations in dissolved oxygen concentrations may be the introduction of air bubbles into the flow through meter during sampling events, as was commonly observed. Finally, the trends in concentrations of chloride, dissolved iron, dissolved manganese, sulfate, methane, and CO_2 were also visually inspected and compared to the baseline conditions (Figure 1.18) in order to determine if the HRC® injections had an impact on the subsurface environment (see Figures 1.19 and 1.20 for CO_2 and methane trends). Only dissolved iron and manganese were considered in this analysis as the bulk of these elements measured in the wells were in the dissolved phase. The results for these analytes do

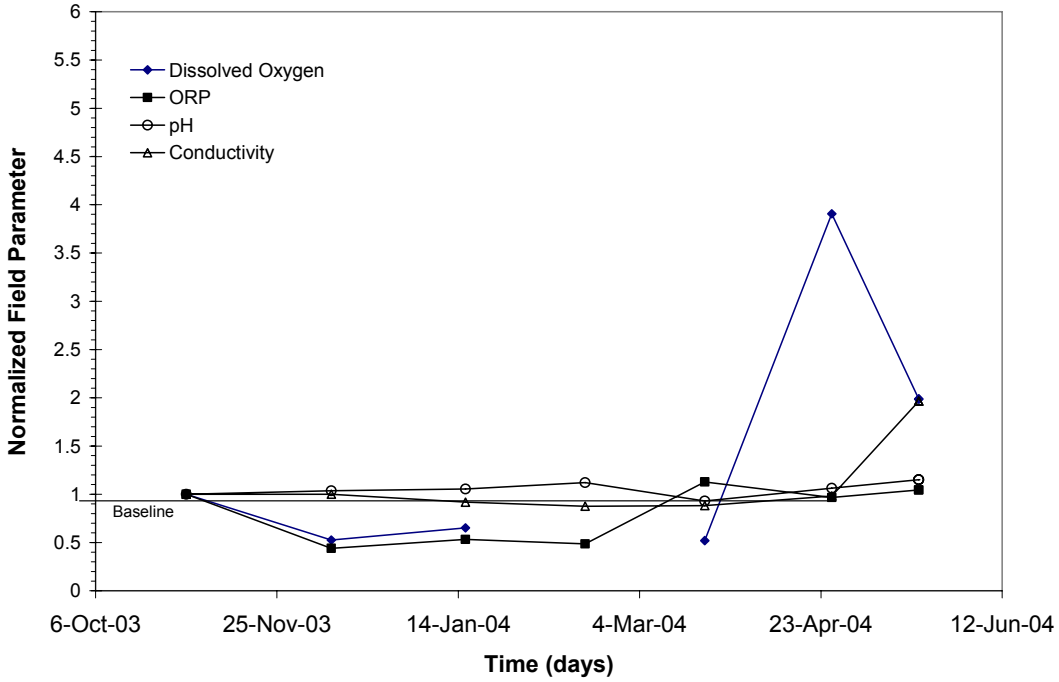

Figure 1.18. TMW-S2 normalized field water quality parameters. Each point represents one sampling event.

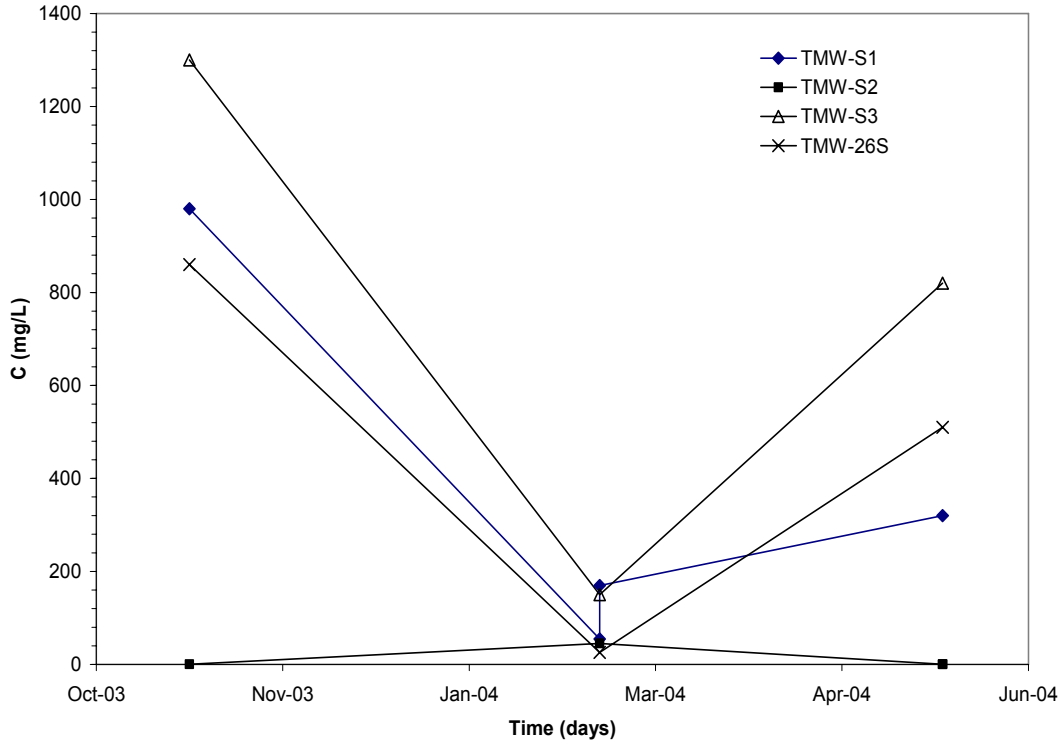

Figure 1.19. RRL-South CO_2 levels.

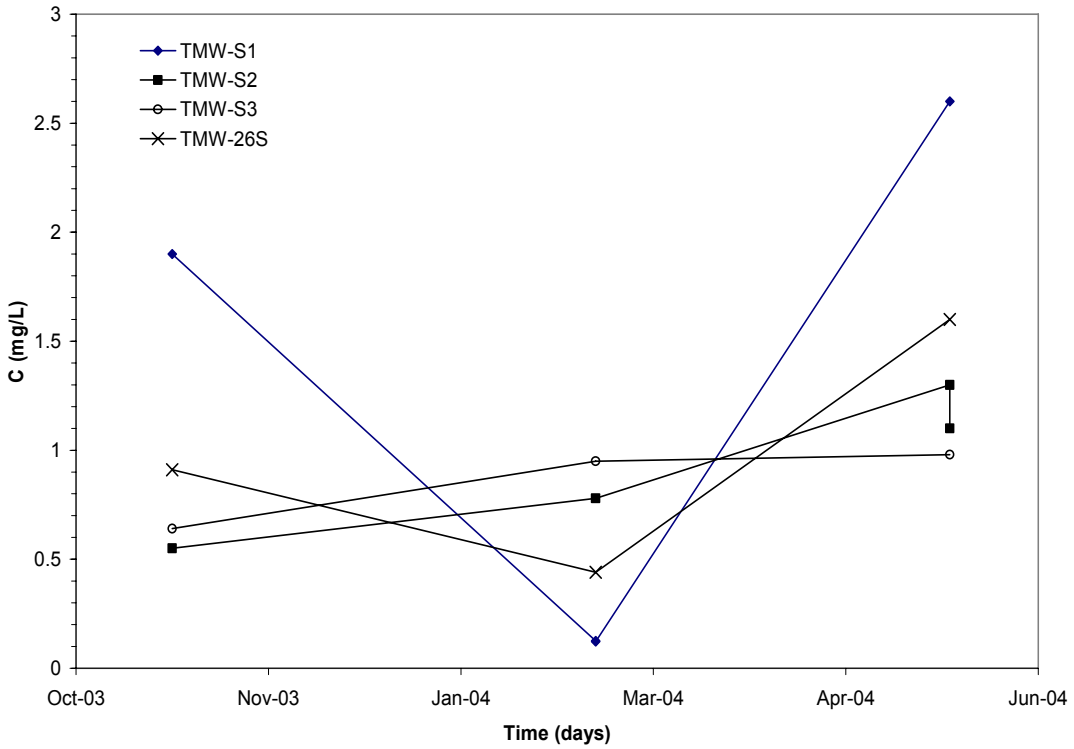

Figure 1.20. RRL-South groundwater methane levels.

not provide any significant trends, with the exception of methane, which increased slightly in all wells, and CO_2, which decreased in wells TMW-S1, -S3, and -26S as would be expected if more reducing conditions were created by the HRC® injections. Slight increases in chloride were observed in wells TMW-S1 and –S2. Additionally, sulfate increased in all wells, except in TMW-26S, where concentrations decreased. Furthermore, dissolved iron increased in all wells, except TMW-S2. This increase in sulfate and dissolved iron are consistent with the pyrite oxidation process discussed in Section 1.3, but not with the anaerobic conditions expected to be created by the HRC® injections.

In summary, based on the analysis of the post-injection results there is no clear evidence that the HRC® had a significant impact on CAH reductions. Furthermore, other indicators, such as the chloride levels, did not show the expected trends that would be observed if an increased reduction of CAHs had occurred. The only indicators suggesting that HRC® was affecting the subsurface environment were methane and CO_2 data. These data indicate that methanogens, competitors of halorespirers, may be consuming the CO_2, along with an electron donor (i.e., hydrogen produced during the fermentation of HRC®), to produce methane. Therefore, overall the trends in the post-injection data are equivocal, but it is clear that the HRC® injection did not have the desired effect.

2.0 SCOPE AND OBJECTIVES

2.1 Review of Pilot Scale Baseline and Post-Injection Results

As reviewed in Chapter 1, historical data at RRL-South suggest that reductive dechlorination has occurred at RRL-South, with decreasing PCE and TCE concentrations and increasing cDCE concentrations. This trend is not surprising, because DCE accumulation occurs frequently in many aquifers contaminated with the more highly chlorinated CAHs, PCE and TCE. For example, upon reviewing degradation trends, one study estimated that approximately half of the soils sampled did not support a microbial population capable of reducing PCE further than cDCE or VC (Hinchee, 1995).

While the accumulation of cDCE has been commonly observed, many practitioners have successfully demonstrated that the complete reduction of cDCE can take place if the necessary microorganisms are present and the site is amended by the addition of electron donors such as molasses (Wu et al, 1998; DiStefano et al, 2001), or lactic acid, e.g., produced through the fermentation of HRC® (Murray et al, 2001). Therefore, assuming that the cause for cDCE accumulation at RRL-South was due to electron donor limitations, the contractor chose to implement a pilot program similar to that of Murray et al (2001), whereby HRC® was injected into the RRL-South formation, as described in Chapter 1. This decision was largely based on the results of the bench scale HRC® treatability study which, as discussed in Section 1.3.1.1, indicated some potential for chlorinated solvent reductions, with a TCE laboratory half-life of 53 days. However, chlorinated ethene concentrations in the field at RRL-

South did not show similar results after the HRC® injections as demonstrated by the data collected after 6 months of post injection monitoring (see Section 1.4).

The findings at RRL-South, which revealed a discrepancy between the laboratory and field results, are not unusual. In fact, numerous authors have reported field degradation rates that do not correspond with those found in the laboratory setting. For example, Davis et al. (2003) reported that upon conducting batch tests on site specific soils, the small scale experiments severely overestimated field rates. Additionally, literature reviews by Haws et al. (2006), and Sturman et al. (1995), indicated that the general consensus is that laboratory degradation rates are always greater than those found in the field, with field rates on the order of 4 to 10 times slower than laboratory derived degradation rates (Sturman et al, 1995). Therefore, based on these typical trends, and given the TCE half-life equal to approximately 53 days, it would be expected that the corresponding field TCE half-life at RRL-South would be approximately 210 to 530 days. Furthermore, we might expect an even longer half-life for reductive dechlorination of cDCE, because the rate of reductive dehalorespiration generally decreases as the degree of halogen substitution decreases (Vogel et al., 1987). Thus, after 180 days of sampling, it is very possible that insufficient time was allowed for sampling to indicate a reduction in chlorinated ethenes has occurred, because some other factor was limiting the microbial processes of interest.

2.2 Nature, Scope, and Objectives

Successful implementation of field-scale *in situ* bioremediation requires an understanding of why field degradation rates are consistently slower than laboratory

rates. The explanation probably ultimately lies in the inherently complex and geologically, chemically, and microbiologically heterogeneous nature of the subsurface environment, which makes the implementation of *in situ* bioremediation technologically challenging (NRC, 1993). The physical and chemical heterogeneities of the subsurface occur at several scales and affect *in situ* biodegradation by controlling the availability of nutrients and substrates that drive microbiological degradation processes.

Despite its importance, the impact of physicochemical heterogeneities on *in situ* biodegradation is still not well understood. Because these subsurface, physical, chemical, and microbiological processes and their interactions are extremely complex, a process engineering approach is necessary to understand them and facilitate the decision making process for the remediation engineer (Sturman et al, 1995; Knapp and Faison, 1997). Following this recommendation, as a first step it is useful to apply the scales of heterogeneity (i.e., micro-, meso-, and macro-scales) as an organizational tool. Secondly, in order to accurately describe the complexities of the interactions between physico-chemical interfaces and biodegradation, and to allow for scale up, dimensionless parameters can be applied to these processes.

In the overall project of which this research is a part, it is hypothesized that using the scales of subsurface heterogeneities and associated interfacial processes as an organizing principle, a quantitative framework based on a set of dimensionless coefficients (described in Chapter 4) can be used to capture the effects of the competing interfacial and biokinetic processes. In turn, the framework results can then aid in defining the limits for the successful application of *in situ* bioremediation

in the field. The goal of the research reported here was to evaluate the utility of such a quantitative framework at the field scale, building on previous modeling (Johnson, 2004) and laboratory (Song, 2005) evaluations of the framework. Specifically, the objectives of this work were as follows:

1) To use a systematic and integrated laboratory and field investigation to obtain quantitative estimates of the key system parameters required for calculation of the dimensionless numbers for the RRL-South field site;
2) To use the results of these experiments, as represented in the dimensionless numbers, along with the quantitative framework to predict the overall rate-limiting process and determine what engineering actions, if any, would positively impact the *in situ* biodegradation rates at the site, and;
3) To evaluate the utility of the quantitative framework for delineating the rate-limiting process and selecting an appropriate *in situ* bioremediation approach by comparing predictions based on the quantitative framework to the results of the pilot-scale study at RRL-South.

The RRL-South site provided an interesting opportunity for evaluating whether the selected dimensionless numbers and framework could be successfully used to reduce the complexity of the field site, determine which process was rate-limiting, and assist field practitioners in remedial alternative selections. For example, given that the addition of an electron-donor source to the RRL-South site using HRC® did not stimulate cDCE biodegradation then if the quantitative framework is successful it

would be useful in defining what action, if any, should be taken to stimulate biodegradation at the site.

In the following chapter, Chapter 3, the key micro-, meso-, and macro-scale subsurface phenomena impacting *in situ* biodegradation are reviewed from the perspective of what a field practitioner needs to understand regarding the current knowledge of the relevant heterogeneous complexities at the respective scales. In Chapter 4, the governing equations for describing reactive transport are provided and used to derive the dimensionless parameters that are incorporated into the quantitative framework of dimensionless numbers. That framework was used in this work to evaluate the interactions between the scale-dependent mass-transport processes and *in situ* biodegradation at the RRL-South site. Then in Chapter 5, the laboratory- and field-scale techniques are described that were used to quantitatively evaluate the key micro-, meso-, and macro-scale phenomena at the RRL-South site. Subsequently, in Chapter 6, the results of the quantitative analyses of the micro-, meso-, and macro-scale phenomena are presented and discussed, followed by application of the results using the quantitative framework and comparison to the pilot-scale remedial activities at RRL-South. Finally, in Chapter 7, the study's conclusions and recommendations for further work are presented.

3.0 BACKGROUND INFORMATION

This chapter presents background information on the key scales of heterogeneities (i.e., micro-, meso-, and macro-scales) derived from relevant contemporary research. The information provided is focused on that crucial for the engineering practitioner who is following a process engineering approach for defining, and evaluating, heterogeneities found at the scales of interest. Specifically, this chapter focuses on the subsurface microbial and physico-chemical heterogeneities, and the latter's effects on the bioavailability of compounds to a microbial population capable of degrading cDCE. However, first the scales of heterogeneities are reviewed. These scales provide the organization framework for this and subsequent chapters.

3.1 Scales of Heterogeneity

In describing the heterogeneities of the subsurface, it is helpful to apply these scales of observation: micro-, meso-, and macro-scale (Sturman, 1995). Understanding the definition of these scales is vital for the work presented here and by others (e.g., Oya and Valocchi, 1997; Karapangioti et al., 2001), which have focused on describing the variability of heterogeneities found within each scale, and developing methods to describe the interfacial transport phenomena at each scale that can limit a successful bioremediation program. Defining the exact size of each scale is arbitrary; nonetheless, a quantitative description provides the type of organization of the subsurface environment that is required in a process engineering approach (Sturman et al., 1995). By becoming familiar with each scale and the extent to which

it affects bioavailability, an engineer will be better able to decide upon an appropriate bioremediation strategy.

The micro-scale is defined as the scale (approximately 10^{-6} to 10^{-5} m) at which chemical and microbiological phenomena may be characterized independent of transport (Sturman et al., 1995). At this scale bioavailability is considered with respect to pore-scale phenomena (micrometers) such as chemical flux from the mobile water phase to the stagnant pore-water, where the most microbes are found. Abundant research has been focused at this scale that attempts to provide data for the first step in site characterization described by Aichberger et al. (2005), i.e., determining biodegradability. Thus, this scale is important as it aids in interpreting the intrinsic ability of native or introduced microbial populations to degrade the compound of interest.

The scale at which transport phenomena and system geometry become apparent (approximately 10^{-5} to 10^{-2} m) is defined as the meso-scale (Sturman et al., 1995). Defining this scale is critical as it greatly influences the bioavailability of compounds used for bioremediation, either through chemical or physical processes. Meso-scale heterogeneities are often influenced by soil and groundwater chemistries, and can be thought of as pore-to-pore scale phenomena. Adding to the complexities of bioavailability are the heterogeneities found at the macro-scale (greater than 10^{-2} m), i.e., the scale at which the physical processes of advection and dispersion are dominant (Sturman et al., 1995). Such larger scale, macro-scale heterogeneities can be affected a range of phenomena including; individual lamina within a formation

(centimeters) or geologic strata (meters). The macro-scale phenomena can be observed at a well-to-well, or a regional scale.

The various physical and chemical heterogeneities that occur at each of these scales create, either directly or indirectly, interfaces, or boundaries between two phases, where there are strong contrasts in physical and chemical properties that exist over short distances (centimeters to meters) (Brockman and Murray, 1997). Specifically, the strong contrasts in physical and chemical properties at these interfaces control moisture flux, nutrient fluxes, and redox conditions, which, in turn, drive the distribution and activity of microbes in the subsurface (Brockman and Murray, 1997; McMahon and Chappelle, 1991).

3.2 Micro-scale Heterogeneities

As described previously, strong contrasts in physical and chemical properties exist over short distances in the subsurface (Brockman and Murray, 1997). Furthermore, at a pore-scale, different mineral phases and types of sedimentary organic matter may exist, which can result in the presence or absence of microbial populations within the span of a few millimeters. For instance, significant microbial growth was reported near the interfaces of porous regions with different permeabilities (Murphy et al., 1997; Szecsody et al., 1994; Oya and Valocchi, 1998), suggesting that a change in parameters within the span of a few millimeters allowed for microbial growth in this specific environment. These microbial populations were able to thrive in a small zone where the conditions sustained their growth. Millimeters away, where mass transfer was possibly limited through meso-scale heterogeneities (see Section 3.3), microbial populations were less abundant.

3.2.1 General Microbiological Effects

There is no question that microbial populations are abundant in the subsurface: bacterial densities in most contaminated aquifers are relatively close to the surface and values can range from 10^4 to 10^7 bacteria/g (dry weight) of soil (Lee et al, 1998; Jones et al, 1988). Commonly, aquifers are characterized macroscopically (>10^{-2} meters) as reducing environments (anaerobic) or oxidizing environments (aerobic) based on the concentrations of dissolved oxygen and the presence, or absence, of anaerobic metabolites (Lee et al, 1998). Once classified as anaerobic or aerobic, it is usually assumed that a microbial population is present that is capable of metabolizing a contaminant under these generalized aquifer conditions. Nevertheless, while measuring the bulk phase parameters (e.g., O_2, pH, ORP, SO_4) aids in defining the macroscale characteristics of an aquifer, many aquifers do not fit this generalization. By macroscopically generalizing aquifer characteristics, the micro-scale (10^{-6} to 10^{-5} meters) or mesoscale (10^{-5} to 10^{-2} meters) heterogeneities that are found at all sites may be ignored, thereby significantly reducing the effectiveness of any *in situ* bioengineered system. For example, heterogeneities due to differences in sediment permeability, channeling of water flow, and proximity to sources of organic contaminants such as fuel hydrocarbons or landfill leachates, may result in aerobic zones residing millimeters from anaerobic environments, with corresponding affects on microbial activity (Lee et al, 1998).

3.2.2 cDCE Biodegradation

The key microbiological phenomena of interest in this research was the biodegradation of cDCE; therefore, this section is a review of the current knowledge

on microbial degradation of chlorinated solvents, in particular cDCE. Numerous studies have been conducted on the degradation of PCE and TCE (e.g., Freedman and Gossett, 1989; Semprini et al., 1990), and the necessary environments required for the degradation of chlorinated ethenes has been described extensively (e.g., Vogel and McCarty, 1987). However, the problem common to most aquifers is that the degradation of PCE and TCE is often observed to stop at cDCE, which then accumulates in the subsurface (Hinchee, 1995). Only within the last ten years has the bioremediation of cDCE gained increased attention.

PCE and TCE, the more oxidized halogenated aliphatics, are susceptible to reductive dechlorination, while the lesser chlorinates, such as cDCE and VC, are in a more reduced state, thereby minimizing the tendency for further reduction (Vogel et al., 1987). Correspondingly, anaerobic conditions have been shown to be favorable for reduction of the more highly chlorinated compounds (i.e., PCE and TCE), and many anaerobic bacteria have been identified which degrade these compounds (Ferguson and Pietari, 2000; Coleman et al., 2002; Semprini et al., 1990; Freedman and Gossett, 1989; Maymó-Gatell et al., 1997, 2001; Major et al., 2002).

Reductive dechlorination of cDCE to VC requires sulfate reducing conditions (Vogel et al., 1987), due to the greater reduction potentials of denitrification, fermentation, and ferric iron reduction (see Table 3.1). Generally speaking, when oxidation and reduction half reactions are coupled, a microbe that can utilize the substrate that yields more energy will have a competitive advantage. For example, when an aquifer's oxidation-reduction potential favors denitrification or iron reduction, the microbes that can reduce nitrate or iron will have an advantage over

microbes that reduce cDCE, as more energy per mole electrons are gained. However, factors other than thermodynamics can also be important (e.g., kinetics), and sulfate has been observed to be inhibitory for the degradation of chlorinated ethenes at some field sites (Harkness et al., 1999).

Table 3.1. Free energy values for reduction of various electron acceptors. (EPA, 1998)

Electron Acceptor	Half-Cell Reaction Product	Free Energy per Electron Transferred (kJ/mole)
NO_3^-	N_2	-120
FeOOH	Fe(II)	-62.9
PCE	TCE	-61.8
TCE	cDCE	-60.6
VC	Ethene	-57.5
cDCE	VC	-50.7
SO_4^-	HS^-	-24
CO_2	CH_4	-16.4

Although sulfate reducing and methanogenic conditions are commonly found in the leachate emanating from landfills, only two microbial species, *Dehalococcoides ethenogenes* and BAV1, have been discovered, that can completely degrade PCE and TCE to ethene under such conditions (Maymó-Gatell et al., 1997, 2001; He et al., 2003). Unfortunately, BAV1 is only capable of PCE and TCE degradation by cometabolism (He et al., 2003). Likewise, *D. ethenogenes* degrades cDCE and VC through cometabolic processes (Maymó-Gatell et al., 1997, 2001), although numerous *D. ethenogenes*-like organisms have been identified which cometabolize cDCE while using VC as a growth substrate (Duhamel et al., 2002; Cupples et al., 2003).

Aerobic degradation of cDCE has been well documented (e.g., Freedman et al., 2001; Klier et al., 1999; Bradley and Chappelle, 1998, 2000), and the processes are predominantly cometabollic. The majority of the microbial species that have been studied are able to cometabolize cDCE through the degradation of VC (Coleman, 2002; Freedman et al., 2001) or methane (Bradley and Chappelle, 1998) as primary growth substrates. According to Klier et al. (1999), the direct oxidation of cDCE has not been verified, however, Bradley and Chappelle (2000) have shown in laboratory experiments that cDCE can be utilized as a sole carbon substrate under aerobic conditions, though no microbial growth was associated with cDCE degradation.

It is obvious from the literature, and from the author's experience, that numerous treatment methods are employed by engineering practitioners for the remediation of chlorinated ethenes in the field due to the different environments required for the growth of microbial populations capable of complete PCE to ethene degradation. In particular, anaerobic environments appear to be the most challenging for engineers to understand and control due to the complexities of the anaerobic aquifer chemistry which can lead to the accumulation of cDCE. Numerous methods have been employed to ensure that the biodegradation under anaerobic conditions does not result in PCE and TCE degradation stalling at cDCE. The first of these methods is the removal of some limiting factor (e.g., via electron donor, or nutrient introduction), or the improvement of environmental conditions (e.g., temperature or pH). Another treatment method is bioaugmentation, i.e., the addition of known chlorinated ethene degrading microorganisms to the aquifer. For example, Harkness et al. (1999) demonstrated that after PCE reduction (stimulated by the addition of

lactate as a growth substrate) stalled at cDCE, only bioaugmentation was able to result in the complete degradation of the compounds to the non-toxic end product, ethene. Additionally, Major et al. (2002) successfully degraded PCE to ethene in the field, only after bioaugmentation with *D. ethenogenes*.

3.3 Meso-scale Heterogeneities

Meso-scale phase interfaces that control the bioavailability of substrates include, but are not limited to; aqueous-solid (sorption/desorption), aqueous-nonaqueous phase liquid (NAPL) (dissolution), and aqueous-aqueous in solution chemistry (diffusion). For example, significant research has been previously conducted on NAPL dissolution rates and their influence on bioavailability (e.g., Davis et al., 2003; Goltz, 2001; Seagren et al.; 1994), as well as the effects of sorption-desorption rates on bioavailability (e.g., Harms and Bosma, 1997; Bosma et al., 1997: Karapangioti et al., 2001). Both of these mass-transfer rates can have an impact on bioavailability, because the majority of compounds that are available for biodegradation are assumed to be in the aqueous phase (Haws et al., 2006; Bosma et al., 1997). Although microbial activity and the associated biokinetics can impact the *in situ* biodegradation rate, as reviewed in Section 3.2, it has been observed that substrate mass transfer through the dissolution of NAPL contaminants, or desorption of sorbed-phase contaminants, not microbial activity, is in most cases the actually the limiting condition (Harms and Bosma, 1997; Bosma et al., 1997). Of these two key rate-limiting phenomena, the focus of this research is on the delivery of sorbed-phase contaminants, because of a NAPL source zone is considered unlikely at the RRL-South field site, given the relative magnitude of the chlorinated ethene concentrations

relative to their aqueous solubilities. Therefore, the remainder of this section is focused on the effects of sorption on biodegradation.

3.3.1 Sorption Effects

Although little research has been specifically conducted on the sorption of chlorinated ethenes, the general trends and models derived from the literature can be applied to most compounds. Sorption (and desorption) processes at the solid-phase/aqueous-phase interface may determine the local physical and/or chemical conditions by effecting biomass distribution through sorption of microbial cells and/or by affecting aqueous concentrations via solute sorption (van Loosdrecht et al., 1990; Ghiorse and Wilson, 1988; Madsen and Ghiorse, 1993). For example, Miller and Alexander (1991) demonstrated that aqueous phase concentrations can be significantly reduced due to a sorption sink which in turn reduces the solutes available for biodegradation and the biodegradation rate. Interestingly, some studies suggest that during injections of substrate amendments for stimulation of *in situ* bioremediation, many sorbed compounds resist hydraulic displacement and later desorb into the aquifer. As a result, the substrate and desorbed compound mixture moves through the formation as a traveling wave, thus increasing bioavailability (e.g., Oya and Valocchi, 1997; Knapp and Faison, 1997).

Sorption can be modeled with either equilibrium or nonequilibrium rate models (Weber et al., 1991; Toride et al., 1993). Although sorption processes are often modeled under equilibrium conditions, nonequilibrium sorption conditions have also been observed at the field scale (e.g., Ball and Roberts, 1993). These nonequilibrium conditions may be due to the presence of co-solutes (i.e., mixed

contaminant plumes), or natural organic matter, which can have a significant affect on aged contaminant plumes (Harms and Bosma, 1997; Alexander, 2000) as the compound of interest is slowly absorbed into the soil organic material, thereby becoming increasingly unavailable. As described in Chapter 4, this research employs a relatively straightforward approach for considering mass transfer kinetics between the soil and aqueous phases, utilizing a linear driving force and a lumped first-order mass-transfer coefficient (adapted from van Genuchten and Wierenga, 1976).

3.4 Macro-scale Heterogeneities

Complex macro-scale heterogeneities within an aquifer, including hydraulic conductivity heterogeneities, can significantly control the success and cost of any project (Knapp and Faison, 1997), and numerous studies indicate that these heterogeneities must be understood for effective *in situ* bioremediation (e.g., McCarty and Semprini, 1993; Sturman et al., 1995; Oya and Valocchi, 1998). Fore example, both advection and dispersion have a significant impact on movement of dissolved constituents, thus, biodegradation rates. Advection controls the bulk transfer of a contaminant plume into a pristine aquifer. The importance of hydraulic conductivity heterogeneities as it relates to advection can be explained by Darcy's law, where the bulk flow rate of groundwater is proportional to the hydraulic conductivity, K, of the formation. Therefore, the heterogeneity in the magnitude of K controls the bulk movement of constituents within the formation. Understanding the macro-scale phenomena are crucial for designing a successful bioremediation system, as diffusion and the heterogeneity-induced mechanical dispersion are the only mixing processes for solutes in the subsurface. Dispersion is a result of molecular diffusion, velocity

differences within pore spaces, and differences in hydraulic conductivities (Goltz et al., 2001), which occur at micro-, meso-, and macro-scales, respectively, thus adding to the difficulty in characterizing heterogeneities at this scale.

Under certain conditions, such as those found at RRL-South, highly stratified lithology can create further macro-scale heterogeneities and hydraulic mixing. These heterogeneities are defined at a laminal or stratum scale where "the contact between subsurface media with different hydrogeologic properties creates an interface that can affect the mass-transport of solutes and the availability of substrates, nutrients and electron acceptors to microbes" (Johnson, 2004). For example, laminal-scale heterogeneities can affect the rate of supply of nutrients and other substrates when variations in hydraulic conductivities exist, such as a clay lens or other fine grained layers. Even small scale variations in K can affect hydraulic mixing, thus, creating zones of "small scale" aqueous chemical heterogeneities that can greatly impact bioremediation. Field studies have concluded that these variations in "small scale" hydraulic conductivities are an important factor controlling *in situ* bioremediation (e.g., Molz and Widdowson, 1988).

4.0 DEVELOPMENT OF QUANTITATIVE FRAMEWORK

In Chapter 4 the mathematical background and derivation of the equations utilized in this research are presented. Specifically, the governing equations that may be used by an engineering practitioner for *in situ* bioremediation are presented, and a system of dimensionless parameters and a quantitative framework for evaluating the equations are developed following the same approach as outlined by Johnson (2004).

4.1 Governing Equations

To quantitatively determine the fate and transport of a compound within a defined system, the starting point is an equation that can be applied for the mass balance. The equation that is often utilized for reactive solute transport modeling in the saturated zones is the advection-dispersion-reaction (ADR) equation. Here, assuming cDCE is biodegraded as a terminal electron acceptor under anaerobic conditions, the ADR is written for cDCE in a two-dimensional domain, with steady flow in the x-direction:

$$\frac{\partial A}{\partial t} = D_x \frac{\partial^2 A}{\partial x^2} + D_z \frac{\partial^2 A}{\partial z^2} - \frac{q_x}{nS_w} \frac{\partial A}{\partial x} \pm G_i \qquad (4.1)$$

where A is the aqueous-phase electron acceptor solute concentration [ML^{-3}], t is time [T]; x is the distance in the direction of flow [L]; z is the distance in the direction horizontally transverse to the direction of flow [L]; D_x is the longitudinal hydrodynamic dispersion coefficient [L^2T^{-1}]; D_z is the horizontal transverse hydrodynamic dispersion coefficient [L^2T^{-1}]; q_x is the specific discharge [LT^{-1}]; n is

the soil porosity; S_w is the water saturation; and G_i is the source/sink term [$ML^{-3}T^{-1}$] where i denotes any number of source or sink equations, of which sorption (G_S), or biodegradation (G_B) kinetic reactions are considered in this work. The partial differential terms on the right side of Eq. 4.1 represent longitudinal dispersion, horizontal transverse dispersion, and longitudinal advection, respectively. The second order differential refers to a change in the "difference" in the mass flux because dispersion is proportional to the concentration gradient.

The description above for Eq. 4.1 is focused on a two dimensional domain with longitudinal and horizontal transverse dispersion because the bedding planes of the Quantico slate formation are vertical in the area of RRL-South, resulting in anisotropic conditions. However, homogeneous hydraulic conductivity, with one-dimensional flow within each vertical layer of the model is assumed; thus, there is no transverse advection term.

In the following sections, the terms on the right of Eq. 4.1 are examined in more detail. First, the advection and dispersion processes are described in greater detail. Specifically, these processes are reviewed from a practitioner's standpoint, thereby clarifying their applications in a field setting. Subsequently, two source/sink terms are developed to represent the reaction processes, G_i, that are important with respect to *in situ* bioremediation at RRL-South: aqueous-phase solute biodegradation, denoted G_B; and kinetic sorption between aqueous-phase solute and solid matrix, denoted G_S.

4.1.1 Advection

The bulk macroscopic process of advection describes solute transport via the motion of flowing groundwater, much like a leaf transported on the surface of a flowing river. In Eq. 4.1, advection is described by the q_x/nS_w term. Typically, flow is assumed to be one-dimensional within a homogeneous layer, as in Eq. 4.1. Under steady-state conditions, with saturated flow (i.e., $S_w = 1.0$) and constant porosity, the term q_x/nS_w can be replaced by v_x. Given that flow is in the x-direction, v_x, is defined as the seepage or average pore velocity in the longitudinal direction (i.e., parallel to flow direction). Seepage or average pore velocity can be defined from Darcy's Law as,

$$v_x = -\frac{K}{n}\frac{dh}{dl} \tag{4.2}$$

where K is the hydraulic conductivity [LT^{-1}], n is the porosity, and dh/dl is the hydraulic gradient based on surface groundwater elevations observed over the region of interest [LL^{-1}] (Freeze and Cherry, 1979).

4.1.2 Dispersion

Dispersion is a function of fluid flow dynamics and the turbulence resulting from obstacles in the one-dimensional flow path, and results in solute spreading away from the path expected based on advective movement alone. In reality, dispersion occurs in three dimensions, however, for simplification, dispersion is often only considered in two dimensions. For this research, dispersion parallel to flow (longitudinal) and dispersion perpendicular to flow (horizontal transverse), are key, and represented by the hydrodynamic dispersion coefficients D_x and D_z [L^2T^{-1}],

respectively, in Eq. 4.1. On a small scale, the hydrodynamic dispersion coefficients are generally defined as representing the combined effects of mechanical and molecular diffusion, and can be represented as,

$$D_i = \alpha_i v_i + D_{diff} \tag{4.3}$$

where D_i represents the hydrodynamic dispersion coefficient in the *i*-direction, α_i is the dynamic dispersivity in the *i*-direction [L], and D_{diff} is the effective coefficient of molecular diffusion in the porous medium [L^2T^{-1}]. The dynamic dispersivity is a mechanical characteristic of the porous medium, and the coefficient of molecular diffusion is a characteristic of the solute (Freeze and Cherry, 1979). For example, the term $\alpha_x v_x$ depends on the degree of micro-scale eddies resulting from flow around non-uniform hydraulic conductivities which can be found at the micro-scale within a subsurface layer. D_{diff} is controlled by the solute concentration gradients, and is described by Fickian motion, which is a "random walk", or flux, of particles from higher to lower concentrations. Usually dispersion resulting from mechanical processes is far greater than dispersion resulting from diffusive processes.

4.1.3 Reactions

The two reaction sink terms, G_i, pertinent to this research are presented in the following sections. They include the linear sorption model, useful for describing sorption of organics onto sediments, and the double-Monod biodegradation equation for describing dual-substrate limited biokinetics.

4.1.3.1 Linear Sorption

For this research it is assumed that the electron acceptor (i.e., cDCE) is subject to sorption, while the electron donors (e.g., H_2) are conservative. As discussed in Chapter 3, sorption processes may be at equilibrium, or non-equilibrium, and appropriate models are required. One simplified equation which can be used to describe the equilibrium sorption of low concentrations onto soil particles is the linear isotherm model:

$$\overline{A} = K_d A \tag{4.4}$$

where $\overline{A}$ is the sorbed electron acceptor concentration [MM^{-1}], K_d is the linear partitioning coefficient [L^3M^{-1}], and A is the electron acceptor solute concentration at equilibrium [ML^{-3}]. The linear partitioning coefficient is sorbent and compound specific, and, thus, is generally modeled as being dependent on the fraction of organic matter present in the sorbent as well as the hydrophobicity of the contaminant.

The sink term for sorption, Gs, can be defined as,

$$G_S = -\frac{\rho_b}{n}\frac{\partial \overline{A}}{\partial t} \tag{4.5}$$

where ρ_b is the particle bulk density, and all remaining terms are described previously. Assuming linear equilibrium sorption, i.e., $\overline{A} = K_d A$, the differential expression on the right side of Eq. 4.5, can be rewritten as,

$$\frac{\partial \overline{A}}{\partial t} = K_d \frac{\partial A}{\partial t} \tag{4.6}$$

Eq. 4.6 can be inserted into Eq. 4.5, which can then be inserted back into the ADR equation (Eq. 4.1). As a result, the left side of Eq. 4.1 becomes,

$$\left(1+\frac{\rho_b}{n}K_d\right)\frac{\partial A}{\partial t}=R_d\frac{\partial A}{\partial t}=\ldots \qquad (4.7)$$

where R_d is defined as the site-specific retardation factor for a given compound, and is equivalent to the ratio of the fluid velocity over the chemical velocity.

While it is useful to determine the retardation of a compound within the aquifer assuming equilibrium conditions, as discussed in Chapter 3, non-equilibrium conditions are also observed. Therefore, this research also focuses on the rate of electron acceptor sorption and its application for the use in a dimensionless parameter framework. There are several approaches available for describing the mass-transfer kinetics between soil aggregates and the water phase. For this work, the following simple linear equation with a linear driving force, was used (Lapidus and Amundson, 1952; van Genutchen and Wierenga, 1976);

$$G_S=\frac{\partial A}{\partial t}=-k_m\left(A-\frac{\overline{A}}{K_d}\right) \qquad (4.8)$$

where k_m is the kinetic mass transfer coefficient [T^{-1}] and K_d is the linear partitioning coefficient, described previously. The term $\overline{A}/K_d$ represents the aqueous concentration of solute that would be in equilibrium with the sorbed electron acceptor concentration. Thus, at equilibrium, the term in the parentheses is zero, and there is no net change in concentration over time. The difference between the sorbed and aqueous phase concentration not in equilibrium can be considered the driving force for sorption, since a greater difference in the A and $\overline{A}/K_d$ values results in a "steeper" gradient. The magnitude of k_m represents rate limitations due to the sorption processes such as availability of sorption sites.

4.1.3.2 Double-Monod Biodegradation

Three conceptual models have been used to describe the biomass mediating biodegradation in the subsurface: (1) the biofilm model, (2) the microcolony model, and (3) the strictly macroscopic model (Baveye and Valocchi, 1989). Odencrantz et al. (1990) concluded that the relatively more complex biofilm and microcolony models were not needed for modeling solute concentrations in most groundwater situations. Therefore, the strictly macroscopic model is used in this research because it does not make assumptions concerning the spatial distribution of biomass that may not conform to reality (Baveye and Valocchi, 1989).

In addition to selecting the conceptual model, it is necessary to implement a model that describes the substrate utilization kinetics. For modeling dual substrate limited biodegradation (e.g., one substrate is the primary electron donor and another is the primary electron acceptor), the multiplicative Monod model can be used. Use of a model such as this takes into consideration the electron acceptor limitations and electron donor limitations that are critical for this research and subsurface bioremediation in general (Sturman et al., 1995). For example, a better understanding of the biodegradation rate of electron donors is vital as this is often the injected limiting substrate in an engineered system for bioremediation of CAHs used as electron acceptors.

Dual substrate limitation, as applied to electron acceptor substrate utilization, can be expressed by the multiplicative Monod model as follows:

$$G_B = \frac{\partial A}{\partial t} = -q_{\max} X \left(\frac{S}{K_S + S} \right) \left(\frac{A}{K_A + A} \right) \qquad (4.9)$$

where q_{max} is the maximum specific substrate utilization rate [$M_{donor}M^{-1}_{cells}T^{-1}$]; X is the total biomass concentration (pore volume basis, i.e., the total concentration of cells per liter of pore water) [$M_{cells}L^{-3}$]; S is the electron donor substrate concentration [ML^{-3}]; A is the electron acceptor substrate concentration (as defined previously) [ML^{-3}]; K_S is the electron donor half-maximum rate constant [ML^{-3}]; and K_A is the electron acceptor half-maximum rate constant [ML^{-3}].

Both q_{max} and K are independent of the biomass concentration and, more importantly, they are only dependent on the compound being degraded and the microbial consortium performing the transformation (Cookson, 1995). For example, if a microbial population capable of mediating the degradation process of interest is present, but the electron donor (*S*) or acceptor (*A*) concentrations are low, the biodegradation rate will decrease. Additionally, if only the electron donor concentration approaches zero, Eq. 4.9 will still approach zero regardless of the electron acceptor concentration.

4.1.4 Biomass

Biomass growth is proportional to substrate utilization described by Eq. 4.9, where the proportionality factor is Y, the true yield coefficient. In addition to biomass growth, loss or death of biomass must also be taken into account, which is represented by kinetic decay term. Therefore, the equation for biomass takes the form,

$$\frac{\partial X}{\partial t} = q_{\max} YX\left(\frac{S}{K_S + S}\right)\left(\frac{A}{K_A + A}\right) - k_d SX \qquad (4.10)$$

where k_d is a biomass decay coefficient [T^{-1}].

4.1.5 Summary of Governing Equations

For the description of contaminant fate and transport in field applications an engineering practitioner requires a relatively simple model. However, the number of equations in the system is dependent upon the number of individual components within the system. For this research it is assumed that there are four key system components: the aqueous electron donor, the aqueous electron acceptor, the sorbed electron acceptor, and the immobile biomass. Therefore, a system of four equations is required to describe the mass entering and leaving the system, as well as the different compartments in which the mass partitions to within the system.

Rearranging the terms in Eq. 4.1 and substituting in the reaction terms of Eqs. 4.8 and 4.9 yields the following governing equation for the electron acceptor substrate:

$$\frac{\partial A}{\partial t} = D_x \frac{\partial^2 A}{\partial x^2} + D_z \frac{\partial^2 A}{\partial z^2} - v_x \frac{\partial A}{\partial x} - k_m \left(A - \frac{\overline{A}}{K_d} \right) - q_{\max} X \left(\frac{S}{K_S + S} \right) \left(\frac{A}{K_A + A} \right) \tag{4.11}$$

where all terms are as previously defined. Although not shown here, a comparable equation could be written for the electron-donor substrate (without the sorption term). The equation for the sorbed electron acceptor substrate could be derived from Eq. 4.8 and the equation for the immobilized biomass is equivalent to Eq. 4.10.

4.2 Dimensionless Parameters

As stated in Chapter 2, a primary goal of this research was to determine if a previously developed dimensionless parameter framework (Johnson, 2004) could be utilized at the field scale. Specifically, the suitability of this framework as an aid in

determining which engineered enhancements, if any, are required to stimulate biodegradation was tested. To accomplish this goal the system of equations developed in the previous sections had to be nondimensionalized by using a set of dimensionless parameters that could be incorporated into the decision making framework. Specifically, a group of dimensionless parameters was developed that can be used to quickly compare the rate of the various processes occurring, e.g., advection, dispersion, sorption, biodegradation, or non-aqueous phase liquid dissolution (Johnson, 2004). Upon a systematic comparison of these relative rates, the rate limiting step can be determined based on the degree of variation from unity. This approach of using dimensionless parameters for comparing complex interactions or rate-limiting processes in contaminated environments has been previously documented (e.g., Seagren et al., 1993; Ramaswami and Luthy, 1997; Oya and Valocchi, 1998; Bruseau et al., 1999; Johnson, 2004; Song, 2005). Such parameters are developed by substituting non-dimensional units of time, mass, and length into the equations developed for the analysis.

The first step in non-dimensionalizing Eq. 4.11 was to substitute non-dimensional units of time (t*), direction (x*, z*), and concentration (S*, A*, and X*). These non-dimensional units as used in this research are summarized in Figure 4.1, where L is the characteristic length (i.e., the height of the saturated zone) [L], S_0 is the initial injected electron-donor substrate aqueous concentration [ML^{-3}], $\overline{A}_0$ is the initial sorbed-phase electron-acceptor concentration [MM^{-1}], A_0 is the initial electron-acceptor aqueous concentration [ML^{-3}], and X_0 is the initial biomass concentration [MM^{-1}]. All initial concentration values reference the background or injected

concentration for the cases where no background concentration of the species is present. Following substitution of the these non-dimensional units, Eq. 4.11 can be rewritten as follows:

$$\frac{\partial A^*}{\partial t^*} = \frac{D_x}{Lv_x}\frac{\partial^2 A^*}{\partial x^{*2}} + \frac{D_z}{Lv_x}\frac{\partial^2 A^*}{\partial z^{*2}} - \frac{\partial A^*}{\partial x^*} - \frac{Lk_m}{v_x}\left(A^* - \overline{A}^*\right) - \frac{q_{maz}X_0 L}{S_0 v_x}X^*\left(\frac{S^*}{K_S^* + S^*}\right)\left(\frac{A^*}{K_A^* + A^*}\right) \quad (4.12)$$

$$x^* = \frac{x}{L} \qquad z^* = \frac{z}{L} \qquad t^* = \frac{t}{Lv_x} \qquad S^* = \frac{S}{S_O}$$

$$\overline{A} = \frac{\overline{A}}{\overline{A}_O} \qquad A^* = \frac{A}{A_O} \qquad K_S^* = \frac{K_S}{S_O} \qquad K_A^* = \frac{K_A}{A_O} \qquad X^* = \frac{X}{X_O}$$

Figure 4.1. Dimensionless units. (e.g., Oya and Valocchi, 1998)

Each of the terms on the right hand side of Eq. 4.12 (dispersion, advection, sink reactions) has an associated dimensionless group of constants that represents the relative rate of change for that term as compared to advection. For example, the rate of change for longitudinal dispersion relative to advection can be observed by inspection of the term D_z/Lv_x. Further, additional relative rate terms can be constructed by comparing the various dimensionless relative rate terms from Eq. 4.12 to each other. For example, comparison of the term that represents the relative rate of biodegradation to advection $\left(q_{\max}X_0 L/A_0 v_x\right)$ to the term D_z/Lv_x, can be performed by rearranging the terms, result in a parameter $q_{\max}X_0 L^2 \Big/ A_0 D_z$, which can be used to compare the relative rate of biodegradation to the longitudinal dispersion.

For this research, additional dimensionless parameters were derived from each of the dimensionless groups of constants on the right-hand side of Eq. 4.12, which are presented in Figure 4.2.

$$\text{Pe}_L = \text{Longitudinal Peclet Number} = \left(\frac{\text{advection}\cdot\text{rate}}{\textit{longitudinal}\cdot\text{dispersion}\cdot\text{rate}}\right) = \frac{v_x L}{D_X}$$

$$\text{Pe}_T = \text{Transverse Peclet Number} = \left(\frac{\text{advection}\cdot\text{rate}}{\textit{transverse}\cdot\text{dispersion}\cdot\text{rate}}\right) = \frac{v_x L}{D_Z}$$

$$\text{St}_2 = \text{Stanton Number 2} = \left(\frac{\text{soil}\cdot\text{mass}\cdot\text{transfer}\cdot\text{rate}}{\text{advection}\cdot\text{rate}}\right) = \frac{Lk_m}{v_x}$$

$$\text{Sh}_2\text{'} = \text{Modified Sherwood Number 2} = \left(\frac{\text{soil}\cdot\text{mass}\cdot\text{transfer}\cdot\text{rate}}{\text{transverse}\cdot\text{dispersion}\cdot\text{rate}}\right) = St_2 \times Pe_T = \frac{L^2 k_m}{D_T}$$

$$\text{Da}_2 = \text{Damköhler Number 2} = \left(\frac{\text{biodegradation}\cdot\text{rate}}{\text{advection}\cdot\text{rate}}\right) = \frac{q_{\max} X_o L}{v_x A_o}$$

$$\text{Da}_5 = \text{Damköhler Number 5} = \left(\frac{\text{biodegradation}\cdot\text{rate}}{\text{soil}\cdot\text{mass}\cdot\text{transfer}\cdot\text{rate}}\right) = \frac{Da_2}{St_2} = \frac{q_{\max} X_o}{A_o k_m}$$

$$\text{Da}_6 = \text{Damköhler Number 6} = \left(\frac{\text{biodegradation}\cdot\text{rate}}{\text{transverse}\cdot\text{dispersion}\cdot\text{rate}}\right) = Da_2 \times Pe_T = \frac{q_{\max} X_o L^2}{A_o D_Z}$$

Figure 4.2. Definition of dimensionless numbers and parameters.

By implementing these parameters, Eq. 4.12 can be rewritten as follows:

$$\frac{\partial A^*}{\partial t^*} = \left(\frac{1}{Pe_L}\right)\frac{\partial^2 A^*}{\partial x^{*2}} + \left(\frac{1}{Pe_T}\right)\frac{\partial^2 A^*}{\partial z^{*2}} - \frac{\partial A^*}{\partial x^*} - St_2\left(A^* - \overline{A}^*\right) - Da_2 X^* \left(\frac{S^*}{K_S^* + S^*}\right)\left(\frac{A^*}{K_A^* + A^*}\right) \tag{4.13}$$

4.3 Dimensionless Parameter Framework

Using the dimensionless parameters presented in Section 4.2, a framework was developed to quantitatively identify the rate-limiting process (after Ramaswami and Luthy, 1997), as previously described by Johnson (2004). The framework, shown in Figure 4.3, presents a flowchart that can be used to identify the rate-limiting process. The first two steps of the flowchart are used to identify the limiting mass-transfer rate (e.g., advection, dispersion, or sorption). The third step compares the limiting mass transfer process with the biodegradation rate to determine the overall rate limiting process for the system. Ramaswami and Luthy (1997) suggest that for conclusive results the dimensionless parameters should be significantly smaller or larger than unity. In practice, the dimensionless parameters are recommended to be less than 0.2 for cases where the value is to be less than unity, and 5 for cases where the value is to be greater than unity (Ramaswami and Luthy, 1997).

4.4 Analysis of Framework at the Field Scale

Whereas previous studies designed to analyze the utility of the dimensionless parameter framework developed in Section 4.3 have focused on modeling (Johnson, 2004), and laboratory-scale (Song, 2005) evaluations, the current study was designed as a field-scale evaluation. Thus, the laboratory and field protocols used for the parameter estimation required for the dimensionless number analysis were designed to provide a useful evaluation of the framework, while being of a nature such that an engineering practitioner could perform similar tests under similar conditions. The results obtained from the framework analysis could then be compared to the ongoing field engineered enhancement at RRL-South for verification purposes. Specifically,

if the framework identified a rate-limiting process which impeded the successful implementation of *in situ* biodegradation, and similar trends were observed in the field, alternate remedial options could then be considered.

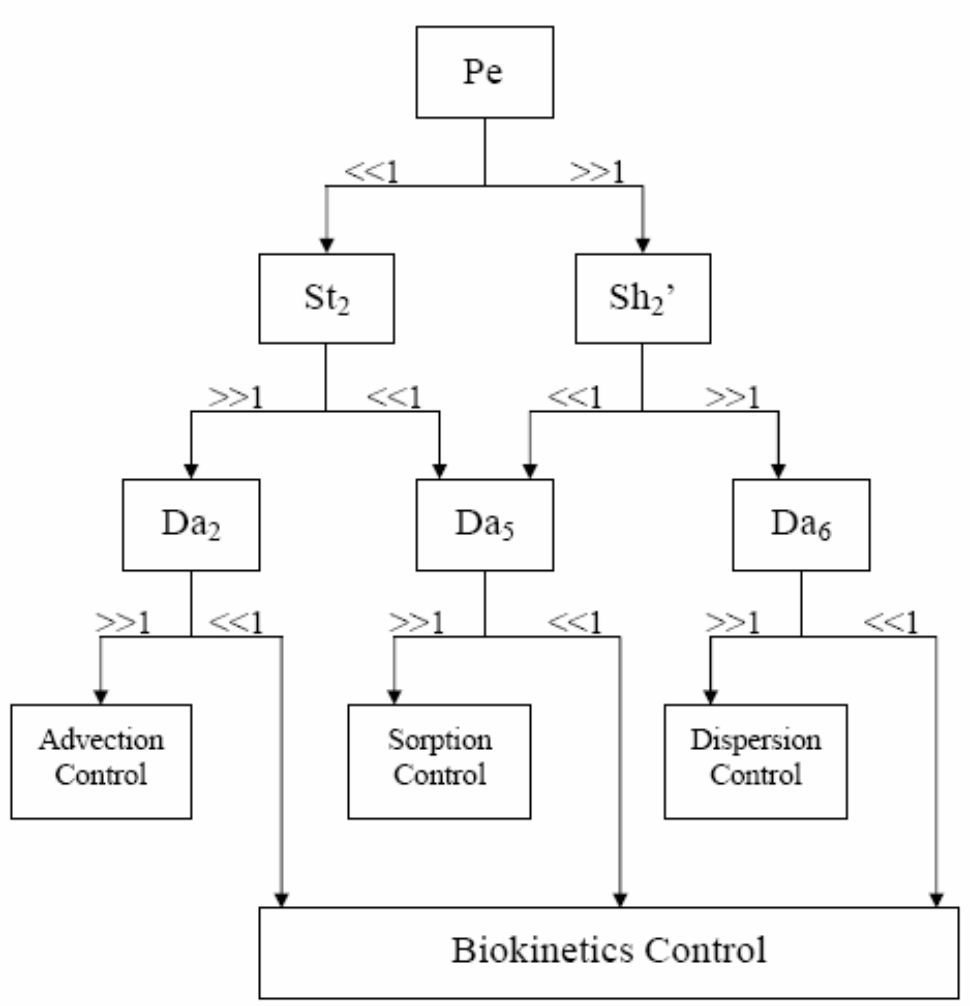

Figure 4.3. Quantitative framework development. (adapted from Ramaswami and Luthy, 1997; Weiner et al., 1999)

5.0 MATERIALS AND METHODS

To apply the quantitative framework proposed in Chapter 4, it is necessary to independently estimate the RRL-South site biokinetics as well as quantifying the physicochemical mass-transfer phenomena that control bioavailability and biotransformation rates at the site (Ramaswami and Luthy, 1997). This was done using a combination of laboratory and field protocols. The laboratory protocols were all performed using soil and groundwater samples taken from the vicinity of RRL-South. Therefore, the first protocols presented in this chapter are those for collecting soil and groundwater samples from the field site, which was discussed in Chapter 1. Second, the methods used for measuring the micro-scale biotransformation rates for chloroethenes are described. Third, the tests are presented that were used to independently measure meso-scale mass-transfer limitations, including equilibrium partitioning and mass-transfer rates. The presence of a dense NAPL source in the vicinity of the test site is unlikely, as described in Chapter 1, Section 1.2.4. Therefore, the evaluation of the meso-scale phenomena was focused on assessment of sorption and volatilization. Fourth, the protocols used for evaluating the macro-scale advective and dispersive transport parameters at the site are described. Specifically, the methods for assessing the site soil densities, porosity, hydraulic conductivity, and dispersion coefficients are outlined. Finally, the analytical methods used during these laboratory and field protocols are presented.

5.1 Field Sample Collection Protocols

5.1.1 Soil Sample Collection

Soil samples used for experiments in this research were obtained from borings in the vicinity of RRL-South. In the following paragraphs, the two different protocols that were employed for the collection of soil samples that were employed are described. The first protocol details the collection of Quantico Slate core samples, and the second describes the collection of soil cuttings, also from the Quantico Slate.

Using a CME 55 ATV drill rig equipped with an 8 inch hollow stem auger, two 1.5 in diameter core samples were aseptically collected from the bottom of bore holes TMW-31 and TMW-26S (~35 fbg) on August 7th, 2003, and September 23rd, 2003, respectively. The collection of these cores was conducted prior to monitoring well installation. The minimize contamination by exogenous microbes, the cores were collected in a plastic liner inserted into a 1.5 inch inner diameter California split spoon sampler, both of which were pre-washed, rinsed with deionized water, and sprayed with a 70% ethanol solution before each use. After preparation, the sampler was lowered to the bottom of each borehole using 15 ft flights of 2" diameter steel rod. Then, using a 150 lb hammer attached to the rig, the sampler was driven into the Quantico Slate to a depth of approximately 18 inches. The sampler was subsequently pulled to the surface where the plastic sleeve was removed from the split spoon. The loose material inside the sleeve was assumed to be drill cuttings from the bottom of the well, and was cut away from the intact sample. The remaining plastic sleeve and sample was then capped at both ends with sterilized plastic and Teflon caps which were subsequently sealed with electrical tape. These protocols were followed in an

attempt to preserve the *in situ* conditions (i.e., anaerobic) within the core. The samples were then placed in additional sterilized plastic bags and stored in a refrigerator at 4°C. These samples were later used in the laboratory measurement of the dispersion coefficient and bulk density, and in the biokinetics studies, as described below.

Cuttings produced during the advancement of the hollow stem auger were collected concurrently with core samples from boreholes TMW-31 and TMW-26S. All the cuttings were collected from depths ranging from 25 to 35 fbg. The cuttings were collected in sterilized baggies using sterilized scoops, and were stored at 4°C. These samples were used in the particle density determination and in the sorption parameter measurements.

As described previously, the Quantico formation is better classified as a slate in the location of RRL-South. This slate is a graphitic dark gray to black, thinly foliated, and extremely friable. In a previous naphthalene sorption study, performed by James Stagge as part of an undergraduate honors thesis at the University of Maryland, soil characteristics of RRL-south aquifer material were determined. These characteristics, provided by Agri Analysis, Inc. (Leola, Pennsylvania), were as follows: cation exchange capacity (CEC) = 8.6, percent organic matter = 1.7, and soil pH = 4.0.

5.1.2 Groundwater Sample Collection

Approximately 10 L of RRL-South site groundwater was collected from monitoring well TMW-31 on March 12, 2005. Groundwater samples were collected using a peristaltic pump (Cole Parmer, Model 7518-00) and ¼" diameter Teflon

tubing, except for the short section of tubing in the pump head, which was Masterflex tubing. The groundwater was pumped into a 20 L clear glass jar wrapped in aluminum foil, and stored in a constant temperature controlled room at 14ºC. This groundwater, upon exposure to the atmosphere, was found to have an orange tint possibly caused by iron oxidation and precipitation. To remove this iron residue, all groundwater samples were first filtered with a glass fiber filter prior to use in any experiment.

5.2 Laboratory Experimental Systems

Some components were common to many of the laboratory experimental systems used. Specifically, the same batch reactor systems and mode contaminants were used in most of the laboratory experiments and are described here before discussing the specific protocols in the following sections.

5.2.1 Batch Reactor

All of the laboratory experiments, with the exception of the laboratory tracer study, were performed using clear glass serum bottles (Fisher Scientific, Inc.), with volumes of approximately 160 ml and 26 ml, as batch reactors. For all calibration curves, and Henry's constant and sorption equilibrium kinetics studies, the 26 ml nominal volume bottles were used. For all biokinetic studies, the 160 ml nominal volume serum bottles were utilized. Before use, each bottle was washed with Alconox, a low foaming detergent, and rinsed with deionized water. Additionally, all bottles were heated to 400°C for 15 minutes to volatilize any remaining chlorinated solvent residue. The serum bottles were later capped with grey butyl Teflon lined

septa and sealed with aluminum crimp caps, which were also washed with Alconox, rinsed with deionized water, and placed into a 105°C oven for one hour before use.

An average bottle volume was calculated for both sizes by weighing five dry bottles, fitted with loose septa and crimp caps, filling them with deionized water at room temperature, sealing, and finally, reweighing them. The volume of the bottles could then be obtained from the total volume of water (calculated from the density of water at 24°C). For 160 ml and 26 ml serum bottles the average volumes were found to be 159.88 ml and 26.2 ml, respectively. For simplicity, bottle volumes are referred to as 160 and 26 ml throughout the text, however, all calculations are based on these average volumes.

5.2.2 Model Contaminants

Two model chlorinated ethene contaminants were used in the laboratory evaluations, as discussed above: cDCE (97% pure, Sigma-Aldrich, St. Louis, MO) and PCE (97% pure, Sigma-Aldrich, St. Louis, MO). The co-solvent methanol was used to increase the solubility of cDCE and PCE for the preparation of all stock solutions used in the laboratory experiments. Gossett (1987) determined experimentally that the addition of a methanol spike to an aqueous solution has little impact on partitioning equilibrium concentrations as long as it is kept relatively small. Specifically, methanol additions of between 0.1 and 2% (v/v) to aqueous solutions showed little variation in headspace concentrations. Therefore, these guidelines were followed in the preparation of the cDCE and PCE methanol stock solutions used in this study.

Using gravimetric methods, two cDCE in methanol stock solutions were prepared using the 26 ml serum bottles. For the Henry's constant estimates (See Section 5.4.2), a cDCE methanol stock solution was prepared with a concentration of 0.432 g/L. A second methanol stock solution, which was used for all other tests, was prepared with a concentration of 0.718 g/L. The bottles were sealed with a Teflon coated rubber septa, wrapped in aluminum foil and stored at 4°C to reduce volatilization into headspace. The PCE in methanol stock solution used in the biokinetics study was previously prepared by Ms. Emily Devillier, an M.S. degree student at the University of Maryland, College Park. The PCE in methanol stock solution was reported as having a concentration of 0.6768 g/L, and had been stored in a freezer prior to use in the laboratory experiments for this study.

5.3 Protocols for Measuring Micro-scale Phenomena

5.3.1 Rate and Extent of Chloroethene Biotransformation

The evaluation of micro-scale phenomena was focused on measuring the kinetics and extent of chloroethene biotransformation in batch microcosm studies. To obtain biokinetic parameters reflective of the RRL-South field site, aseptically-obtained core samples were used as the innoculum source. In addition, to minimize heterogeneity effects, the soil sample size was maximized by use of 160 ml serum bottles. In addition to the studies reported here, during the initial site investigation, Regenesis (2003) conducted a plate count and bench scale test, as described in Chapter 1, Section 1.3.2.1., and determined that the site soil contained a large number of indigenous microbes capable of degrading TCE. The Regenesis bench-scale results are provided in Appendix C.

5.3.2 Soil Samples (Innoculum)

The innoculum used for the batch microcosm study was taken from the core sample collected at well boring TMW-31, as described in Section 5.1.1. Because of the aseptic methods used for the collection of the core samples, it was assumed that soil from the cores was less likely to be contaminated by non native microbes compared to the soil cuttings. Because only a 12 in. long x 1.5 in. diameter core was available for use as the innoculum, the mass of soil (dry weight) that could be used in each microcosm was limited. Therefore, it was decided to follow the methodology for slurry sample preparation described by Häggblom et al. (1993), and use a 10% (v/v) soil to liquid ratio. To facilitate setting up the microcosms, the moisture content was determined following procedures described in Section 5.4.1, and was approximately 10.5%.

5.3.3 Microcosm Preparation

A total of 28 batch microcosms were prepared for the biokinetics estimation, comprising four different environmental systems. These systems consisted of anaerobically-prepared and aerobically-prepared bottles, a sterilized control, and an uninnoculated control (i.e., no soil added). Within these systems, a total of seven different treatments were prepared. In each treatment, which are described further below, different substrate amendments were added that were expected to potentially stimulate cDCE metabolism. The total mass of substrate added to each bottle was determined by first calculating the total mass required to completely degrade the entire mass of cDCE within a single bottle. Based on these stoichiometric calculations an over abundance of substrate was then added to ensure substrate

concentrations were not a rate-limiting condition. Four replicate bottles were constructed for each of the seven treatments, with two bottles stored in a 14ºC temperature controlled room (bottles 1 and 2 for each treatment) and two stored in a 30ºC incubator (bottles 3 and 4 for each treatment).

Subsequently, all equipment was first autoclaved for 30 minutes, including the serum bottles, Teflon-lined caps, glass pipettes, and approximately 2000 L groundwater (split into two 1000 L bottles, one closed with a screw cap for the anaerobic experiment, and the other with a stir bar and closed with a gauze/cotton plug to be used for aerobic experiments). Before autoclaving, the serum bottles and all other equipment were covered and wrapped in aluminum foil. Prior to establishing anaerobic or aerobic conditions, soil from core TMW-31 was added to a sterilized bag, where large clasts were broken up under finger pressure. The finger-pulverized soil was then added to all bottles requiring innoculum through gravimetric methods. Given the previously calculated soil moisture, the mass of soil added to each bottle, except the uninnoculated controls, was approximately 12.91 grams, in order to obtain a dry mass of approximately 11.55 grams.

5.3.3.1 Anaerobic Microcosm Systems

Three different electron-donor substrate amendment treatments were performed using anaerobic microcosms: molasses, HRC®, and lactate. To prepare for the amendment additions, twelve bottles with soil added, were labeled MOL-1 through -4, HRC-1 through -4, and LAC-1 though -4, loosely covered with grey Teflon septa and aluminum crimp caps and placed in an anaerobic glove box, which was filled with nitrogen and CO_2 gas, for 72 hours. Also placed in the anaerobic

glove box at this time were a sample of food grade pure molasses (Grandma's® (manufactured by Mott's) supplied by Emma Shinn) and a 160 ml sample of HRC® that was taken in the field prior to injection. Both the molasses and HRC® sample were stored in a 160 ml glass serum bottle capped with a grey butyl Teflon lined septa and aluminum crimp cap, and were kept at 4ºC prior to use. Additionally, a loosely capped 1000 L bottle of autoclaved groundwater, 50 ml pipette, and 3 one ml sterilized syringes were also placed in the anaerobic chamber.

After 72 hours, 50 ml of groundwater was aseptically added to each sample. For all bottles labeled MOL-#, 1.2 ml of molasses was added to each bottle with a 1 ml syringe. This volume of molasses was added based on studies conducted by Wu et al. (1997) and DiStefano et al. (2001) in which similar substrate to soil mass ratios were used for the degradation of chlorinated ethenes. In addition, 1.38 ml of HRC® was added to each of the bottles marked HRC-#, with another sterilized 1 ml syringe. This volume was equivalent to that used by Regenesis in the initial bench scale microcosm tests, described previously. Then, while still inside the anaerobic glove box, all of the microcosm bottles were capped.

Following removal from the glove box, the four remaining unmodified capped anaerobic bottles were aseptically injected with 0.4 ml of sodium lactate taken from a stock solution previously prepared by Ms. Emily Devillier. This stock solution was injected using a sterilized 1 ml syringe (Cole Parmer, 0.45 µm pore size) and a sterilized syringe filter, giving a concentration of approximately 5 mM as lactate. The sodium lactate in deionized water stock solution, with a concentration of 56.1 g/L, as lactate, as previously prepared by Emily Devillier, and stored in a 160 ml glass serum

bottle, capped with a rubber septum and aluminum crimp cap, at room temperature. After spiking, the bottles were then labeled LAC-1 through LAC-4.

All previously prepared anaerobic microcosms were then spiked with approximately 70.4 µl of a cDCE in methanol stock solution, which contained cDCE at a concentration of 0.718 g/L. This volume of stock solution was introduced using a 10 µl glass Hamilton syringe to achieve an aqueous concentration of approximately 1.0 mg/L. Because the cDCE stock was added volumetrically, the initial concentration was determined by headspace analysis using a gas chromatograph (GC) with a flame ionization detector (FID) as described in Section 5.6.2.1. As noted above, for all three anaerobic treatments, bottles marked with -1, and -2 were incubated in a temperature controlled room at 14ºC, while samples marked -3 and -4 were placed in the 30 ºC incubator. Subsequently, the anaerobic microcosms were periodically monitored by headspace analysis for cDCE using a GC with an FID or electron capture detector (ECD), and for methane, ethene, and VC using a GC with an FID, as described in Sections 5.6.2.1 and 5.6.2.2.

5.3.3.2 Aerobic Microcosm Systems

Four different treatments were performed using the aerobic microcosms: (1) a cometabolic cDCE transformation (COM) stimulation, (2) aerobic oxidation of cDCE (DO) stimulation, (3) a sterilized (STER) control, and (4) an uninnoculated (UC) control. Prior to setting up the treatments the1000 L bottle of autoclaved groundwater that was fitted with a sterile gauze ball at the mouth, was placed on a magnetic stirrer and allowed to equilibrate with the atmosphere for 72 hours. At the end of this period, 50 ml of groundwater was aseptically added to each bottle labeled COM-1

through -4, DO-1 through -4, STER-1 though -4, and UC-1 through -4. All bottles were then sealed with grey butyl Teflon septa and an aluminum crimp cap.

To stimulate aerobic cometabolism of cDCE, methane was added to the headspace of the COM treatment bottles, using a Scotty bottle (Supelco, 99.0% pure). Replicating the 3% methane headspace concentration used by Lorah et al. (1997), 3.13 ml of the 99.0% methane was added to the bottles marked COM-# using a 1 ml Hamilton gas-tight syringe. The DO treatment bottles designed to evaluate aerobic oxidation of cDCE received no additional amendments other than the aerated groundwater, as did the uninnoculated (no soil) control (UC) treatment bottles. The sterile control bottles, marked STER-# were autoclaved for 1 hour on three consecutive days. All bottles were then spiked cDCE in methanol stock solution, using the same technique as described above for the anaerobic bottles, to achieve an aqueous concentration of approximately 1.0 mg/L. As described for the anaerobic aqueous concentrations, the final aerobic cDCE aqueous concentrations were determined using a GC. Additionally, the bottles were labeled in a manner identical to the anaerobic samples, with those marked -1, and -2 incubated at 14ºC, and those marked -3 and -4 incubated at 30 ºC. The incubated aerobic microcosm samples subsequently analyzed by headspace analysis for cDCE using a GC with an FID or ECD, and for methane (COM bottles only), ethene and vinyl chloride using the GC equipped with an FID, as described in Sections 5.6.2.1 and 5.6.2.2.

5.3.3.3 PCE Additions

Approximately one month after the start of the biokinetics study, PCE was added to the MOL, HRC, LAC, and STER treatment bottles. This was done because

no cDCE transformation had occurred and it was thought this might be due to a lack of cDCE degraders at the site. Thus, the PCE was added to monitor for cDCE accumulation. All bottles were spiked with approximately 73.8 µl of a 0.6768 g/L PCE in methanol stock solution, using a 1 ml sterile syringe and filter, to achieve a concentration of approximately 1.0 mg/L. Similar to the cDCE spiked microcosms, the final PCE aqueous concentration was determined by headspace analysis using a GC equipped with an ECD, as described in Section 5.6.2.2.

5.3.3.4 pH Adjustment

After the biokinetics study had been running approximately 1.5 months, the pH in the samples was analyzed and found to be in the range of 2.5 to 3.5. These levels were possibly too low to support microbial degradation of chloroethenes. Therefore, the pH of every bottle was adjusted to approximately 7.0 with a 1 N solution of sodium hydroxide. Using the sample bottle STER-1 as a test, the volume of 1 N sodium hydroxide required to adjust the 50 ml samples to pH 7 was found to be 4 ml. Accordingly, 4 ml of the 1N sodium hydroxide solution was added to each bottle. To check the effectiveness of the NaOH addition, approximately 0.2 ml was removed from each of the STER-4 and DO-4 bottles and tested with pH paper. Both samples were at approximately pH 7; therefore, it was assumed that all bottles had been adjusted to this pH. All volume changes due to the NaOH additions and pH checks (subtractions) were recorded and subsequent aqueous concentration calculations reflected the changes.

5.4 Protocols for Measuring Meso-scale Phenomena

A series of batch experiments were performed to quantify the key meso-scale mass-transport processes for the site. Specifically, studies were performed to estimate appropriate values for the Henry's constant and activity coefficient for cDCE with the site groundwater, as well as to estimate the linear sorption distribution coefficient (K_d) for cDCE and the Quantico slate.

5.4.1 Aquifer Material (Sorbent)

Soil samples to be used for these studies were taken from cuttings collected during monitoring well TMW-31 installation (see Section 5.1.1). Air dried samples were required for use in K_d studies, therefore, the soil cuttings were initially prepared by spreading the soil sample onto aluminum foil to a depth of no greater than ¼". The soil was then allowed to air dry for 7 days, or until the difference in the mass of a pre-weighed sample was less than 5% per 24 hour period. The moisture content of the air-dried soil was calculated through the following steps: (1) pre-weigh a dry porcelain sample dish, (2) place a small amount (approximately 5 g) of air dried sample into the dish, (3) reweigh dish and soil sample, (4) place dish in 105ºC for 1 hour, and (5) reweigh oven dried sample. The mass of the dish was then subtracted from the total sample mass (i.e., the oven dried soil sample) to obtain the total mass of oven dried soil. The percent mass of water was calculated using the following equation:

$$W\% = \frac{M_{AD} - M_{OD}}{M_{AD}} \times 100 \qquad (5.1)$$

where M_{OD} is the oven dried sample and M_{AD} is the initial air-dried sample mass. Using this method the moisture content of the air dried samples was found to be approximately 0.23%. This water content was determined to be negligible and, therefore, was not considered when calculating the total mass of water in each batch system.

5.4.2 EPICs Method For Henry's Constant and Activity Coefficient

When calculating aqueous concentrations based on headspace sample analysis, as done in this study, a value for the Henry's constant (H') is required, which relates equilibrium gas phase (C_g) and aqueous concentrations (C_w) in a closed system using the equation,

$$H' = C_g/C_w \qquad (5.2)$$

Initially, a dimensionless Henry's constant of 0.124 was used in this work based on a study conducted by Shimotori and Arnold (2003), who determined H' values for cDCE in water at a range of temperatures between 1.8 and 70°C. Henry's constants, however, vary widely due to sampling procedures, impurities within aqueous samples, and many other factors. Therefore, a new H' was calculated for this study using the cDCE methanol stock solution and RRL-South groundwater, described previously, and the equilibrium partitioning in closed systems (EPICs) method.

The EPICs method has been shown to be an effective technique for determining the Henry's constants of volatile organic compounds in water when the dimensionless Henry's constant is less than 3 (Garbarini and Lion, 1985). The method is based on the comparison of mass balances between two similar closed

systems. Garbarini and Lion (1985) provide the following equation for H' given two closed systems (bottles 1 and 2) containing the same total mass of organic compound, but different liquid and gas volumes:

$$H' = \frac{\left(C_{g1} / C_{g2}\right) \cdot V_{l1} - V_{l2}}{V_{g2} - \left(C_{g1} / C_{g2}\right) \cdot V_{g2}} \qquad (5.3)$$

where H' = dimensionless Henry's constant; C_{g1} and C_{g2} = headspace concentrations of bottles 1 and 2, respectively; V_{l1} and V_{l2} = volume of liquid within bottles 1 and 2, respectively; and V_{g1} and V_{g2} = volume of gas within bottles 1 and 2, respectively.

Garbarini and Lion (1985) also report that an adaptation of the EPICs method is useful in the determination of activity coefficients (γ). For the calculation of γ, a comparison of mass balances was again used similar to the calculation of H'. The activity coefficient relates the concentration of a compound in solution to its thermodynamic activity (Garbarini and Lion, 1985). The activity coefficient, by definition, is the measure of how a specific real system deviates from some ideal reference system. In this study the specific real system is a microcosm set up with groundwater, and the ideal reference system is a microcosm set up with deionized water. Therefore, assuming an equal volume of ideal and non-ideal liquids within bottles 1 and 2, with an equal mass of volatile solute (i.e., cDCE) added to each system, the following equation can be used to obtain γ (Garbarini and Lion, 1985):

$$\gamma = \frac{V_1 / H'}{\left(C_{g1} / C_2\right) \cdot \left(V_g + V_1 / H'\right) - V_g} \qquad (5.4)$$

where all terms have been described previously.

An advantage of the EPICs method for the determination of H', and K_d, as described in the following subsection, is that numerous samples can be paired together to increase the accuracy in estimation. For example, if 6 bottles are prepared, 3 with 40 ml and 3 with 80 ml liquid, then a total of 9 different sample pairs are available for comparison using the EPICs method for Henry's constant. Following this example, for this study six Henry's constant (labeled HC-1 thru HC-6) and two activity coefficient samples (AC-1 and AC-2) were prepared gravimetrically in 160 ml clear glass serum bottles as described by Garbarini and Lion (1985). Three of the Henry's constant serum bottles were half-filled with groundwater to an approximate volume of 40 ml, and the remaining three were filled with groundwater to approximately 80 ml. Both activity coefficient bottles were filled with approximately 80 ml water, but AC-1 contained deionized water, and AC-2 contained groundwater. Using the methanol stock solution containing cDCE at a concentration of 0.432 g/L, all six samples were spiked with approximately 85 µg of cDCE. All samples were kept in a 14°C incubator for 24 hours, at which time duplicate headspace analyses were conducted on each sample using a GC equipped with an ECD, as described in Section 5.6.2.2.

Six Henry's constant serum bottles were prepared, as described previously, and allowed to equilibrate with constant mixing on an end-over-end mixer in a 14ºC temperature controlled room. Using the sampling and analysis methods, as described in Section 5.6.2.2, the headspace cDCE concentrations were analyzed. Duplicate headspace samples were collected from each sample and an average peak area was

calculated. From the sample data as presented in Appendix E, Figure 1, a dimensionless Henry's constant (H'), was estimated using Eq. 5.3.

5.4.3 EPICS Method For Sorption Coefficient (K_d) Estimation

When H' and γ have been determined, the equilibrium serum-bottle head space gas concentrations can serve as a direct measure of equilibrium aqueous concentrations. Upon rearranging the equation for the Henry's constant (Eq. 5.2), the following equation can be used to determine the aqueous concentration within the serum bottles:

$$C_l = \frac{C_g}{H' \cdot \gamma} \tag{5.5}$$

where γ is described previously, and is inserted into Eq. 5.5 to adjust the aqueous concentrations to RRL-South groundwater conditions.

The EPICs method can be extended to the examination of sorption equilibrium (Garbarini and Lion, 1985). Garbarini and Lion (1985) provide the equations for the estimation of sorption percentage per total sorbent mass, given equal liquid (V_l) and gas volumes (V_g), and total compound mass (M_T), in two bottles, on that contains liquid only (Bottle 1) and one that contains liquid plus sorbent (Bottle 2). First, the total compound mass in each bottle is calculated as follows:

Bottle 1:
$$M_T = C_{g1} V_g + \frac{C_{g1}}{H' \cdot \gamma} V_l = C_{g1} \left(V_g + \frac{V_l}{H' \cdot \gamma} \right) \tag{5.6a}$$

Bottle 2:
$$M_T = C_{g2} \left(V_g + \frac{V_l}{H' \cdot \gamma} \right) + X \tag{5.6b}$$

where X = mass of contaminant sorbed. Thus, by setting Eq. 5.6a equal to Eq. 5.6b, Garbarini and Lion (1985) provide the following equations for percent contaminant sorbed:

$$X = \left(C_{g1} - C_{g2}\right)\left[V_g + \left(\frac{V_l}{H' \cdot \gamma}\right)\right] \tag{5.7}$$

Subsequently, by combining Eq. 5.6a with Eq. 5.7 then,

$$\%\ \text{sorbed} = \frac{X}{M_T} x100 = \frac{\left(C_{g1} - C_{g2}\right)}{C_{g1}} \times 100 \tag{5.8}$$

and,

$$\mathrm{X} = \frac{\%sorbed \cdot (M_T)}{100} \tag{5.9}$$

Garbarini and Lion (1985) also provide the necessary equations for determining the distribution coefficient (K_d) of the sorbed mass, assuming a linear sorption isotherm. Therefore, the EPICs method can be utilized for the calculation of K_d directly from headspace analysis by first writing Equations 5.5 and 5.6 in terms of aqueous concentrations:

$$M_T = C_{l1}(\gamma H' V_g + V_l) \tag{5.10}$$

and,

$$M_T = C_{l2}(\gamma H' V_g + V_l) + X \tag{5.11}$$

As discussed above, it is assumed in this approach that sorption onto the RRL-South aquifer material can be described by a linear isotherm. Therefore, the following equation is used:

$$q = {}^{X}\!/_{M} = K_d C_{eq} \tag{5.12}$$

where C_{eq} is the aqueous phase concentration in equilibrium with the sorbent, and *M* is equal to the mass of sorbent employed.

By equating the total mass of sorbate in bottles with and without sorbent (Eqs. 5.10 and 5.11), the following equation for equilibrium concentrations in both systems is obtained.

$$X = (C_T - C_{eq})(\gamma H' V_g + V_l) \qquad (5.13)$$

where; $C_T = C_{l1}$, and is equal to the equilibrium concentration in the aqueous phase of the system without sorbent, and; $C_{eq} = C_{l2}$, which is also equal to the equilibrium concentration in the aqueous phase of the system with sorbent (Garbarini and Lion, 1985). Finally, the value of K_d can be determined by inserting Eq. 5.12 into Eq. 5.13, yielding;

$$K_d = \frac{\left\{\left[\left(\frac{C_{g1}}{C_{g2}}\right)\left(\gamma \cdot H' \cdot V_{g1} + V_l\right)\right] - \left(\gamma \cdot H' \cdot V_{g2} + V_l\right)\right\}}{M} \qquad (5.14)$$

To use the EPICs method to obtain a value for K_d, equilibrium between the aqueous phase and sorbed phase concentrations must be achieved. Therefore, the time required for equilibrium must first be determined. This was accomplished in sorption kinetics experiments by setting up bottle pairs according to the EPICs method, as described above, where one sample contained soil and groundwater, and the other only groundwater. The sampling protocol was to sample the bottle pairs at predetermined time intervals until equilibrium was established. However prior to

applying the EPICs method the concentrations were normalized using the following equation (Garbarini and Lion, 1985),

$$C_{\text{g·normalized}} = C_{\text{g·obed}} \frac{\left(V_l + \gamma H' V_g\right)_{\text{obed}}}{\left(V_l + \gamma H' V_g\right)_{\text{standard}}} \qquad (5.15)$$

where the term 'obed' refers to the concentration of interest, and 'standard' refers to the bottle used as a comparison in each experiment, i.e., a sample containing only the model compound and groundwater. Normalizing the concentrations with Eq. 5.15 is important because the gaseous volumes varied between bottles due to unequal liquid and/or soil additions. The EPICs method is based on comparing the gas phase mass in each bottle, therefore, the concentrations must be normalized against a baseline concentration. Accordingly, the normalized concentrations were calculated by randomly selecting a standard bottle, and using the gaseous concentration for all normalizations.

Two separate sorption kinetic experiments were conducted following a procedure modeled after that of DeWulf et al. (1998). The first was begun on July 14th, 2005, and consisted of six pairs of samples, labeled: 4/B4, 16/B16, 24/B24, 48/B48, 72/B72, and 96/B96, with the sample ID indicating the approximate time (hrs) at which each pair was sampled following test initiation, and the B referring to the blank bottle with no soil added to the system. All bottles in this first sorption experiment were prepared gravimetrically by first weighing the dry serum bottle and recording the mass. Next, unscreened soil samples, weighing 5.2 g each, were randomly taken from the total mass of air-dried soil cuttings and were added to the sample bottles labeled with only the sample time. The combined serum bottle and

soil sample was then reweighed to obtain the actual mass of soil added to each bottle. Following the ASTM Standard D 5285-03 (ASTM, 2003), a volume of water was added to each bottle such that the mass to mass ratio, in this case approximately 1:2 (soil to water), allowed for the maximum sorption of cDCE onto RRL-South aquifer materials. Therefore, approximately 10.4 ml groundwater was added to each bottle. Finally, after sealing with Teflon coated butyl-rubber septa and aluminum crimps, each bottle was spiked with cDCE methanol stock solution (using a 10µl Hamilton syringe) so the initial aqueous concentration was approximately 1.0 mg/L. Subsequently, the first sorption kinetics study was initiated by placing the samples in a 14ºC temperature controlled room where the samples were continuously stirred with an end-over-end mixer. Headspace analyses were taken, in duplicate, at 4, 16, 24, 47.5, 93, and 136.75 hours (e.g., sample pair 4/B4 was sampled at 4 hrs, sample 24/B24 at 24 hrs, etc.), and analyzed for cDCE using the methods detailed in Section 5.6.2.2.

As discussed in Chapter 6, the data collected from the first kinetics estimate indicated that equilibrium occurred after approximately 50 hours, however, variability in the data made it difficult to clearly define the time to reach equilibrium. Therefore, a second kinetics study was conducted to clarify the time needed to reach equilibrium and to better describe the rate of sorption. One possible cause for the variation in concentrations over time in the first kinetics study may have been due to the non-uniform sediment particle sizes used for that test. Therefore, to ensure that more uniform soil particle sizes were used in the second sorption kinetics study, only air dried soil that passed a #80 sieve was used. Using this soil, seven bottle pairs, labeled

5/B5, 29/B29, 53/B53, 77/B77, 101/B101, 125/B125, and 149/B149, were set up by following the same procedures as in the first kinetics study. Subsequently, the bottles were placed in a 14ºC temperature controlled room in an end-over-end mixer. Headspace analyses were conducted, in duplicate, at 4.5, 28.5, 52, 72, 102, 124.5, and 1475 hrs, using the methods detailed in Section 5.6.2.2.

Once the time to equilibrium had been estimated, additional experiments were performed to define the equilibrium condition by using the EPICs method to estimate K_d. As described in the section regarding H' estimation via the EPICs approach, the greater the number of sample bottles, the greater the accuracy of estimation. Accordingly, 9 sample bottles, labeled KD-1 through KD-9 were prepared gravimetrically following the same procedures as described above. Sample bottles KD-1, -2, and -3 were prepared with air dried soil, while bottles KD-7, -8, and -9 were prepared without soil. To provide controls for possible biotic reductions in cDCE, sample bottles KD-4, -5, and -6 were also prepared with air dried soil, however, approximately 0.3 g of 40% formaldehyde solution was added to each of these three bottles. On August 3rd 2005, all bottles were sealed and placed in a 14ºC temperature controlled room on an end-over-end mixer.

Based on the sorption kinetics studies, the samples for the EPICs method were to be collected after approximately 72 hours, however, it was discovered that the cooler had malfunctioned and the samples were at approximately 40ºC. Therefore, all of the samples were subsequently removed and placed in a refrigerator at 4ºC to reduce biological activity until a suitable temperature controlled environment could be found. On August 17th, 2005, fourteen days after the experiment was first stopped,

the samples were placed in a temperature-controlled circulating water bath at 14ºC. The serum bottles were shaken by hand every day to increase the mass transfer of cDCE between the aqueous phase and the sorbent. On August 22nd, 2005, after sufficient time was allowed for the bottles to achieve equilibrium at 14ºC (approximately 72 hours) duplicate headspace analyses were conducted on all sample bottles using procedures described in Section 5.6.2.2.

5.5 Protocols for Measuring Macro-scale Phenomena

Much of the basic information required for describing the macro-scale parameters (e.g., porosity and hydraulic conductivity) was not previously collected at RRL-South. Therefore, to quantify the macro-scale transport phenomena numerous additional studies were required for this research. Specifically, soil bulk and particle densities were determined based on soil cores, described previously, and used to estimate formation porosity. In addition, field-scale hydraulic conductivities were measured at RRL-South using single well slug tests. These values were used only with the site hydraulic gradient and Darcy's law to estimate the average groundwater pore-water velocity. Finally, field and laboratory tracer studies were conducted to determine the dispersivity within the Quantico formation aquifer. These laboratory and field measurements, when analyzed jointly, aided in determining the site specific dispersion coefficient, while the field tracer measurements also were used to confirm the average pore-water velocity at the site.

5.5.1 Soil Density and Porosity

To obtain samples for determining the bulk density at the site, two sections, 1.9 and 1.5 inches in length, were cut from the 1.5 inch diameter plastic sleeve-encased core collected from TMW-31, which was described previously. These two soil sub-cores yielded volumes of 42.23 and 36.50 cm^3, respectively. The weights of two pre-dried porcelain dishes were recorded and subsequently filled with the soil from the two cores. The plastic sleeves were also placed in the dishes due to the retention of soil particles on the sleeve walls. The dish-soil-sleeve samples were then reweighed and placed into a 105°C oven until the weight stabilized between two consecutive readings taken approximately every half hour, after the first hour. When the readings stabilized, the dishes were then reweighed. Next, the sleeves were removed, washed of any sediment, and dried for 10 minutes in a 105°C oven. Finally, the sleeves were removed from the oven and their weights were recorded. The final dry weight of the sleeve and the initial tare weight of the dishes was then subtracted from the total dry weight to obtain the total dry soil mass. Bulk densities were then obtained by dividing the oven dried soil mass by the total volume of sample.

Particle densities were then determined using the remaining oven-dried soil samples. Following the method described by Klute (1982), approximately 500 ml of water was boiled and allowed to cool, thus driving off any air bubbles within the water sample. Next, 50 g of the oven dried soil was added to a dry, pre-weighed, 100 ml volumetric flask. The outside and neck of the flask were cleaned of any loose soil and the total weight was recorded. Then, the flask was filled approximately half full

with distilled water and allowed to gently boil for several minutes. While boiling, frequent gentle agitation was applied to the sample to prevent soil loss due to foaming. After cooling the contents of the flask, previously boiled water was added until the water level reached the calibration mark. The filled flask was subsequently reweighed, and the temperature was recorded. The contents (i.e., DI water and soil) of the flask were then removed and the flask was refilled with the previously boiled water to the calibration mark, weighed, and the temperature was recorded. The following equation could then be used to calculate ρ_s (Klute, 1982):

$$\rho_s = \frac{d_w(W_s - W_a)}{(W_s - W_a) - (W_{sw} - W_w)} \qquad (5.15)$$

where;

d_w = density of water in grams per cubic centimeter at temperature observed
W_s = weight of flask plus soil sample
W_a = weight of flask filled with air
W_{sw} = weight of flask filled with soil and water
W_w = weight of flask filled with water at temperature observed

Based on the soil bulk and particle densities, the soil porosity, η, could then be calculated using the following expression (EPA, 1998):

$$\eta = 1 - \frac{\rho_b}{\rho_s} \qquad (5.16)$$

5.5.2 Hydraulic Conductivity Estimation

A slug test estimates the hydraulic conductivity of a formation based on the groundwater head response to an introduced "slug". Ideally, slug tests are performed through a nearly instantaneous change in water level that is induced by adding or removing a weight, referred to as the slug. This slug must be capable of displacing a

measurable volume of water. For the slug tests performed at RRL-South, a slug was constructed using a 70 inch section of 1.5 inch inner-diameter PVC pipe, which was filled with sand for weight and capped by 1.5" PVC caps, one having an eye hook attached. All parts were fastened together using PVC cement. The dimensions of the slug were selected to produce a volume of displaced water that would be great enough as to obtain data representative of the formation in wells screened both above and below the groundwater interface. The slug tests in the pilot area (see Figure 5.1) were performed in wells TMW-S2, -S3, and 26-S.

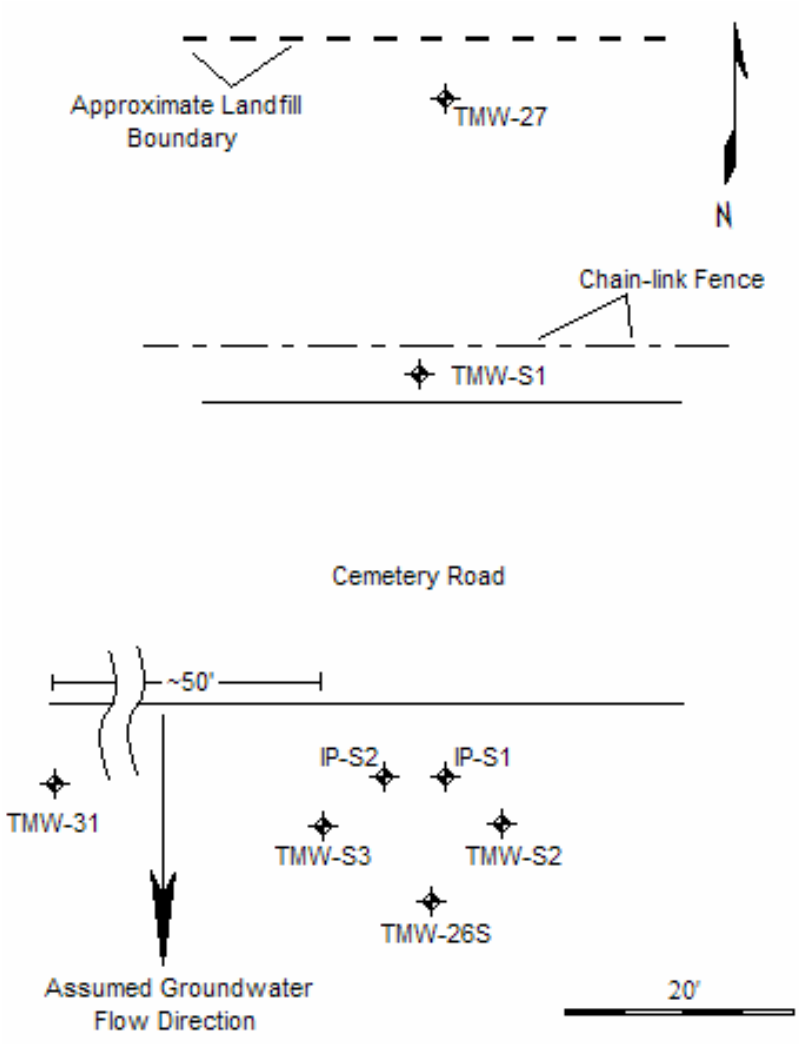

Figure 5.1. RRL-South site plan.

In *The Design, Performance, and Analysis of Slug Tests*, Butler (1997) describes performing similar slug tests that rarely displaced water elevations greater than 1 meter; therefore, the amount of displacement created during tests for this study was chosen to not exceed 1 meter. In addition, the Quantico slate formation was expected to have very low hydraulic conductivity. This assumption, based on previous well sampling activities, also implied that a low rate for rebound to local static water levels should be encountered. Therefore, based on slug tests designed by Butler (1997), coupled with the expected low conductivity and rebound rate, the amount of displacement was chosen to be approximately 3 feet, thereby allowing for reasonable testing times, while keeping the displacement levels close to those described in Butler (1997).

To measure the slow hydrostatic rebound at each well, ASTM D 404-91 (ASTM, 1991) recommends using a pressure transducer because a manual measuring device may not provide measurements of adequate frequency. Following this guideline, an 18.3 mm outer diameter miniTROLL transducer (In-Situ Inc., Ft. Collins, CO), capable of taking elevation measurements every second, was used during the slug tests. The transducer could be attached to a polyurethane quick-connect cable for communication between the
transducer and a personal digital assistant (PDA). The PDA was installed with Pocket-Situ software (Version 1), by In-Situ Inc., to download and view data. The PDA could then be docked with a PC installed with Win-Situ 4 (Version 4.53) , by Microsoft, where the data could be imported to, and viewed by, Excel (2000 version).

Prior to transducer introduction, the total water column depth in each well was

measured in order to establish the ideal depth at which to seat the instrument. An electronic water level indicator (Solinst, Model 101, Georgetown, Ontario), which measures to the nearest tenth-of-a-foot, was used to record baseline groundwater and the bottom-of-well elevations (see Table 5.1). Based on the difference between these two elevations, the height of water columns within wells TMW-S2, -S3, and -26S were 12.6, 14.9, and 14.2 feet, respectively.

Table 5.1. Groundwater and well characteristics on March 30 and 31, 2005.

Well ID	Depth to Bottom of Well (ft)[1]	Top of Screened Interval Depth (ft)[2]	Depth to Ground-water (ft)	Water Column (ft)	Transducer Depth (ft)	Well Inner Diam. (in)	Boring Diam. (in)
TMW-26S	34.0	31.5	21.4	12.6	32	2	8
TMW-S2	32.5	19.0	17.6	14.2	28	2	8
TMW-S3	33.0	19.0	18.8	14.9	28	2	8

Notes: 1) May not be true depth of well, but depth to a sediment well plug
2) Calculated by subtracting known screened interval from depth of well reported in Monitoring Well Completion Diagrams (Battelle, 2003), provided in Appendix B.

To avoid agitation of settled sediment within a well, which can affect instrument accuracy, In-Situ, Inc. recommends the transducer be set no lower than two feet above the bottom of each well. In addition, no less than 70 inches should be left between the groundwater surface and the top of the transducer to allow for the complete submersion of the slug. The transducer depths selected, which were based on these criteria, are summarized in Table 5.1.

The transducer was attached to the polyurethane cable before the start of each testing event, and was subsequently lowered to the chosen depth, and, finally, secured to the top of the monitoring well via a clip attached to the end of the cable. The

transducer was then programmed with the PDA to record water depths changes in groundwater elevations every three seconds.

To confirm the validity of conventional slug-test theory for the analysis of slug tests in unconfined aquifers, Butler (1997) recommends that at least three tests be conducted at any one well, and that two or more different values for the initial displacement (varying by at least a factor of two) be collected. Therefore, following this recommendation, two sets of slug tests were performed during this study, with different degrees of displacement. For the first data set, collected on March 30, 2005, at TMW-S2 & -S3, and April 13, 2005, at TMW-26S, the greatest volume of displacement was induced by lowering the entire slug below the surface of the groundwater. The second data set, collected on March 31, 2005, at TMW-S2, induced a volume of displacement equal to half the first set. This was done by lowering only half of the 70 inch slug below the groundwater surface. The same procedure was followed for each data set, regardless of the degree of displacement, as described in the following paragraphs.

Prior to lowering the slug into a well, an appropriate length of nylon twine for achieving the desired displacement was cut and tied to the end of the slug. The opposite end of the twine was fastened to the well and the slug was then lowered into the well, but not allowed to contact the water. Before introducing the slug into the groundwater, the transducer was turned on with the PDA to establish baseline water levels. Finally, the slug was quickly lowered into the well to achieve, as best as possible, near-instantaneous slug introduction. This introduction of the slug resulted in a rise in head, followed by a declining head, which was used for a falling head test.

As suggested by Wiedemier et al (1995), each slug addition that was used to perform a falling head test was followed by the removal of a slug, resulting in a rising head test as the groundwater levels recovered. For example, at the completion of a falling head test and prior to the start of a rising head test, the transducer was restarted and allowed to collect new baseline measurements for the next test. Subsequently, the slug was rapidly withdrawn from the groundwater and secured at a level within the well above the water table. Groundwater levels were then initially lower than the baseline followed by an increase in head. Upon completion of the rising head test the transducer was again stopped and reprogrammed for another falling head test. The sequence of falling and rising head tests were performed as frequently as time allowed. However, due to the slow groundwater response to slug introduction, only two rising and two falling head tests were conducted in TMW-S2 for both volumes of displacement. Similarly, only one falling and one rising head test could be conducted in wells TMW-S2 and -26S. The average time allowed for both falling and rising head tests in all wells was 83.7 minutes, with the shortest test interval, collected in TMW-S3, equal to 21.15 minutes.

The protocols for determining K within the RRL-South aquifer in this study were based on the procedures described in *The Design and Analysis of Slug Tests* (Butler, 1997). The procedures provided by Butler (1997) vary based on the aquifer type and well configuration. For example, a well screened the entire width of a confined aquifer requires a specific set of calculations, as described by Butler (1997), for the determination of K. Alternately, the RRL-South aquifer is considered to be unconfined, requiring procedures suited to these conditions, also described in Bulter

(1997). Included in the calculations for unconfined aquifers are two sub-methodologies required for different well configurations within unconfined aquifers, as defined further by Butler (1997). For example, when the screened interval is below the groundwater surface the Bouwer and Rice method can be used. For wells screened across the water table a modification to the Bouwer and Rice method, described in the following paragraphs, can be used.

Assuming that the soil boring logs are accurate (see Appendix B), the data listed in Table 5.1 indicates that all wells at RRL-South were screened below the water table when the slug tests were conducted. However, Butler (1997) suggests that if the top of the screened interval is close to the groundwater surface, then the wells should be defined as being screened across the water table. The exact depth for wells screened close to the groundwater surface was not defined, however, Butler (1997) only used the method for wells screened below the water table if the top of the screened interval was well below the water table (i.e., >100 ft). Therefore, when calculating K in this study, it will be assumed that all wells, including TMW-26S, which is screened approximately 10 ft below the water table, will be defined as being screened across the water table. The only major difference in the two methods is the determination of r_c, discussed below. For TMW-26S both methods were followed to determine K. The results of this comparison indicated that the difference in K values ranged between 46 to 51%, with higher conductivity values calculated using the modified Bouwer and Rice method. However, based on the suggestions set forth by Butler (1997), the modified Bouwer and Rice method was used to calculate K for each well. As discussed further in Chapter 6, this method also more accurately

describes the groundwater velocity determined in the field tracer study.

For wells screened across water table, Butler (1997) suggests using The Bouwer and Rice Method for determining K. Although this method is best for interpreting data for wells screened below the water table, it can also be effective for interpretation of data for wells screened across or near the water table (Butler, 1997). As described by Butler (1997) and Hyder et al (1994), Bouwer and Rice (1976) initially developed a method to interpret groundwater response data based on a partial differential equation that describes the steady-state flow in response to an instantaneous change in the water level (due to a slug introduction or withdrawal) at a central well screened in a porous formation (Bouwer and Rice, 1976):

$$\frac{\partial^2 h}{\partial r^2} + \frac{1}{r}\frac{\partial}{\partial r} + \frac{K_z}{K_r}\frac{\partial^2 h}{\partial z^2} = 0 \qquad (5.17a)$$

where: h = deviation of hydraulic head in the formation from static conditions
r = radial direction
K_r = radial component of hydraulic conductivity
K_z = vertical component of hydraulic conductivity
z = vertical direction

With the initial conditions written as:

$$H(t = 0) = H_0 \qquad (5.17b)$$

$$h(r,z=0,t) = 0,\ r_w < r < R_e,\ t > 0 \qquad (5.17c)$$

Subject to the following boundary conditions:

$$\frac{\partial h(r,B,t)}{\partial z} = 0,\ r_w < r < R_e,\ t > 0 \qquad (5.17d)$$

$$h(r = R_e,z,t) = 0,\ 0 \le z \le b,\ t > 0 \qquad (5.17e)$$

$$h(r = r_w,z,t) = H(t),\ d \le z \le (d + b),\ t > 0 \qquad (5.17f)$$

$$2\pi r_w K_r \int_d^{d+b} \frac{\partial h(r = r_w, z, t)}{\partial r} dz = \pi r_c^2 \frac{dH(t)}{dt}, \; t > 0 \qquad (5.17g)$$

$$\frac{\partial h(r_w, z, t)}{\partial r} = 0, \; 0 \le z < d, \; d + b < z \le b, \; t > 0 \qquad (5.17h)$$

where: H(t) = deviation of head in well from static conditions
H_0 = magnitude of initial displacement
r_w = effective radius of the boring (0.33 ft)
R_e = effective radius of the slug test
B = formation thickness
t = time
b = screen length
d = z position of end of screen closest to water table
r_c = effective radius of well casing (1 inch)

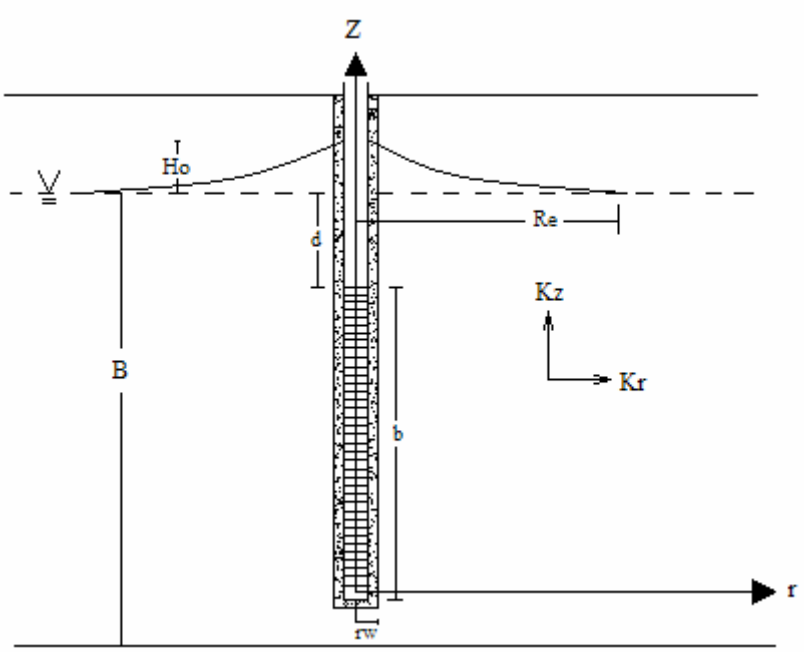

Figure 5.2. Diagram of well characteristics for partially penetrating well screened below the water table.

As described by Zlotnik (1994), Hvorslev (1951) developed data analysis methods primarily in confined aquifers. To describe flow in unconfined aquifers Bouwer and Rice (1976) made several simplifying assumptions to the mathematical

description of flow to a well (Hyder and Butler, 1995). These assumptions neglect; (1) specific storage of a formation; (2) changes to the global position of the water table during a slug test; (3) the possibility of flow above the water table; (4) well skin (created during well installation); and most importantly, (2) anisotropy (Hyder and Butler, 1995).

In an assessment of The Bouwer and Rice method by Hyder and Bulter (1995), the authors noted that many natural systems are characterized by an anisotropy in hydraulic conductivity ($K_z > K_r$). They also noted that if anisotropy, as well as other formation characteristics, such as large storage parameters (defined as $\alpha\left(\frac{2r_w^2 S_s b}{r_c^2}\right)$, where S_s is the specific storage) and high aspect ratios (b/r_w) are present within the formation, an error in the estimate of K_r can arise. Zlotnik (1994) recommends that when using the Bouwer and Rice method, a modification to r_w be applied to account for anisotropy due to unknown storage parameters and poorly defined aspect ratios, where:

$$r_w^* = r_w\left(K_z / K_r\right)^{1/2} \qquad (5.18)$$

where the term $(K_z/K_r)^{1/2}$ is the anisotropy ratio. As mentioned previously, it is assumed that the formation is isotropic and, as a result, during the calculation of the effective well radius (r_w*), the radial conductivity (K_r) is equal to 1. A value of 1, though, may not be representative of the RRL-South Quantico formation conditions. This is because the formation consists of vertically dipping, finely bedded, shales which may yield greater values of K in the x-direction (longitudinal) compared to the y-direction (transverse). Therefore, the vertical conductivity (K_z) is most likely

greater than the radial conductivity. This being said, Butler (1997) recommends that without the benefit of additional data the conductivity ratio, for simplicity, should equal 1. Using the value of 1 for the anisotropy ratio the term r_w* is therefore equal to r_w.

Even if K_r is not equal to 1, except in the case of interbedded high- and low-conductivity material, the anisotropy ratio $((K_z/K_r)^{1/2})$ for natural systems should usually lie between 0.3 and 1.0 (Freeze and Cherry, 1979, Butler, 1997). Given this range, errors in the K_r estimate introduced through uncertainty about anisotropy should not exceed 20% (Butler, 1997). Further error estimates are provided by Hyder and Butler (1995), who advise caution when analyzing data from a formation with high degrees of anisotropy with the Bouwer and Rice method as significant changes in the anisotropy ratio can impact Kr estimates by as much as 50%.

An analytical solution of Eq. 5.17a, defined by Eqs. 5.17b to 5.17h, while considering anisotropic flow due to unknown storage parameters and poorly defined aspect ratios (i.e., Eq. 5.18), can be written as (Bouwer and Rice, 1976, Zlotnik, 1994, Bulter, 1997):

$$\ln\left(\frac{H(t)}{H_0}\right) = -\frac{2K_r bt}{r_c^2 \ln\left(R_e / r_w^*\right)} \qquad (5.19)$$

Additionally, because the wells are screened across the water table, Butler (1997) recommends that the effective casing radius be modified in order to account for the displaced water entering the filter pack, thus skewing the value for initial height of water displacement (H_0). Accordingly, the term for effective casing radius, r_c, is further defined as:

$$r_c = r_{nc}\sqrt{\frac{H_0^*}{H_0^+}} \qquad (5.20)$$

where: H_0*= expected value for the initial displacement determined from volumetric considerations.
H_0^+= apparent value for the initial displacement determined for the y- intercept of the best-fit straight line
r_{nc} = nominal radius of the well screen.

When the slug test response data is collected and subsequently plotted on a graph of normalized head response versus time, as discussed in Section 6.4.1.2, a trend line is fitted to the data. After fitting the trend line to the best representative data (see Section 6.4.1.2), determined visually or quantitatively (Butler, 1997), the slope of the trend line (equal to $-1/T_0$) is used in the following expression, which is derived from rearranging Eq. 5.19 for estimation of K_r (Butler, 1997):

$$K_r = \frac{r_c^2 \ln\left(R_e / r_w^*\right)}{2bT_0} \qquad (5.21)$$

The R_e term in Eq. 5.21 is not the actual effective radius of the slug test, but is an empirical parameter (Butler, 1997). As described in Butler (1997), Bouwer and Rice (1976) present empirical expressions for the estimation of R_e based on a series of electrical-analog simulations of the mathematical model defined by Eqs. 5.17a to 5.17h. For simplification Butler (1997) presents the following equation for R_e, which is written in terms of $\ln(R_e/r_w^*)$:

$$\ln\left(R_e / r_w^*\right) = \left[\frac{1.1}{\ln\left((d+b)/r_w^*\right)} + \frac{A + B\left(\ln\left[\left(B^o - (d+b)\right)/r_w^*\right]\right)}{b/r_w^*}\right]^{-1} \qquad (5.22)$$

where: A,B = dimensionless coefficients
B^o = formation thickness

Bouwer and Rice note that when the $\ln[(B^o-(d + b))/r_w^*]$ term in Eq. 5.22 is greater than 6.0, 6.0 should be used instead of the actual value (Butler, 1997). For all wells tested at RRL-South, the formation thickness, while not clearly defined, is assumed large enough to make this expression greater than 6.0. Accordingly, a value of 6.0 is used for all calculations of $\ln(R_e/r_w^*)$.

Van Rooy (1988) fit polynomial equations to a series of curves created by Bouwer and Rice (1976), which were plots of various aspect ratios versus the dimensionless coefficients presented in Eq. 5.22. Butler (1997) presents these equations for the dimensionless coefficients A and B determined by Van Rooy (1988):

$$\mathbf{A} = 1.4720 + 3.537\times10^{-2}(b/r_w^*) - 8.148\times10^{-5}(b/r_w^*)^2 + 1.028\times10^{-7}(b/r_w^*)^3 - 6.484\times10^{-11}(b/r_w^*)^4 + 1.573\times10^{-14}(b/r_w^*)^5$$

$$\mathbf{B} = 0.2372 + 5.151\times10^{-3}(b/r_w^*) - 2.682\times10^{-6}(b/r_w^*)^2 - 3.491\times10^{-10}(b/r_w^*)^3 + 4.738\times10^{-13}(b/r_w^*)^4$$

5.5.3 Dispersion Coefficient Estimation

5.5.3.1 Laboratory Estimates

A soil column was constructed in the laboratory for estimates of one dimensional dispersion coefficients in the Quantico slate by using a plastic sleeve encased soil core, which was collected from the bottom of boring TMW-26S, as discussed previously. The Quantico slate foliation, as described in Section 5.1.1, is near vertical in the area of RRL-South; therefore, when the soil core was taken the vertical foliation was preserved within the core. This foliation was observed in the core when the sub-cores were created by cutting off the ends of the main core sample,

as discussed in Section 5.5.1. Because flow through the core would be parallel to the observed lamination, these laboratory tracer tests were assumed to be as representative of field conditions as possible.

The core was prepared for the column construction by first trimming away the excess soil from either end, which was believed to be loose soil caused by borehole cuttings or rough handling. Next, a gap of approximately 1/8" was created between the rim of the plastic liner and the end of the soil by gently brushing away loose soil. Both ends were then thoroughly cleaned with deionized water to remove any loose debris. When all loose soil was removed, the length of the soil column measured at 12 inches. Finally, the gaps were filled with loosely packed Pyrex filter fiber wool, capped with 1.5" PVC end caps, and all fittings were attached and sealed with aquarium silicone sealant.

Prior to their attachment, the PVC end caps were prepared by drilling a ¼" hole into the end of each cap, which was fitted with Teflon connectors that allowed for 1/8" Teflon tubing to be attached. Again, all fittings were connected and sealed with aquarium silicone sealant. The outlet cap tubing was connected to a ¼" outer diameter (OD) section of Masterflex silicone tubing, with a tubing clamp at the outlet for stopping flow. The effluent water was collected in a 1 L glass graduated cylinder. The inlet cap tubing was connected with a reducer fitting to 1/16" Masterflex silicone tubing and sealed with parafilm at the connection. The 1/16" inlet tubing was passed through a Cole Parmer pump head, connected to a Cole Parmer peristaltic pump (Model # 7518-00), which was operated with a Masterflex solid state speed control. The free end of the inlet tubing was inserted into a 1 L glass bottle filled with influent

solution. See Figure 5.3 for a photograph of the bench-scale tracer column setup. Once assembled, the silicone caulking was allowed to dry for no less than 48 hours before initiating the tracer studies.

After column assembly and before the tracer tests were begun, trapped air was removed from the core by purging the sealed column with deaerated deionized water. This was accomplished by first boiling 1 L of deionized water for approximately 10 minutes, and subsequently allowing the container to cool to room temperature. Next, approximately three pore volumes (230 ml) of the deaerated water was pumped though the column, which was then allowed to sit undisturbed for approximately 54 hours

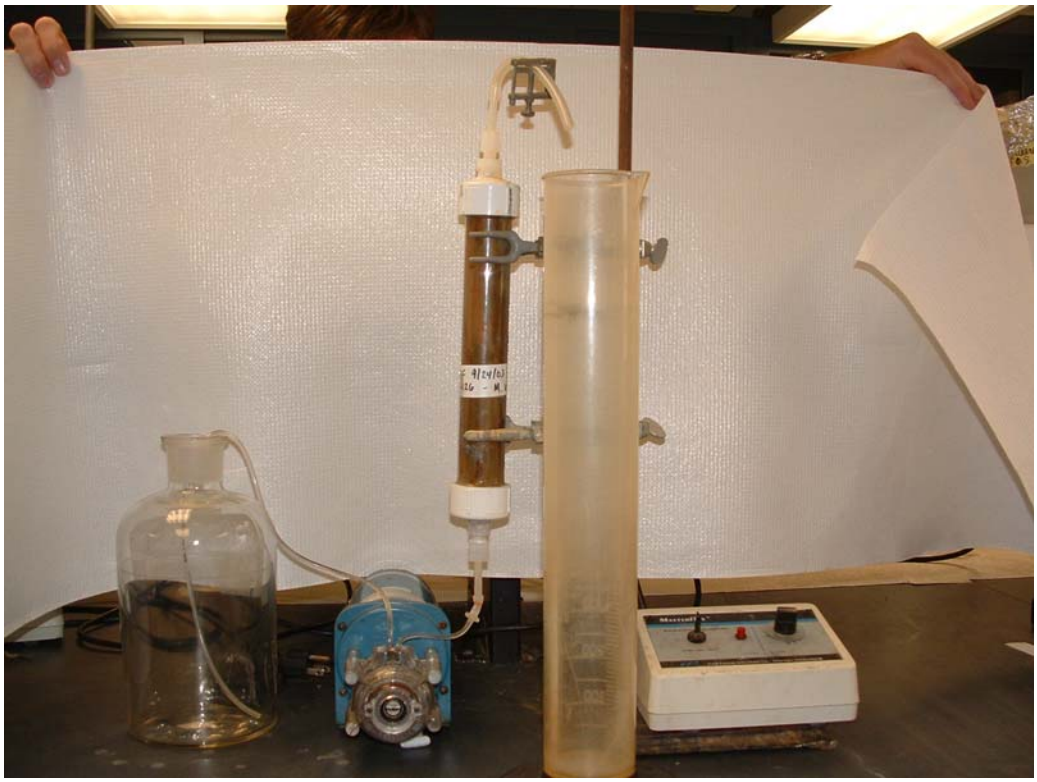

Figure 5.3. Bench scale tracer column setup. From left to right: bromide stock solution, Cole Parmer peristaltic pump, 12" soil column, effluent collection, Masterflex flow meter.

so that all trapped air would have a chance to dissolve back into the porewater. After the deaeration of the column was completed, four step-input, one dimensional tracer breakthrough curve experiments were performed. To establish the ideal sampling and flow rate conditions a trial test was first conducted.

Before beginning the first trial tracer test, the flow rate was determined by pumping deionized water through the system and measuring the time required to collect a defined volume of water in a 25 ml graduated cylinder, marked in 0.2 ml increments. This information was used to obtain a flow rate (Q), and calculate the seepage velocity $\left(V = \left[Q/\left(A \cdot n\right)\right]\right)$, which was found to be 16.13 m/d (52.92 ft/d) (see Table 5.2). The 1/16" inlet tubing was then inserted into a 1 L bromide stock solution with a concentration of 497.7 mg/L made using NaBr (99%+, Sigma-Aldrich, St. Louis, MO). At the start of each test (t = 0) a sample was collected from the feed bottle to establish a Br^- baseline level. The pump was then turned on, and the test begun when it was believed the influent feed solution had entered the column (approximately 15 seconds were required for the solution to travel through inlet tubing and glass wool filter). Subsequently, samples were taken approximately every seven minutes, during which time 12.5 ml samples were collected and then diluted to 25 ml for analysis. The bromide analysis was performed as described in Section 5.6.1 using the Orion electrode; however, as discussed further in Section 5.6.1, due to the reduced size of the samples, the volume of an ionic strength adjuster (ISA) was adjusted accordingly to achieve the ratio of 1 ml ISA:100 ml sample.

Table 5.3. Column flow characteristics.

Test	*Q (L/min)*	*V (m/d)*
Trial	0.0028	16.13
1	0.0016	9.23
2	0.0013	7.49
3	0.0014	8.06

Upon the completion of each tracer test the column was flushed with approximately 500 ml of deionized water. Background Br- levels were checked at the completion of the flushing, and if levels of Br^- were above 3.0 mg/L, the purging process was repeated until aqueous concentrations were below this level.

The trial laboratory tracer test resulted in an irregular breakthrough curve (see Figure 6.17) due to infrequent sampling times and possibly from too great of a bromide stock solution flow rate. Therefore, the procedures for the first test were identical to the trial test, with a few changes. One, the concentration used for Test 1 was decreased to 48.1 ppm. Two, the flow rate was reduced to 0.0016 L/min. Finally, the frequency of sample collection was increased and samples volumes were reduced to 5 ml and diluted to 25 ml. This was done to reduce possible dilution effects caused by the larger samples.

Test 2 was performed following the same protocol as for Test 1, except that the Br- analysis was performed using a Cole Parmer electrode (see Section 5.6.1). However, before test three was begun a small leak developed in the seal between the Teflon connector and the influent end cap. Additionally, a small gap formed in the soil column apparently as a result of a fracture that formed perpendicular to the plastic casing due to sampling activities. The gap was approximately 1 inch from the inlet end of the column. To remove this gap the column length was reduced

approximately 1.5 inches and the inlet end was refitted with cleaned fittings. The column and caulking was then allowed to dry for 48 hours. The resulting new column length was 10.5 inches. To minimize air from being reintroduced into the column during these procedures, all gaps and both influent and effluent tubing were filled with deionized water before reattachment.

Tracer test 3 was conducted in a manner identical to Test 2 as well, except that the 5 ml samples collected during the test were diluted two times, giving a final total volume of 10 ml per sample. The bromide analysis procedures were as described in Section 5.6.1; however, the ISA solution addition was adjusted to give a ratio of 2 ml ISA:100 ml sample.

5.5.3.1.1 Laboratory Tracer Data Analysis Protocols

For the interpretation of breakthrough curves, provided in Section 6.3.2, a Fortran program, written by Dr. Eric Seagren of the University of Maryland, was used to obtain dispersivity estimates for the RRL-South core section laboratory tracer study. This program, presented in detail in Appendix F, calculates the sum of the squares of either the absolute or relative residuals between the normalized experimental bromide tracer data and the normalized flux-averaged concentration calculated using the one-dimensional non-reactive solute transport model of Parker and van Genuchten (1984). For this data, the sum of the squares of the absolute residuals provided the most reliable results, as the relative residual results could not be calculated using the data from the experiment.

Additionally, this program calculates the best fit hydrodynamic dispersion coefficient (D_x) and average pore water velocity (which is used to calculate the best

fit porosity), if an initial estimate is provided for both. These best fit parameters are obtained using a modified Levenberg-Marquardt method to minimize the sums of the squares of the residuals between observed and calculated concentrations. Although the original program was written to describe conservative tracer dispersion through a packed bed column with a square cross section, the program is assumed to be applicable to the RRL-South round column. The initial conditions (required for the program) from the three laboratory tracer tests are provided in Table 5.4.

Table 5.4. Laboratory tracer study initial conditions.

Test	Length (cm)	Flow (Q) (L/min)	Cross Sectional Area (cm^2)	Pore Water Velocity (m/d)	D_x (m^2/d)	# of Data-points
1	30.48	0.0014	11.40	8.06	0.0048	18
2	26.67	0.0013	11.40	7.49	0.0052	17
3	26.67	0.0014	11.40	8.06	0.0048	19

The porosity of the Quantico slate, estimated in Section 6.3.1.1, was used to calculate the pore water velocity, estimated at the start of each tracer test. The dispersion coefficient estimates were arbitrarily chosen, however, after running the program with D_x estimates ranging from 0.002 to 100, the final best fit D_x varied by less than 0.5%. As a result, a value of approximately 2.00, an estimate close to that measured in Section 6.3.2.2, was used for all calculations.

5.5.3.2 Field Estimates

Two field-scale conservative tracer studies were conducted for field estimation of the dispersion coefficient. Unfortunately, ongoing remedial pilot activities at RRL-South, during the course of this study, necessitated the periodic

injection of HRC® and the subsequent monthly monitoring of all wells in the pilot area, all of which greatly constrained the time during which these studies could be performed. As a result, periods comprising a total of only 7 and 29 days in the duration were allowed for undisturbed tracer migration during tracer injection events 1 and 2, respectively. The two tracer injection events were conducted during the months of April and June, 2005. Specifically, the tracer, described in the following subsection, was injected into TMW-27 and IP-S2 on April 13th (Event 1), and only into IP-S2 on June 29th (Event 2). To perform these tracer studies it was necessary to select a conservative tracer and suitable concentrations, and to design the tracer study procedures.

5.5.3.2.1 Tracer Selection and Preparation

Bromide (Br^-) is commonly used as a groundwater tracer (in the form of sodium bromide salt, NaBr) because it has relatively low toxicity, usually exists at low concentrations in the environment, and is simple to measure, inexpensive, and assumed to be conservative (Davis et al, 1980; Korom, 2000). Prior to tracer test initiation at RRL-South, a bromide background check was conducted on groundwater collected from TMW-31, a well adjacent to the RRL-South pilot area (see Figure 5.1), in order to verify the absence of naturally occurring and/or introduced Br^-, and to support the use of the bromide salt rather than other tracers such as Cl^- or I. Natural Br^- background concentrations, measured in TMW-31, were approximately 1.0 mg/L. This low concentration suggested that Br^- was not present in the groundwater naturally or from other sources, and that sodium bromide would be an effective tracer for this study.

Once Br^- had been selected as the conservative tracer for the field tracer study, the next step was to select the concentration to inject. Selection of an appropriate Br^- concentration is important because if the initial tracer concentration is too high, there is the possibility that the tracer plume will sink in the formation. Furthermore, if the initial concentration is too low, there is a chance that the tracer concentrations at the sampling locations will be too dilute for accurate measurement. The exact concentration at which density effects are observed is unclear due to variations in site conditions and injection procedures. Due to these uncertainties, the concentrations used for field tracer studies in the literature were used as a guide for this study. However, Br^- concentrations described in the literature varied widely. For example, reported concentrations ranged from 100 mg/L, used by Smith et al (1996) in a sand and gravel aquifer at a site located in Cape Cod, to approximately 1000 mg/L, used by Smith et al (1991), at the same site. Additionally, in a study by LeBlanc et al. (1991), also at the Cape Cod site, used a tracer with the concentration of 640 mg/L. The concentration of 640 mg/L showed only slight density effects after a distance of roughly 300 meters. Taking these effects into account, it was assumed that Br^- density effects at a concentration of 640 mg/L would not be significant because the distances between injection and monitoring wells at RRL-South are no more than 30 feet. Although the dispersion of bromide within the Quantico slate is unknown, concentrations used at RRL were chosen to be in the range between 400 and 640 mg/L to ensure measurable concentrations down gradient of injection wells.

To achieve the desired Br^- concentration in the water column within the injection wells, it was decided to add relatively small volumes of high concentration

stock solutions that would then be mixed with the water column *in situ* to achieve the desired concentration range. For all tracer tests the stock solutions were prepared in the lab prior to field activities, using the sodium bromide (99+%, Sigma-Aldrich), as described in Section 5.5.3.1. For Event 1, a 100mL stock solution with a concentration of 0.134 mg/L as Br^- was prepared with deionized water, and stored in a small Nalgene® bottle. For Event 2, a 100mL stock solution with a concentration of 0.1 mg/L as Br^- was prepared and stored in a similar manner.

5.5.3.2.2 Tracer Field Procedures

The field tracer studies were performed using radially divergent tests, with wells IP-S2 and TMW-27 used for the tracer injection locations in order to maximize the number of down-gradient sampling wells (see Figure 5.1). IP-S2 was used as a tracer injection well for both Events 1 and 2, while TMW-27 was only used as an injection well, concurrently with IP-S2, during Event 1. Additionally, this configuration was selected because the groundwater was believed to flow due south, however, even if this assumed flow direction was not exactly right, the down gradient well configuration would still be able to capture the plume given the number of wells down gradient from each injection point.

The decision to perform two simultaneous injections during Event 1 arose from two issues. First, as mentioned previously, time constraints allowed for only seven days of undisturbed radial tracer flow during Event 1. Therefore, running two tests simultaneously allowed for the collection of the most data from RRL-South during the available time. Second, the injection of Br^- in IP-S2 would yield data at a local scale, while the concurrent injection of Br^- into TMW-27 would provide data for

a slightly lager scale. By increasing the size of the tracer test area it was also hoped that coupling the larger scale data with the smaller scale test would provide a more complete description of dispersion due to heterogeneities within the Quantico Slate. The larger scale test conducted in TMW-27, however, was unsuccessful as the tracer plume emanating from TMW-27 was never detected in TMW-S1, or the other down gradient monitoring wells during Event 1. Therefore, TMW-27 was not used as an injection well during Event 2, and the following sub-sections only discuss tracer injections within IP-S2.

In addition to selecting where to inject the tracer for the radially divergent tests, it was also necessary to decide how to inject the tracer, i.e., as a step- or pulse-input. As discussed in Chapter 6, the average hydraulic conductivity (K) value for Quantico slate within RRL-South aquifer were estimated in this study to be 0.04 m/day (0.131 ft/d). While consistent with values determined by others (Peterson, 1954; Young et al., 1964; Davis, 1969; Moran et al., 1976) for similar formations (i.e., slates), the corresponding groundwater flow rate was deemed to be too slow to use a step tracer injection method. For example, Harvey and Garabedian (1991) used the radial divergent method, with an injection of the tracers used (Br^-, bacteria, and Cl^-) that could be characterized as a pseudo-step input. All tracers were introduced at a rate equal to the groundwater flow, e.g., a 90 L sample with a Br^- concentration of 150 mg/L was introduced into the formation at a rate of 0.85 L/min, matching the natural flow of the aquifer. However, due to the low K values at RRL-South, a step-input of bromide was not feasible as the time required to introduce the tracer would

be too great. Therefore, a pulse-input of a predetermined bromide concentration was added to the injection wells.

Injection of the pulse tracer input was complicated by the fact that the tests had to be performed using the pre existing wells within the RRL-South pilot area. While attempting to follow previously described methods in the literature as closely as possible. One of the biggest challenges was due to the screened intervals of the existing wells. For example, previously reported radially divergent tests conducted in controlled field environments have incorporated wells that were installed primarily for the use of tracer introduction, either via a single well (Smith et al, 1991; Harvey and Garabedian, 1991), or via multiple injection wells (LeBlanc et al, 1991), coupled with down gradient monitoring wells equipped with multi-level sampling ports (Smith et al, 1991; Harvey and Garabedian, 1991; LeBlanc et al, 1991; Smith et al, 1996). Importantly, the screened intervals for the tracer injection wells described in the literature were relatively small (compared to those at RRL), averaging approximately 1 meter. Use of such a small screen length allows for introduction of a more localized tracer plume into the aquifer. However, for both tracer events at RRL-South, the screen length of the injection wells was 15 feet. For this reason, it was decided to attempt to create a uniform initial Br^- concentration throughout the entire water column in the screened interval, which proved challenging as discussed below. By applying such an approach, it was hoped that the bulk of the resulting tracer plume would, therefore, be captured in the downgradient wells which were of similar construction (e.g., 15-foot screen lengths) and set at identical depths. However, sampling the tracer over the first screened interval was also difficult, and required

development of a method to create sampling conditions in the monitoring wells similar to those described in the literature (e.g., multilevel sampling ports). Specifically, a method was developed for sampling at RRL which utilized two ¼" heat fused Teflon lined tubing samplers that were cut so that the influent end of one tube extended to approximately 31 fbg, while the second influent end extended to approximately 26 fbg. This in effect created a dual level sampling port to measure baseline concentrations within injection wells and monitoring wells (see Figure 5.4).

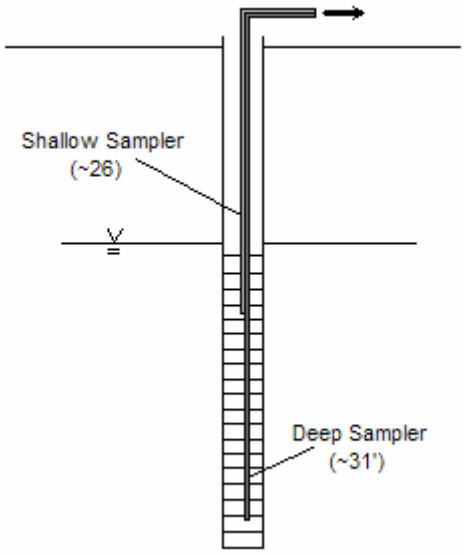

Figure 5.4. Dual Level Samplers capable of sampling within injection or monitoring wells.

For both Events 1 and 2, the specific procedures for the tracer introduction and sampling were identical, although, the initial concentrations in the injection well columns varied due to different tracer injection procedures and varying bromide stock solution concentrations. The first step in the procedure was to determine what volume of the above mentioned Br^- stock solutions to inject to achieve the target initial tracer concentration. First, the total volume of the water column (V_{wc}) within

the injection well (excluding the water within the gaps between screen slots and in the filter pack pore space) was calculated based on measured depths to the bottom of the well and to the water surface, both of which were taken prior to injection. For IP-S2, V_{wc} was 10.9 L and 7.2 L, for Events 1 and 2, respectively. Next, based on V_{wc}, the appropriate volume of Br^- stock needed to achieve the bromide mass required to create a water column tracer "slug" with uniform concentrations of approximately 640 mg/L (Event 1) and 400 mg/L (Event 2) was calculated. Therefore, during Event 1, 52.4 ml of 0.134 mg/L stock solution was needed, and during Event 2, 29 ml of 0.1 mg/L Br^- stock solution was required. For both events, the stock solution volumes were then mixed with approximately 500 ml deionized water to facilitate the tracer injection.

After determining the stock solution requirements, the next step was to inject the stock solutions. However, before starting the tracer injections, a length of Teflon tubing sufficiently long to reach the bottom of the injection well was lowered to a depth approximately 6" above the bottom of the well. Then, the influent end of the injection tubing was attached to the ¼" Masterflex tubing in the pump head of a peristaltic pump (Cole Parmer, model 7518-00, with Masterflex solo state speed control). Subsequently, the 500 ml of diluted Br^- stock solution was slowly pumped into the well at a rate of approximately 2.5 ml/min. Due to the low groundwater velocity, the time allowed for tracer introduction was not a concern as minimal loss of tracer mass was expected to occur due to migration into the formation before the measurement of baseline concentrations could be made.. While pumping, the tubing was slowly pulled out of well at a rate of approximately 2 feet per minute, all the

while taking precautions so the tubing would not be completely withdrawn from the water. If the water surface was reached before all the tracer solution had been injected, the same tubing was slowly lowered back into the well, at approximately the same rate, until all the stock solution had been injected. Next, in an attempt to gently mix the stock solution with the groundwater in the well, a rapid withdrawal and insertion of the tubing was performed across the entire length of the water column. This gentle mixing method was employed because of concerns that vigorous mixing may cause the tracer solution to mix with pore water in screen slot gaps and in the filter pack, thus decreasing initial concentrations within the water column to levels which may not be observable in down gradient monitoring wells upon tracer plume migration.

All field tracer study samples in the injection and monitoring wells were collected using the previously described dual level sampler (Figure 5.4) and peristaltic pump configuration. Using this equipment, the groundwater samples (approximately 75 ml from each depth) were drawn at a flow rate of approximately 50 ml/min. However, before collecting the 75 ml groundwater samples, approximately 50 and 25 ml of purge water was removed from the 31 and 26 ft sample depths, respectively. After each sampling event, the tubing was rinsed with distilled water, and air dried before use in the next well. Initially (the first three sampling events), the collected groundwater samples were field-analyzed for the Br^- concentration using an Orion 94-35A bromide specific electrode; however, this method proved difficult. As a result, the bulk of the samples were collected in pre-washed 200 ml Nalgene® bottles and stored for no longer than one week before being

analyzed in the laboratory using the bromide specific electrode method, as described below.

5.6 Analytical Methods

5.6.1 Bromide Analysis

Two different Br^- specific electrodes and meters were used for bromide analysis. During the laboratory tracer studies (laboratory trial and Test 1), and the first three sampling events for Event 1 of the field tracer test, an Orion 94-35A solid state ion specific bromide electrode was used, along with an Orion digital research analyzer (Model 501). The procedures for analyzing bromide concentrations with the Orion 94-35A electrode were identical, whether applied in the field or laboratory. Initially, the 10 ml (laboratory Test 3), 25 ml (laboratory trial, and Test 1 & 2), or 50 ml (groundwater sub-sample) was transferred into an appropriately sized glass beaker, with a Teflon coated stir bar, and then placed on a magnetic stir plate and gently stirred. Next, the Orion 94-35A solid state ion specific electrode and an Orion temperature reference electrode were suspended in the sample, and the meter was turned on and set to read mV. Next, an ionic strength adjuster (ISA) was added to each sample at a ratio of 1 ml ISA per 100 ml sample, and the solution was allowed to stabilize for approximately 5 minutes before recording the meter reading. Unfortunately, during field tracer Event 1 the electrode/meter readings began to drift at lower concentration (e.g., <5 mg/L) and, as a result, an accurate calibration curve could not be created. Therefore, use of the Orion 94-35A electrode was discontinued on July 7, 2005, and a new electrode was required to measure the remaining samples for laboratory tracer Tests (2) and (3) and field tracer Events 1 and 2.

The remaining measurements were made using a Cole Parmer solid state ion selective bromide electrode (Model EW-27502-05) filled with KNO_3 electrolyte, along with an Orion 520A meter. The sample analysis procedures for this electrode/meter were identical to those described for the Orion electrode, except that a greater ratio of ISA to groundwater was required during analysis (i.e., 2 ml ISA per 100 ml sample). Additionally, no temperature reference electrode was required while using the Cole Parmer electrode. As with the Orion 94-35A electrode, when analyzing the sample the meter was set to read mV. For concentrations greater than 5.0 mg/L the readings were allowed to stabilize for approximately 5 minutes. At the lower concentrations (e.g., <5.0 mg/L) the time for stabilization increased to an average of 10 minutes.

For the Orion 94-35A bromide specific electrode, a 5-point calibration curve was created approximately every 5^{th} use. This curve was prepared using sodium bromide (99.0%+, Sigma Aldrich) dissolved in deionized water at a concentration range of 0.5 to 1000 mg/L Br^-. For the Cole Parmer electrode, a 5-point calibration curve was also created. However, a new calibration curve was prepared prior to every use, and concentrations ranged from 0.5 to 75 mg/L Br^-. This lower concentration range was used because concentrations within the collected field and laboratory samples were not expected to be greater than 75 mg/L. When concentrations were found to be above 75 mg/L (e.g., when sampling the injection wells to determine the water column concentrations), then two additional standards at 500 and 750 mg/L Br^- were added to the standard curve. In addition to the frequent calibration curve preparation, a slope check was simultaneously conducted prior to

every sampling event when using the Cole-Parmer electrode. The slope check was a further verification that the electrode was working properly. For example, the electrode was considered accurate if the difference between the readings of two 100 ml bromide standard solution samples with a 10-fold difference in concentration, was 57 ± 3mV (i.e., the acceptable mV range established by the manufacturer).

5.6.2 Headspace Gas Analyses

5.6.2.1 Gas Chromatograph With FID Method

A Hewlett-Packard (HP) 5890 Series II Plus Gas Chromatograph (GC) with an FID and a 1% SP-1000 on 60/80 Carbopak-B (Supelco) (2.44-m x 3.2 mm) packed column was used to measure ethene, methane, VC and cDCE in headspace gas samples. The injector and detector temperatures are set at 200 ^{o}C and 250 ^{o}C, respectively. Helium (Ultra Pure Carrier Grade, Air Gas) was the carrier gas at a flow rate 40 ml/min. Air (Ultra Pure Carrier Grade, Air Gas) and hydrogen (Ultra Pure Carrier Gas, Air Gas) were used to fuel the FID at flow rates of 400 and 40 ml/min, respectively. The temperature program was as follows: (1) hold isothermally at 60 ^{o}C for 2.00 min, (2) ramp at 20 ^{o}C/min to 150 ^{o}C, and (3) ramp at 10 ^{o}C/min to 200 ^{o}C for 4.2 min. Under these conditions, retention times for ethene, methane, VC and cDCE were approximately 0.44, 0.6, 2.5 and 5 minutes, respectively. Injection volumes of 0.5 ml were made using the same 1 ml Hamilton gas tight syringe with a side-port valve that was used for headspace sampling.

5.6.2.2 Gas Chromatograph With ECD Method

An HP 5890 Series II Plus GC with an ECD and a DB-624 (30 m x .53 mm (ID) x 3 um film thickness) capillary column was used to analyze cDCE and PCE headspace concentrations. The injector and detector temperatures were 200 ^{o}C and 300 ^{o}C, respectively. The carrier and make-up gases were helium and nitrogen, with flow rates of 6 and 60 ml/min, respectively. The temperature program was as follows: (1) hold isothermally at 30 ^{o}C for 5 min, (2) ramp at 4^{o}C/min. to 60 ^{o}C, hold for 5 min., and (3) ramp at 15 ^{o}C/min to 140 ^{o}C. Under these conditions, the retention time for cDCE and PCE were 7.2 and 27 minutes, respectively. Injection volumes were 50 µl, and were made using the Hamilton 100 µl gas tight syringe used to collect the headspace samples.

In the following paragraphs, the procedures are described that were used to produce standard curves for analysis of the chloroethenes, cDCE and PCE, and methane. Ethene was never detected and, thus, no standard curve was ever produced.

5.6.2.3 Chloroethene Calibration Curves

As discussed in Section 5.3, chloroethene additions to the microcosms included cDCE and PCE. Therefore, calibration curves were required to determine the aqueous concentrations of cDCE and PCE, as well as the aqueous concentrations of methane. Importantly, because headspace analyses were performed, it was necessary that the calibration curves were prepared with standards at the same temperature at which the corresponding biokinetics and sorption microcosms and the Henry's constant determinations were being conducted. As a result, calibration curves were prepared for the following compounds and conditions: cDCE at 14ºC and 30 ºC

using both GCs; PCE at 30 ºC using the GC equipped with the FID, and methane using the GC equipped with the FID. Furthermore, the EPICs method, as described in Section 5.4.4, was also used to determine all aqueous phase concentrations based on the calibration curves detailed below.

5.6.2.3.1 cDCE Calibration Curves

A calibration curve for cDCE using eight standards was prepared in deionized water at 14°C and 30°C using both GCs. For the samples analyzed using the GC equipped with an ECD, calibration points ranged in aqueous concentrations from approximately 0.05 to 2.4 mg/L. These calibration points, labeled C-1 thru C-8, were prepared gravimetrically in the 26 ml nominal volume serum bottles. Specifically, the points were prepared by adding approximately 13 ml of deionized water to the previously weighed and dried 26 ml bottles. Next, the combined weights were recorded for each bottle, which were then sealed with Teflon coated butyl-rubber septa and aluminum crimps.

To obtain aqueous standard concentrations of approximately 0.05, 0.1, 0.2, 0.5, 1, 1.5, 2.0, and 2.4 mg/L, a 10 µl Hamilton syringe was used to transfer the required volumes of cDCE methanol stock solution, described in Section 5.4.2, to the serum bottles. Once the cDCE methanol stock solution was injected into each standard bottle, the total mass of cDCE methanol stock added was determined by reweighing the serum bottles and subtracting the difference. Based on the density of methanol, and assuming the density of cDCE was negligible, the total volume of stock solution injected into each bottle could then be calculated. From the calculated total volume of cDCE methanol stock solution in each bottle, and from the cDCE

methanol stock solution concentration, the cDCE aqueous concentrations could then be calculated. The standardized solution serum bottles were then stored in the dark at 14°C and 30°C for 24 hours. Once equilibrium conditions were established, the headspace was analyzed, in triplicate, using the GC with the ECD following the procedures described in Section 5.6.2.2.

Following the FID calibration procedures described above, a five point calibration curve was prepared for samples analyzed using the GC equipped with an FID. These calibration standards were prepared with aqueous cDCE concentrations of approximately 0.05, 0.2, 0.5, 1.0, and 1.5 mg/L. The samples were then stored at 14ºC and 30ºC and allowed to equilibrate for 24 hours. Headspace analyses were conducted, in triplicate, using the GC with the FID following sampling procedures described in Section 5.6.2.1.

5.6.2.3.2 PCE Calibration Curve

PCE was only added to the 30ºC anaerobic microcosm laboratory experiments, as discussed in Section 5.3.3.3. Thus, for the determination of aqueous PCE concentrations, a calibration curve was prepared using the GC with the ECD, and the standards were stored in a 30ºC incubator. The PCE calibration points were prepared following the same procedures described in Section 5.6.2.3.1, to produce standard PCE aqueous concentrations of approximately 0.05, 0.2, 0.5, 1.0, and 1.5 mg/L. After the injection of the required volumes of PCE in methanol stock solution, and the determination of the actual PCE concentrations based on the methods described previously, the samples were placed in a 30ºC incubator and allowed to

equilibrate for 24 hours. Headspace sampling and analyses were conducted, in triplicate, following the same sampling procedures described in Section 5.6.2.2.

5.6.2.3.3 Methane Calibration Curve

A Scotty bottle of methane (Supelco, 99.0% pure), was used for the cometabollic microcosm experiments, as described in Section 5.3.3.2, and for the methane calibration curve as described in the following paragraphs. To collect appropriate gas phase samples, a 1 ml Hamilton air tight syringe was connected to a Scotty bottle equipped with a syringe port for sampling. Next, the gas port was opened to allow a small flow of methane. This flow rate was kept at a minimum so that the pressure would not build up within the syringe. While the gas was flowing the syringe was slowly flushed with methane three times. Next, the syringe was filled to the appropriate volume (either 25, 100, 250, or 600 µl), the valve was closed and the needle withdrawn, and the contents were then injected into the GC with the FID following the procedures described in Section 5.6.2.2. This method was repeated twice for each standard and the average peak between the two was recorded. These injected methane volumes of 25, 100, 250, or 600 µl, yielded gaseous concentrations of 1, 4, 10, and 24 µmol, respectively.

The calibration methods for the smaller methane mass standard points (corresponding to 0.05 and 0.25 µmol) was as follows: First, a 160 ml serum bottle, sealed with a butyl rubber stopper and containing two glass beads to aid in mixing, was flushed with N_2 gas, making sure to vent while flushing to ensure that the contents are at atmospheric pressure. Next, the flushing needle was withdrawn followed immediately by the venting needle. After removing the vent needle, 2 ml of

methane gas was taken from the Scotty bottle, described previously, using a 1 ml Hamilton air-tight syringe, and added to the serum bottle while simultaneously inserting a vent needle. The bottle was then shaken vigorously, and a 1 ml gastight Hamilton syringe was used to obtain a 0.1 ml and 0.5 ml samples from the bottle for the 0.05 µmol and 0.25 µmol samples, respectively. These samples were then injected into the GC with an FID, following the methods described previously.

5.6.3 Dissolved Oxygen Estimation

Dissolved O_2 (DO) concentrations were obtained using a micro O_2 electrode and meter (Model 16-730, Microelectrode, Inc., Bedford, NH). To analyze for DO, small sample volumes (0.20 – 0.25 ml) were collected from all DO and COM aerobic sample bottles using a 1 ml sterile syringe and filter. Accordingly, all withdrawn sample volumes were subtracted from calculated aqueous concentrations to correct for the liquid loss. Next, the syringe was attached to the electrode flow cell. Then the liquid samples were injected into the microelectrode flow cell and allowed to flow past the electrode until readings in percent O_2 stabilized. Using the following equation, provided in the Microelectrode manual, the O_2 concentration (moles/L) could then be calculated from the percent O_2 (output):

$$S = \left(\frac{a}{22.414}\right)\left[\left(\frac{760 - p}{760}\right)\left(\frac{r\%}{100}\right)\right] \qquad (5.23)$$

where; S is the solubility of gas in mg per liter; *a* is the absorption coefficient of gas at 14 ºC and 30ºC, which is equal to 0.03486 and 0.02608, respectively, based on the chart provided in the Microelectrode manual (not provided); p is the vapor pressure of

water (mm Hg) at the given temperature (14 ºC and 30ºC), and; r% is the actual reading in percent oxygen.

The microelectrode was calibrated using a two-point calibration standard, which consisted of an ambient air point and a sample with DO equal to zero. The ambient air calibration point was carried out by pumping air into the microelectrode flow cell using the syringe. The zero DO sample was prepared by adding an excess mass of sodium sulfite, Na_2SO_3, and a trace of cobalt chloride, $CoCl_2$, to approximately 10 ml of deionized water (APHA et al., 1995). A small sub-sample of the zero DO solution was then injected into the microelectrode flow cell and the meter was adjusted accordingly. The relative accuracy, which was given by the manufacturer of the microelectrode was reported by

at 0.04 mg/L for a temperature of 24^{o}C.

6.0 RESULTS AND DISCUSSION

This chapter presents the results from the micro-, meso-, and macro-scale experiments discussed is Chapter 5. Specifically, the scale dependent experimental results are provided in this chapter and analyzed such that key parameters (e.g., bio-kinetics, sorption, porosity, advection rate, etc.) can be evaluated quantitatively. The dimensionless values obtained from these results are then incorporated into the appropriate dimensionless parameter presented in Figure 4.2, which are obtained from the dimensionless ADR equation, as described by Eq. 4.13. These dimensionless parameters are then analyzed through the flow chart presented in Figure 4.3. Using this systematic engineered approach, a quantitative assessment of the overall rate-limiting process is offered for the RRL-South pilot-scale engineered bioremediation system.

6.1 Micro-scale Parameter Results

Following the protocols described in Section 5.3.3 a total of 28 batch microcosms were prepared for the biokinetics estimation, comprising four different environmental systems. The microcosm experimental data are provided in Appendix G, including peak area counts. The intent of the microcosms study was to better understand the capabilities of the indigenous RRL-South microbial populations in site materials under various conditions expected to enhance cDCE degradation: cometabolic stimulation with methane (COM), aerobic oxidation stimulation with DO (DO), and reductive dechlorination stimulation with various electron donor substrates (molasses, MOL; HRC; lactate, LAC) Ultimately, the goal was to determine the optimum growth conditions for stimulating cDCE biodegradation by the native

microbes, and for this ideal system then estimate the growth rate parameters (i.e., substrate utilization rate, and substrate and electron acceptor half-maximum rate constants) required for the double-Monod biokinetics model. Biodegradation in the various treatments was evaluated by monitoring for changes in cDCE, and in some cases PCE (MOL, HRC, LAC all at 30^{o}C) concentrations in comparison to the uninnoculated (UC) and sterilized (STER) controls. In addition, supporting evidence was obtained by monitoring for methane consumption in the cometabolic (COM) treatment, methane production in the anaerobic treatments (MOL, HRC, LAC) and DO uptake in the aerobic treatments (COM and DO).

As noted in Section 5.6.2.2, while cDCE was detected on both of the GCs with FID and ECD, at the dosed concentrations within the samples, PCE was only detected using the GC with the ECD, and methane was only detected using the GC equipped with the FID. Given that both cDCE and PCE were analyzed using the GC with the ECD, all of the chlorinated ethene data given in the following figures are those collected on the GC with the ECD, while only methane aqueous concentrations are presented based on peak areas determined by the GC with the FID.

6.1.1 cDCE Concentrations

The duplicate batch microcosms for each treatment at 14^{o}C and at 30^{o}C, were sampled at approximately 4 day intervals. The resulting aqueous cDCE concentration data with time are summarized in Figures 6.1 though 6.7. Note that the aqueous concentrations provided in these figures are the normalized concentrations, which were calculated using Eq. 5.15. For the determination of normalized cDCE

concentrations, as well as PCE and methane concentrations, the standard bottle used for comparison was randomly chosen to be sample bottle UC-1.

From Figures 6.1 through 6.7, and from the groundwater concentrations in Appendix G, Figure 3, the average maximum concentrations of cDCE in all of the 14°C and 30°C sample bottles were approximately 0.7 mg/L and 1.3 mg/L, respectively. This is consistent with the initial addition of cDCE, which was designed to achieve an aqueous concentration of approximately 1.0 mg/L at 14°C. However, the initial concentrations were slightly lower for all samples. The same mass was added to the 30°C bottles, but due to the higher temperature, more partitioned into the headspace. In all samples, the initial concentrations were slightly lower than the

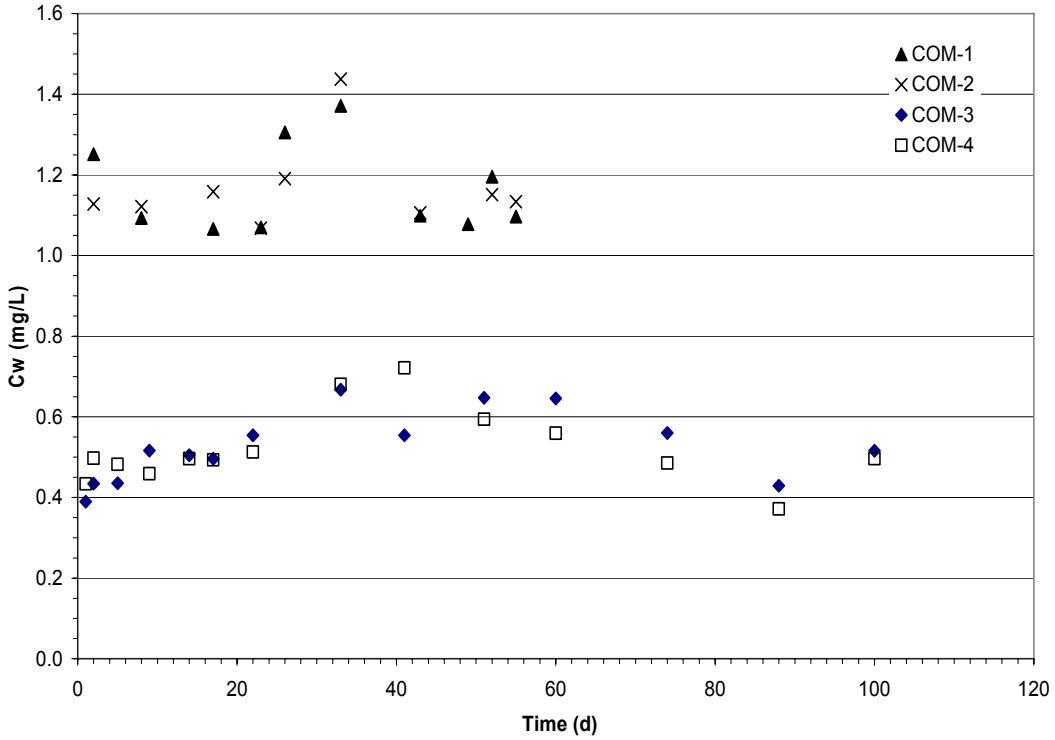

Figure 6.1. Aqueous cDCE concentration in aerobic cometabolism microcosms at 14°C (COM-1, COM-2) and 30°C (COM-3, COM-4). Each point represents a single GC headspace injection sample.

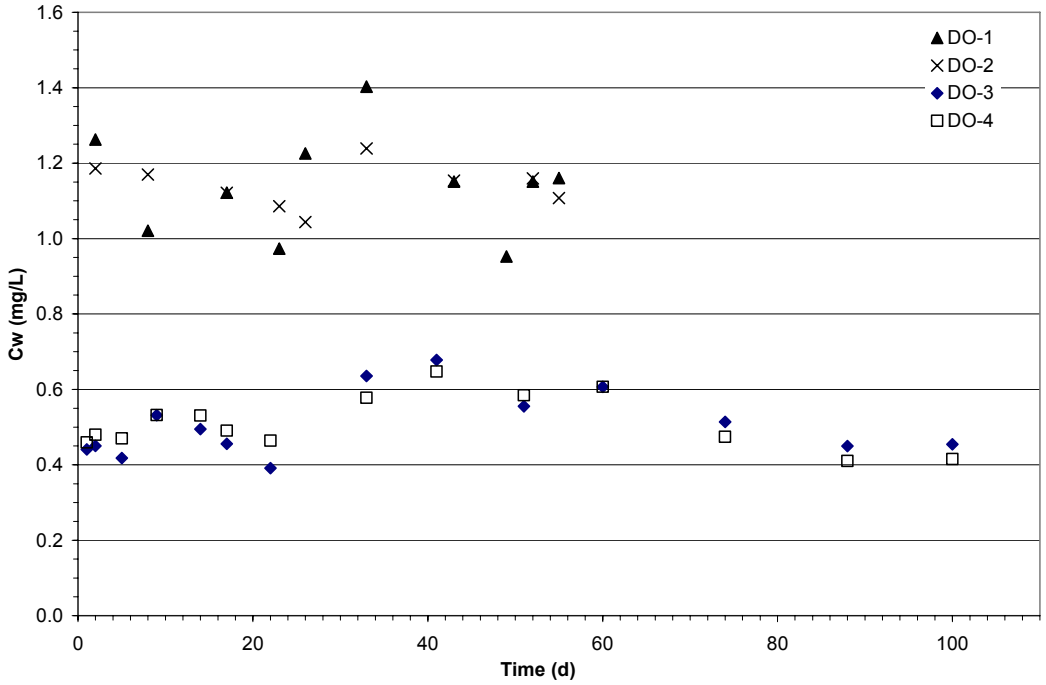

Figure 6.2. Aqueous cDCE concentration in aerobic oxidation microcosms at 14°C (DO-1, DO-2) and 30°C (DO-3, DO-4). Each point represents a single GC headspace injection sample.

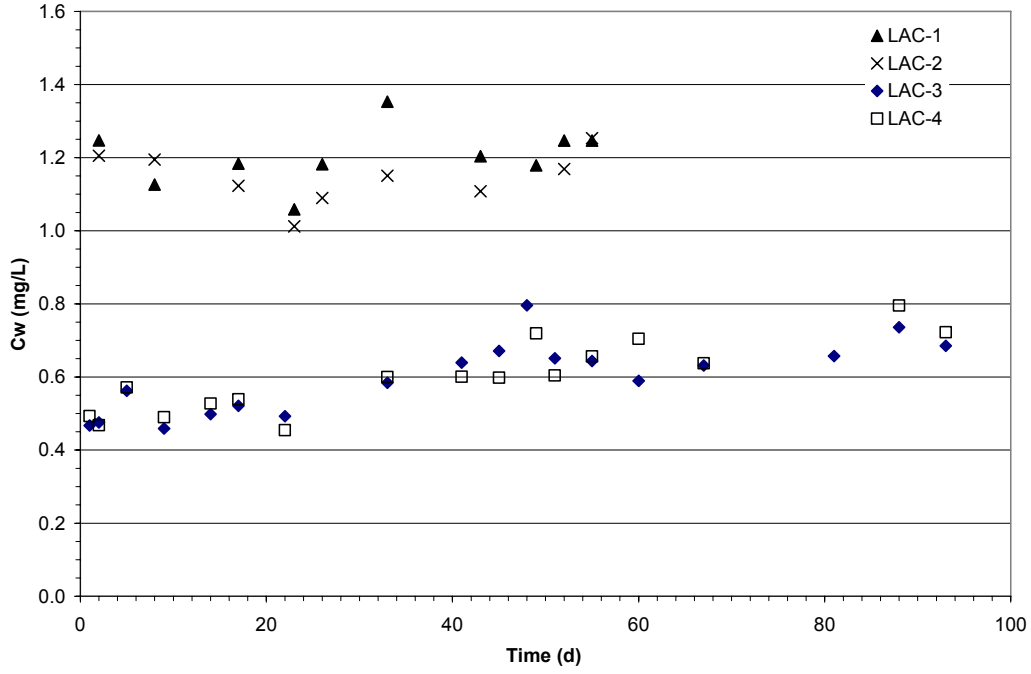

Figure 6.3. Aqueous cDCE concentration in anaerobic reductive dechlorination microcosms with lactate at 14°C (LAC-1, LAC-2) and 30°C (LAC-3, LAC-4). Each point represents a single GC headspace injection sample.

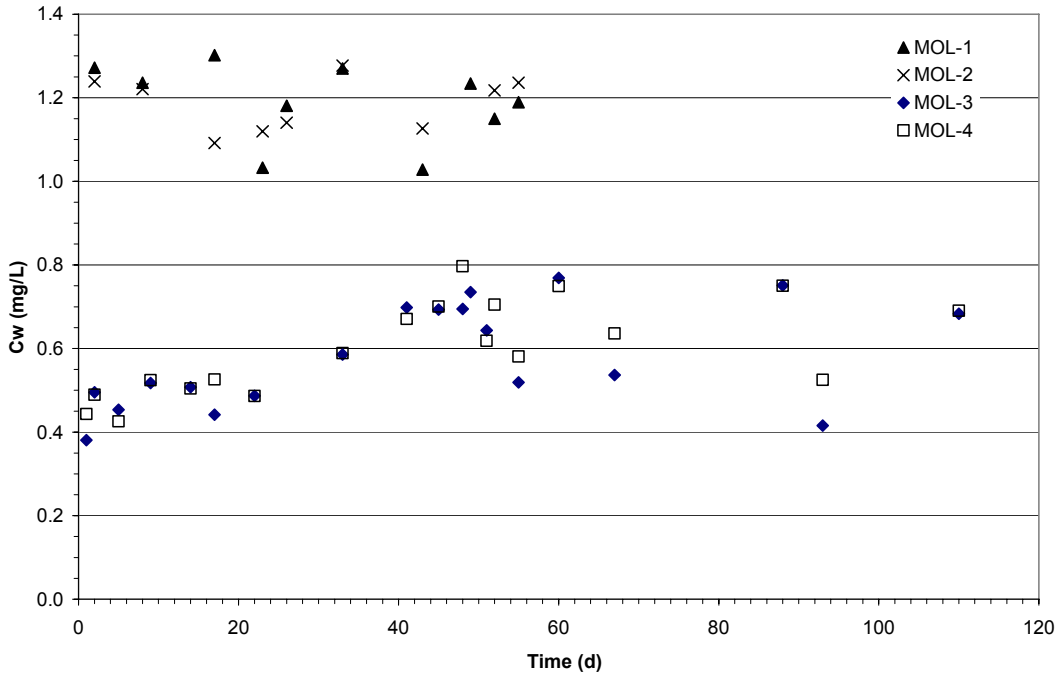

Figure 6.4. Aqueous cDCE concentration in anaerobic reductive dechlorination microcosms with molasses at 14°C (MOL-1, MOL-2) and 30°C (MOL-3, MOL-4). Each point represents a single GC headspace injection sample.

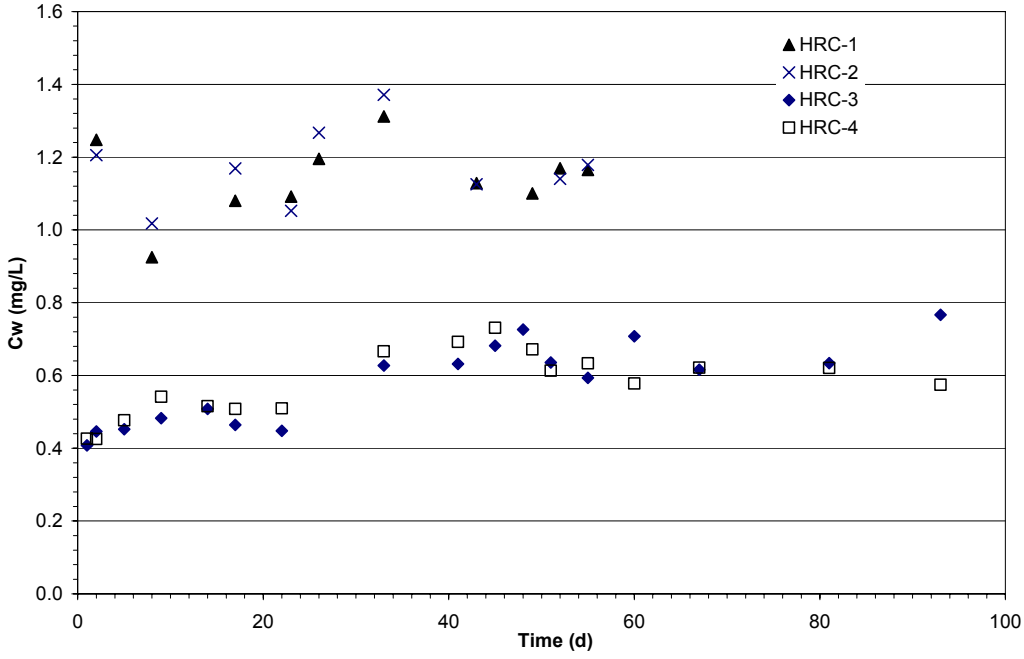

Figure 6.5. Aqueous cDCE concentration in anaerobic reductive dechlorination microcosms with HRC at 14°C (HRC-1, HRC-2) and 30°C (HRC-3, HRC-4). Each point represents a single GC headspace injection sample.

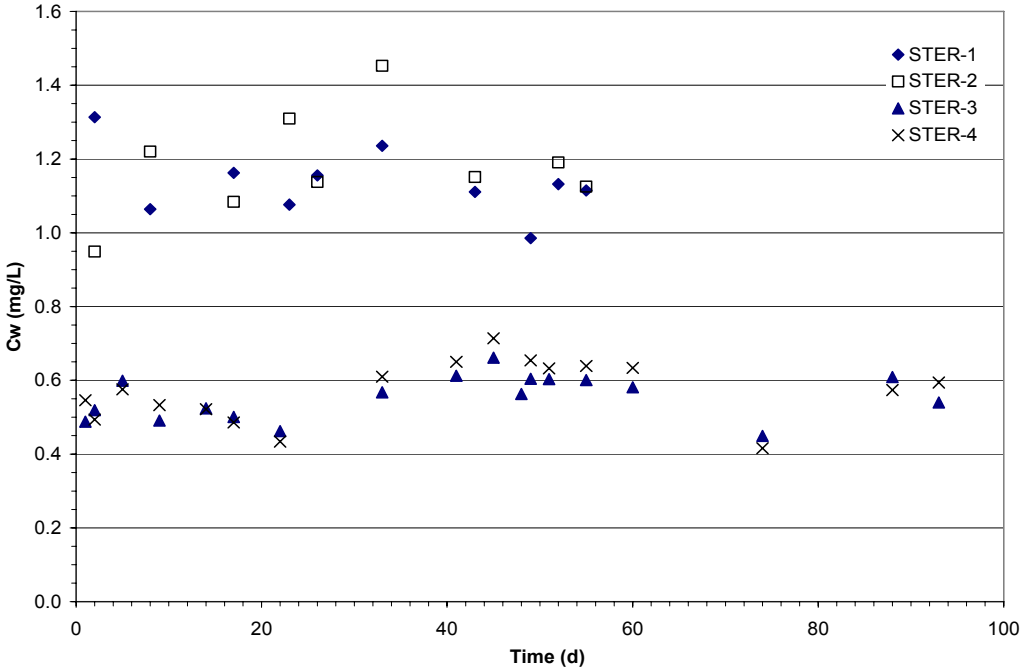

Figure 6.6. Aqueous cDCE concentration in sterilized microcosms at 14°C (STER-1, STER-2) and 30°C (STER-3, STER-4). Each point represents a single GC headspace injection sample.

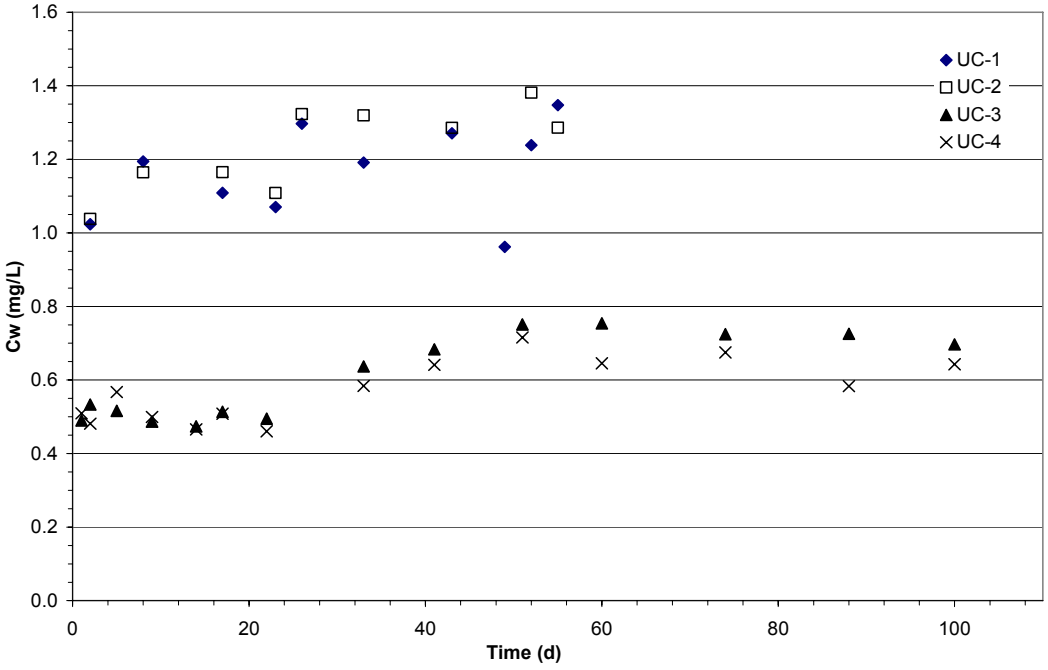

Figure 6.7. Aqueous cDCE concentration in uninnoculated control microcosms at 14°C (UC-1, UC-2) and 30°C (UC-3, UC-4). Each point represents a single GC headspace injection sample.

maximum concentrations, as noted previously, and the concentrations fluctuate somewhat over time. These fluctuations are possibly due to the slightly fluctuating temperatures at which the samples were stored. Although the temperatures were observed prior to every sampling event, the possibility of a 1 to 2 degree Celsius temperature change may have occurred in the samples due to the constant opening of the incubator required during sampling events, and was not corrected for when calculating the final aqueous concentrations. However, on October 15, 2005, the temperature within the incubator was recorded as approximately 60^{o}C. The duration at which the samples were incubated at this temperature is unknown. Upon this discovery the incubator was re-set to 30^{o}C and the aqueous concentrations within the sampled bottles were corrected for the higher temperatures.

This being said, no clear trend of cDCE loss through the first 55 days was observed. Sampling was concluded in the 14^{o}C bottles after 55 days to focus sampling and analysis efforts on the 30^{o}C samples, because it was anticipated that the more favorable growing conditions in these microcosms would provide useful results more quickly. Nevertheless, after a total of approximately 110 days of sampling the 30^{o}C bottles, the aqueous concentrations never significantly decreased, although there is possibly a decreasing trend in the cDCE concentrations in the cometabolic (Figure 6.1) and aerobic (Figure 6.2) treatments over the last 55 days. Similar trends can also be observed in the cDCE aqueous concentrations graphs, provided in Appendix G, for the cometabolic and aerobic treatments that were analyzed using the GC with the FID.

The conclusion that little or no cDCE biodegradation occurred is further supported by the correlation between the treatment microcosm results and the sterilized controls (labeled STER-#). The fact that the sterilized control samples showed similar aqueous concentration to the treatment microcosms supports the conclusion based on the field data that a microbial population capable of biodegrading cDCE is absent from the aquifer sediments at RRL-South, as discussed further below. In addition, the observation that the uninnoculated control aqueous concentrations (labeled UC-#) are nearly identical to all other microcosm sample concentrations, supports the findings discussed in Section 6.2, that there was minimal sorption of the cDCE to the aquifer solids in the bottles. Specifically, because similar cDCE masses were introduced to all sample bottles, if the mass of cDCE sorbing to the aquifer sediments were large, then the corresponding equilibrium aqueous and gaseous concentrations would be correspondingly lower, but they are not. Furthermore, the sterilized samples showed similar aqueous concentrations supporting the assumption that a microbial population capable of biodegrading cDCE is absent from the sediments.

6.1.2 PCE Concentrations

As described above, the lack of significant change in the cDCE concentrations in the microcosms indicated that little or no cDCE was being degraded in any of the treatments, consistent with the field data. However, historic field data indicated that reductive dechlorination of PCE and TCE to cDCE might be occurring. Therefore, to confirm this and determine if the collected sediments were still representative of the RRL-South field conditions, PCE was dosed to the anaerobic 30^{o}C sample bottles

containing HRC®, molasses, lactate, and to the sterilized bottles as a control. This approach was supported by the Regenesis bench scale tests, which indicated that TCE was degraded by RRL-South indigenous microbes under anaerobic conditions after approximately 30 days. Therefore, assuming that PCE would be degraded under similar laboratory conditions, the selected microcosm treatment bottles were spiked with a PCE stock solution (see Section 5.3.3.3). The sample bottle data and results for the PCE analysis are provided in tabular form in Appendix G, or graphically in Figures 6.8 through 6.11 for aqueous PCE concentrations with respect to time for all dosed sample bottles.

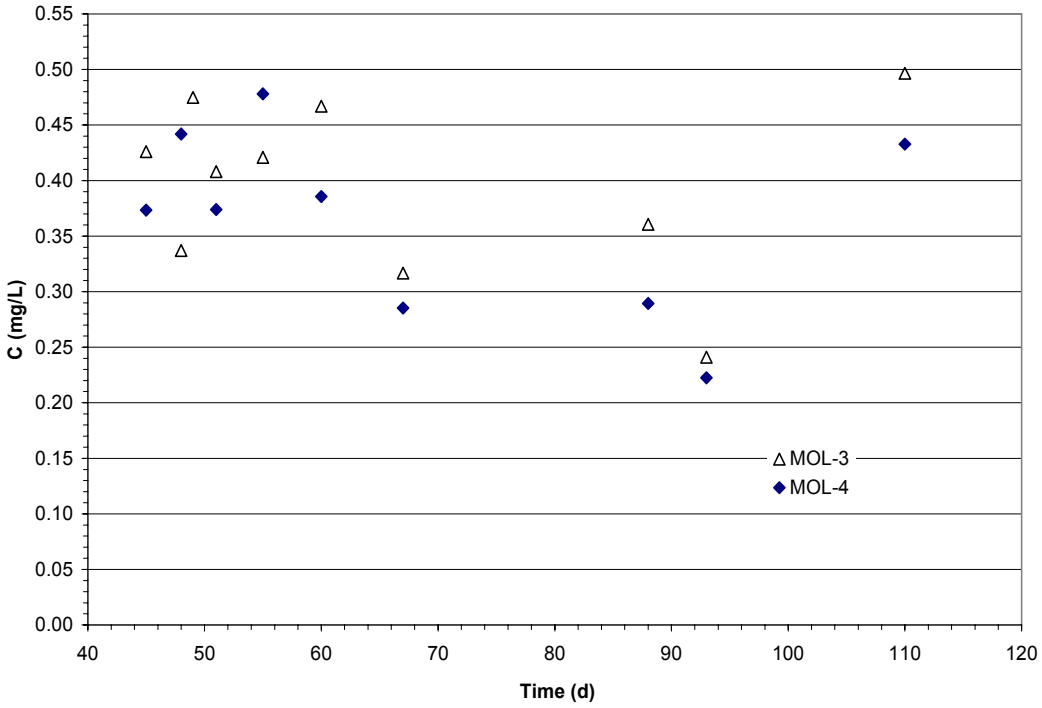

Figure 6.8. Aqueous PCE concentration in anaerobic reductive dechlorination microcosms with molasses at 14°C (MOL-1, MOL-2) and 30°C (MOL-3, MOL-4). Each point represents a single GC headspace injection sample.

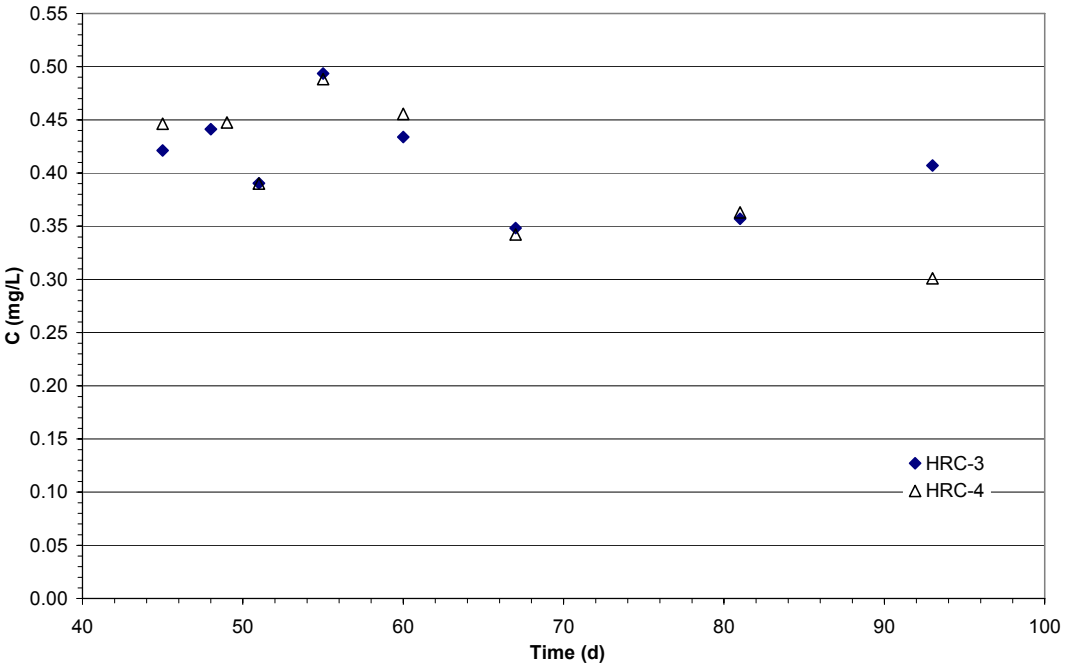

Figure 6.9. Aqueous PCE concentration in anaerobic reductive dechlorination microcosms with HRC at 14°C (HRC-1, HRC-2) and 30°C (HRC-3, HRC-4). Each point represents a single GC headspace injection sample.

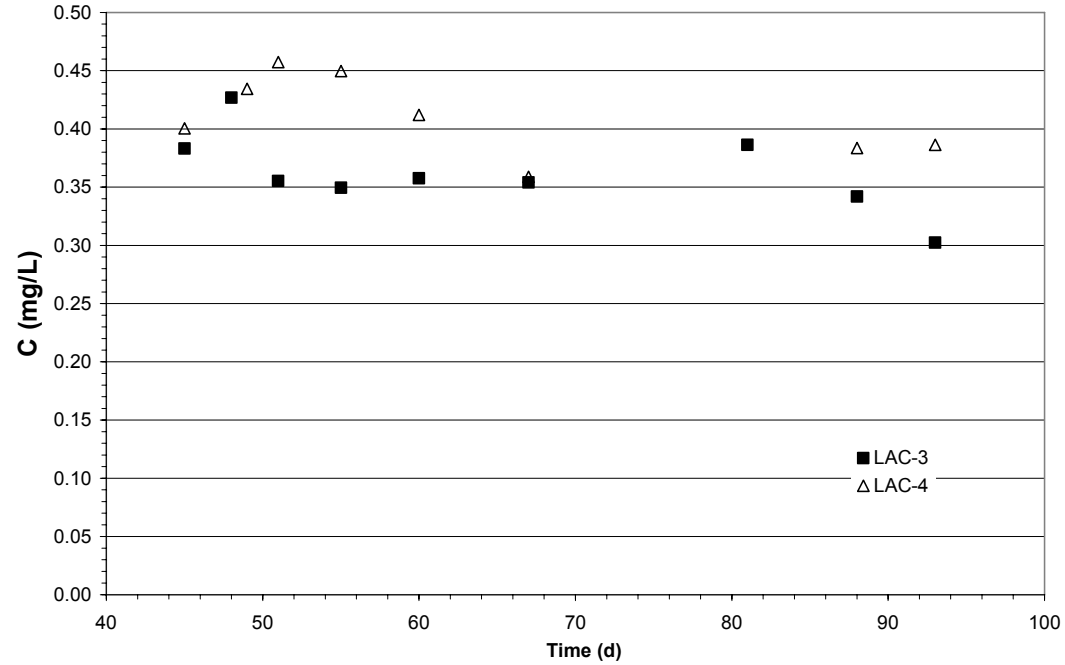

Figure 6.10. Aqueous PCE concentration in anaerobic reductive dechlorination microcosms with lactate at 14°C (LAC-1, LAC-2) and 30°C (LAC-3, LAC-4). Each point represents a single GC headspace injection sample.

The initial aqueous PCE concentrations were approximately 0.4 mg/L, consistent with the added mass, which was designed to achieve an aqueous concentration of 0.2 mg/L. The concentration trends in all bottles are similar, and suggest little or no degradation was occurring. There is a slight decrease over time from the initial baseline concentrations for all three treatments, approximately 5 days after the PCE addition. However, the PCE aqueous concentrations in the sterilized controls (Figure 6.11) exhibit a very similar trend, which suggests that the concentration decreases were not biologically mediated.

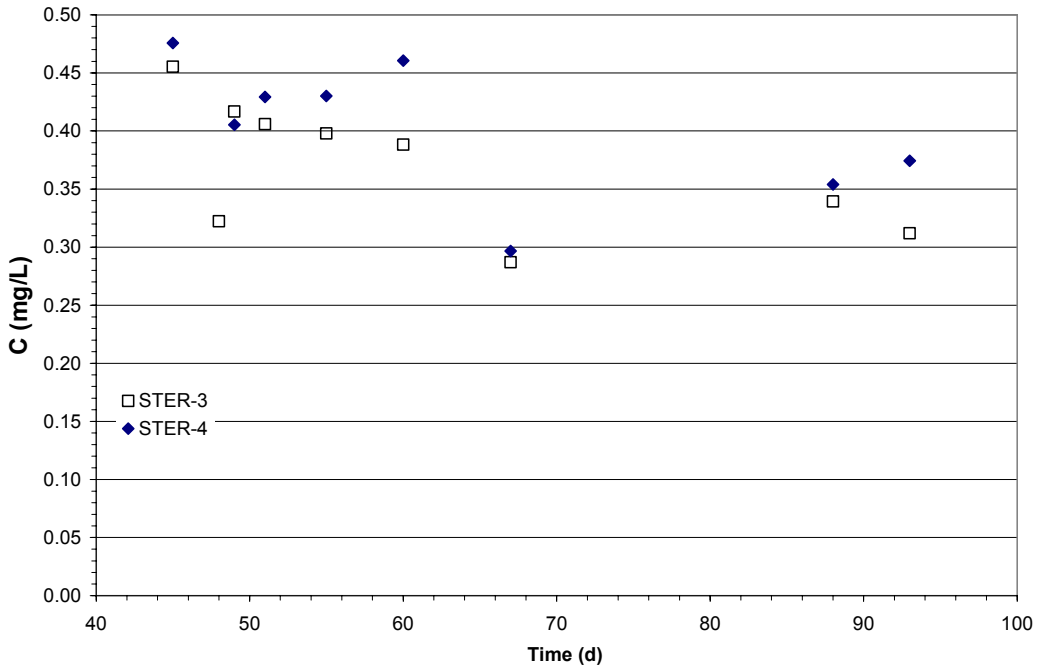

Figure 6.11. Aqueous PCE concentration in sterilized microcosms at 14°C (STER-1, STER-2) and 30°C (STER-3, STER-4). Each point represents a single GC headspace injection sample.

6.1.3 Methane Concentrations

To provide supporting evidence of any degradation of cDCE via cometabolism in the COM-# treatment bottles, the aqueous methane concentrations

were monitored using the GC equipped with the FID. The initial methane aqueous concentrations, first recorded 10 days after the start of the microcosm experiments, were approximately 170 µmol/L in the 14°C bottle marked COM-2, and 400 µmol/L in the 14°C COM-1 and the 30°C samples. These concentrations are greater than expected from the initial addition of cDCE, which was designed to achieve an aqueous concentration of approximately 3 µmol/L at 30°C. Subsequently, aqueous methane concentrations (Figure 3.12) appear to remain constant until approximately 60 days after the tests were began. At this point, which corresponded to possibly a small decrease in cDCE (Figure 6.1), the methane concentrations show a slight decrease over time in the COM treatments. As noted above, the cause for this

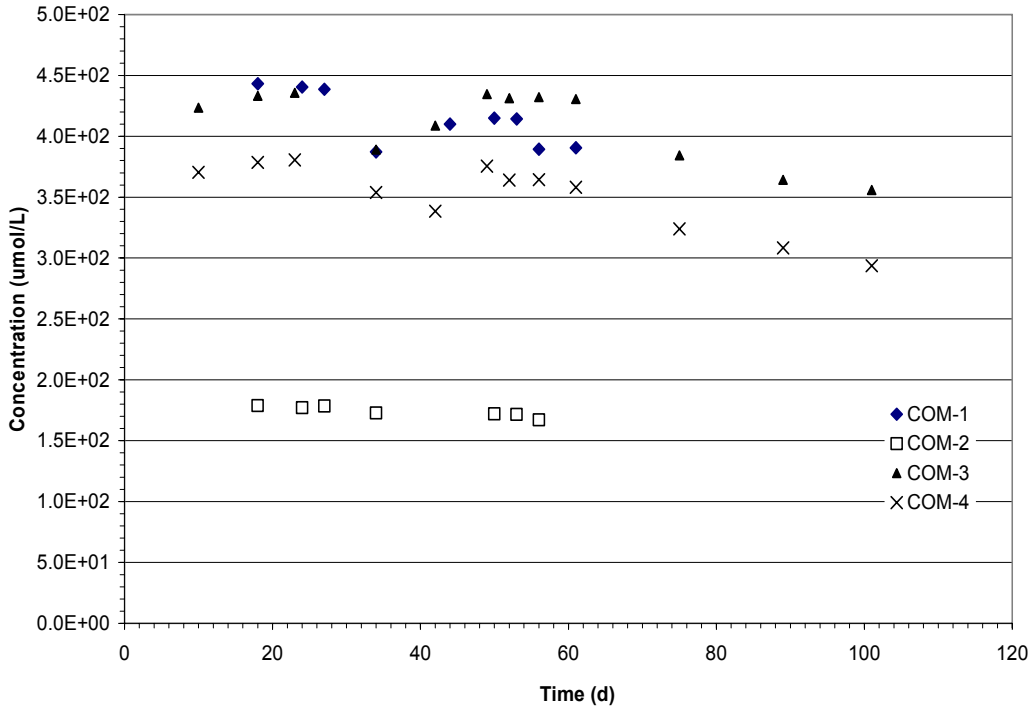

Figure 6.12. Aerobic cometabolic microcosm methane concentrations at 14°C (COM-1, COM-2) and 30°C (COM-3, COM-4). Each point represents a single GC headspace injection sample.

decrease in methane may have been the result of the pH adjustment to the sample bottles that occurred approximately 51 days after the start of the tests.

The anaerobic treatment microcosms, on the other hand, were monitored for increases in the methane concentrations in the samples, as evidence of methanogenic activity (see Appendix G). For example, in the molasses sample (MOL-#) (see Figure 6.13), and HRC samples (not shown), the methane aqueous concentrations increased approximately 0.15 µmol/L at around the time of the pH adjustment, after which levels slowly decreased with time toward initial conditions. Correspondingly, after the pH adjustment the pressure within MOL samples increased from a baseline level of 1.0 psi to approximately 17.0 and 16.9 psi in samples MOL-3 and MOL-4, respectively. Similarly, the HRC-3 and -4, and LAC-3 and -4 sample bottle pressures

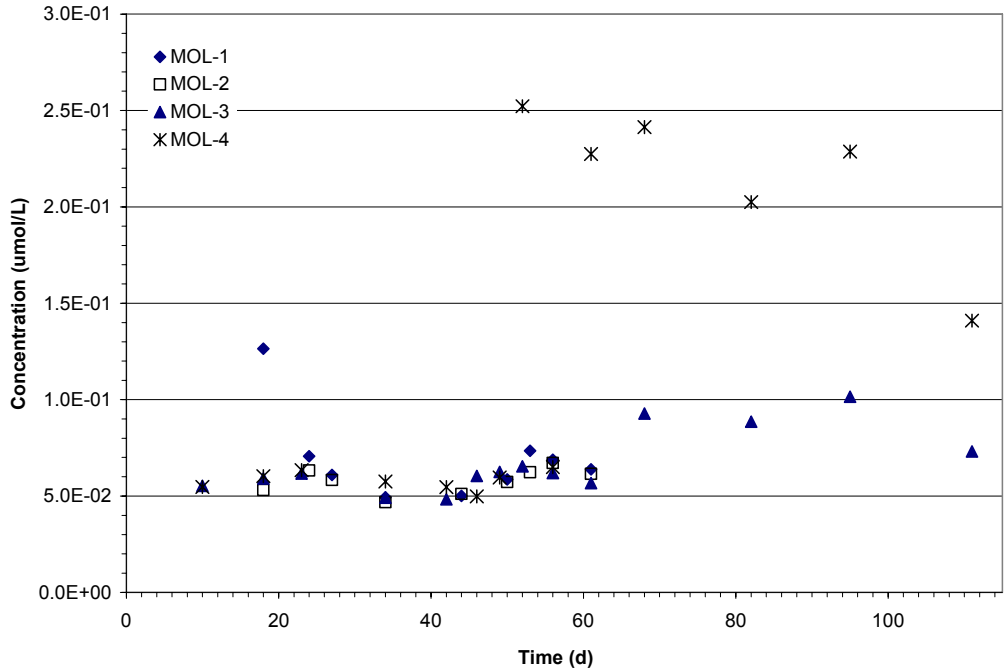

Figure 6.13. Anaerobic molasses-amended microcosm methane concentrations at 14°C (MOL-1, MOL-2) and 30°C (MOL-3, MOL-4). Each point represents a single GC headspace injection sample.

doubled from a baseline of 1.0 psi after the pH adjustment. Furthermore, both MOL-3 and MOL-4 sample colors changed from clear to brownish-orange possibly indicating the presence of iron precipitate. These results suggest that the pH adjustment may have also increased anaerobic microbial activity, but apparently not reductive dechlorination as evidenced by the lack of clear trends in the cDCE and PCE data.

6.1.4 Oxygen Concentrations

As another indicator of biological activity, the oxygen concentrations were monitored in the aerobic microcosm treatments, following the protocols described in Section 5.6.3, and using Eq. 5.23. Aqueous oxygen, given as percent O_2, was first recorded in the aerobic samples approximately 27 days after the start of the biokinetics tests. As shown in Table 6.1 the percent oxygen in the 30^{o}C aerobic

Table 6.1. Change in percent O_2 for 30^{o}C samples DO-3, DO-4, COM-3, COM-4, STER-3, and STER-4. Sample bottles first sampled 42 days after onset of biokinetics study (9/16/06) and again 82 days after onset of study (10/20/06) for a total time interval of 40 days.

Sample ID	*% O_2*		*% O_2 Decrease*
	42 days	82 days	
DO-3	16.0	10.5	34.4
DO-4	15.8	15.0	5.1
COM-3	14.6	14.3	20.1
COM-4	17.3	13.1	24.3
STER-3	14.7	13.8	6.1
STER-4	14.0	13.3	5.0

bottles has decreased with time, indicating that oxygen has possibly been consumed, although the decrease in some of the treatment bottles is similar to or less than that in

the sterilized control. This is consistent with the cDCE aqueous concentration trends, discussed previously, do not support significant biodegradation of CAH as a result of O_2 consumption.

6.1.5 Microcosm Discussion

Upon review of the data presented in the preceding sections there is no indication that cDCE was significantly biodegraded in any of the controlled systems during the time frame of the study. There was, however, some evidence of cDCE removal in the cometabolic and aerobic treatments, after the pH adjustment, supported by corresponding decreases in methane and oxygen. Similarly, there was some evidence of increased biological activity in the anaerobic treatments after the pH adjustment (e.g., an increase in methane concentrations), but in these cases no correlation could be made between these observed conditions and the reduction of cDCE or PCE.

There are several possible explanations for these findings. One possibility is that the experimental observation period was insufficient. From the results of the Regenesis bench scale study, it was anticipated that cDCE, or at the least PCE reduction, would occur after approximately 30 days of incubation. However, the samples used in this study were very different than those used by Regenesis. First, the time lag between sample collection and the onset of microcosm tests by Regenesis was on the order of days, while the lag in this study was on the order of months. Specifically, the core sample used as the innoculum in the microcosms had been stored at 4^{o}C for nearly 18 months. Though microorganisms are extremely resilient and capable of surviving long periods under adverse conditions, the time spent in

storage for this experiment may have negatively impacted the activity and numbers of the indigenous RRL-South microbial populations. Certainly, lower microbial numbers could have contributed to a longer lag phase.

Another important factor in contributing to these observations was probably the low pH recorded in the microcosms prior to adjustment, which was approximately 2 -3. This pH was lower than seen in the field, probably due to continued sulfide oxidation in the sediments during storage. Importantly, this pH range is not suitable for most dehalorespiring organisms. A pH level between 6 and 8 is generally considered favorable for CAH reduction (EPA, 2000). Indeed, after the pH was adjusted there was some indication of possible cDCE removal which was observed in the cometabollic and aerobic treatments, supported by methane and DO data, along with increased anaerobic activity in the anaerobic microcosms.

Based on these findings, however, overall the biodegradation of cDCE appears to be extremely limited. As discussed above, these observations may be, at least in part, due to the microbial innoculum and slurry pH. Nevertheless, the conclusion that there is limited cDCE biodegradation potential at the site is consistent with the field observations. Unfortunately, with the available data it cannot be discerned if the lack of biodegradation is due to a lack of the appropriate microorganisms or the environmental conditions. With respect to the dimensionless parameter evaluation, it is not possible to fit any kinetic parameter to these data and the biokinetics are simply assumed to be very limiting compared to other processes.

6.2 Meso-scale Parameter Results

6.2.1 Henry's Constant and Activity Coefficient

The volatilization and subsequent gas phase partitioning of CAHs into the vadose zone is common in many aquifers contaminated with such compounds (Washington, 1996). However, volatilization of cDCE or other chlorinated ethenes is not a major concern at RRL-South because of the depth to groundwater, temperature within the aquifer, and low aqueous concentrations. Nevertheless, it was required to determine the Henry's constant, which is a direct measure of the volatility of a compound, and the activity coefficient in order to determine the headspace concentrations within the laboratory microcosms set up at 14^{o}C. Additionally, these estimates for H' and γ were required for the EPICs method utilized to determine the sorption coefficient for cDCE in the RRL-South aquifer sediments, which were also established at 14^{o}C.

A few steps were required prior to creating the cDCE calibration curve for samples at 14ºC specific to this study. As discussed in Chapter 5, an initial H' estimate, adapted from Shimotori and Arnold (2003), was required for the calculation of cDCE concentrations in the development of an early 14^{o}C cDCE calibration curve. From the initial concentrations determined from the GC peak areas and the H' estimate (i.e., 0.124), a new H' could then estimated from the EPICs method using Eq. 5.3. This method yielded a Henry's constant value specific for RRL-South aquifer conditions at 14^{o}C. This specific H' value, equal to 0.15±0.04 (average ± standard deviation) (Table 6.2), was subsequently reinserted back into the original

calibration data, and a new calibration curve was recalculated based on the original 5-point standard aqueous concentrations also used in the early calibration curve.

For the cDCE and PCE calibration curve calculations using the GC with the ECD and FID at 30ºC, a specific estimate for H' was not carried out for this study. For simplification, the H' estimates used to create a calibration curve for cDCE and PCE concentrations at 30ºC were determined by fitting an exponential regression trend line to the Henry's constant data provided by Shimotori and Arnold (2003), who gave H' values for temperatures ranging from 1.8 ^{o}C to 70^{o}C (Appendix E). From the regression equation, H' values were estimated to be 0.2 and 0.795 (Table 6.2) for cDCE and PCE, respectively, at 30^{o}C.

Table 6.2. Henry's constants for select temperatures calculated from laboratory estimates and literature values.

Compound	Temperature (^{o}C)	H'	Source
cDCE	14	0.15±0.04	Laboratory Estimate
cDCE	30	0.20	Shimotori and Arnold (2003)
PCE	30	0.795	Shimotori and Arnold (2003)

As discussed previously, temperature fluctuations occurred periodically in the chilled and heated incubators. If a temperature change was discovered (a thermometer was stored in the 30^{o}C incubator and the chilled room had a temperature monitor), the Henry's constant regression equations calculated for cDCE and PCE were used to calculate a new H', which was then reinserted to the calibration data to generate a revised calibration curve for the observed temperature.

The values obtained in this study for Henry's constant are comparable to others available in the literature. This being said, the values available in the literature varied from source to source. For instance, Gossett (1987) provided a range for

dimensionless Henry's constant values of 0.074 and 0.111, which were calculated at 10.3 and 17.5^{o}C, respectively. Additionally, Shimotori and Arnold (2003) provided cDCE H' ranges of 0.09±0.03 and 0.14±0.02 at 1.8 and 21.6^{o}C, respectively. Furthermore, Ashworth et al. (1988) estimated H' values, for cDCE at 10, 15, and 20^{o}C, to be 0.116, 0.138, and 0.15±0.04, respectively. Given the range in H' values, e.g., H' at 10.3^{o}C equal to 0.0741 (Gossett, 1987), compared to H' at 10^{o}C equal to 0.116 (Ashworth et al., (1988), the H' value of 0.15±0.04 calculated in this study seems reasonable, albeit marginally higher than the literature values at approximately the same temperature.

6.2.2 Sorption Rate

To determine the rate of sorption of cDCE onto Quantico slate, two meso-scale sorption tests were conducted following the protocols described in Section 5.4.3.1. The test conditions properties and results for both studies are presented in Appendix H. Figure 6.14 is a plot of the cDCE aqueous concentrations versus time for both tests.

Based on the results of the first test, the time to equilibrium could not be easily established due to the fluctuations in aqueous concentrations, especially the last three data points. As discussed Chapter 5, it was thought that these fluctuations may have been caused by non-uniform particle sizes. Therefore, the second test was performed using the sieved aquifer sediments, and additional data points were taken. The second test was allowed to run for approximately 150 hrs, at which time the aqueous concentrations appeared to have stabilized. Despite the differences, both data sets have a spike in aqueous concentrations after approximately 24 hours,

followed by a rapid decrease in the aqueous concentrations between 24 and approximately 48 hours. Subsequently, only the second test appears to have reached equilibrium after approximately 72 hours, as indicated by the relatively stable aqueous concentrations shown in the later sampling events. Thus, based on the observed equilibration time required in the second sorption rate experiment, the experiments used to estimate the equilibrium K_d values were required to equilibrate for no less than 100 hours, as discussed in the next subsection.

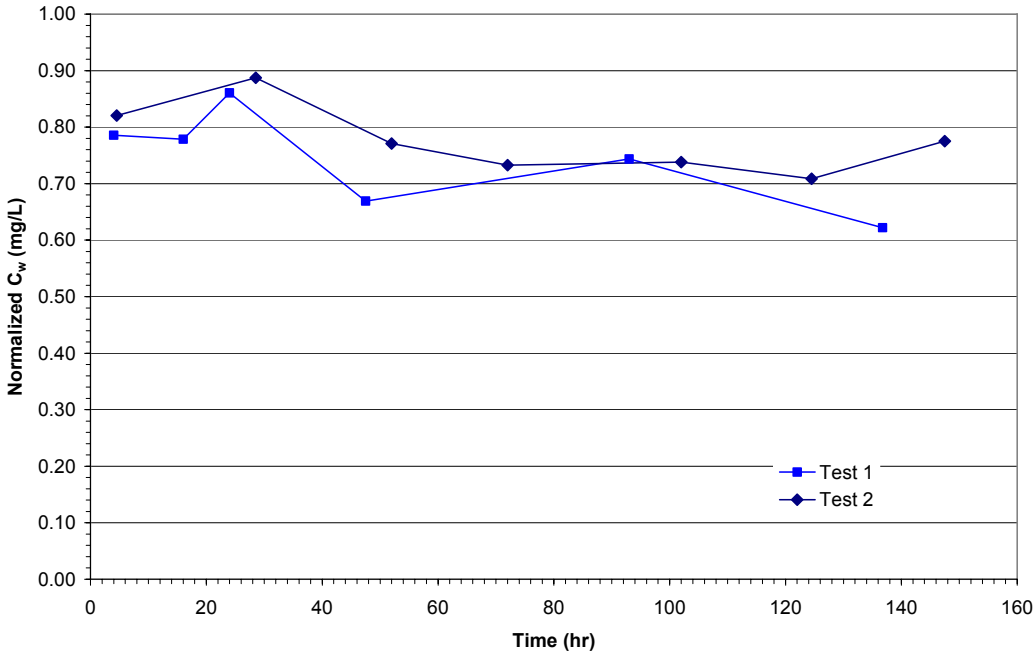

Figure 6.14. Normalized cDCE concentration ($C_{groundwater\ only}/C_{soil\ +\ groundwater}$) as a function of time for the cDCE rate of sorption experiments at 14°C. (Each data point represents the aqueous concentration determined based on headspace analysis of a sacrificial bottle.

To obtain a sorption rate constant, the simple first-order rate model presented in Chapter 4 was applied:

$$\frac{\partial A}{\partial t} = -k_m\left(A - \frac{\overline{A}}{K_d}\right) \qquad (4.8)$$

The data used for this analysis were those from sorption rate tests 1 and 2 prior to, and immediately after the aqueous cDCE concentration had peaked, i.e., from 4 hr to 47.5 hr for test 1 and from 4.5 hr to 52 hr for test 2. Specifically, the first three data points in test 1, recorded at 4, 16, and 24 hr, were paired with the fourth data point, recorded at 47.5 hr. Similarly, the first two data points in test 2, recorded at 4.5 and 28.5 hr, were paired with the third data point, recorded at 52 hr. At these times in each test, sorption was obviously at its most rapid rate, and it is reasonable to assume that at the time of the range of initial concentrations (e.g., 4, 16, and 24 hr for test 1), the aqueous concentrations in equilibrium with the sorbed concentration (i.e., the $\overline{A}/K_d$ term in Eq. 4.8 above) was relatively small compared to the aqueous concentration (A). In that case, the $\overline{A}/K_d$ term in Eq. 4.8 can be ignored at these early times, and Eq. 4.8 reduces to,

$$\frac{\partial A}{\partial t} = -k_m A \tag{6.1}$$

which can be integrated to solve for k_m a follows:

$$k_m = \frac{\ln\left(A_o/A\right)}{t - t_o} \tag{6.2}$$

Applying Eq. 6.2 to the three data pairs from test 1 and the two data pairs in test 2, a value for k_m is calculated for each data pair (Table 6.3) and an average sorption rate is estimated from these five data pairs. The average k_m value is estimated at 0.005±0.003 hr^{-1}, or 0.127±0.074 d^{-1} (average ± standard deviation). This value is probably an underestimate of the actual rate because by the time of the

second data point used in the calculations above, the term $\overline{A}/K_d$ is no longer insignificant compared to *A*.

Table 6.3. Sorption rate constant estimates calculated from tests 1 and 2 sorption data pairs.

Test #	Sample Pairs	k_m (hr^{-1})
1	4 & 47.5 hr	0.0037
	16 & 47.5 hr	0.0048
	24 & 47.5 hr	0.0107
2	4.5 & 52 hr	0.0013
	28.5 & 52 hr	0.0060
Average ± standard deviation:		0.0053±0.0031

6.2.3 Equilibrium Sorption Coefficient (K_d)

The equilibrium sorption coefficient was estimated following the EPICs method, as described in Section 5.4.4, by comparing two sets of microcosms, one set with soil and groundwater and the other without soil but still containing an equal volume of groundwater. Consistent with the results of the sorption rate study, the microcosms were assumed to reach equilibrium at a temperature of 14°C after 72 hours (see Section 5.4.3.1) before sampling. Additionally, the K_d estimate microcosms were vigorously shaken once a day to increase the cDCE mass-transfer onto the sediment.

The data for the microcosms used for the K_d determination are provided in Appendix H. There are a total of nine serum bottle samples, but not all were used in the K_d calculation. First, one of the samples without soil was discarded because the equilibrium cDCE levels were found to be far too low, indicating that a leak had

developed in the bottle seal allowing for cDCE volatilization to the atmosphere. Second, the three bottles that contained formaldehyde were not used in K_d calculations because in two out of the three bottles, the normalized aqueous concentrations were similar to, or greater than the equilibrium concentrations in the bottle with groundwater only. The formaldehyde was added to inhibit biodegradation, but it appears that it instead interfered with partitioning to the soil. It is possible that formaldehyde was competing for sorption sites on the soil, thus increasing the aqueous concentrations. In addition, the formaldehyde was added in the form of formalin, which includes methanol which could have increased partitioning into the aqueous phase. In any case, it was not important given the low levels of biodegradation.

The data from three soil and groundwater bottles were paired with two groundwater-only bottles (i.e., KD-1 with KD-7, KD-1 with KD-9, KD-2 with KD-7, etc.) giving 12 pairs, which were used with Eq. 5.14, whereby a K_d value could be obtained for each pair. Then the K_d values for all the soil and groundwater bottle pairs were averaged. Table 6.4 provides the estimated K_d values for their respective sample bottles pairs, as well as the overall average value.

A retardation factor (R_d) was calculated for cDCE in the Quantico formation based on Eq. 4.7, and was estimated to be approximately 4.6. This indicates that the migration of cDCE in the Quantico formation is 4.6 times slower than the advective rate. Although not important to the dimensionless parameter framework, the retardation of a compound in the subsurface may aide an engineer practitioner with predicting the horizontal extent of the plume boundary.

Table 6.4 Sorption partitioning coefficient estimation.

Sample Pairs	*Kd (L/kg)*
KD-1 & KD-7	0.32
KD-1 & KD-9	0.35
KD-2 & KD-7	0.29
KD-2 & KD-9	0.32
KD-3 & KD-7	0.48
KD-3 & KD-9	0.51
Average Kd (±Std Deviation):	0.38±0.08

The final sorption partitioning coefficient estimate of 0.38±0.08 L/kg is over five times lower than the one reported value of 2.07 (DeWulf et al., 1998), however this reported value was derived from a soil with an f_{oc} value of 4.12±0.08 %, which is a far greater organic fraction than estimated for RRL-South, which is approximately 1.7 %. Not surprisingly, the higher organic fraction in these reported soils gives a greater K_d value. This occurs because K_d is proportional to organic carbon content, as shown by the following equation,

$$K_d = K_{oc} f_{oc} \qquad (6.3)$$

where f_{oc} is equal to the fraction of organic material, and K_{oc} is defined as the organic carbon partition coefficient. Based on Eq. 6.3, the K_{oc} value used in the study by DeWulf et al. (1998) can be compared to the K_{oc} value obtained in this study. Given the DeWulf et al. K_d and f_{oc} values defined above, and K_d and f_{oc} values of 0.38 and 0.017 (kg/kg), respectively, for this study, the K_{oc} values for DeWulf et al. and this study are 50.2 and 22.4, respectively. As expected, after correcting for the organic fraction variation within soils, the K_{oc} values are more similar than the K_d values, with the remaining difference perhaps due to differences in the nature of the organic carbon.

Furthermore, the following general equation which relates K_{oc} to K_{ow} can be used for the calculation of K_d,

$$K_{oc} = 0.33K_{ow} \quad (6.4)$$

Using a K_{ow} for cDCE equal to 72.44 (Schwarzenbach et al., 2004), from Eq. 6.4 K_{oc} is equal to 23.9. Then inserting the value of K_{oc} into Eq. 6.3 gives a K_d value of 0.41. This value is consistent with the value estimated in this study.

6.3 Macro-scale Parameter Results

The following sub-sections present the results of the laboratory and field protocols used to estimate the parameters describing the macro-scale transport processes of advection and dispersion. However, as described in Sections 5.5.1 and 5.5.2, prior to estimating the parameters describing advection and dispersion, it was first necessary to determine some of the basic physical properties of the RRL-South aquifer. The first of these properties were the soil bulk and particle densities, which were be used to determine the porosity. The second characteristic, which was required to determine the groundwater seepage velocity, was the hydraulic conductivity (K), which was estimated during slug tests. Together, the porosity, the hydraulic conductivity, and the site hydraulic gradient were used to determine the seepage velocity, as discussed in Section 4.1.1, which represents the advection rate within the RRL-South aquifer. Additionally, results from the laboratory and field tracer studies are presented, which were used to provide estimates for the longitudinal dispersivity at the site, which was then used to estimate the dispersion coefficient. The laboratory tracer experiments were compared to the field tracer study results to

provide a quantitative and qualitative comparison of laboratory and field scale heterogeneity differences.

6.3.1 RRL-South Advection Rate Calculations

6.3.1.1 Soil Densities and Porosity

As discussed in Section 5.5.1, the bulk density was calculated by dividing the oven-dry soil mass by the total volume of the sample. Additionally, the average particle density was calculated using Eq. 5.15. The results of these analyses for the Quantico slate are provided in Table 6.5. Based on the average bulk and particle densities, an average porosity was determined from Eq. 5.16 to be 0.229.

Typical values of porosity for shales, which is the rock type most representative of the Quantico formation at RRL-South, range from 0 to 20%, and sometimes higher (Fitts, 2002). Considering this range in values, the porosity

Table 6.5. Quantico slate soil properties.

Test #	Volume (cm^3)	ρ_b (g/cm^3)	ρ_s (g/cm3)
1	42.23	2.19	2.82
2	36.50	2.15	2.81
	Average	2.17	2.815
		Average η	0.229

estimated in this study is reasonable, albeit slightly higher than reported values. The somewhat high estimate for the porosity may be due to voids created during sampling activities (e.g., cracks perpendicular to the column sleeve, and gaps between the sample and columns sleeves). The presence of such voids would have resulted in the soil in the core being less compacted than in the field, and may help explain why the

estimated bulk density for Quantico slate is lower than the reported values of 2.65 g/cm^3. The effect of ρ_b on *n* is compounded by the relatively high estimated particle density of 2.815 g/cm^3 for the Quantico slate. This value indicates that more dense particles, such as quartz or possibly iron containing minerals are present within the Quantico slate samples. Nevertheless, the porosity estimate is reasonable and, without the benefit of a reference for the Quantico slate's physical properties, the porosity of 0.229 was used for all calculations in the remainder of this work.

6.3.1.2 Hydraulic Conductivity (K) and Seepage Velocity

To calculate the radial conductivity (K_r) using the Bouwer and Rice method (discussed in Chapter 5), a plot of the normalized change in head vs. time is required. The first step in normalizing the data requires each head measurement to be corrected so that the baseline is equal to zero. For example, falling head tests are corrected so that the change in head decreases to zero, and rising head tests increase to zero. Accordingly, for falling head tests the head recorded at any time (t) is subtracted from the baseline value, and the opposite is done for rising head tests, i.e., the baseline is subtracted from each rising head data point. Then each corrected data point is divided by the greatest corrected displacement value. An additional adjustment to the collected data involves the correction of time in order to represent the true start of the test. The true test starting time is defined as the moment of instantaneous slug introduction (i.e., the first reading where a change in head is measured). Finally, the normalized response data are plotted versus the corrected time. A data set typical of that collected for all the monitoring wells is presented in Table 6.6. The data shown are the falling head groundwater response for TMW-S3 (for simplicity only the first

60 seconds of data are shown). The normalized head groundwater response and corrected start time are shown in columns 6 and 7. The slug data for all wells, up to 150 seconds, are provided in Appendix I.

Table 6.6. TMW-S3 falling head groundwater response data for test performed on April 13, 2005.

Date	*Time*	*ET (sec)*	*Pressure (Feet H_2O)*	*Ho-H(t)*	*Normalized (H(t)/Ho)*	*Adjusted t*
3/30/2005	9:54:59	96	11.821	0		
3/30/2005	9:55:02	99	11.819	0		
3/30/2005	9:55:05	102	11.826	0	**Baseline**	
3/30/2005	9:55:08	105	14.037	2.211	1.000	0
3/30/2005	9:55:11	108	13.363	1.537	0.695	3
3/30/2005	9:55:14	111	13.523	1.697	0.768	6
3/30/2005	9:55:17	114	13.26	1.434	0.649	9
3/30/2005	9:55:20	117	13.288	1.462	0.661	12
3/30/2005	9:55:23	120	13.207	1.381	0.625	15
3/30/2005	9:55:26	123	13.205	1.379	0.624	18
3/30/2005	9:55:29	126	13.118	1.292	0.584	21
3/30/2005	9:55:32	129	13.088	1.262	0.571	24
3/30/2005	9:55:35	132	13.021	1.195	0.540	27
3/30/2005	9:55:38	135	13.031	1.205	0.545	30
3/30/2005	9:55:41	138	12.874	1.048	0.474	33
3/30/2005	9:55:44	141	12.966	1.14	0.516	36
3/30/2005	9:55:47	144	12.9	1.074	0.486	39
3/30/2005	9:55:50	147	12.914	1.088	0.492	42
3/30/2005	9:55:53	150	12.889	1.063	0.481	45
3/30/2005	9:55:56	153	12.863	1.037	0.469	48
3/30/2005	9:55:59	156	12.843	1.017	0.460	51
3/30/2005	9:56:02	159	12.82	0.994	0.450	54
3/30/2005	9:56:05	162	12.799	0.973	0.440	57
3/30/2005	9:56:08	165	12.778	0.952	0.431	60

The next step in the slug test data analysis requires that a trend line be fitted to the graphic representation of the data that best represents steady state flow due to the slug introduction. Butler (1997) explains that this line can be drawn through visual inspection or through the use of an automated linear regression routine. Upon visual inspection of the normalized graphs for each slug test in this study (Appendix I), it

was determined that the normalized response data in the range of approximately 30 and 40% (i.e., H_t/H_o = 0.3 to 0.4) corresponded to steady state flow. If this range was not achieved during a particular test due to time constraints, then a comparison was made between all the normalized graphs for that well to determine what range would be best for representing the steady state flow. Specifically, through visual inspection of a template graph, usually the first test ran in that well, the shape of the two curves were compared and a range which best matched the curve of the template was then used for slope determination of the test which did not achieve 30 to 40% recovery. For this study, the trend lines were added to the normalized plots in the selected ranges by using the least squares linear regression analysis in Excel (2000 version). As an example, the slope estimation graph for TMW-S3 is provided in Figure 6.15.

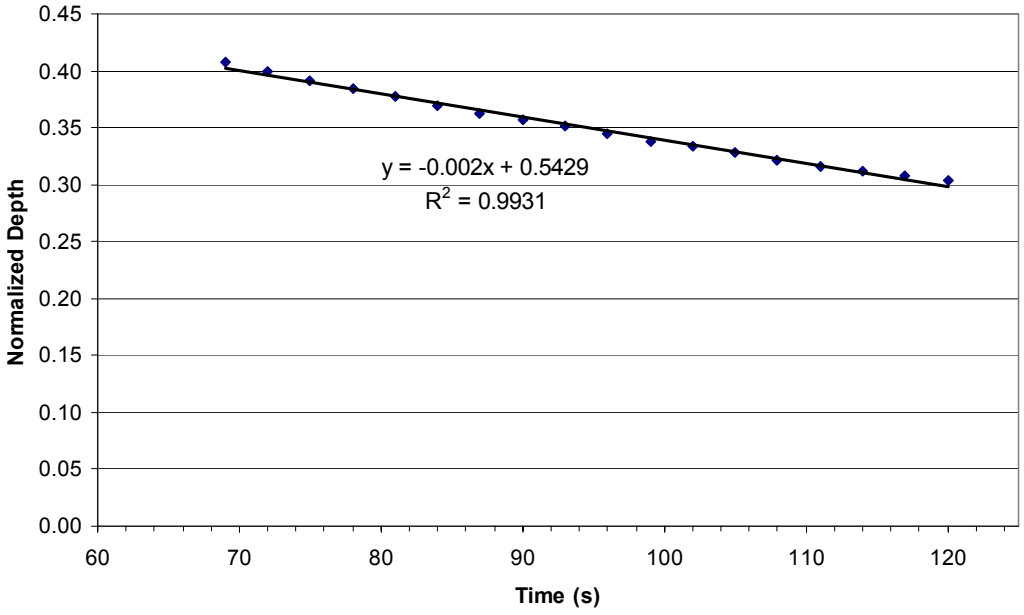

Figure 6.15. Slope calculation for TMW-S3 from falling head test response data presented in Table 6.6.

The normalized data range used, trend line equations, and associated R-squared values that were obtained by following these procedures are presented in Table 6.6 for all slug tests, including the full and half-slugged wells. In addition, all slug test slope calculations are provided in Appendix I.

The slopes of the trendlines in Table 6.6 were used in Eq. 5.21 to calculate K_r. However, several other parameters were also required. The aquifer thicknesses (*b*) are summarized in Table 6.8. In addition, the dimensionless parameters **A** and **B** required to calculate $\ln(R_e/r_w^*)$ using Eq. 5.22 along with the resulting $\ln(R_e/r_w^*)$ values are also provided in Table 6.8.

The final parameter required for estimating K_r was r_c, as defined by Eq. 5.20. However, first the terms H_0^*, H_0^+, and r_{nc}, used in Eq. 5.20 had to be determined. As discussed previously, H_0^* is the expected volume of the initial displacement within

Table 6.7. Trendline equations and R-squared values for all slug tests.

Well ID	***Test Type & Number***	***Normalized Data Range Used***	***Trendline Equation***	***R^2***
TMW-26S	Falling Head (1)	35 – 40%	y = -1E-04x + 0.6138	0.9442
	Rising Head (1)	97 – 99%	y = -2E-04x + 0.9923	0.9133
TMW-S2	Falling Head (1)	30 – 40%	y = -2E-04x + 0.3966	0.9682
	Rising Head (1)	54 – 45%	y = -3E-04x + 0.5263	0.9242
	Falling Head (2)	30 – 40%	y = -2E-04x + 0.3879	0.9517
	Rising Head (2)	30 – 40%	y = -6E-04x + 0.3815	0.8769
	½ Falling Head (1)	31 – 40%	y = -4E-05x + 0.4436	0.9301
	½ Rising Head (1)	30 – 40%	y = -2E-04x + 0.3933	0.8941
	½ Falling Head (2)	60 – 70%	y = -7E-04x + 0.7509	0.9457
	½ Rising Head (2)	10 – 20%	y = -9E-04x + 0.2212	0.9507
TMW-S3	Falling Head (1)	30 – 40%	y = -2E-03x + 0.5429	0.9931
	Rising Head (1)	27 – 35%	y = -9E-04x + 0.5121	0.9412

Table 6.8. Well characteristics and dimensionless parameters.

Well ID	*b*	*A*	*B*	*ln(R_e/r_w*)*
TMW-S2	15	2.70E+00	4.28E-01	2.45E+00
TMW-S3	15	2.91E+00	4.64E-01	2.41E+00
TMW-26S	2.5	1.73E+00	2.76E-01	1.63E+00

the casing, assuming all the displaced water were to remain within the well upon slug introduction. For the larger and smaller displacements (i.e., 70 and 35 inch slugs), a displacement of 3.28 and 1.64 linear feet was calculated for H_0^*, respectively, based on the slug dimensions. H_0^+, the apparent value for the initial displacement, was determined by continuing the trend line obtained in the slope calculations to the y-intercept, or, if the line was calculated using the linear regression analysis the y-intercept is provided in the equation for the line. This point on the y-intercept, as illustrated in Figure 6.16 is equal to approximately 0.54, which corresponds to an H_0* value of 1.195 (see Table 6.6). Finally, the nominal casing radius (r_{nc}) is defined as half the diameter of the casing (i.e., 1 inch). Table 6.9 provides the calculated values of r_c for each slug test, as well as the radial hydraulic conductivity, as defined by Eq. 5.22. Also shown in Table 6.9 are the corresponding values for the seepage velocity, which were estimated by using Darcy's equation (Eq. 4.2) with the given K_r, the porosity from Section 6.3.1.1, and the local RRL-South hydraulic gradient, which between wells TMW-S3 and TMW-26S is estimated at approximately 0.56 (ft/ft) Using the data from Table 6.9, average values for K_r and v were calculated for each well, as summarized in Table 6.10. However, the half slug readings for falling head (2) and rising head (2) in TMW-S2 were not used to estimate the average hydraulic conductivity and velocity for that because these points

were not representative of the site based on the values obtained for the first six readings in TMW-S2.

Table 6.9. Hydraulic conductivity and seepage velocity estimates.

Well ID	Test Type & Number	r_c	K_r (ft/s)	K_r (m/day)	Velocity (m/day)
TMW-26S	Falling Head	0.12	3.8e-7	0.009	0.024
	Rising Head	0.11	6.9e-7	0.018	0.046
TMW-S2	Falling Head (1)	0.25	1.0e-6	0.027	0.070
	Rising Head (1)	0.18	7.5e-7	0.021	0.049
	Falling Head (2)	0.25	9.8e-7	0.027	0.064
	Rising Head (2)	0.22	2.4e-6	0.064	0.155
	½ Falling Head (1)	0.38	4.6e-7	0.012	0.030
	½ Rising Head (1)	0.32	1.7e-6	0.046	0.107
	½ Falling Head (2)	0.31	5.5e-6	0.146	0.354
	½ Rising Head (2)	0.52	2.0e-5	0.536	1.31
TMW-S3	Falling Head	0.15	3.7e-6	0.098	0.238
	Rising Head	0.17	2.0e-6	0.052	0.128

Table 6.10. Average conductivity and velocity estimates.

Well ID	K_r Average (ft/day)	K_r Average (m/day)	Average *v* (ft/day)	Average *v* (m/day)
TMW-26S	0.05	0.02	0.12	0.05
TMW-S2	0.11	0.03	0.26	0.08
TMW-S3	0.25	0.08	0.60	0.20
RRL-South Averages:	0.14±0.08[1]	0.04±0.03	0.33±0.20	0.10±0.07

[1] Average ± standard deviation.

As discussed in Chapter 5, using the modified Bouwer and Rice method resulted in hydraulic conductivity values that were 46 to 51% greater than those obtained when using the unmodified method. The only difference in the two methods is the determination of r_c, which requires a slight modification when using the Bouwer and Rice method for wells screened at or near the groundwater surface in

unconfined aquifers. Following the suggestion of Butler (1997) the modified method was used to calculate K_r for this study based on the proximity of the tops of screened intervals to the groundwater surface.

Linsley et al. (1992) (cited in Masters (1998)) provides an average shale conductivity value of 0.041 m/day (0.134 ft/d), while Freeze and Cherry (1979) state that values of the hydraulic conductivity of intact samples of shale tested in the laboratory are rarely larger than 8.6×10^{-5} m/day (2.8×10^{-4} ft/d) and are commonly in the range of 8.6×10^{-6} to 8.6×10^{-8} m/d (2.8×10^{-5} to 2.8×10^{-7} ft/d) (Peterson, 1954; Young et al., 1964; Davis, 1969; Moran et al., 1976). The estimated Quantico slate hydraulic conductivities in Table 6.10 are much greater than those reported by Freeze and Cherry. However, these K values are comparable to the value estimated by Linsley et al. (1992). A possible cause for these greater K values, compared to those reported by Freeze and Cherry (1979), may be due to the geologic structure of the Quantico formation in the area of RRL-South. As discussed in Chapter 1 the Quantico slate in the area is more representative of shale. Furthermore, given the friable nature of the formation in the area of RRL-South, the composition of the rock may even be less competent than a "true" shale, thus, increasing the porosity of the formation (see Section 6.3.1.1). The friability of the RRL-South Quantico slate may be a result of fracturing present in the formation, as discussed in Chapter 1. These fractures may have also resulted in the greater hydraulic conductivity values and, thus, the greater seepage velocity values by creating secondary porosity (Freeze and Cherry, 1979).

The average seepage velocities shown in Table 6.10 are slightly higher than would be expected given the relatively low K_r values. The cause for the greater velocity values is the large hydraulic gradient at RRL-South due to the road cut adjacent to the site (see Section 1.2.3), coupled with the high estimated porosity for the Quantico slate at RRL-South, as calculated in Section 6.3.1.1. Nevertheless, these values correspond with the velocity estimated from the field tracer studies, as discussed in the following section 6.3.2.2.

6.3.2 RRL-South Dispersivity Calculations

6.3.2.1 Laboratory Measurements

Following the protocols described in Chapter 5, dispersivity estimates were obtained in the laboratory by performing conservative tracer studies using a core sample collected from the RRL-South area. The column operating parameters used in these tests are provided in Table 5.4. Tracer concentrations in the collected effluent water were plotted with respect to time for the three tests described in Section 5.5.3.1, and the resulting breakthrough curves (BTCs) are presented in Figure 6.16.

The best fit model results, obtained by following the analysis protocols described in Section 5.5.3.1.1, are provided in Table 6.11. In addition, the best fit

Table 6.11. Best fit parameters for laboratory column tracer study.

Test	***Porosity***	***Seepage Velocity (m/day)***	***D_x (m^2/day)***
1	0.40	4.44	0.12
2	0.31	5.36	0.21
3	0.34	5.26	0.23
Average:	0.35±0.04[1]	5.02±0.41	0.19±0.05

[1] Average ± standard deviation

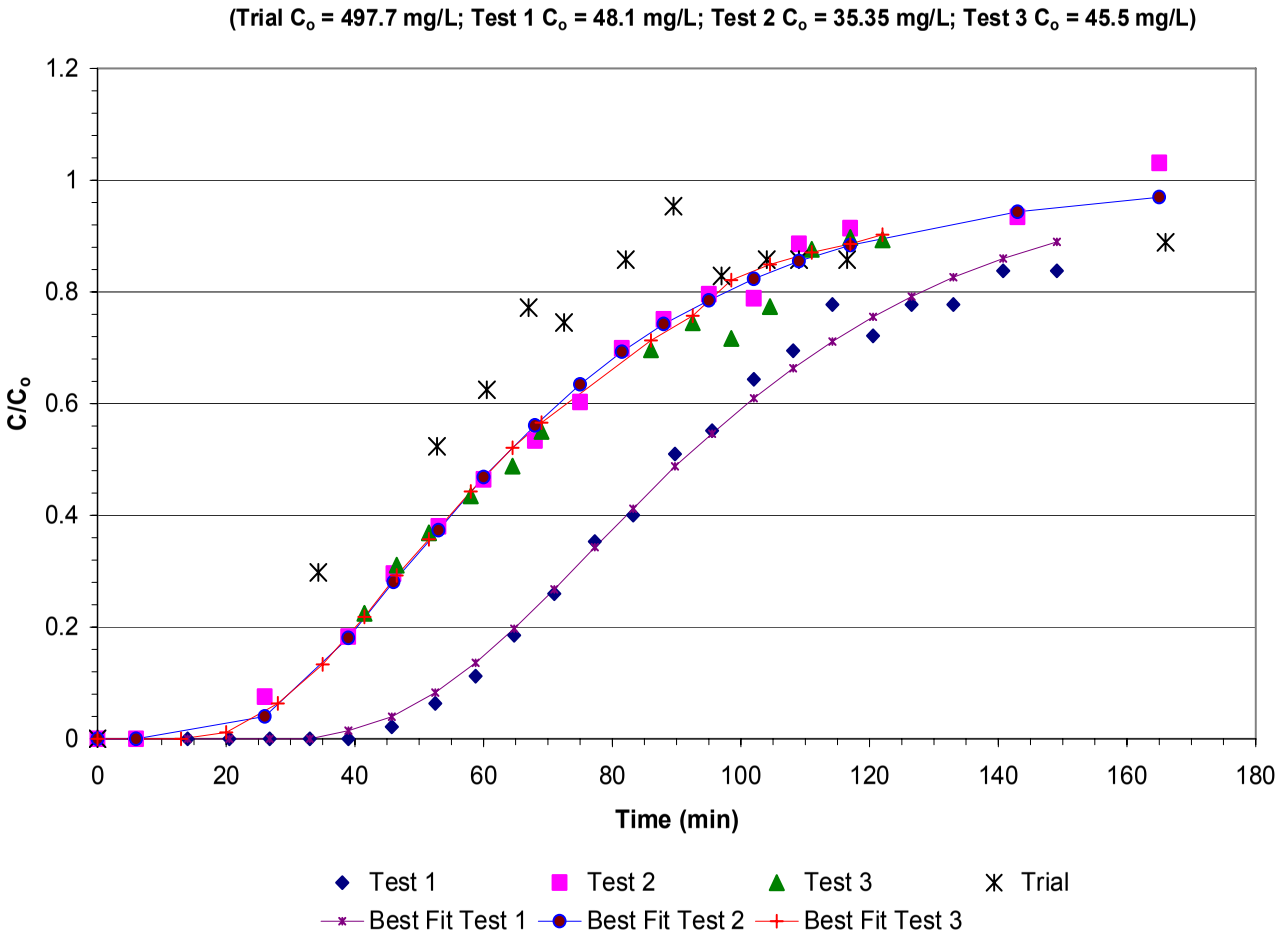

Figure 6.16. Laboratory bromide tracer breakthrough curves with model best fit.

output results for all laboratory tracer tests, which were generated using the Fortran program, (described previously) are provided in Appendices F and K.

The average porosity best fit parameter is much higher than was calculated based on the bulk and particle densities in Section 6.4.1.1, and higher than expected for the Quantico slate aquifer material. The higher porosity value obtained in the column studies may be the result additional pore space formed along the column wall, or through cracks in the sample, both of which may have resulted from sampling activities and from the disturbance of the soils during the construction of the laboratory column. For these reasons, the porosity value of 0.229, estimated based on the bulk and particle densities, was used in the dimensionless parameter calculations.

Using the average best-fit dispersion coefficient calculated above, the dispersivity of the Quantico slate can then be calculated by rearranging Eq. 4.3, to yield the following equation:

$$\alpha_L = \frac{D_L - D_{diff}}{v} \qquad (6.3)$$

where D_{diff} is the effective diffusion coefficient for bromide in the porous medium, and v is the average seepage velocity. Assuming that the diffusion of bromide within the Quantico slate aquifer is extremely small, e.g., on the order of approximately 10^{-5} m^2/day (1.07 x 10^{-4} ft^2/d), then $D_{diff} << D_L$. Therefore, Eq. 6.3 can be rewritten to describe the longitudinal dispersivity as follows:

$$\alpha_L = \frac{D_L}{v} \qquad (6.4)$$

From Eq. 6.4 the average laboratory estimate of α_L for the Quantico slate is approximately 0.04 m (0.12 ft).

6.3.2.2 Field Measurements

The seepage velocity and longitudinal dispersivity were also estimated from the breakthrough curve generated during field tracer study (Figure 6.17), as described in Section 5.5.3.2. During the field tracer study only monitoring wells TMW-S3 and TMW-26S were consistently sampled. However, as shown in Appendix K, TMW-26D was also sampled after the peak concentration was detected in TMW-26S (see Figure 6.17), and no bromide was detected within this well. Consequently, the only well that provided a BTC was TMW-26S, while the samples from similar depths within TMW-S3 did not provide measurable results, as illustrated by the curves in Figure 6.18.

Bromide was assumed to be a conservative tracer, so that the seepage velocity could be calculated from the known distance between the injection point and the sampling point (x_1) and the time to the peak concentration (t_{peak}) for the breakthrough curve (Smith et al., 1991; Harvey & Garabedian, 1991):

$$v = \frac{x_1}{t_{peak}} \tag{6.5}$$

The distance between TMW-IPS2 and TMW-26S, x_1, was approximately 9.65 ft, and from the BTC, shown in Figure 6.18, t_{peak} is approximately 23 days. Therefore, the fluid velocity, based on field tracer estimates, and Eq. 6.5, is approximately 0.13 m/day (0.42 ft/day). This estimate is very comparable to the seepage velocity of 0.10±0.07 m/day (0.33±0.2 ft/day) that was estimated from the slug test data (Section 6.3.1.2). However, given that the average seepage velocity was more directly measured by the field tracer study and the similarity between field tracer and slug

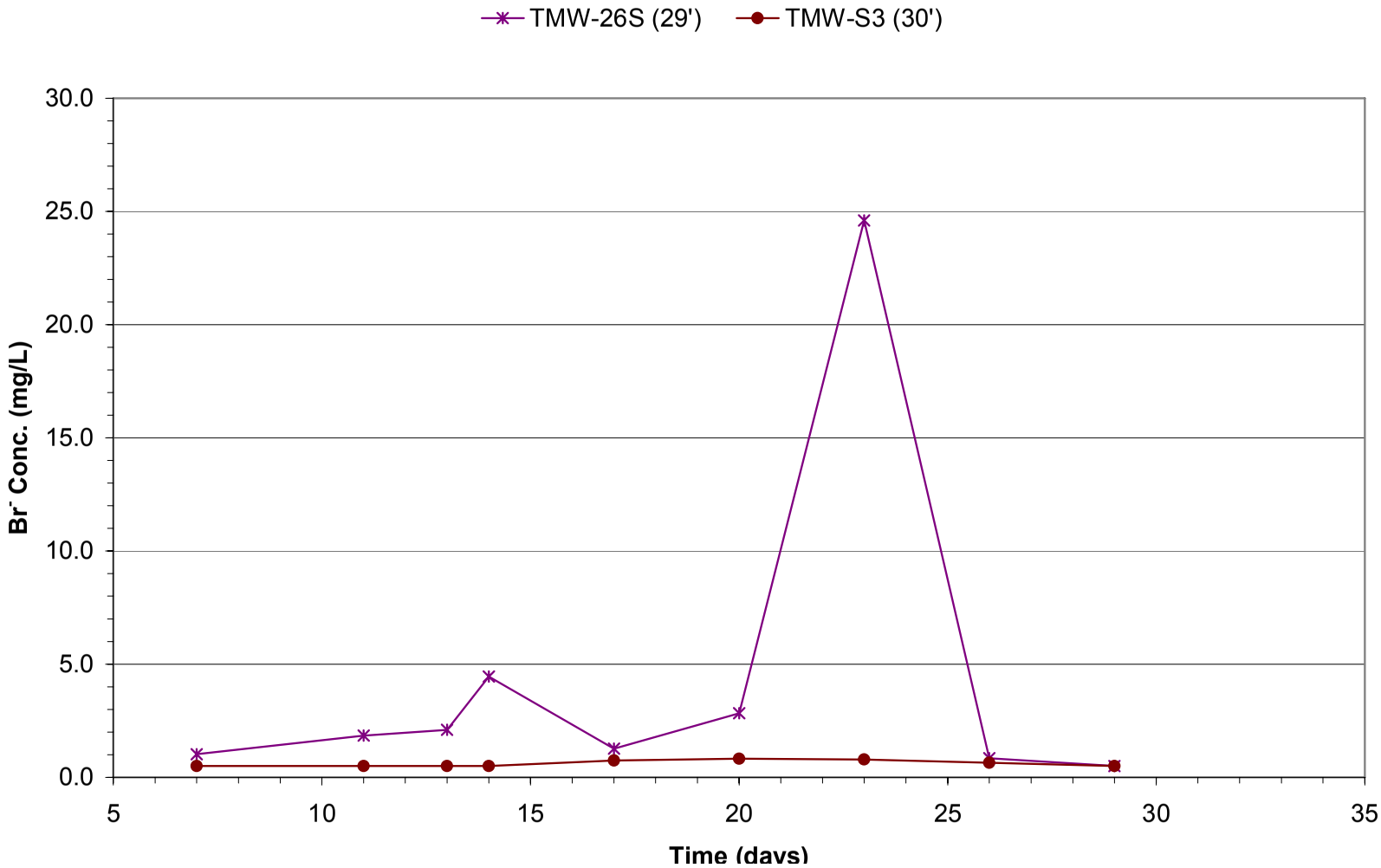

Figure 6.17. Field bromide breakthrough curve at TMW-

velocity estimates, a range of *v* was, therefore, set equal to 0.03 – 0.17 m/d (0.10 – 0.56 ft/d) in the all dimensionless number calculations.

To calculate the longitudinal dispersivity parameter (α_L) from the field tracer study data, the following relationship, obtained from the one dimensional solution of the advection dispersion equation (described in Chapter 4), was applied to the breakthrough curve (Smith, et al., 1991; Harvey and Garabedian, 1991):

$$\alpha_L = \frac{x_1\left(\Delta t / t_{peak}\right)^2}{16\ln(2)} \qquad (6.6)$$

where Δt is the duration of the breakthrough curve when $Br_{(t)} > 0.5\ Br_{max}$, and Br_{max} is the peak concentration. From the field tracer breakthrough curve Δt is equal to approximately 3.5 days, and Br_{max} = 24.6 mg/L (Figure 6.18). Therefore, from Eq. 6.6, α_L is approximately 6.1 x 10^{-3} m (0.02 ft). Finally, by rearranging Eq. 6.4 and inserting the value obtained for the field α_L estimate, and the longitudinal dispersion coefficient (D_L) was estimated to be 6.1x10^{-4} m^2/day (6.6 x 10^{-3} ft^2/d). This estimate of α_L is much smaller than the value of 0.04 m (0.12 ft) obtained in the laboratory column tracer study. It was actually expected that the field-scale α_L value would be larger than the laboratory-scale value due to the fact that at the field-scale there is typically additional heterogeneity induced dispersion, in addition to the mechanical dispersion and molecular diffusion described by Eq. 4.3.

In order to explore the effect of the range of α_L values on the dimensionless parameter framework results, both the field and laboratory-scale tracer study derived values for α_L were used to obtain a range of values dimensionless parameter values in all calculations for the dimensionless framework.

6.4 Dimensionless Parameter Framework Analyses

To achieve the overall goal of this research, which was to quantify the rate-limiting factors that may influence biodegradation at RRL-South, the results from the biokinetics, mass-transfer kinetics, and macro-scale studies were evaluated using the dimensionless parameter framework discussed in Chapter 4. Additionally, the results of the quantitative framework analysis were used to interpret the results of the ongoing pilot remediation study and evaluate whether or not the current approach should be altered based on the final outcome.

The first step in the quantitative framework analysis was to select the system parameters to use and then define the dimensionless numbers. The system parameters used are summarized in Table 6.12. For the biokinetics study, as discussed previously, the results were inconclusive. Although there were slight decreasing trends for cDCE after the pH adjustment in the cometabolic and aerobic treatment bottles, there was no clearly defined trend in degradation and it was not possible to obtain any biokinetic parameters, e.g., q_{max}. Therefore, for this dimensionless parameter analysis the biokinetics are assumed to be the rate-limiting step, and the dimensionless parameters related to biokinetics, e.g., Da_2, Da_5, and Da_6, are set << 1. Given this assumption, it was not necessary to obtain a value for the initial biomass, X_o.

The results of the mass-transfer kinetics experiments indicated that the sorption of cDCE onto the Quantico slate aquifer sediments was relatively limited but rapid, with an estimated k_m of 0.127±0.074 d^{-1}. This estimated k_m value range was used in the dimensionless numbers related to mass-transfer kinetics, e.g., St_2, and

Sh_2'. The sorption rate range was then propagated to the dimensionless parameter framework. Therefore, the high and low values could be compared separately in the Stanton and Modified Sherwood numbers.

Table 6.12. Parameters used for quantitative framework analysis at RRL-South.

System Parameter	Definition	Value Used in Dimensionless Evaluation
$\hat{q}$	Maximum specific substrate utilization rate	Very small ~ 0
X_o	Initial biomass concentration	Unknown
A_o	Initial cDCE concentration	0.382 mg/L[1]
k_m	Sorption mass-transfer coefficient	0.053 – 0.201 d^{-1}
L	Characteristic length (i.e., saturated zone thickness)	4.24 m (13.9 ft) [2]
v	Average seepage velocity	0.03 – 0.17 m/d (0.10 – 0.56 ft/d)
α_T	Horizontal transverse dispersivity = $\alpha_L/10$	$6.1x10^{-4}$ – 0.004 m (0.020 – 0.013 ft)
D_T	Horizontal transverse dispersion = $\alpha_T v$	$1.8x10^{-5}$ – $9.6x10^{-4}$ m^2/d ($5.9x10^{-5}$ – $3.1x10^{-3}$ ft^2/d)

[1] Average baseline cDCE field concentration from Table 1.5.
[2] Average water column depth from Table 5.1.

Finally, for the macro-scale study, the analysis was based on a combination of laboratory and field results. As discussed in Section 6.3, the values for the seepage velocity determined in the field (e.g., slug and tracer tests) and the longitudinal dispersion coefficient that were determined in both the field and laboratory tracer studies were considered to be the most robust, and are used as the starting point here. To calculate a value range for the horizontal transverse dispersion, the low and high seepage velocity values that were obtained from the slug and field tracer tests (Table 6.12) were compared to the lowest and highest horizontal transverse dispersivity values obtained in the field and laboratory tracer studies (i.e., $6.1x10^{-4}$ to 0.004 m).

Thus, a horizontal dispersion value range was calculated as 1.8×10^{-5} to 9.6×10^{-4} m^2/d (5.9×10^{-5} to 3.1×10^{-3} ft^2/d), thereby resulting in a value range for the transverse Peclet number used in the dimensionless framework.

By comparing the lowest and highest values for the seepage velocity and D_T, and given the characteristic length equal to the effective aquifer depth of 4.24 m (13.91 ft), a range of Pe_T was approximately 750 to 7,066, and the values are much greater than 1 (Table 6.13). Thus, transverse dispersion is a far more limiting mass-transfer process than advection. As a result, the next step in the dimensionless parameter analysis framework (Figure 6.19), is to compare the sorption rate and the transverse dispersion rate using the modified Sherwood No. 2 (see Table 6.13).

Table 6.13. Quantitative framework used to identify the overall rate limiting process at RRL-South

Dimensionless Parameter	Definition	Value Range		Outcome
		Low	High	
Pe_T	= Transverse Peclet No. $= \frac{v_x L}{D_T}$	750	7,066	>>1
Sh_2'	=Modified Sherwood No. 2 $= \frac{k_m L^2}{D_T}$	3,764	$5.2 \times 10_4$	>>1
Da_6	= Damköhler No. 6 = $\frac{q_{max} X_o L^2}{A_o D_T}$	~0*	~0*	<<1*

*Assuming q_{max} approaches zero.

Given the discrepancy between the field and laboratory obtained values for α_L, it is interesting to see if only using the laboratory value for α_L has an effect on the

outcome of the analysis. For the laboratory experimental estimate, the transverse Again, by comparing the low and high values of k_m to the low and high D_T values, a Sh_2' value range of approximately $3.7x10^3$ to $5.3x10^4$ was obtained, which is much greater than 1. This indicates that transverse horizontal dispersion is a more limiting mass-transfer process than adsorption to the soil, which is consistent with the relatively fast and limited sorption observed in this study.

Thus, based on the first two steps of qualitative framework, the limiting mass-transfer process at RRL-South is horizontal transverse dispersion. As a result, the final step in the dimensionless parameter analysis, as illustrated in figure 6.14, was to

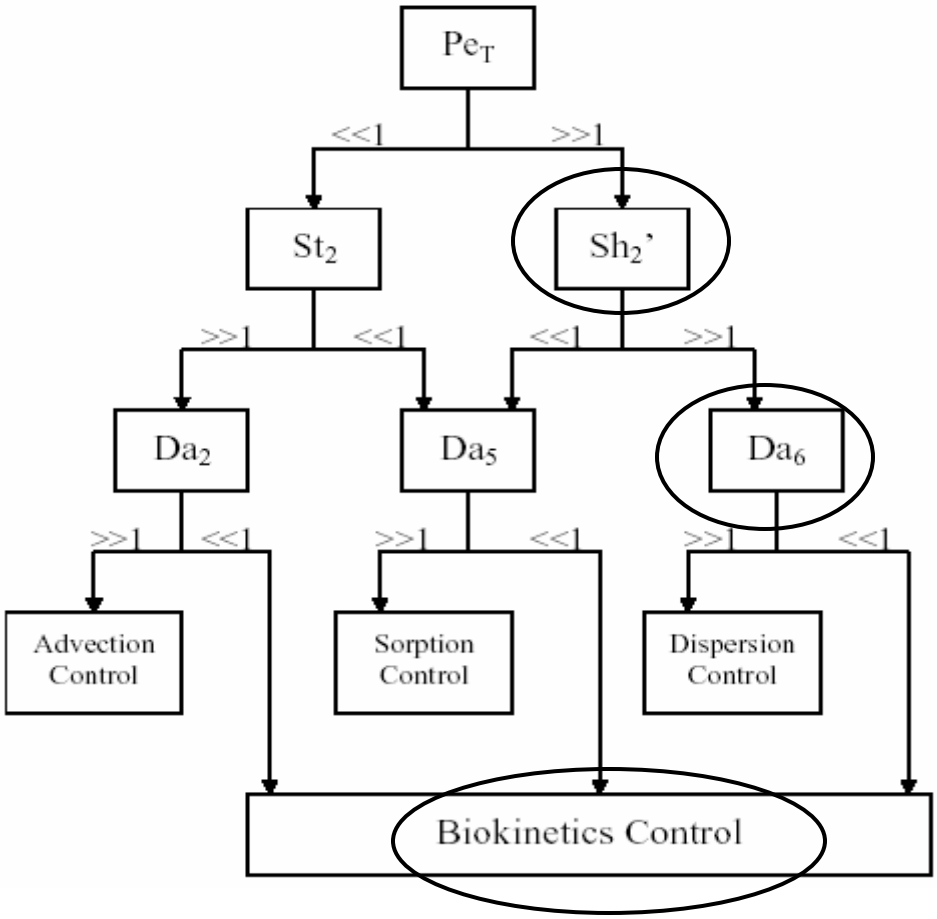

Figure 6.18. Dimensionless parameter framework outcome based on the study estimates of biokinetic, mass-transfer, advective, and dispersive rates.

compare horizontal transverse dispersion to the biokinetics. Considering the very limited biodegradation observed, biokinetics is probably the overall rate-limiting factor that controls *in situ* cDCE biodegradation (Table 6.13).

The outcome depicted in Figure 6.18 may, however, be different if the slightly decreasing trends noted for the aqueous cDCE concentrations in the cometabolic (COM) and the aerobic (DO) treatments represent actual biodegradation of cDCE. These trends, however, could not be verified possibly because of experimental time constraints for this study. If these contaminant reduction trends did indeed indicate biodegradation of cDCE, then the biokinetics may not be as rate-limiting as thought, and the biokinetics may be such that Da_6 is not $<<1$ under cometabolic or aerobic conditions. Assuming this to be the case at RRL-South, then the dimensionless parameter framework outcome would indicate that horizontal transverse dispersion is controlling biokinetics, as illustrated in Figure 6.19. This is consistent with the field tracer study which indicated that the magnitude of transverse dispersion was small compared to longitudinal dispersion based on the lack of tracer observed in TMW-S3. Although this scenario is plausible, without the benefit of further biodegradation data this outcome remains an assumption. Nevertheless, it appears likely that transverse dispersion or biokinetics, or both processes are the overall rate-limiting process controlling the rate of in situ biodegradation at RRL-South.

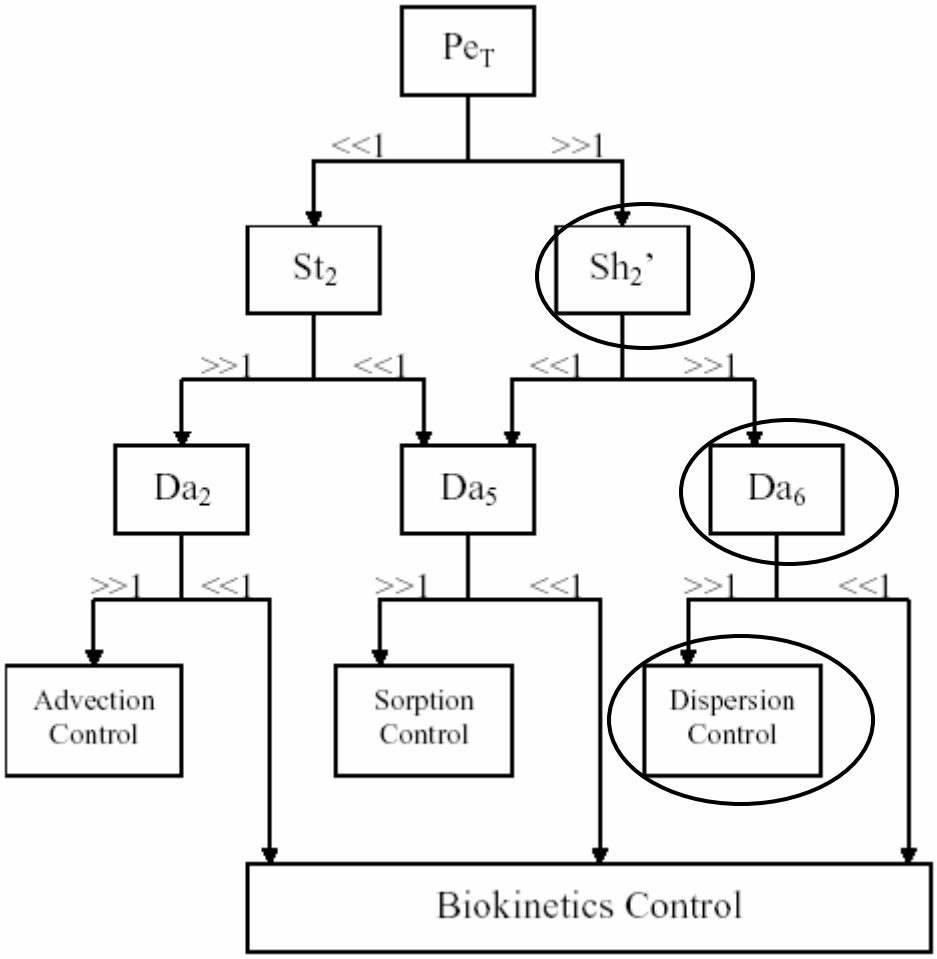

Figure 6.19. Dimensionless parameter framework outcome based on the assumption aerobic biodegradation occurs and transverse dispersion is the rate-limiting step.

7.0 SUMMARY AND CONCLUSIONS

Low concentrations of cDCE have been detected in the groundwater emanating from the Russell Road landfill located on the Marine Corps Base in Quantico, Virginia. Specifically, the contaminant plume in the RRL-South area has shown historic PCE, TCE, and cDCE concentrations above the EPA (2003) established MCLs of 0.005, 0.005, and 0.07 mg/L, respectively. The historic concentration of cDCE in the RRL-South area has been the greatest of the three, with levels exceeding 0.3 mg/L, while the other CAHs were near, or below, the MCLs. Based on the anaerobic conditions of the landfill source zone coupled with the low concentrations of the more highly chlorinated ethenes (i.e., PCE and TCE) and the high concentration of cDCE, it has been concluded that reductive dechlorination is occurring in the RRL-South contaminant plume to create the lesser chlorinated ethene daughter product, cDCE, with minimal further transformation.

To determine if the concentrations of cDCE could be further reduced by reductive dechlorination, Battelle, of Columbus, Ohio, implemented a pilot-scale bioremediation program which involved the periodic injection of HRC® directly into the groundwater. This remedial approach was largely selected based on results from a bench-scale test conducted by Regenesis, the manufacturer of HRC®, which indicated that microbial species were present in the Quantico formation that were capable of degrading small levels of TCE over time when additional electron-donor source in the form of HRC® was added. Based on these results, the first pilot injection of HRC® was conducted at RRL-South in November 2003.

Groundwater sampling was conducted approximately 30 days after the first HRC® injection and continued for 6 months, with sampling events occurring every month. The results from these post-injection analyses were compared to a baseline sampling event, which occurred a few days prior to the HRC® injections. Upon review of the CAH data and other indicators of reductive dechlorination, e.g., increased chloride levels, the author concluded that a clear trend indicating enhanced contaminant reduction had not occurred. In fact, based on post-injection results it was clear that little or no biodegradation of CAHs was occurring at RRL-South. In order to determine the overall rate-limiting step that was preventing *in situ* bioremediation from occurring, a systematic approach was employed. The approach used was based on a quantitative framework of dimensionless numbers, which had previously been applied in modeling (Johnson, 2004) and laboratory-scale studies (Song, 2005). First, following the steps suggested by Sturman et al. (1995), the relevant scales of observation (i.e., micro-, meso-, and macro-scales) were identified. Then, the key system parameters were identified at each scale (e.g., biokinetics, mass-transfer kinetics, and advective and dispersion rates) and analyzed through a series of laboratory and field experiments. Subsequently, these parameter values were used to calculate a set of dimensionless parameters that were systematically compared using a flowchart framework in order to quantitatively identify the overall rate-limiting steps limiting *in situ* biodegradation. The goal was to demonstrate that the results of the framework could be used by a remediation engineering practitioner to identify the overall rate-limiting process, and, therefore, be able to enhance the subsurface

appropriately by selecting the best approach for overcoming the rate-limiting process and thereby stimulating biodegradation.

Accordingly, at the micro-scale a biokinetics study was conducted using groundwater and sediment from the RRL-South site. For this study a total of 7 systems were analyzed, including two aerobic and three anaerobic microcosm treatments. Of these microcosms, only the aerobic treatments, one of which was dosed with both oxygen and methane in an attempt to stimulate cometabolic biodegradation of cDCE (labeled COM-#), and the other dosed solely with oxygen (labeled DO-#) to stimulate aerobic oxidation of cDCE, showed a slight reduction in aqueous cDCE levels. The anaerobic treatments, which were spiked with HRC®, molasses, and lactate, as the electron donor substrates, did not show any clear trends in cDCE reduction. Furthermore, to verify that the samples were representative of RRL-South, PCE was injected into the HRC®, molasses, and lactate bottles stored at 30^{o}C. Similar to the cDCE trends, no PCE reduction was observed in any of the treatment bottles. The lack of degradation was verified through other indicators in the microcosms, such as methane concentrations and oxygen levels, which remained relatively stable throughout the experiments, except in the COM and DO treatments. It is not surprising that the cometabolic and aerobic treatments showed the most, albeit limited, potential for cDCE removal given that at the RRL-South location there is a natural mixing of cDCE, methane, and oxygen. Nevertheless, it was difficult to determine exactly what at the micro-scale was limiting *in situ* biodegradation of cDCE. One possibility is that the appropriate microbial species capable of degrading cDCE, either via cometabolism, aerobic oxidation, or reductive dechlorination, are

not present, or are present in such few numbers that the lag time required for observable degradation to occur was longer than was allowed for in this study. Furthermore, the degradation rates for field-scale contaminant reductions is considerably longer compared to laboratory scale degradation rates (Sturman, 1995), and given that contaminant reductions still had not been observed at RRL-South, the lack of cDCE within the treatments is not surprising.

Another possibility is that the relatively low site groundwater pH is inhibitory to cDCE biodegradation via the mechanisms test. The fact that the only possible removal in the biokinetics study occurred after the pH was adjusted from a range of 2 – 3 to neutral, suggests that this might be at least part of the explanation. There was also the issue that the core sample used as the microcosm innoculum was stored in a 4^{o}C refrigerator for 18 months prior to the start of the experiments, and that the cores were disturbed during sampling activities.

At the meso-scale, a cDCE sorption mass-transfer rate experiment, as well as an equilibrium partitioning study, utilizing the EPICs method, was conducted using RRL-South aquifer sediments and groundwater. From these tests a range for the sorption rate was determined to be between 0.053 and 0.201 d^{-1}. Additionally, using the EPICs method, the average K_d value for the Quantico formation was determined to be approximately 0.38 L/kg, which was consistent with the findings of others from the literature (DeWulf et al., 1998). These results indicated the cDCE sorption to the aquifer solids occurred relatively rapidly, but was also relatively limited in magnitude.

Finally, the macro-scale parameters describing the advection and dispersion rates were also determined. First, the Quantico formation physical properties (i.e., bulk and particle densities, and porosity), and the formation hydraulic conductivity were determined from a series of laboratory and field slug tests, respectively. From laboratory experiments the bulk and particle density were determined to be 2.815 g/cm^3, and 2.815 g/cm^3, respectively, which were then used to calculate a porosity value of 0.229. Based on these calculations and the results from numerous slug tests, the hydraulic conductivity was estimated to be 0.04 m/day, which is greater than most reported values for shales. However, given the geology of the site, the comparison between the Quantico formation at RRL-South and a true shale, may be slightly misleading. Specifically, the observed fracturing and the extremely friable nature of the site formation may result in increased secondary porosity, and therefore, increased hydraulic conductivity. To calculate the average seepage velocity at RRL-South, the estimates for porosity and hydraulic conductivity were used in Darcy's equation, along with the local hydraulic gradient, in the area of TMW-26S, which was found to be approximately 0.56. This high gradient, which was caused by the road cut to the south of TMW-26S, yielded and average velocity estimate of 0.1 m/d.

As verification for this velocity estimate, and to determine the field scale dispersion rate, a radially divergent tracer test was performed at RRL-South. Using the well IP-S2 as the injection point, the conservative tracer, bromide, was introduced as pulse input and allowed to migrate with the natural groundwater flow. Only monitoring well TMW-26S yielded detectable levels of bromide as a result of this injection, with a breakthrough peak of approximately 23 days. From this

breakthrough curve, the longitudinal dispersivity, α_L, was estimated at $6.1x10^{-3}$ m, and the seepage velocity, v_x, was approximately 0.13 m/day, a value consistent with the velocity estimated from the slug tests. In addition to the field tracer study, laboratory tracer tests were conducted on a 1.5 in x 12 in core sample from the RRL-South site, again using bromide as the tracer. The results from the laboratory tracer test gave a greater value for the longitudinal dispersivity equal to 0.04 m, possibly due to additional porosity in the laboratory column. Because of the variability in these parameter estimates, the range in v values from the field, and α_L from the laboratory and field were used in the dimensionless parameter evaluation. Furthermore, although transverse dispersion was not specifically calculated in this study, based on findings by Gelhar et al. (1992), the horizontal transverse dispersion is typically 10 times less than the longitudinal dispersion. Therefore, the range of field scale horizontal transverse dispersivity was estimated as approximately $6.1x10^{-4}$ to 0.004 m.

The key, scale-dependent parameters calculated in this study were then used to calculate a series of dimensionless parameters that could be systematically compared using a quantitative framework. The first two stages in the framework were used to determine the rate-limiting mass-transfer process, as detailed in Chapter 4. First, the transverse Peclet number was found to be >>1 based on the laboratory and field dispersion and advection values, indicating that horizontal transverse dispersion was more limiting than advection. Then the sorption mass-transfer rate and the transverse dispersion rate was compared using the modified Sherwood Number 2, which also was >>1, indicating that horizontal transverse dispersion was more limiting than

sorption. The final step in the framework was the calculation of the Damköhler Number 6, which is defined as the ratio of the degradation rate per the transverse dispersion rate. Because the biokinetics results were inconclusive it was not possible to quantitatively calculate Da_6, but biokinetics appear to represent the limiting rate. Thus, biokinetics control biodegradation rates, and $Da_6 >> 1$. Nevertheless, there is the possibility that the biokinetics studies underestimated the biodegradation potential because of the condition of the samples prior to and during the experiments, i.e., the innoculum storage and pH issues discussed above. If the biokinetics were impacted in any way due to these factors then Da_6 could potentially be $<< 1$, given the relatively small magnitude of the horizontal transverse dispersion process. Despite these uncertainties, from these findings it is evident that biokinetics and/or transverse dispersion are the rate-limiting steps controlling *in situ* biodegradation at RRL-South.

It is interesting to consider the outcome of the quantitative framework analysis in light of the results obtained in the ongoing pilot-scale program for HRC® injections at RRL-South. One, the framework prediction that biokinetics are rate-limiting suggests that the contractor's decision to add an electron donor to stimulate the microbial-mediated reductive dechlorination of cDCE was not fundamentally wrong, in the sense that they were trying to stimulate the micro-scale biokinetics. However, it was not demonstrated that: (1) reductive dechlorination was the best cDCE degradation mechanism to try to stimulate, (2) the electron donor substrate was what was limiting the occurrence of reductive dechlorination of cDCE, nor (3) microbes capable of mediating that transformation were present. In addition, the pilot-program did not address the occurrence of sulfide oxidation in the RRL-South aquifer sediments and

the fact that the resulting low pH may be limiting all possible cDCE biodegradation mechanisms.

Two, the use of an injected, low water solubility substrate like HRC®, may not be the best choice considering that the dimensionless framework indicates that transverse dispersion is the rate-limiting mass-transfer process. Specifically, as a substrate like HRC® breaks down to form lactate that can be fermented to H_2 and acetate, the only way that the resulting electron donor substrates can be transported into the formation is by advection and dispersion away from the injection point. The fact that dispersion was so limiting means that the horizontal and vertical movement of the H_2 and acetate into the formation and, hence, to the microorganisms, will be very limited. On the other hand, if a soluble limiting substrate were used in such a situation and circulated through the contaminated zone via a controlled use of groundwater pumping and injection, the increased groundwater flow would result in increased dispersion (recall $D_i = \alpha_i v_i + D_{diff}$), thus there would be improved mixing into the formation and, thereby, a better supply of substrates to the microbes.

For future work it is apparent that adequate biokinetics studies need to be performed prior to selecting a microbial substrate amendment. Additionally, these studies must be conducted relatively quickly after sampling to avoid microbial viability loss, and the tests should be conducted under site conditions on the contaminant of interest. For example, the Regenesis bench-scale biokinetics study was applied to collect data for the degradation of TCE at RRL-South, which is a contaminant that historically has been near or below the MCLs. Furthermore, based on the possibility of transverse dispersion being the rate-limiting step, coupled with

the field tracer results, the current configuration of injection and monitoring wells at the site may not be delivering the electron donor substrate effectively into the Quantico formation aquifer.

Although there have been several numerical modeling studies that incorporate the interactions between key physical/chemical heterogeneities and bioremediation (e.g., Wood et al, 1994; Karapangioti et al, 2001; Johnson, 2004), few experimental studies (Murphy et al, 1997; Szecsody et al, 1994; Song, 2004) have been reported that evaluate several phenomena at more than one scale and how they relate to bioremediation. Thus, field-scale research reported here represents a step toward the development of a useful quantitative tool for defining when *in situ* bioremediation will work, and when an engineered or intrinsic approach is best. Such a tool is needed as the general practitioner has neither the time nor financial resources to devote to establishing a sophisticated numerical modeling approach.

7.1 Recommendations for Future Research

The goal of this research was to determine the applicability of a dimensionless parameter framework for predicting rate limiting conditions affecting the *in situ* bioremediation of cDCE at RRL-South. Although the results indicated that such a framework was capable of predicting rate limiting conditions, as shown through the comparison of framework out comes and ongoing pilot-scale program results, there remains the question of the general applicability to additional field sites. From the results of this study a few comments can be made to help with future applications of this framework at sites other than RRL-South. Specifically, the degree of library research coupled with laboratory and field investigations are clarified in order to

minimize the labor and time required to determine the parameters required for the framework analyses.

The first process for obtaining data required in the framework analyses may simply involve a library review for sorption and biodegradation potentials based on the site groundwater and soil characteristics, which can be determined through a basic site characterization. For example, in the current study, the fraction of organic carbon within the Quantico slate was already known and, therefore, when applied to Eq. 6.3 an estimate for the sorption partition coefficient could be calculated. As seen in Eq. 6.3, however, the value for K_{oc} must be estimated. Most compounds have a linear regression equation which relates the octanol water partition coefficient to K_{oc}, or the simplified Eq. 6.4 can be applied to the calculations. Additionally, from these K_d estimates the retardation factor may be applied to determine if the degree of sorption could be considered an overall rate limiting process. As described in Section 4.1.3.1, the greater the retardation factor the more likely sorption will be limiting.

Based on the library research, and from various other sources, i.e., retardation factor, an assumption can be made as to the potential role of sorption or biodegradation as a limiting factor for in situ bioremediation. If the literature review suggests that sorption or biodegradation may be important processes, then the pertinent rates should be determined experimentally to determine whether or not these processes are rate limiting.

Although certain processes such as sorption and biodegradation may be initially analyzed based on a literature review, it must also be understood that the remaining processes such as transverse dispersion and advection should be determined through

laboratory and/or field experiments. For example, the horizontal transverse dispersion estimates for the RRL-South aquifer would have been greatly overestimated if only the literature values were considered. Furthermore, the question of which value to use, laboratory or field derived estimates, remains. For most sites that have time and financial constraints, the choice may be left up to the funding and time available to complete the job. To help resolve this situation, more studies should be conducted which will support whether field or laboratory experiments should be used for the determination of these macro-scale processes.

Appendices

Appendix A: Historic CAH Trends (Tetra Tech, 2002)

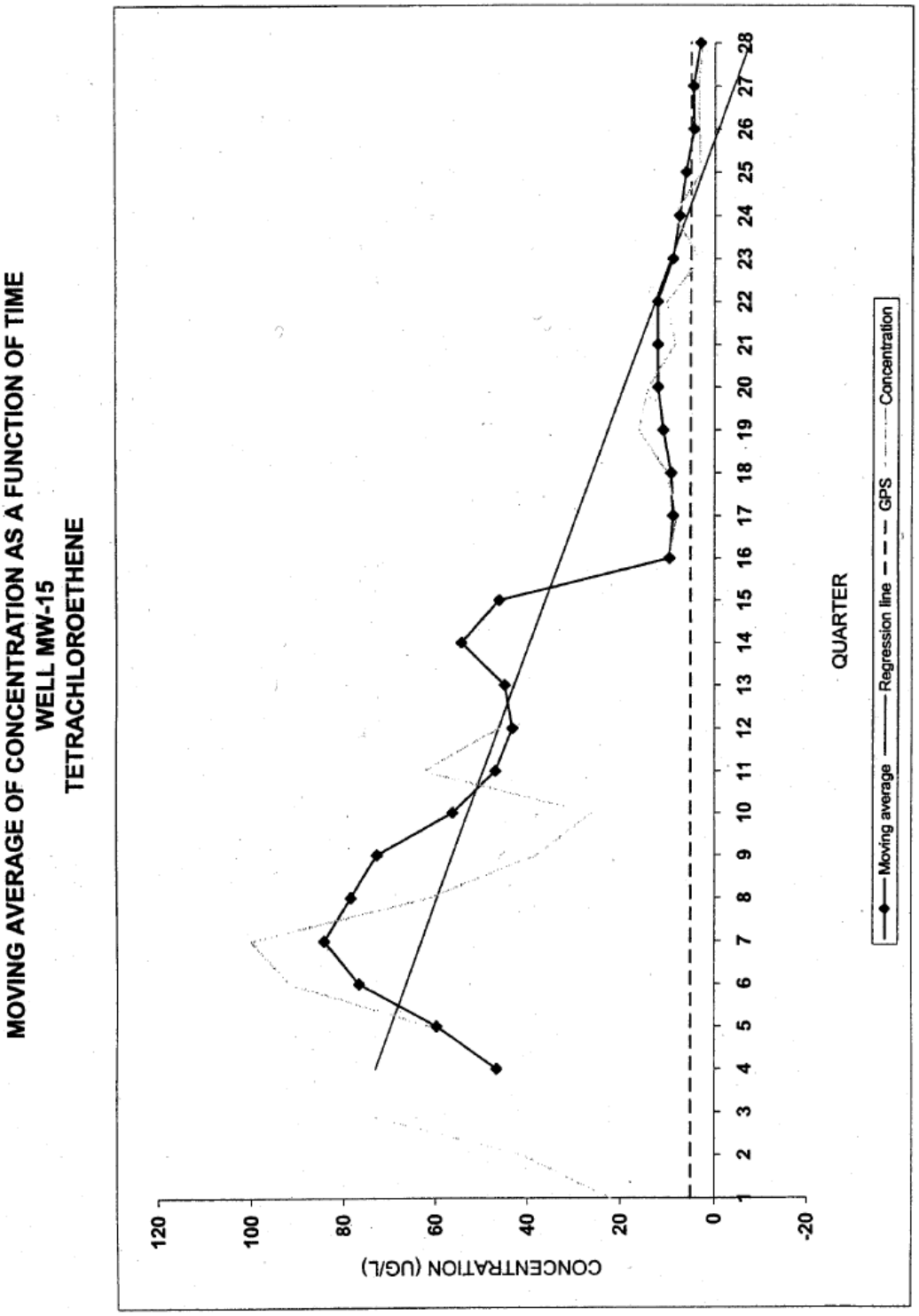

Appendix A: Historic CAH Trends (Tetra Tech, 2002)

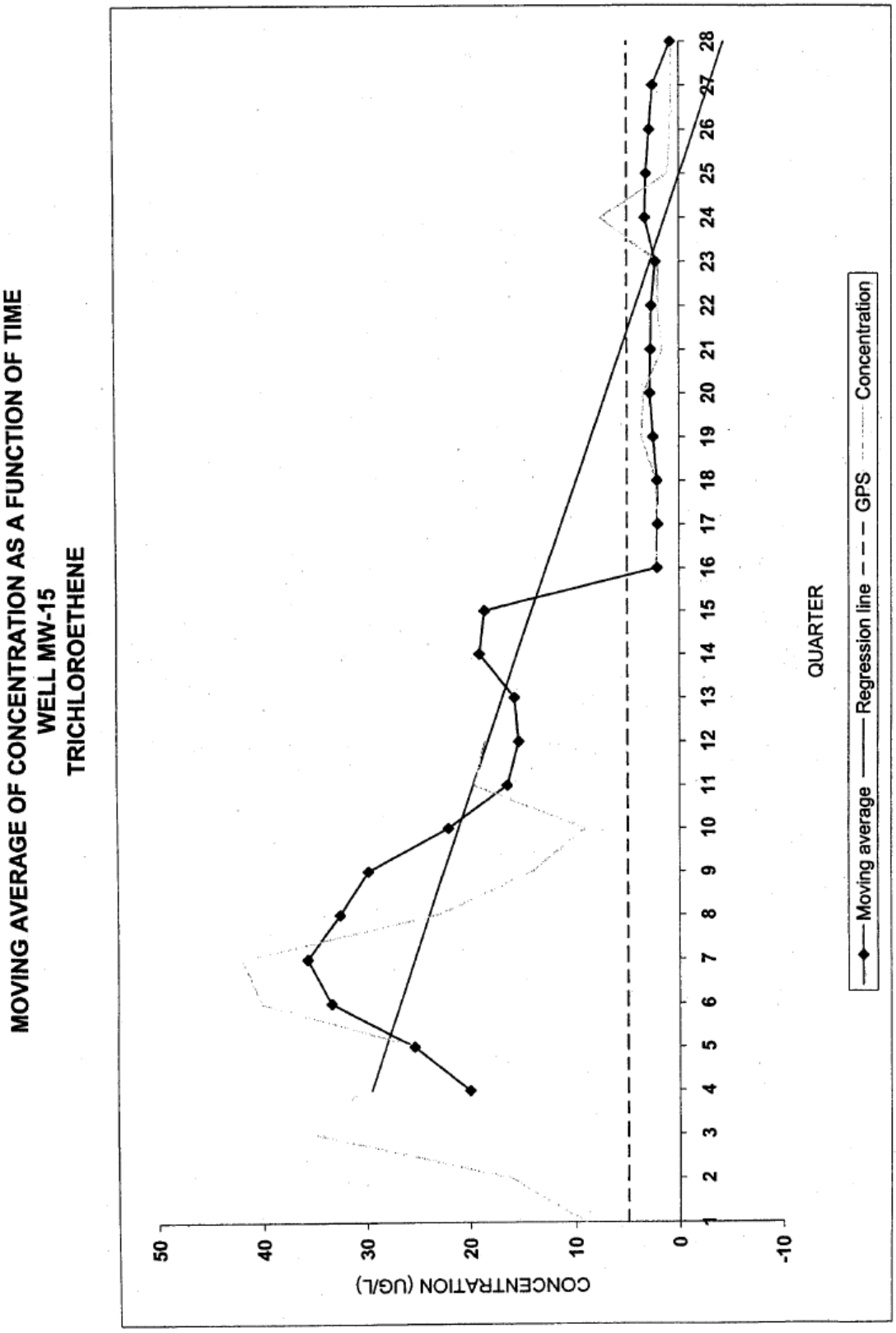

Appendix A: Historic CAH Trends (Tetra Tech, 2002)

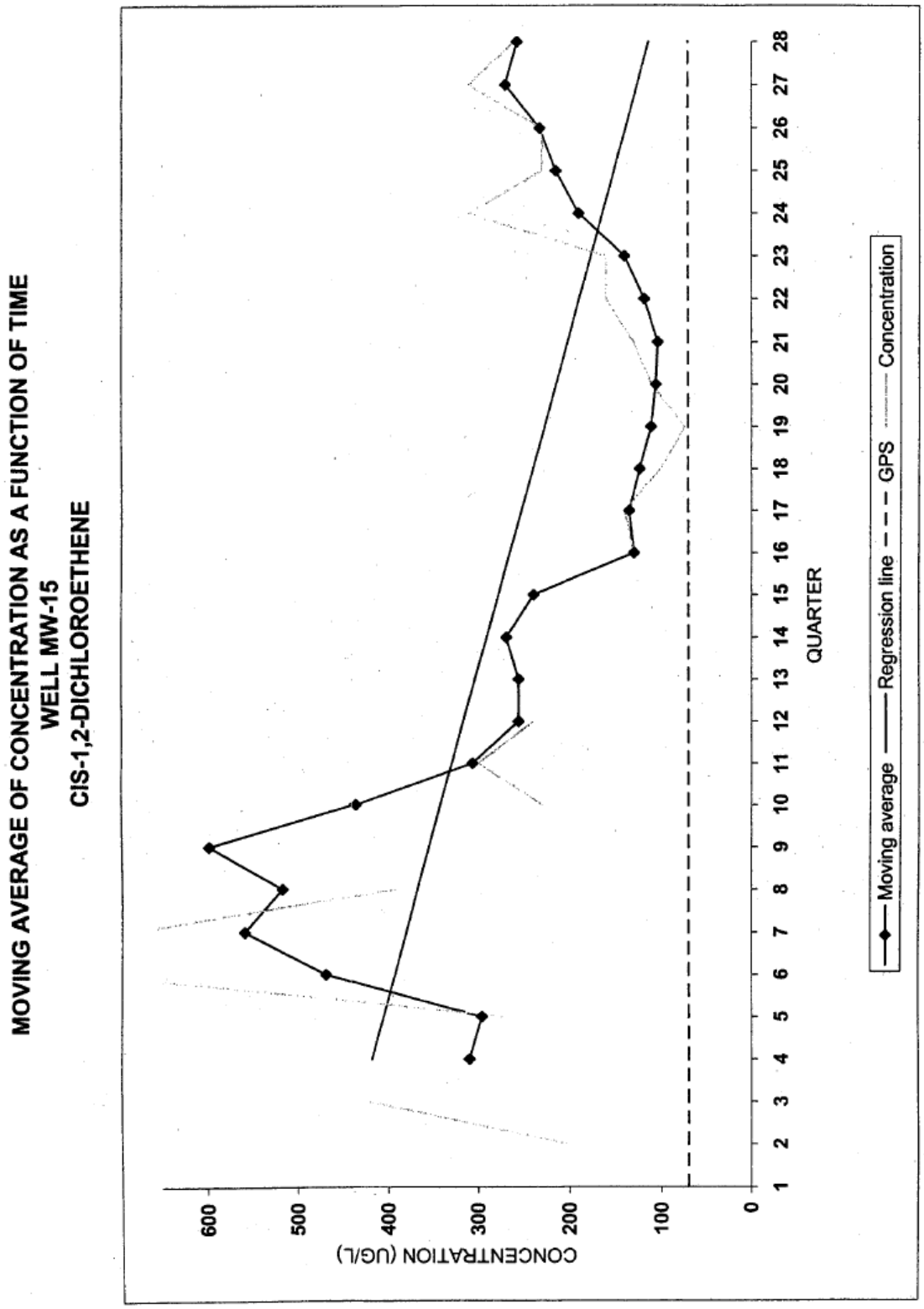

Appendix A: Historic CAH Trends (Tetra Tech, 2002)

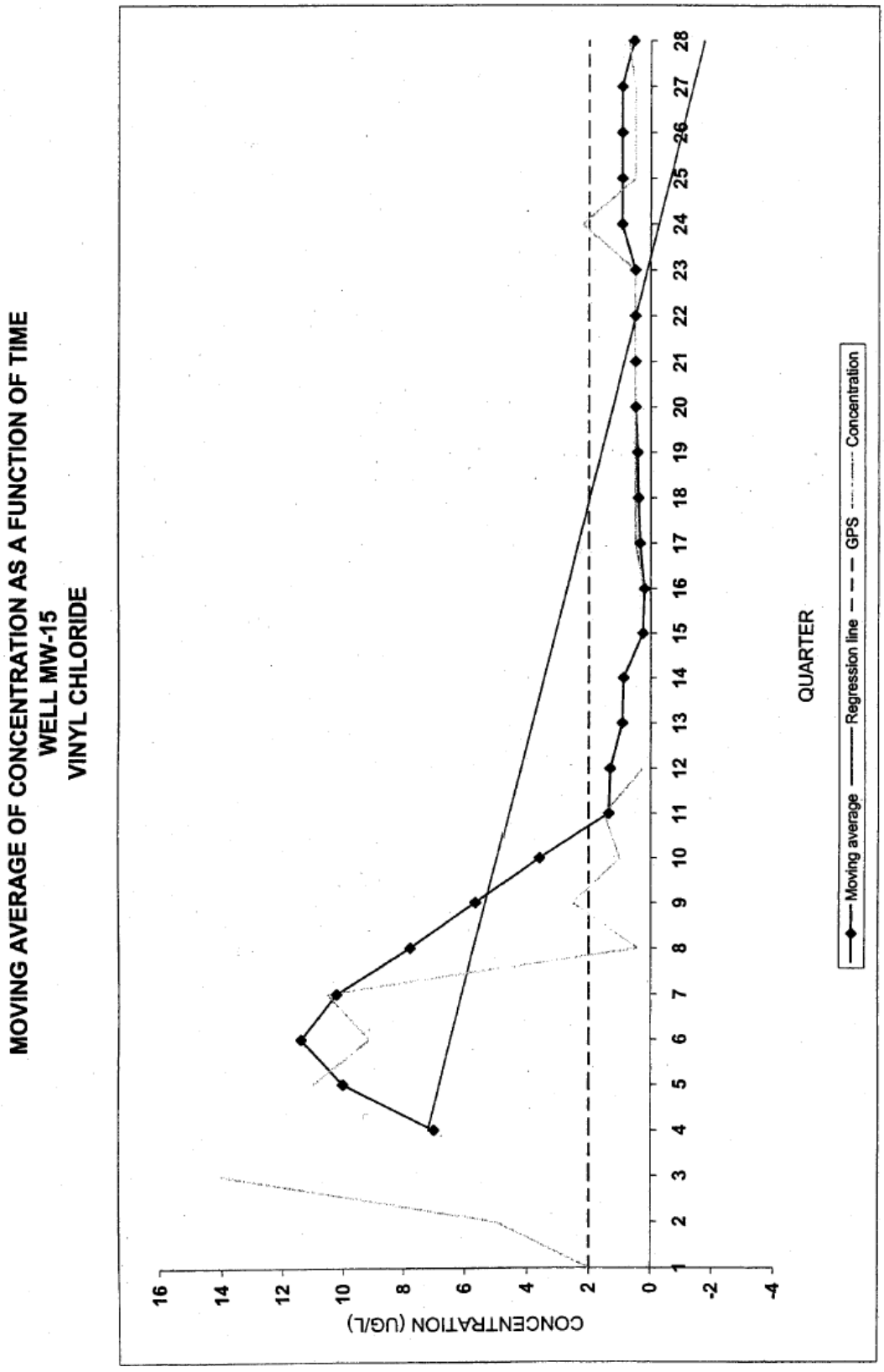

Appendix B: Boring and Well Construction Logs (Battelle, 2003)

Battelle
... Putting Technology To Work

MCB QUANTICO - T.O. 50
BORING LOG - TMW-S1

Permit Number: Project Number: G486050-71 Boring Location: TMW-S1 Date Logged: 09/22/03 Geologist: M. Gaberell Total Depth: 35' Reviewed by:	Drilling Contractor: Chesapeake Geosystems Driller: Darnell Green Drilling Equipment: Mobile B57 ATV Drilling Method: HSA Boring Diameter: 4" auger 8" borehole Sampler Type: NA Hammer Type: NA	Northing (NAD 83): Easting (NAD 83): Surface Elevation (NAVD 88): Borehole Abandoned: __Yes _X_No Backfill Method: Monitoring Device Installed: X Yes __No Type: 2" PVC riser/15' stainless steel screen monitoring well

Depth (feet bgs)	Lithology	USCS Symbol	Sample Description	Sample ID	Comments
0		ML	Silty CLAY, soft, slightly plastic, orange brown, dry		
5			Silty CLAY , trace gravel, dry Qtz. vein with gravel size pieces		
10			SLATE, dark gray-brown, metallic, weathered slate, dry		
15			SLATE, dark gray, metallic slate, dry, fine grained cuttings		
20			SLATE, dark gray, metallic slate		
25			SLATE, dark gray, metallic gravel zone ~2' thick		
30			SLATE, dark gray metallic gravel zone ~1' thick		
35			TD=35 ft @ 1140		

3 drums generated

Page 1 of 1

TMW-S1.GDR

Appendix B: Boring and Well Construction Logs (Battelle, 2003)

Battelle
. . . Putting Technology To Work

MCB QUANTICO - T.O. 50
MONITORING WELL COMPLETION DIAGRAM
TMW-S1

Project #: G486050-71	Site: MCB Quantico - T.O. 50	Well #: TMW-S1	Northing (NAD 83):
Drilling Contractor: Chesapeake Geosystems	Rig Type and Drilling Method: HSA	Date: 09/23/03	Easting (NAD 83):
Reviewed by: M. Gaberell	Driller: Darnell Green	Geologist: M. Gaberell	Surface Elevation (NAVD 88):

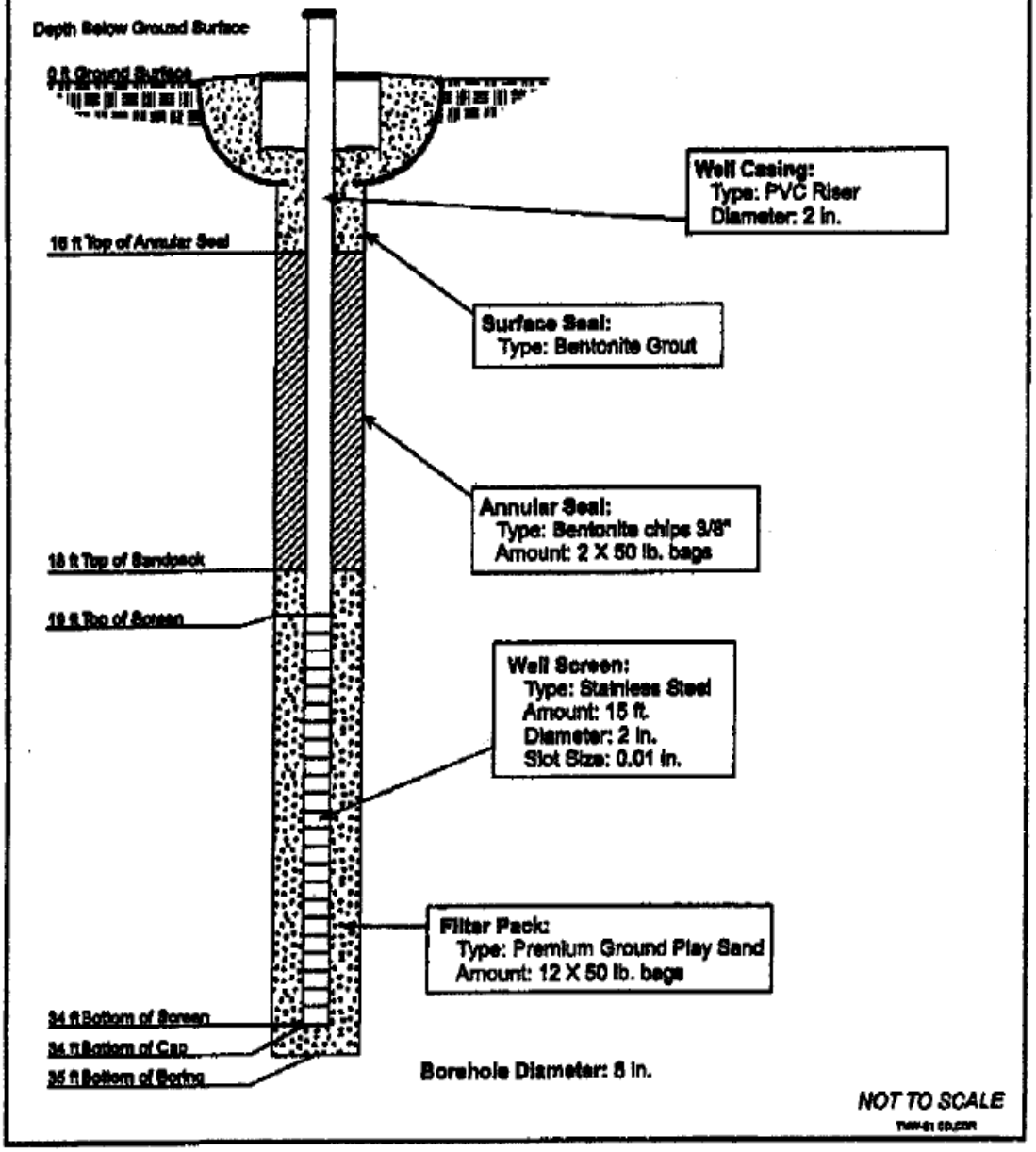

Appendix B: Boring and Well Construction Logs (Battelle, 2003)

Battelle
... Putting Technology To Work

MCB QUANTICO - T.O. 50
BORING LOG - TMW-S2

Permit Number: Project Number: G486050-71 Boring Location: TMW-S2 Date Logged: 09/23/03 Geologist: M. Gaberell Total Depth: 37' Reviewed by:	Drilling Contractor: Chesapeake Geosystems Driller: Darnell Green Drilling Equipment: Mobile B57 ATV Drilling Method: HSA Boring Diameter: 4" auger 8" borehole Sampler Type: NA Hammer Type: NA	Northing (NAD 83): Easting (NAD 83): Surface Elevation (NAVD 88): Borehole Abandoned: _Yes X No Backfill Method: Monitoring Device Installed: X Yes _No Type: 2" PVC riser/15' stainless steel screen monitoring well

Depth (feet bgs)	Lithology	USCS Symbol	Sample Description	Blow Counts	Sample Interval	Sample ID	Comments
0		ML	Silty CLAY, slightly plastic, orange brown, dry				
5			same as above				
			(7'-10') Qtz. vein				
		CL	Silty CLAY, brown weathered slate, fine drill cuttings				
10			SLATE, metallic dark gray, dry, fine drill cuttings				
			SLATE, dark grey				
15			SLATE, metallic dark gray, dry, fine drill cuttings				
20			same as above				
			more resistance, gravel size pieces of slate mixed in with cuttings				
25			same as above, moist				
30			same as above				
35			same as above TD=37 ft @ 1538				

Page 1 of 1

Appendix B: Boring and Well Construction Logs (Battelle, 2003)

Battelle
. . . Putting Technology To Work

MCB QUANTICO - T.O. 50
MONITORING WELL COMPLETION DIAGRAM
TMW-S2

Project #: G466050-71	Site: MCB Quantico - T.O. 50	Well #: TMW-S2	Northing (NAD 83):
Drilling Contractor: Chesapeake Geosystems	Rig Type and Drilling Method: HSA	Date: 09/23/03	Easting (NAD 83):
Reviewed by: M. Gaberell	Driller: Darnell Green	Geologist: M. Gaberell	Surface Elevation (NAVD 88):

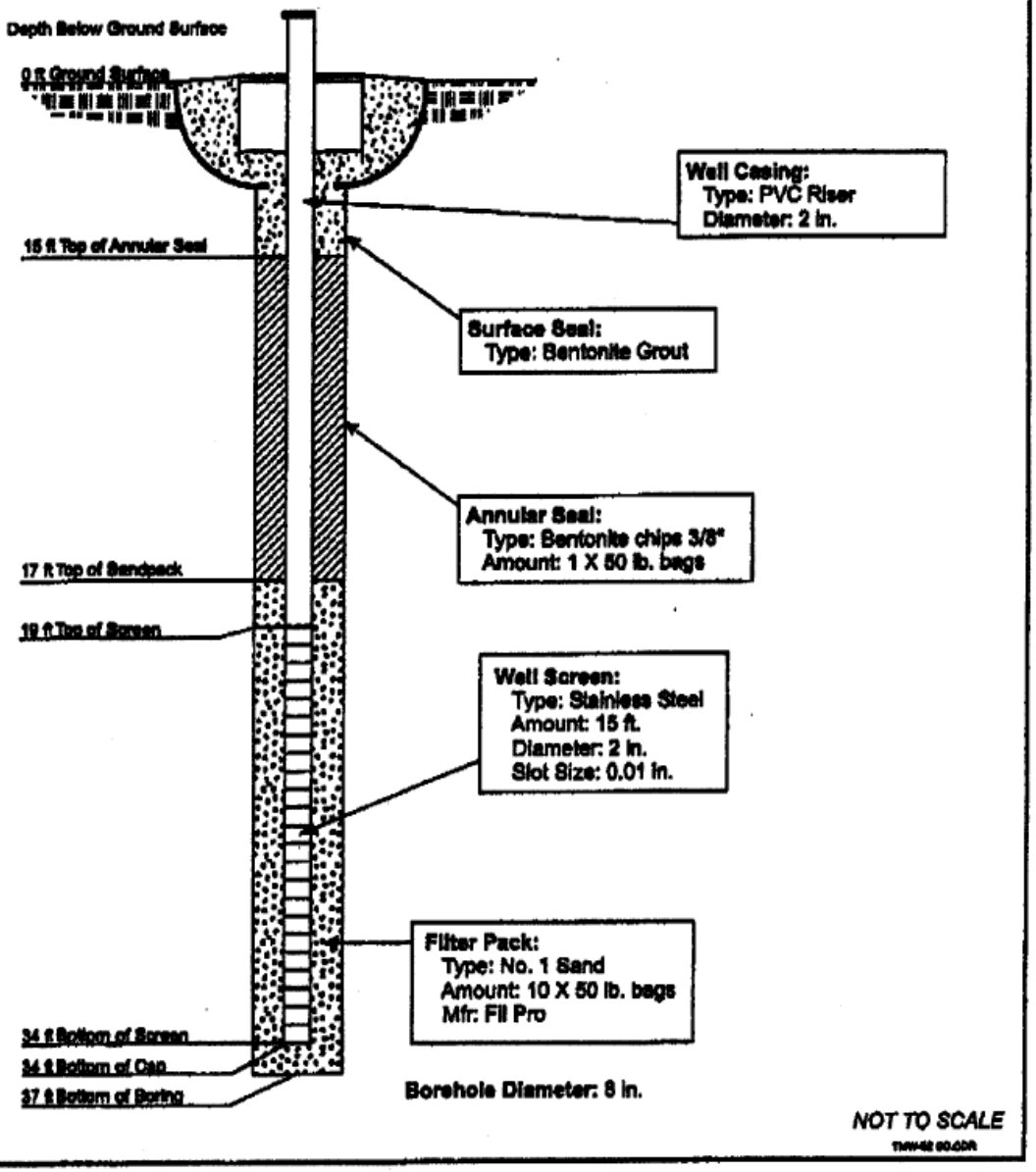

Appendix B: Boring and Well Construction Logs (Battelle, 2003)

Battelle
... Putting Technology To Work

MCB QUANTICO - T.O. 50
BORING LOG - TMW-S3

Permit Number: Project Number: G486050-71 Boring Location: TMW-S3 Date Logged: 09/24/03 Geologist: M. Gaberell Total Depth: 37' Reviewed by:	Drilling Contractor: Chesapeake Geosystems Driller: Darnell Green Drilling Equipment: Mobile B57 ATV Drilling Method: HSA Boring Diameter: 4" auger 8" borehole Sampler Type: NA Hammer Type: NA	Northing (NAD 83): Easting (NAD 83): Surface Elevation (NAVD 88): Borehole Abandoned: __Yes X No Backfill Method: Monitoring Device Installed: X Yes __No Type: 2" PVC riser/15' stainless steel screen monitoring well

Depth (feet bgs)	Lithology	USCS Symbol	Sample Description	Grading % Gravel	% Sand	% Fines	Bore Cuttings	Sample Interval	Sample ID	Organic Vapor	Comments
0		ML	Silty CLAY, slightly plastic, orange brown, dry								
5			Silty CLAY, orange brown, slightly plastic, dry								
			(8') Qtz. vein with clayey silt, orange brown								
		CL	Silty CLAY, orange brown, some plastic tan clay								
10			SLATE, metallic gray changed to metallic brown, fine drill cuttings								
			SLATE, dark gray, fine drill cuttings, dry								
15			SLATE, brown								
			SLATE, dark gray								
20			SLATE, dark metallic gray, dry								
25			SLATE, dark metallic gray, moist								
			Quartzite pebbles up to ½" wide								
30			SLATE, metallic dark gray, moist								
			more resistance at 33'								
			TD=37 ft @ 1038								
35											

3 drums generated

Page 1 of 1

TMW-S3.COR

Appendix B: Boring and Well Construction Logs (Battelle, 2003)

Battelle
. . . Putting Technology To Work

MCB QUANTICO - T.O. 50
MONITORING WELL COMPLETION DIAGRAM
TMW-S3

Project #: G486050-31	Site: MCB Quantico - T.O. 50	Well #: TMW-S3	Northing (NAD 83):
Drilling Contractor: Chesapeake Geosystems	Rig Type and Drilling Method: HSA	Date: 09/24/03	Easting (NAD 83):
Reviewed by: M. Gaberell	Driller: Darnell Green	Geologist: M. Gaberell	Surface Elevation (NAVD 88):

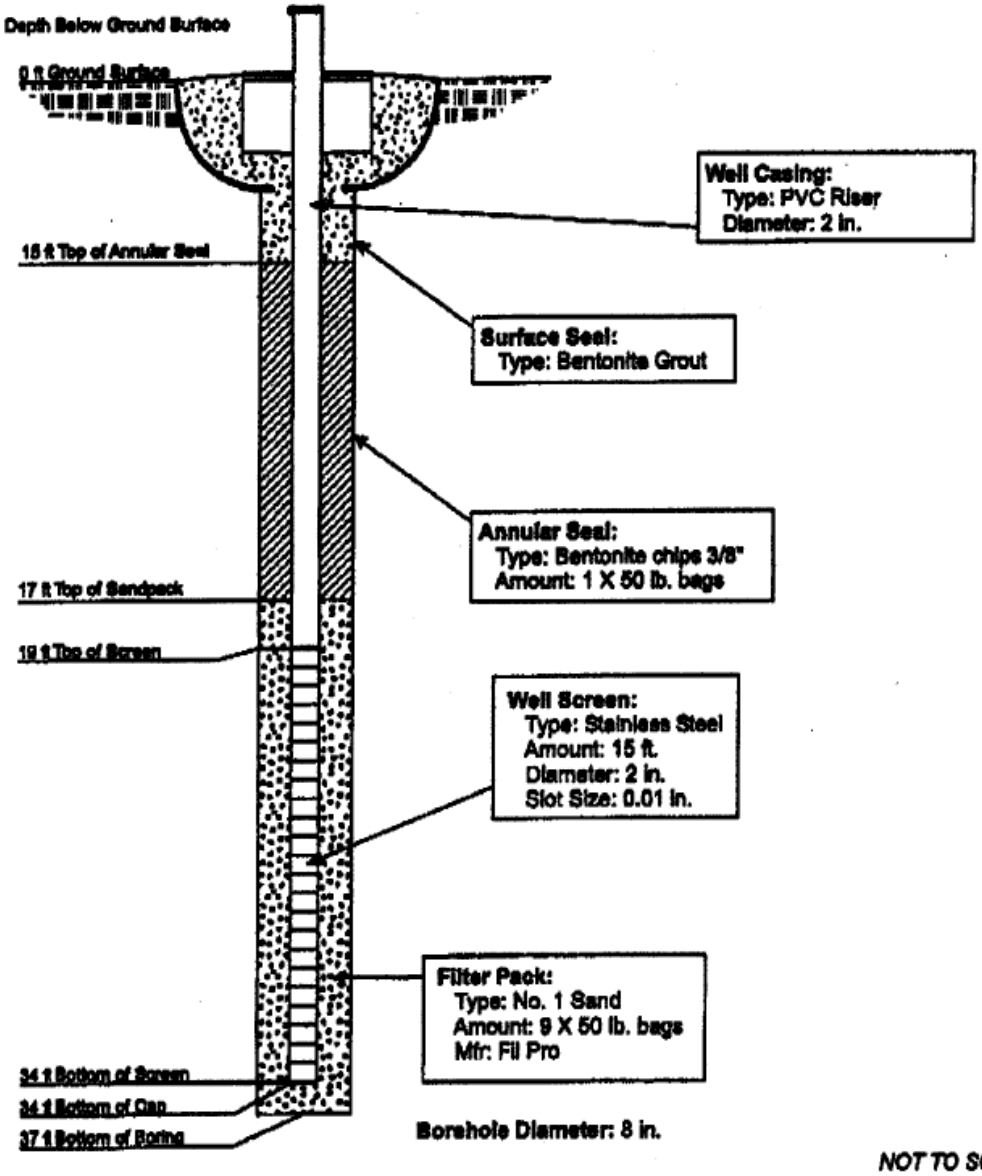

Appendix B: Boring and Well Construction Logs (Battelle, 2003)

Battelle
. . . Putting Technology To Work

MCB QUANTICO - T.O. 50
BORING LOG - TMW-26

Permit Number: 3-120 Project Number: G466050-31 Boring Location: TMW-26 S/D Date Logged: 7/31/03 Geologist: M. Gaberell Total Depth: 48' Reviewed by:	Drilling Contractor: Chesapeake Geosystems Driller: Jay Comon Drilling Equipment: Mobile B57 ATV Drilling Method: HSA Boring Diameter: 12" OD, 6.5" ID Sampler Type: NA Hammer Type: NA	Northing (NAD 83): Easting (NAD 83): Surface Elevation (NAVD 88): Borehole Abandoned: _Yes X No Backfill Method: Monitoring Device Installed: X Yes _No Type: Nested Well 2X2" PVC Monitoring Well, 2.5' Stainless Steel Screen

Depth (feet bgs)	Lithology	USCS Symbol	Sample Description	Sample ID	Comments
0			Silty SAND, fine, some clay		
5			Silty SAND, fine, some clay, orange brown (7') Quartz cobbles		
10			brown metallic weathered schist brown metallic weathered schist		
15			Same as above (18') copper-brown metallic weathered schist		
20			(22') gray metallic weathered schist		
25			Same as above		
30			(32') more resistance, possibly another qtz. vein (~3' thick) gray metallic weathered schist, damp		
35			gray metallic schist, (more resistance)		
40			Same as above, moist		
45			Same as above, saturated TD=48 ft @ 1257		
50					
55					
60					

Page 1 of 1

Appendix B: Boring and Well Construction Logs (Battelle, 2003)

Battelle
. . . Putting Technology To Work

MCB QUANTICO - T.O. 50
MONITORING WELL COMPLETION DIAGRAM
TMW-26 S/D

Project #: G486050-31	Site: MCB Quantico - T.O. 50	Well #: TMW-26 S/D	Northing (NAD 83):
Drilling Contractor: Chesapeake Geosystems	Rig Type and Drilling Method: HSA	Date: 07/31/03	Easting (NAD 83):
Reviewed by: M. Gaberell	Driller: Darnell Green	Geologist: M. Gaberell	Surface Elevation (NAVD 88):

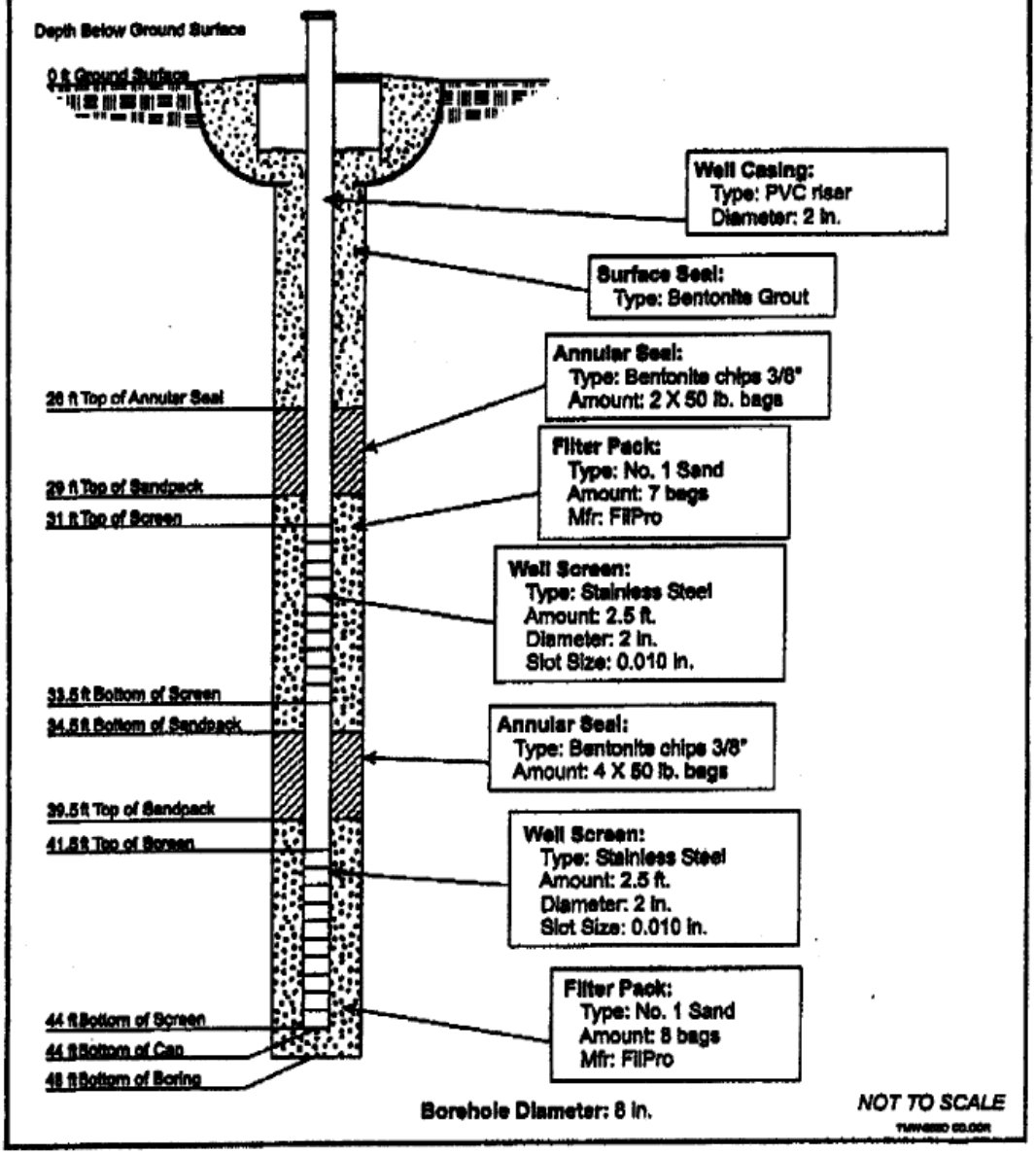

Appendix B: Boring and Well Construction Logs (Battelle, 2003)

Battelle
... Putting Technology To Work

MCB QUANTICO - T.O. 50
BORING LOG - TMW-27

Permit Number: 3-120 Project Number: G466050-31 Boring Location: TMW-27 Date Logged: 08/01/03 Geologist: M. Geberell Total Depth: 35' Reviewed by:	Drilling Contractor: Chesapeake Geosystems Driller: Darnell Green Drilling Equipment: Mobile B57 ATV Drilling Method: HSA Boring Diameter: 8" OD, 4" ID Sampler Type: NA Hammer Type: NA	Northing (NAD 83): Easting (NAD 83): Surface Elevation (NAVD 88): Borehole Abandoned: _Yes X No Backfill Method: Monitoring Device Installed: X Yes _No Type: 2" PVC Monitoring Well with 15' Stainless Steel Screen

Depth (feet bgs)	Lithology	USCS Symbol	Sample Description	Blow Counts	Sample ID	Organic Vapors	Comments
0			GRAVEL (road bed)				
5			CLAY, tan-brown				
10			brown, metallic weathered mica schist				
15 ▽			Same as above				
20			Grey metallic weathered mica schist				
25			Same as above				
30			Same as above, damp				
35							

Page 1 of 2 TMW-27.GDR

Appendix B: Boring and Well Construction Logs (Battelle, 2003)

Battelle
... Putting Technology To Work

MCB QUANTICO - T.O. 50
BORING LOG - TMW-27

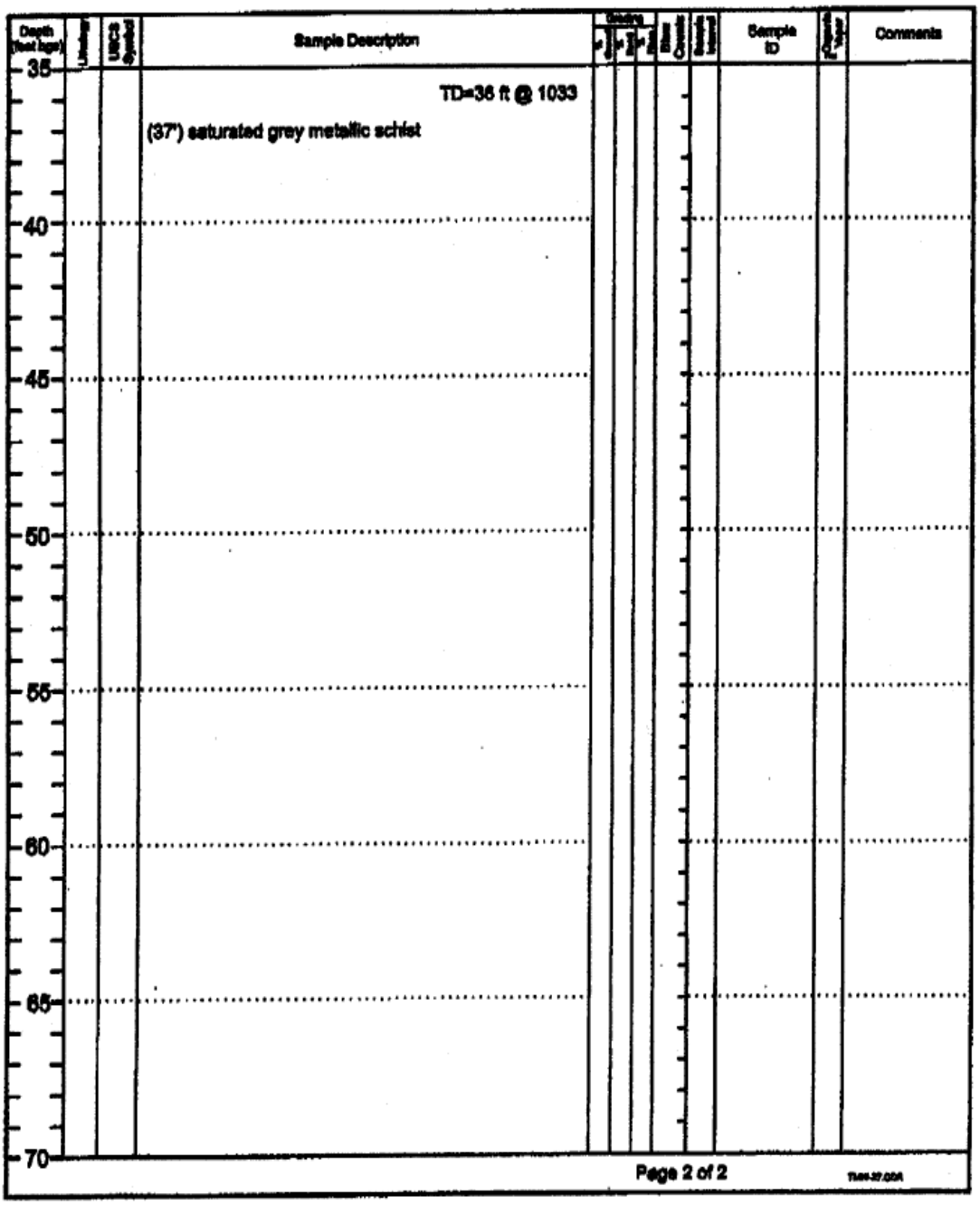

Appendix B: Boring and Well Construction Logs (Battelle, 2003)

Battelle
. . . Putting Technology To Work

MCB QUANTICO - T.O. 50
MONITORING WELL COMPLETION DIAGRAM
TMW-27

Project #: G466060-31	Site: MCB Quantico - T.O. 50	Well #: TMW-27	Northing (NAD 83):
Drilling Contractor: Chesapeake Geosystems	Rig Type and Drilling Method: HSA	Date: 08/01/03	Easting (NAD 83):
Reviewed by: M. Gaberell	Driller: Jay Corron	Geologist: M. Gaberell	Surface Elevation (NAVD 88):

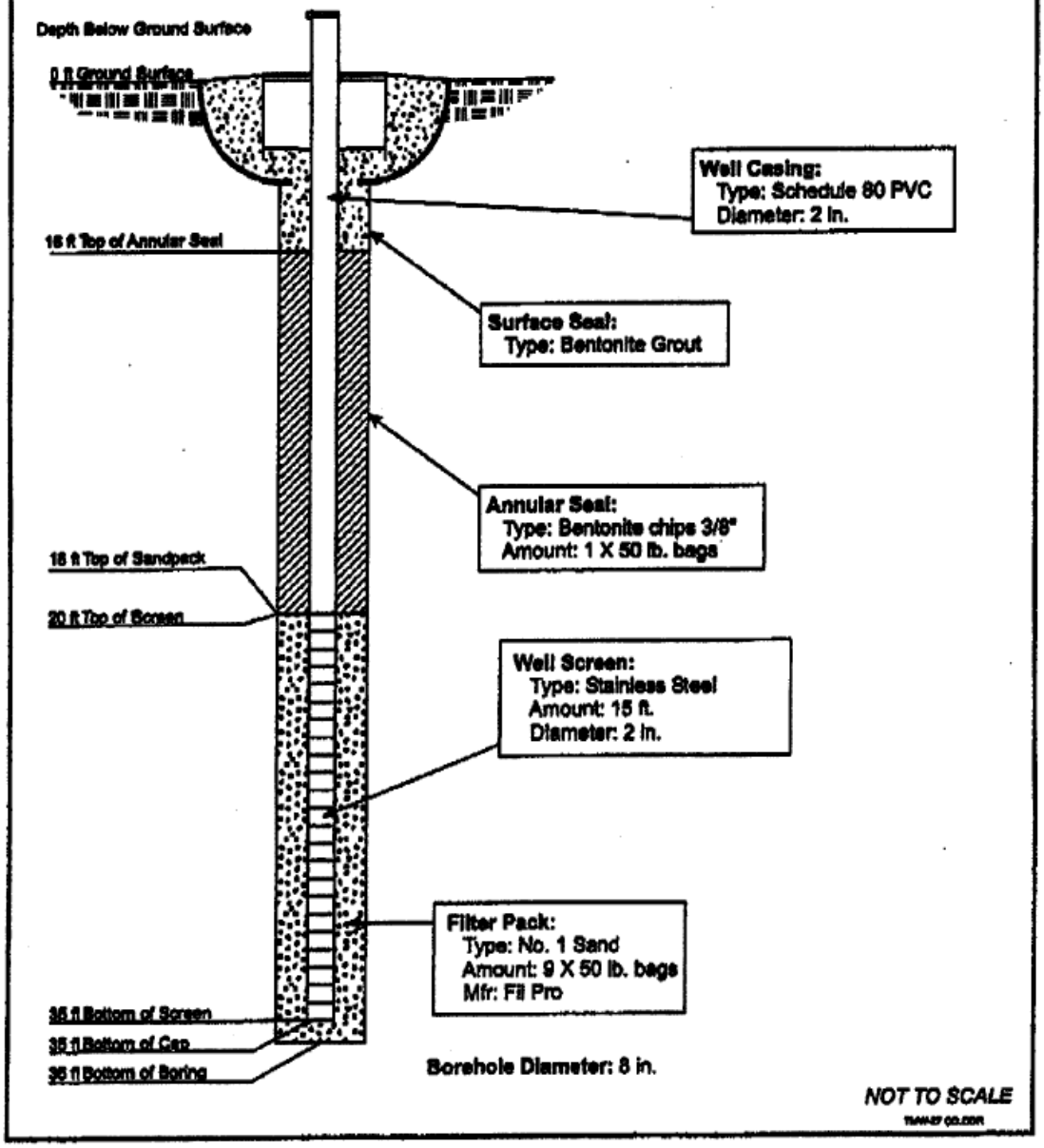

Appendix B: Boring and Well Construction Logs (Battelle, 2003)

Battelle
... Putting Technology To Work

MCB QUANTICO - T.O. 50
BORING LOG - IP-S1

Permit Number: Project Number: G486050-71 Boring Location: IP-81 Date Logged: 09/22/03 Geologist: M. Gaberell Total Depth: 35' Reviewed by:	Drilling Contractor: Chesapeake Geosystems Driller: Darnell Green Drilling Equipment: Mobile B57 ATV Drilling Method: HSA Boring Diameter: 4" auger 8" borehole Sampler Type: NA Hammer Type: NA	Northing (NAD 83): Easting (NAD 83): Surface Elevation (NAVD 88): Borehole Abandoned: _Yes X No Backfill Method: Monitoring Device Installed: X Yes _No Type: 2" PVC Injection Point

Depth (feet bgs)	Lithology	USCS Symbol	Sample Description	Grading	Blow Counts	Sample Interval	Sample ID	Depth (feet bgs)	Comments
0		ML	Silty CLAY, plastic, orange brown, dry						
5			Silty CLAY, orange brown, dry (7'-8') Qtz. vein, gravel-cobble size pieces						
10		CL	Silty CLAY, orange brown Silty CLAY, orange brown SLATE, brown metallic, dry						
15			SLATE, brown metallic, dry, very fine cuttings						
20			SLATE, metallic gray, dry, very fine cuttings						
25			SLATE, metallic gray, some solid slate pieces						
30			same as above						
35			TD=35 ft @ 1725						

3 drums generated

Page 1 of 1

Appendix B: Boring and Well Construction Logs (Battelle, 2003)

Battelle
. . . Putting Technology To Work

MCB QUANTICO - T.O. 50
MONITORING WELL COMPLETION DIAGRAM
IP-S1

Project #: G456050-71	Site: MCB Quantico - T.O. 50	Well #: IP-S1	Northing (NAD 83):
Drilling Contractor: Chesapeake Geosystems	Rig Type and Drilling Method: HSA	Date: 09/22/03	Easting (NAD 83):
Reviewed by: M. Gaberell	Driller: Darnell Green	Geologist: M. Gaberell	Surface Elevation (NAVD 88):

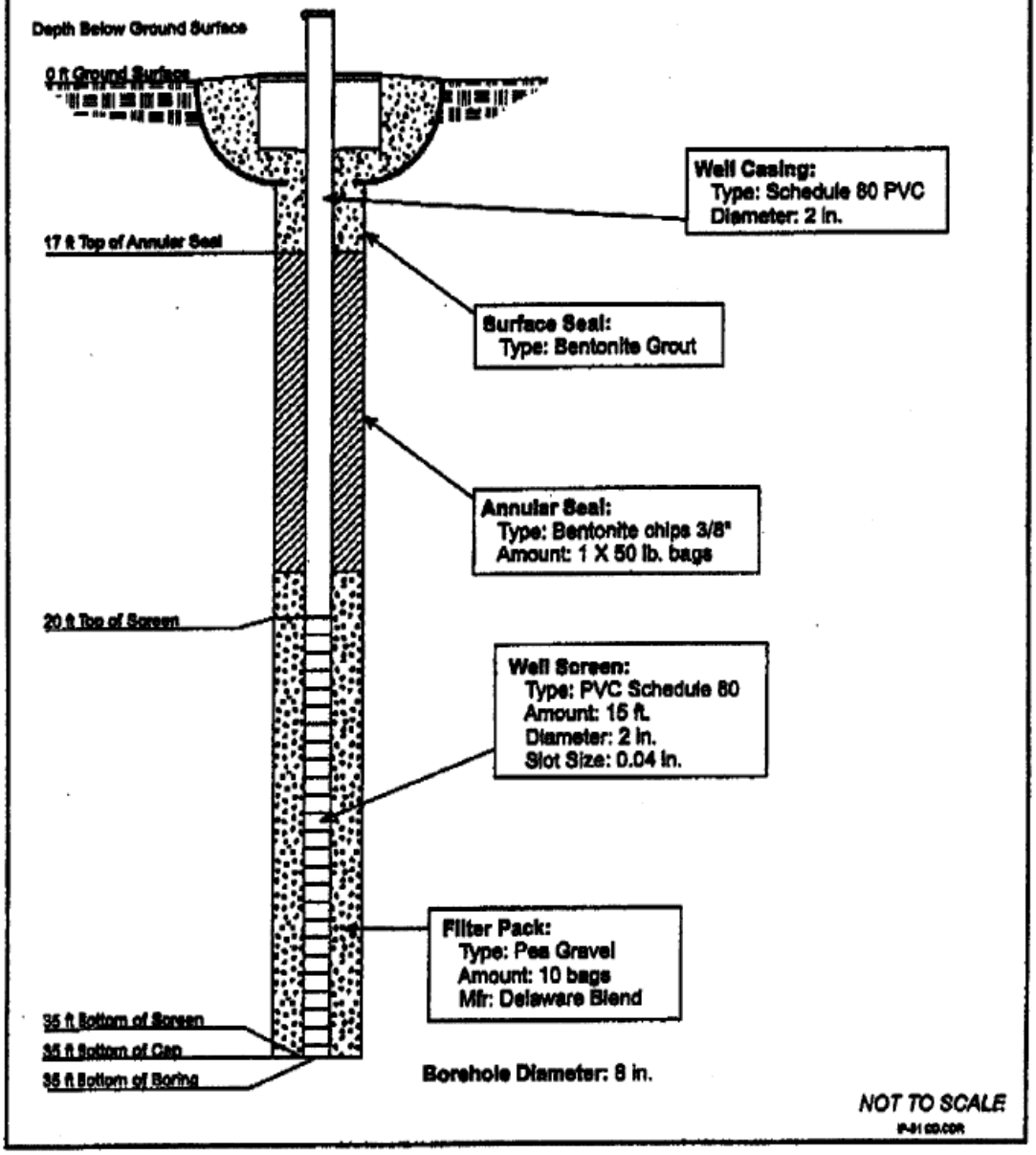

Appendix B: Boring and Well Construction Logs (Battelle, 2003)

Battelle
... Putting Technology To Work

MCB QUANTICO - T.O. 50
BORING LOG - IP-S2

Permit Number: Project Number: G486050-71 Boring Location: IP-S2 Date Logged: 09/23/03 Geologist: M. Gaberell Total Depth: 35' Reviewed by:	Drilling Contractor: Chesapeake Geosystems Driller: Darnell Green Drilling Equipment: Mobile B57 ATV Drilling Method: HSA Boring Diameter: 4" auger 8" borehole Sampler Type: NA Hammer Type: NA	Northing (NAD 83): Easting (NAD 83): Surface Elevation (NAVD 88): Borehole Abandoned: _Yes X No Backfill Method: Monitoring Device Installed: X Yes _No Type: 2" Injection Pt., Sch. 80 PVC with 15' Screen

Depth (feet bgs)	Lithology	USCS Symbol	Sample Description	Graphics	Blow Counts	Sample ID	Comments
0		ML	Silty CLAY, slightly plastic, orange brown, dry				
5			Silty CLAY , orange brown				
			(7'-9') Qtz. vein				
10		CL	Silty CLAY , orange brown, dry				
			SLATE, brown, weathered				
			SLATE, gray metallic				
15			SLATE, metallic gray drill cuttings are fine, but some gravel-size slate pieces evident				
20			SLATE, metallic gray				
25			Same as above, drilling becomes more difficult at 25'				
30			same as above				
35			TD=35 ft @ 1022				

3 drums generated

Page 1 of 1

IP-S2.CDR

Appendix B: Boring and Well Construction Logs (Battelle, 2003)

Battelle
... Putting Technology To Work

MCB QUANTICO - T.O. 50
MONITORING WELL COMPLETION DIAGRAM
IP-S2

Project #: G486060-71	Site: MCB Quantico - T.O. 50	Well #: IP-S2	Northing (NAD 83):
Drilling Contractor: Chesapeake Geosystems	Rig Type and Drilling Method: HSA	Date: 09/23/03	Easting (NAD 83):
Reviewed by: M. Gaberell	Driller: Darnell Green	Geologist: M. Gaberell	Surface Elevation (NAVD 88):

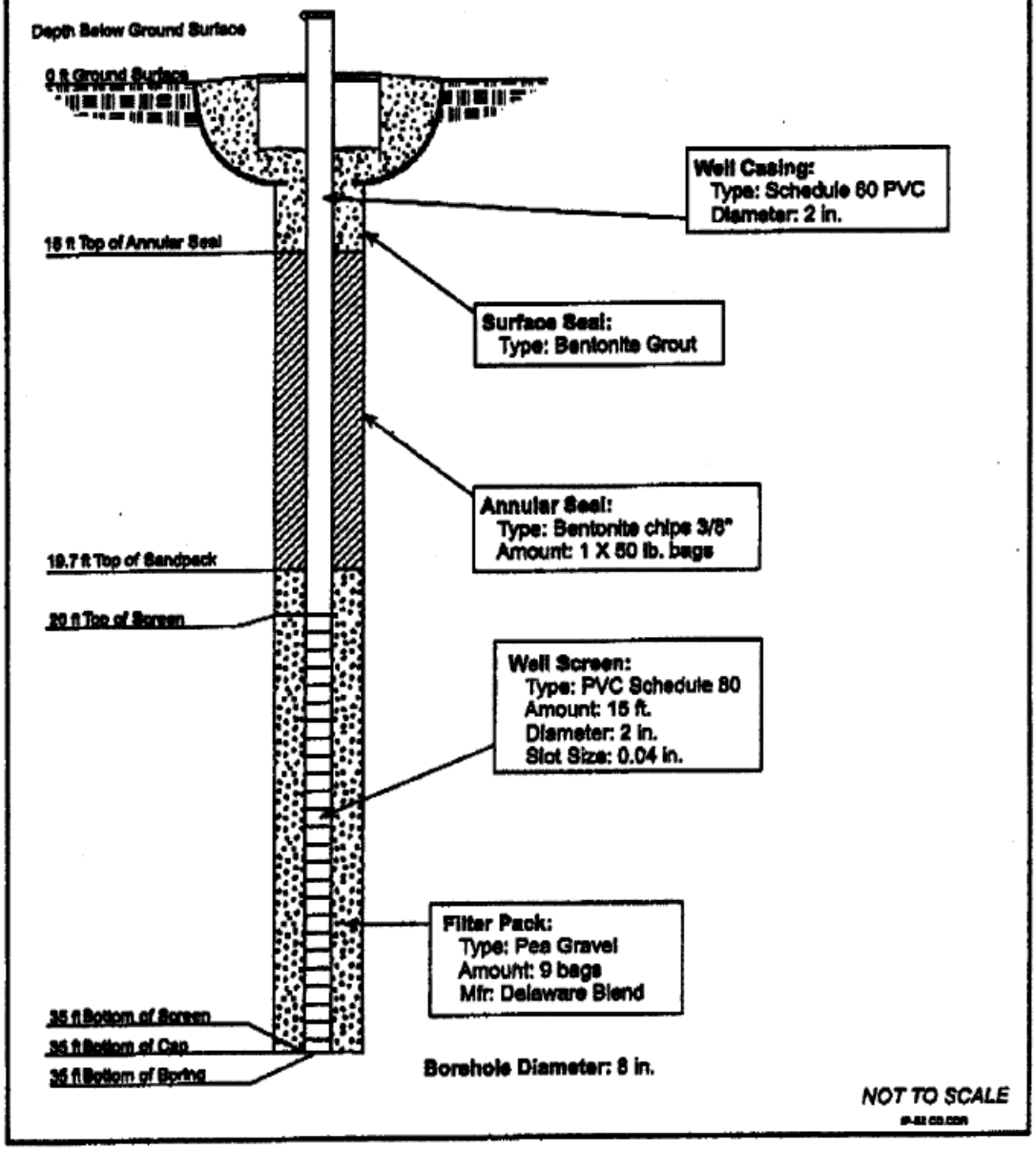

Appendix C: Regenesis Bench-Scale Biokinetics Results

FINAL REPORT

Treatability Study

Russell Road Landfill

For

Regenesis Bioremediation Products, Inc.

By

Applied Power Concepts, Inc.
411 E. Julianna Street
Anaheim, CA 92801

September 11, 2003

TEL (714) 502-1150
FAX (714) 502-2450
E-mail tracy@appliedpowerconcepts.com

Summary:

A soil sample from a Russell Road Landfill site was studied using the Protocol for the Regenesis Bench Scale Experiment for the Bioremediation of Trichloroethylene (TCE). The purpose of the study was to determine whether the site is a candidate for anaerobic remediation of the chlorinated hydrocarbon, TCE.

The bench scale test provides an accelerated response to anaerobic remediation. The focus is on the determination of whether the soil contains a population of bacteria that a) are suitable to perform the remediation and b) respond to an increase in both the biochemical energy and the hydrogen generated from HRC (Hydrogen Release Compound) under the anaerobic conditions of the test.

The test was started on August 8, 2003. A total of 15 test tubes set were set up. The test tubes were sampled and analyzed once a week. Three test tubes were analyzed at each sampling interval for statistical comparisons. At each sampling interval a new set of three test tubes were opened to eliminate any losses due to reopening test tubes each time to sample.

Analyses of this type are usually done every seven days and the test is normally run for 4 weeks. The initial concentration of TCE was targeted at 10 ppm. The initial average concentration measured in the test tubes at time zero was 10.87 ppm of TCE. By the end of the test we see a reduction of TCE to an average value of 8.84 ppm, DCE had an average value of 1.35 ppm, which includes t-DCE, c-DCE and 1,1-DCE. VC had an average value of 0.61 ppm.

Microbial counts in the test were in the higher range of what we usually see for aerobic counts and anaerobic counts. We would have expected to see a greater amount of bioremediation which such high microbe counts. SRB are present at reasonable levels which indicate that aquifer conditions may be suitable for complete reductive dechlorination.

According to published criteria for bioremediation of chlorinated hydrocarbons, acclimatization under actual field conditions could take several months. These results are not like any results we have seen in the past. Remediation in this case is extremely slow, yet the microbial counts are extremely high.

Remediation rates in small systems are not a good indication of rates in the field. One should not use the rates in this study to extrapolate to expected rates in the field.

Experimental Methods:

The soil samples are homogenized by manual stirring and a 10-gram aliquot is added to each of the 15 test tubes of approximately 200-ml total volume. In all of the test tubes 150 ml of distilled water containing approximately 15 mg/L of TCE solution is added along with 1.5 grams of Glycerol Polylactate (GPL) HRC.

TCE and its daughter products are measured by gas chromatography using a silica column on a SRI GC outfitted with both a PID (Photoionization Detector) and a FID (Flame Ionization Detector) detector. Toluene is used as the internal standard in a gas phase (head space) measurement. The hydrocarbons methane and ethane are also detected on this column but the column conditions are not adequate to allow separation and quantification of the mixed hydrocarbons due to the presence of methane from the HRC degradation process.

The organic acids, lactic, pyruvic, acetic, propionic and butyric are measured using liquid chromatography with a Restek C18 column and an UV detector. Citric acid is used as the internal standard. In this test the column was quantitatively calibrated for the lactic, pyruvic and acetic measurements.

Bacterial counts are made using standard plate pour techniques. Three populations are measured. The first population is aerobic total plate counts (TPC) based on a glucose nutrient agar plate. This is the normal test used for groundwater. The results are reported as the number of Colony Forming Units per ml. We use the same test media for anaerobes but incubate the plates anaerobically under nitrogen. These counts are reported as anaerobic TPC. Finally we also use the standard AWWA (American Water Works Association) test for sulfate reducing bacteria to measure the SRB (Sulfate Reducing Bacteria) content in the water. The rationale for this test is that the SRBs thrive at a redox potential that is close to the optimum for dechlorination. Although the dechlorinators are not necessarily SRBs, the presence of SRB indicates that aquifer conditions may be suitable for reductive dechlorination. It is generally agreed that high rates of dechlorination, especially for recalcitrant chlorinated materials (e.g. dichloroethane) are expected at Oxidation Reduction Potentials in the –200 mv to –250 mv range, the range in which SRBs thrive.

In the nomenclature used in plate counts, a "spreader" is a plate that has become so overgrown that colonies merge making identification of individual colonies impossible. This usually occurs when the sample contains an organism that will grow rapidly when provided an adequate carbon source. A "TNTC" (Too Numerous To Count) is a plate that has so many individual colonies making it impossible to count. A contaminated plate (Cont.) is easy to identify since invariably contamination in plating is due to fungus that overgrows the plate. This is not the case in spreaders that have microbes clearly growing into the agar.

Complete detailed methods are on file for all of the procedures used at APC (Applied Power Concepts, Inc.). Also available are GLP (Good Laboratory Practices) Protocols even though they are

not required. APC generally follows GLP methodology. The Regenesis protocols do not require a GLP study for each of the treatability experiments. This reduces administrative time and costs and allows more flexibility in sample collection, duration of the tests, etc.

Results and Discussion:

The test tube system has been studied extensively for TCE as the test substance before it was used for site treatability screening. A supplementary document explaining the test is available from Regenesis. The system has been tested with various levels of bacteria and with various levels of CH (Chlorinated Hydrocarbons) to determine the range of useful parameters. When a fully acclimated bacterial system is used, remediation occurs in a matter of days. Russell Road Landfill soil sample was studied to determine if remediation would occur in the time frame of the test.

We began the treatability test on Russell Road Landfill sample on 8/8/03. The data from the test are given in the tables.

The microbial counts are shown in Table 3. The anaerobic microbial counts are in the higher range than normal. Facultative organisms can show up in both counts, although an organism will reproduce more quickly to become a visible colony in the conditions it favors most. Reasonable SRB counts are to be expected given the fact that dechlorinating bacteria appear to prefer a redox environment similar to SRBs.

Conclusions and Recommendations:

Former Russell Road Landfill site could be a candidate for a field application. This appears to be a case where the bio-inoculum could enhance the results. In actual field trials HRC, as well as lactic acid, have shown they can provide a large increase in remediation rate over background.

Table 1
Chlorinated Hydrocarbon Data
(Concentration values are in mg/l)

Time In Days	0	7	14	21	28
CH					
TCE	10.87	9.47	8.84	8.16	8.84
t-DCE	0.0	0.0	0.0	0.0	0.056
c-DCE	0.0	0.15	0.10	0.15	0.90
1,1-DCE	0.0	0.25	0.10	0.18	0.39
VC	0.0	0.29	0.30	0.49	0.61

Table 2
Organic Acid Data
(Concentration values are in mg/l)

Time In Days	7	14	21	28	7
Acids					
Lactic	0	1762	3905	3020	5954
Pyruvic	0	18.52	41.77	33.57	70.65
Acetic	0	577.03	400.45	1235.27	1130.83

Table 3
Microbial Counts in CFU's

	Aerobic	Anaerobic	
Sample	TPC	TPC	SRB
A1	27375	30000	10875
B1	11328	11083	7958
C1	15312	37813	12857

Legend: In table 3, samples A1, B1 and C1 are the last set of triplicate test tubes

Appendix D: Post Injection Pilot Area Monitoring Well Data

TMW-S1

(post injection results)

Date	PCE ug/L	TCE ug/L	cis-1,2-DCE ug/L	trans-1,2-DCE ug/L	1,1-DCE ug/L	Vinyl Chloride ug/L	DO mg/L	ORP mV	pH	Conductivity	Turbidity	Temp C	Normalized Field Parameters DO	ORP	pH	Cond.
Oct-03	59	31	520	1.9	0.50	5.7	1.02	247	5.66	0.326		15.72	1	1	1	1
Dec-03	50	30	480	2.5	0.95	4.4	0.93	106	5.34	0.289	10.8	16.33	0.91	0.43	0.94	0.89
Jan-04	82	36	710	4.15	4.65	3.75	0.95	142	5.48	0.339	6.7	15.32	0.93	0.57	0.97	1.04
Feb-04	15	6.3	130	0.85	0.95	0.75	1.11	116	5.36	0.232	10.1	13.77	1.09	0.47	0.95	0.71
Feb-04	15	7.2	140	0.85	0.95	0.75	1.11	116	5.36	0.232	10.1	13.77	1.09	0.47	0.95	0.71
Mar-04	15	8.1	130	0.85	0.95	0.75	0.93	336	4.99	0.230	7.3	15.59	0.91	1.36	0.88	0.71
Apr-04	62	29	460	2.5	0.36	3.4	0.92	258	5.51	0.309	9.1	14.84	0.90	1.04	0.97	0.95
May-04	39	23	430	1.5	0.185	2.5	2.98	275	5.65	0.336	8.7	16.05	2.92	1.11	1.00	1.03

Date	Chloride mg/L	Total Fe mg/L	Dissolved Fe mg/L	Total Mn mg/L	Dissolved Mn mg/L	Nitrate mg/L	Sulfate mg/L	Sulfide mg/L	Methane mg/L	Ethane mg/L	Ethene mg/L	Alkalinity mg/L	TOC mg/L	CO2 mg/L	Lactic acid mg/L	Pyruvic acid mg/L	Acetic acid mg/L	Propionic acid mg/L	Butyric acid mg/L
Oct-03	60	27.3	26.2	5.42	5.80	0.032	7.7	0.65	1.9	0.001	0.002	30	19.7	980	50	1900	5.0	0.29	0.55
Feb-04	54	3.00	1.24	0.605	0.648	0.32	21	0.85	0.125	0.001	0.002	15	15.0	55	50	50	6.26	0.29	0.55
Feb-04	52	2.80	1.29	0.577	0.644	0.011	21	0.85	0.122	0.001	0.002	120	15.2	170	50	50	6.26	0.29	0.55
May-04	75	46.7	49.7	6.07	6.29	0.32	16	1.75	2.6	0.0025	0.002	47	9.85	320	50	50	0.81	0.29	0.55

Reported as BRL with a U flag (the compound was analyzed for but not detected); Use 1/2 Method Detection Limit (MDL)

Reported with a J flag (results between MDL and Reporting Limit); Using 1/2 Reporting Limit IF the result is LESS THAN 1/2 Reporting Limit

Reported with a J flag (results between MDL and Reporting Limit); Using the reported value IF the result is MORE THAN 1/2 Reporting Limit

Appendix D: Post Injection Pilot Area Monitoring Well Data

TMW-S2

(post injection results)

Date	PCE ug/L	TCE ug/L	cis-1,2-DCE ug/L	trans-1,2-DCE ug/L	1,1-DCE ug/L	Vinyl Chloride ug/L	DO mg/L	ORP mV	pH	Conductivity	Turbidity	Temp C	Normalized Field Parameters: DO	ORP	pH	Cond.
Oct-03	75	27	510	2	0.5	5.1	1.5	263	4.91	0.171		15.06	1	1	1	1
Dec-03	62	24	530	1.8	0.5	4.2	0.79	116	5.09	0.171	9.8	14.97	0.53	0.44	1.04	1.00
Jan-04	82	25	660	4.15	4.65	3.75	0.98	140	5.18	0.157	10.1	13.76	0.65	0.53	1.05	0.92
Feb-04	22	7.8	220	1.65	1.85	1.5	6.96	128	5.50	0.150	58	13.64	4.64	0.49	1.12	0.88
Mar-04	61	28	840	2.5	0.95	3.4	0.78	297	4.57	0.151	8.1	13.98	0.52	1.13	0.93	0.88
Apr-04	50	22	510	2.5	0.36	1.9	5.86	254	5.22	0.168	7.3	14.22	3.91	0.97	1.06	0.98
May-04	65	29	670	2.5	0.5	3.6	0.58	411	4.39	0.192	6.6	15.73	0.39	1.56	0.89	1.12
May-04	66	28	680	2.5	0.185	3.3	0.58	411	4.39	0.192	6.6	15.73	0.39	1.56	0.89	1.12

Date	Chloride mg/L	Total Fe mg/L	Dissolved Fe mg/L	Total Mn mg/L	Dissolved Mn mg/L	Nitrate mg/L	Sulfate mg/L	Sulfide mg/L	Methane mg/L	Ethane mg/L	Ethene mg/L	Alkalinity mg/L	TOC mg/L	CO2 mg/L	Lactic acid mg/L	Pyruvic acid mg/L	Acetic acid mg/L	Propionic acid mg/L	Butyric acid mg/L
Oct-03	19	13.8	15.6	4.78	5.58	0.9	4.3	1.6	0.55	0.021	0.002	80	4.65	0.5	50	50	5.45	5.0	0.55
Feb-04	25	16.8	9.84	4.52	4.43	0.94	9.9	0.85	0.78	0.021	0.002	18	6.00	45	50	50	6.25	5.0	0.55
May-04	24	4.50	5.93	8.09	7.36	2.2	38	0.85	1.3	0.003	0.002	0.4	3.95	0.5	50	50	0.81	0.29	0.55
May-04	24	4.86	6.44	7.79	7.32	2.3	37	0.85	1.1	0.003	0.002	1.5	3.25	0.5	50	50	0.81	0.29	0.55

Reported as BRL with a U flag (the compound was analyzed for but not detected); Use 1/2 Method Detection Limit (MDL)

Reported with a J flag (results between MDL and Reporting Limit); Using 1/2 Reporting Limit IF the result is LESS THAN 1/2 Reporting Limit

Reported with a J flag (results between MDL and Reporting Limit); Using the reported value IF the result is MORE THAN 1/2 Reporting Limit

Appendix D: Post Injection Pilot Area Monitoring Well Data

TMW-S3

(post injection results)

Date	PCE ug/L	TCE ug/L	cis-1,2-DCE ug/L	trans-1,2-DCE ug/L	1,1-DCE ug/L	Vinyl Chloride ug/L	DO mg/L	ORP mV	pH	Conductivity	Turbidity	Temp C	Normalized Field Parameters: DO	ORP	pH	Cond.
Oct-03	43	20	250	0.72	0.19	2.5	0.89	196	6.05	0.316		15.15	1	1	1	1
Dec-03	50	23	370	0.85	0.95	0.75	0.57	102	5.48	0.280	89	15.23	0.64	0.52	0.91	0.89
Jan-04	50	22	350	1.65	1.85	1.5	1.20	131	5.65	0.290	8.4	13.89	1.35	0.67	0.93	0.92
Feb-04	27	12	350	1.65	1.85	1.5	0.32	108	5.49	0.284	9.9	14.55	0.36	0.55	0.91	0.90
Mar-04	46	26	540	1.65	1.85	1.5	1.33	199	5.32	0.276	9.0	14.21	1.49	1.02	0.88	0.87
Mar-04	43	26	480	1.65	1.85	1.5	1.33	199	5.32	0.276	9.0	14.21	1.49	1.02	0.88	0.87
Apr-04	47	23	350	2.5	0.36	1.0	5.02	243	6.00	0.265	8.6	14.18	5.64	1.24	0.99	0.84
May-04	56	31	470	1.6	1.6	1.6	0.71	468	5.47	0.278	8.2	14.79	0.80	2.39	0.90	0.88

Date	Chloride mg/L	Total Fe mg/L	Dissolved Fe mg/L	Total Mn mg/L	Dissolved Mn mg/L	Nitrate mg/L	Sulfate mg/L	Sulfide mg/L	Methane mg/L	Ethane mg/L	Ethene mg/L	Alkalinity mg/L	TOC mg/L	CO2 mg/L	Lactic acid mg/L	Pyruvic acid mg/L	Acetic acid mg/L	Propionic acid mg/L	Butyric acid mg/L
Oct-03	28	42.1	41.7	5.69	6.05	0.032	18	1.4	0.64	0.021	0.002	77	8.57	1300	50	50	27.8	7.54	5.00
Feb-04	29	50.8	48.1	6.64	6.48	0.011	31	0.85	0.95	0.021	0.002	53	10.6	150	50	50	6.25	0.29	0.55
May-04	31	49.0	50.9	7.13	7.08	0.40	29	3.5	0.98	0.0025	0.002	59	3.55	820	50	50	0.81	0.29	0.55

Reported as BRL with a U flag (the compound was analyzed for but not detected); Use 1/2 Method Detection Limit (MDL)

Reported with a J flag (results between MDL and Reporting Limit); Using 1/2 Reporting Limit IF the result is LESS THAN 1/2 Reporting Limit

Reported with a J flag (results between MDL and Reporting Limit); Using the reported value IF the result is MORE THAN 1/2 Reporting Limit

Appendix D: Post Injection Pilot Area Monitoring Well Data

TMW-26S

(post injection results)

Date	PCE ug/L	TCE ug/L	cis-1,2-DCE ug/L	trans-1,2-DCE ug/L	1,1-DCE ug/L	Vinyl Chloride ug/L	DO mg/L	ORP mV	pH	Conductivity	Turbidity	Temp C	Normalized Field Parameters DO	ORP	pH	Cond.
Oct-03	25	9.9	250	0.5	0.185	2.6	0.95	198	5.99	0.553		14.96	1	1	1	1
Dec-03	24	12	280	0.57	0.185	2.2	1.32	95	5.89	0.553	10.3	14.56	1.39	0.48	0.98	1.00
Jan-04	26	9.8	310	1.65	1.85	1.5	0.74	112	6.08	0.571	5.9	13.56	0.78	0.57	1.02	1.03
Feb-04	63	33	560	4.15	4.65	3.75	1.88	93	5.84	0.540	8.8	14.15	1.98	0.47	0.97	0.98
Mar-04	35	15	360	1.65	1.85	1.5	0.75	129	5.43	0.282	5.7	14.65	0.79	0.65	0.91	0.51
Apr-04	33	14	380	2.5	0.36	1.8	1.19	234	6.33	0.498	5.3	15.05	1.25	1.18	1.06	0.90
May-04	31	13	410	0.66	0.185	2.1	0.37	305	5.92	0.520	9.3	15.21	0.39	1.54	0.99	0.94

Date	Chloride mg/L	Total Fe mg/L	Dissolved Fe mg/L	Total Mn mg/L	Dissolved Mn mg/L	Nitrate mg/L	Sulfate mg/L	Sulfide mg/L	Methane mg/L	Ethane mg/L	Ethene mg/L	Alkalinity mg/L	TOC mg/L	CO2 mg/L	Lactic acid mg/L	Pyruvic acid mg/L	Acetic acid mg/L	Propionic acid mg/L	Butyric acid mg/L
Oct-03	29	35.3	32.2	5.16	5.27	0.032	99	1.8	0.91	0.021	0.002	120	15.5	860	50	50	15.4	5.0	5.0
Feb-04	34	58.4	48.7	7.79	7.32	0.60	81	1.75	0.44	0.001	0.002	16	52.4	26	50	50	12.3	23.4	20.0
May-04	31	60.2	58.6	7.85	8.20	0.35	56	0.85	1.6	0.0025	0.002	180	27.4	510	50	50	14.5	5.0	0.55

Reported as BRL with a U flag (the compound was analyzed for but not detected); Use 1/2 Method Detection Limit (MDL)

Reported with a J flag (results between MDL and Reporting Limit); Using 1/2 Reporting Limit IF the result is LESS THAN 1/2 Reporting Limit

Reported with a J flag (results between MDL and Reporting Limit); Using the reported value IF the result is MORE THAN 1/2 Reporting Limit

Appendix D: Post Injection Pilot Area Monitoring Well Data

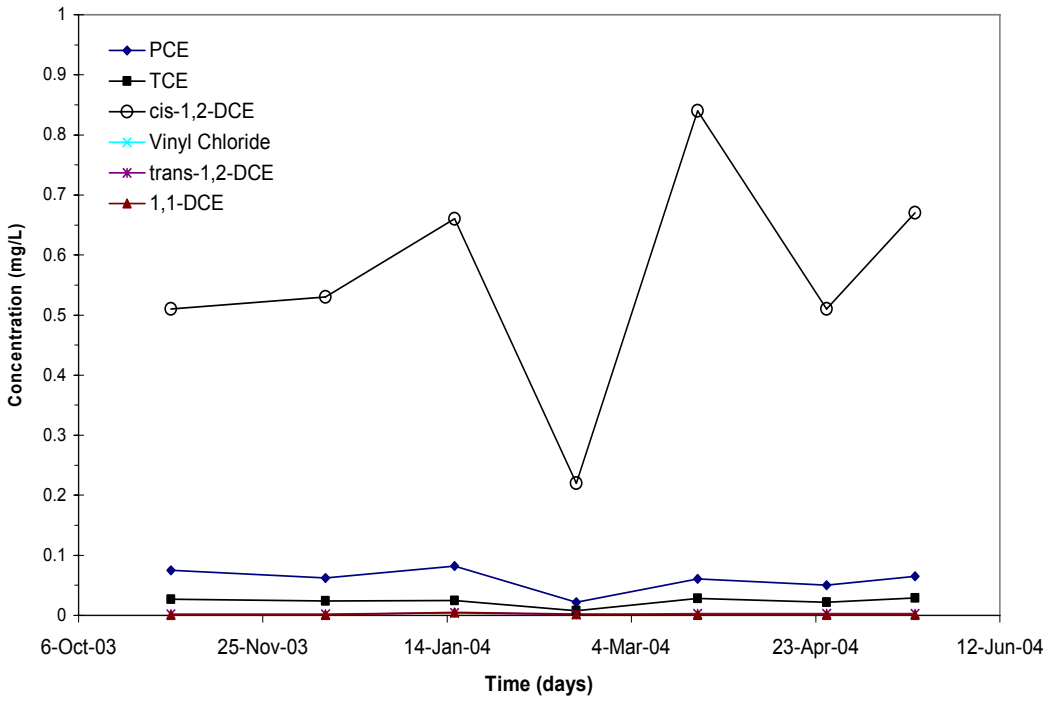

TMW-S2 CAH Trends

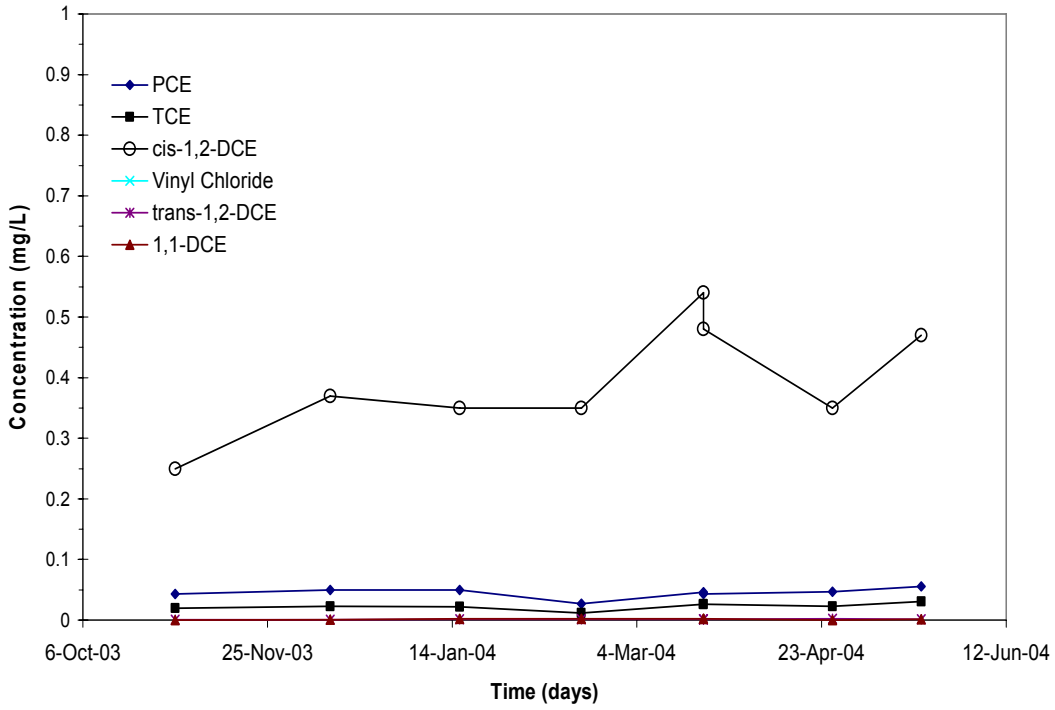

TMW-S3 CAH Trends

Appendix D: Post Injection Pilot Area Monitoring Well Data

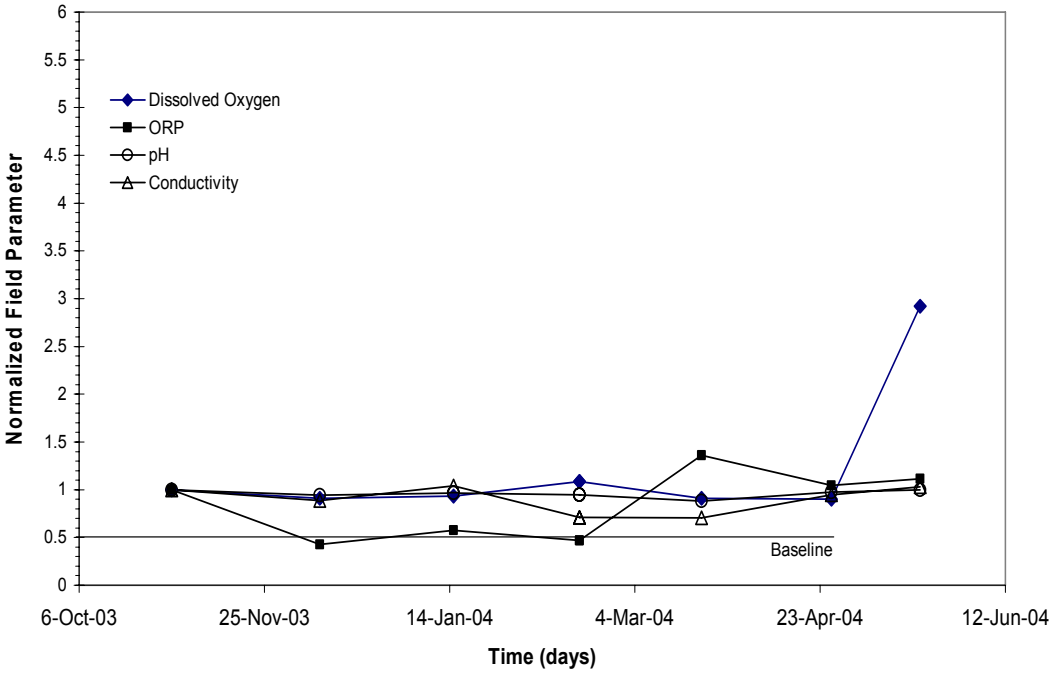

TMW-S1 Normalized Field Water Quality Parameters

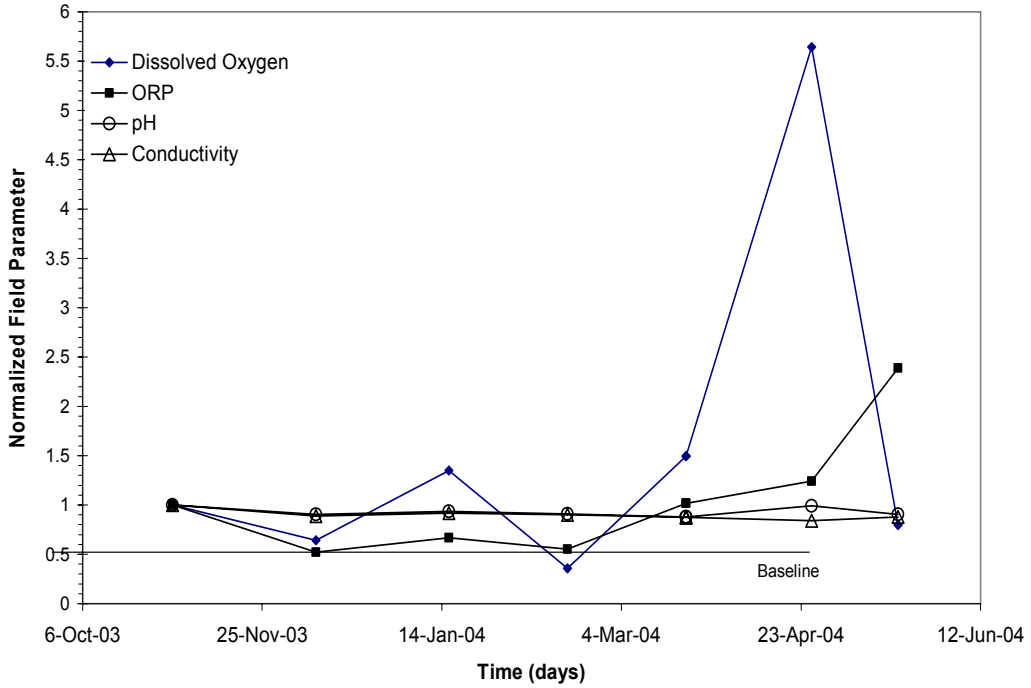

TMW-S3 Normalized Field Water Quality Parameters

Appendix D: Post Injection Pilot Area Monitoring Well Data

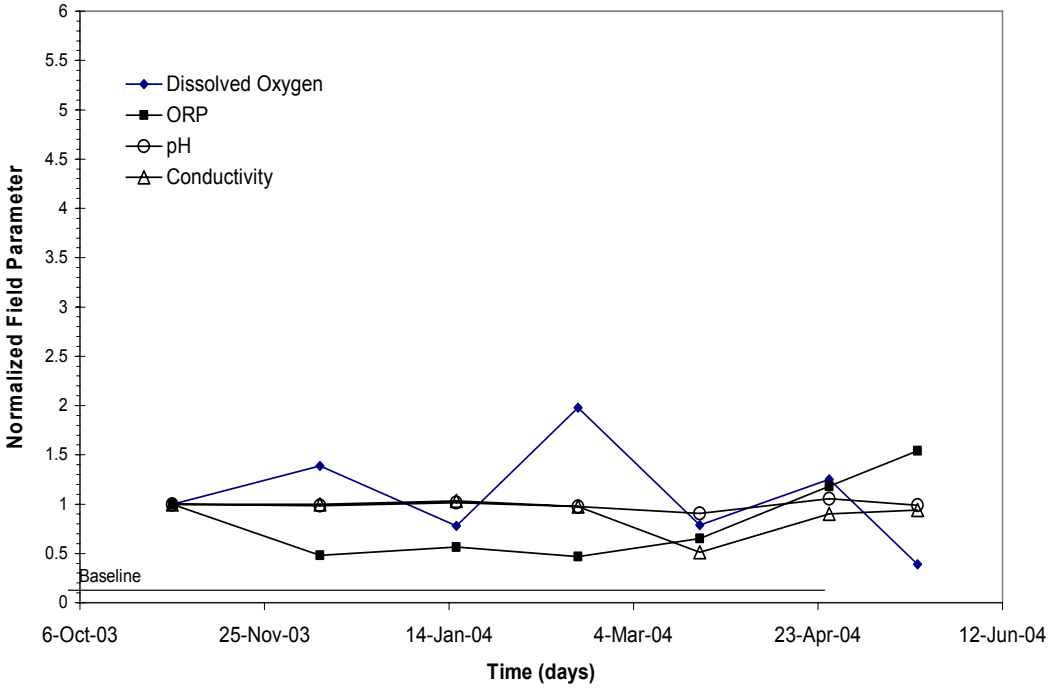

TMW-26S Normalized Field Water Quality Parameters

Appendix E: Henry's Constant and Activity Coefficient Data

Figure 1

Henry's Constant (H') and Activity Coefficient (γ) Data and Calculations

ρ_{water} (25°C) = 9.97E-01 g/ml Stock Conc= 4.32E-03 mg/µl

Bottle vol= 159.88 ml H' = 0.15

Sample ID	Dry Wt. (g)	Wet Wt. (g)	Wet - Dry wt. (g)	Vol Water (ml)	Vol Gas (ml)	Wt. w/ DCE stock (g)	Total Stock added (mg)	Vol Stock (µl)	Total Mass DCE (µg)	Estimated Cw (µg/L)	Area Counts (avg)	Cw (mg/L)	Cg (mg/L)
HC1	102.52	142.29	39.77	39.88	120.00	142.30	15.90	20.08	86.75	2175.43	8067.16	2.07	0.31
HC2	102.88	142.68	39.79	39.90	119.98	142.69	16.40	20.71	89.48	2242.48	7570.64	1.94	0.29
HC3	103.01	142.84	39.83	39.93	119.95	142.85	15.60	19.70	85.11	2131.32	7249.25	1.85	0.28
HC4	102.91	182.48	79.57	79.78	80.10	182.50	15.60	19.70	85.11	1066.81	4856.49	1.22	0.18
HC5	103.18	182.83	79.65	79.87	80.01	182.85	15.80	19.95	86.20	1079.35	4725.29	1.19	0.18
HC6	102.86	182.21	79.35	79.56	80.32	182.22	15.40	19.45	84.02	1056.08	4992.03	1.26	0.19
AC1	103.34	183.01	79.67	79.89	79.99	183.02	15.70	19.83	85.66	1072.24	4553.63	1.14	0.17
AC2	103.41	183.14	79.73	79.95	79.93	183.15	15.20	19.20	82.93	1037.31	4977.83	1.26	0.19
BG	102.80	182.55	79.75	79.97	79.91	182.56	15.10	19.07	82.38	1030.22	5718.90	1.45	0.22

COMBO	Hc'
1+4	0.10
1+5	0.08
1+6	0.12
2+4	0.15
2+5	0.13
2+6	0.17
3+4	0.19
3+5	0.17
3+6	0.22
Avg H':	**0.15**
γ=	**1.11**

Appendix E: Henry's Constant and Activity Coefficient Data

Reported Henry's Constants and Estimates For cDCE and PCE At 30°C

T(°C)	H' (DCE)[1]	H' (PCE)[1]
1.8	0.09	0.22
21.6	0.14	0.64
40	0.29	1.33
50	0.37	1.77
60	0.48	2.52
70	0.67	4.16

Calculated (from Figure 5)

T(°C)	H' (DCE)	H' (PCE)
10	1.10E-01	3.47E-01
19	1.44E-01	5.04E-01
30	2.00E-01	7.95E-01
31	2.07E-01	8.28E-01
32	2.13E-01	8.63E-01
33	2.19E-01	9.00E-01
34	2.26E-01	9.38E-01
35	2.33E-01	9.77E-01

[1]Source: Shimotori, T., Arnold, W.A., Measurement and Estimation of Henry's Law Constants of Chlorinated Ethylenes in Aqueous Surfactant Solutions, *Journal of Chemical Engineering Data*. 2003. 48: 253-261

Appendix E: Henry's Constant and Activity Coefficient Data

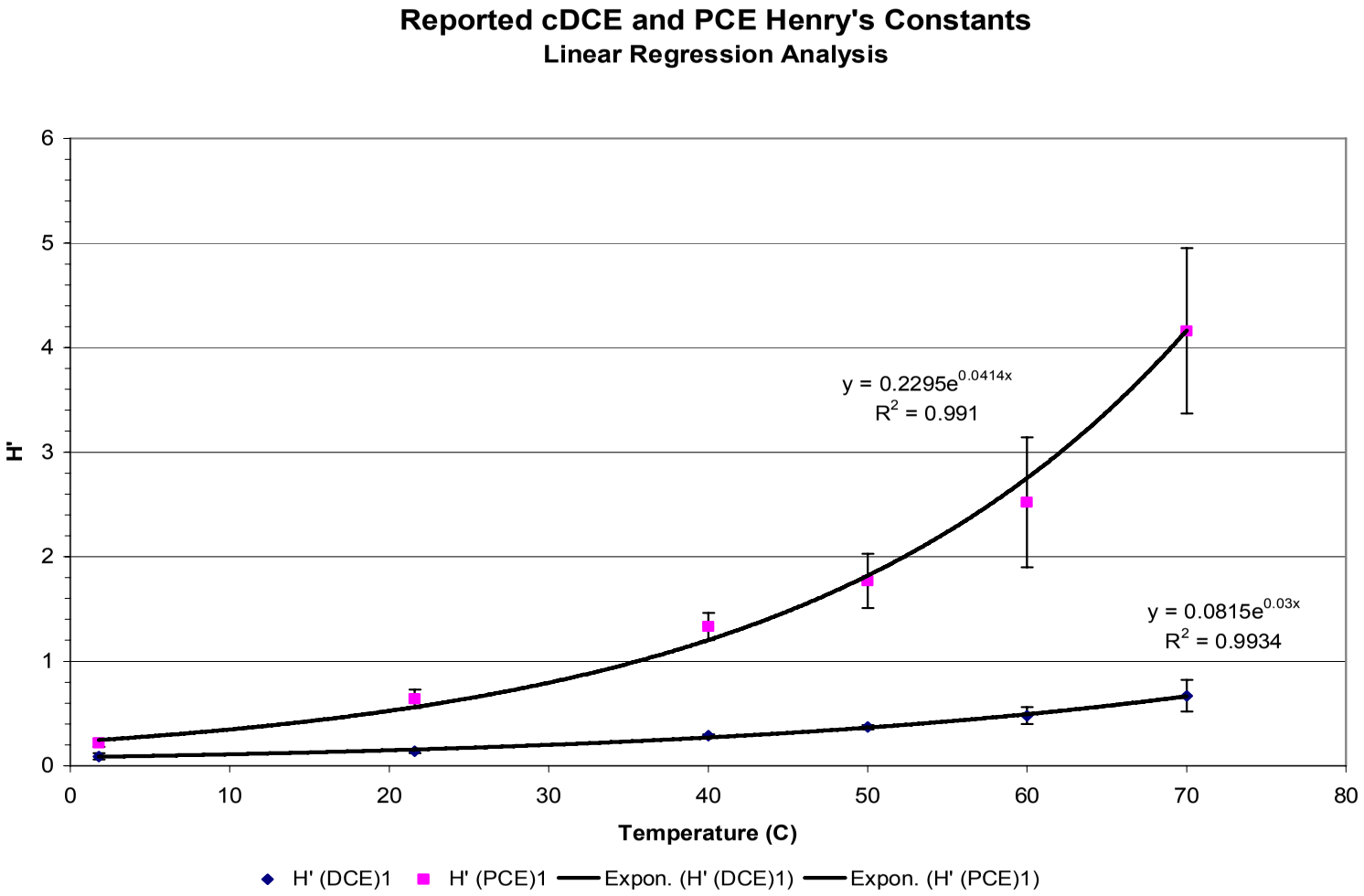

Appendix F: FORTRAN Dispersion Program and Output Pages

```
      PROGRAM trafit1d
C
C THIS IS A FORTRAN PROGRAM THAT CALCULATES THE SUM OF THE SQUARES OF
C EITHER THE ABSOLUTE OR RELATIVE RESIDUALS BETWEEN THE NORMALIZED
C EXPERIMENTAL CONSERVATIVE TRACER DATA AND THE NORMALIZED FLUX-
C AVERAGED CONCENTRATION CALCULATED USING THE ONE-DIMENSIONAL NON-
C REACTIVE SOLUTE TRANSPORT MODEL OF PARKER AND VAN GENUCHTEN (1984)
C AND THE BEST FIT HYDRODYNAMIC DISPERSION COEFFICIENT, DH, AND AVERAGE
C PORE WATER VELOCITY, V (WHICH IS USED TO CALCULATE THE BEST FIT PORO-
C SITY).  THE BEST FIT PARAMETERS ARE OBTAINED USING A MODIFIED LEVEN-
C BERG-MARQUARDT METHOD TO MINIMIZE THE SUMS OF THE SQUARES OF THE
C RESIDUALS BETWEEN OBSERVED AND CALCULATED CONCENTRATIONS.  THE EXPER-
C IMENTAL DATA ARE FROM A PACKED BED COLUMN WITH A SQUARE CROSS-SECT.
C
C THE MAIN PROGRAM CALLS FIVE SUBROUTINES:
C     INPUT:  READS INPUT FROM A DATA FILE CALLED INDAT1D.
C     DUNLSF: AN IMSL SUBROUTINE THAT SOLVES A NONLINEAR LEAST SQUARES
C             PROBLEM USING A MODIFIED LEVENBERG-MARQUARDT ALGORITHM
C             AND A FINITE-DIFFERENCE JACOBIAN.
C     FCN:    CALCULATES EITHER THE ABSOLUTE OR RELATIVE RESIDUAL
C             VECTOR.
C     EXER:   CALCULATES EXP(A) ERFC(B)
C
C VARIABLES:
C     AREA - COLUMN CROSS SECTIONAL AREA (CM^2).
C     BSTPOR - BEST FIT FOR POROSITY;CALCULATED FROM VELOCITY BEST FIT.
C     CEX(I) - NORMALIZED EXPERIMENTAL EFFLUENT CONCENTRATION AT EACH
C              SAMPLING TIME.
C     CMOD(I) - CALCULATED NORMALIZED FLUX-AVERAGED EFFLUENT CONCENTRA-
C               TION AT EACH SAMPLING TIME, USING OPTIMUM FIT PARAMETER
C               VALUES.
C     DATPTS - NUMBER OF EXPERIMENTAL OBSERVATIONS.
C     VD(I) - ESTIMATED VALUES FOR AVERAGE PORE WATER VELOCITY AND
C              HYDRODYNAMIC DISPERSION COEFFICIENT, RESPECTIVELY.
C     FJAC(I,J) - FINITE DIFFERENCE APPROXIMATE JACOBIAN AT SOLUTION.
C     FLOW - EXPERIMENTALLY DETERMINED BULK FLOW RATE (ML/HR).
C     FSCALE(I) - DIAGONAL SCALING MATRIX FOR FUNCTION.
C     LENGTH - LENGTH OF COLUMN (CM).
C     N - NUMBER OF PARAMETERS TO BE ESTIMATED.
C     PGUESS(I) - INITIAL GUESS FOR AVERAGE PORE WATER VELOCITY (CM/HR)
C                 AND HYDRODYNAMIC DISPERSION COEFFICIENT (CM^2/HR) ,
C                 RESPECTIVELY.
C     PSCALE(I) - DIAGONAL SCALING MATRIX FOR VARIABLES.
C     RESID(I) - ABSOLUTE OR RELATIVE RESIDUALS.
C     RPARAM(I) - PARAMETER VECTOR FOR OPTIMIZATION SUBROUTINE.
C     SUMSQ - SUM OF SQUARES OF ABSOLUTE OR RELATIVE RESIDUALS.
C     TIME(I) - COLUMN EFFLUENT SAMPLING TIMES (HR).
C
C-----------------------------------------------------------------------
C
C DECLARATION OF VARIABLES
C
      DOUBLE PRECISION TIME(30), CEX(30), CMOD(30), RESID(30), VD(2),
     *RPARAM(7), FJAC(30,2), PSCALE(2), PGUESS(2), FSCALE(30)
      DOUBLE PRECISION EXER, SUMSQ, LENGTH, FLOW, AREA, BSTPOR, STDDEV
C
      INTEGER SSE, DATPTS, I, LDFJAC, IPARAM(6), N
C
      COMMON/OBS/LENGTH, TIME, CEX, CMOD, SSE
C
```

```
      EXTERNAL FCN, INPUT
C
C OPEN FILES
C
      OPEN (5, FILE='INDAT1D', STATUS='OLD')
      OPEN (6, FILE='BSTFIT1D', STATUS='UNKNOWN')
C
C READ INPUT VARIABLES
C
      CALL INPUT (LENGTH, FLOW, AREA, PGUESS, SSE, DATPTS, TIME, CEX)
C
C INITIALIZE OPTIMIZATION SUBROUTINE ARGUMENTS
C
      N=2
      DO 90 I=1,N
         PSCALE(I)=1.0
   90 CONTINUE
      DO 100 I=1,30
         FSCALE(I)=1.0
  100 CONTINUE
      IPARAM(1)=0
      LDFJAC=30
C
C CALL THE OPTIMIZATION SUBROUTINE TO SOLVE FOR THE BEST-FIT PARAMETERS
C
      CALL DUNLSF(FCN, DATPTS, N, PGUESS, PSCALE, FSCALE, IPARAM,
     *RPARAM, VD, RESID, FJAC, LDFJAC)
C
C CALCULATE THE SUM OF THE SQUARES OF THE RESIDUALS
C
      SUMSQ=0.0D0
      DO 120 I=1,DATPTS
         SUMSQ=SUMSQ+RESID(I)**2
  120 CONTINUE
C
C CALCULATE THE STANDARD DEVIATION OF THE ABSOLUTE OR RELATIVE
C RESIDUALS
C
      STDDEV=DSQRT(SUMSQ/DFLOAT(DATPTS-2))
C
C CALCULATE THE BEST FIT POROSITY FROM THE BEST FIT AVG. PORE WATER
C VELOCITY, FLOW, AND CROSS-SECTIONAL AREA
C
      BSTPOR=FLOW/(AREA*VD(1))
C
C WRITE RESULTS TO OUTPUT FILE
C
      WRITE (6, 130)
  130 FORMAT (8X, 'THE BEST-FIT PARAMETERS ARE:')
      WRITE (6, 140) VD(1), BSTPOR, VD(2)
  140 FORMAT (10X, 'VELOCITY =', X, F6.3, 4X, 'POROSITY =', X, F5.3, 4X
     *, 'DH =', X, F6.3,/)
      IF(SSE.EQ.1) THEN
      WRITE (6, 150)
  150 FORMAT (10X, 'TIME', 8X, 'C/C''(exp)', 4X, 'C/C''(model)',
     *4X, 'ABS RESIDUAL', /)
         ELSE
      WRITE (6, 160)
  160 FORMAT (10X, 'TIME', 8X, 'C/C''(exp)', 4X, 'C/C''(model)',
      *4X, 'REL RESIDUAL', /)
      ENDIF
      DO 200 I=1, DATPTS
         WRITE (6, 190) TIME(I), CEX(I), CMOD(I), RESID(I)
```

```
  190    FORMAT (8X, F6.2, 8X, F6.4, 9X, F6.4, 8X, E10.4)
  200 CONTINUE
      WRITE (6,*)
      WRITE (6, 210) SUMSQ
  210 FORMAT (18X, 'THE SUM-OF-SQUARED RESIDUALS IS: ', G10.4)
      WRITE (6, 220) STDDEV
  220 FORMAT (7X, 'THE STANDARD DEVIATION OF THE RESIDUALS IS: ', G10.4
     *)
C
      STOP
      END
C
C*********************************************************************
C
      SUBROUTINE INPUT (LENGTH, FLOW, AREA, PGUESS, SSE, DATPTS, TIME,
     *CEX)
C
C THIS SUBROUTINE READS INPUT FROM A DATA FILE CALLED INDAT1D
C
C IF SSE=1, THE ABSOLUTE LEAST SQUARES (ALS) CRITERION IS USED;
C IF SSE=2, THE RELATIVE LEAST SQUARES (RLS) CRITERION IS USED.
C
C---------------------------------------------------------------------
C
      DOUBLE PRECISION TIME(30), CEX(30), PGUESS(2)
      DOUBLE PRECISION LENGTH, FLOW, AREA
      INTEGER SSE, DATPTS, I
      READ (5,2) LENGTH, FLOW, AREA, PGUESS(1), PGUESS(2)
    2 FORMAT(F6.3)
      READ (5,4) SSE, DATPTS
    4 FORMAT(I2)
      DO 10 I=1, DATPTS
         READ (5,6) TIME(I), CEX(I)
    6 FORMAT(F7.4, X, F6.4)
   10 CONTINUE
      RETURN
      END
C
C *********************************************************************
C
      SUBROUTINE FCN(DATPTS, N, VD, RESID)
C
C THIS SUBROUTINE COMPUTES THE ANALYTICAL SOLUTION TO THE NON-REACTIVE
C SOLUTE TRANSPORT EQUATION.  THE POSITION (X), TIME (T), PORE WATER
C VELOCITY (VD(1)), AND THE DISPERSION COEFFICIENT (VD(2)) ARE INPUTS.
C THE OUTPUT IS THE NORMALIZED FLUX-AVERAGED CONCENTRATION (C/Co) AT
C THE GIVEN POSITION AND TIME (PARKER AND VAN GENUCHTEN, 1984).  THIS
C REQUIRES AN EXTERNAL FUNCTION EXER(A,B), WHICH COMPUTES THE VALUE OF
C EXP(A)*ERFC(B). THE SUBROUTINE USES THESE VALUES TO THEN CALCULATE
C EITHER THE ABSOLUTE OR RELATIVE RESIDUAL VECTOR.
C
C---------------------------------------------------------------------
C
C DECLARE VARIABLES
C
      DOUBLE PRECISION TIME(30), CEX(30), CMOD(30), VD(2), RESID(30),
     *LENGTH
C
      INTEGER DATPTS, N, SSE, I
C
      COMMON/OBS/LENGTH, TIME, CEX, CMOD, SSE
C
C DECLARE LOCAL VARIABLES
```

```
C
      DOUBLE PRECISION A(30), B(30), E(30), EXER
C
C COMPUTE THE VALUES OF THE LOCAL VARIABLES
C
      DO 300 I=1,DATPTS
      A(I)=(LENGTH-VD(1)*TIME(I))/(2.0D0*DSQRT(VD(2)*TIME(I)))
      B(I)=VD(1)*LENGTH/VD(2)
      E(I)=(LENGTH+VD(1)*TIME(I))/(2.0D0*DSQRT(VD(2)*TIME(I)))
  300 CONTINUE
C
C COMPUTE THE NORMALIZED FLUX-AVERAGED CONCENTRATION AT X,T; THIS
C REQUIRES AN EXTERNAL FUNCTION EXER(A,B) WHICH COMPUTES THE VALUE
C OF EXP(A)*ERFC(B).
C
      DO 310 I=1,DATPTS
      CMOD(I)=0.5D0*EXER(0.0D0,A(I))+0.5D0*EXER(B(I),E(I))
  310 CONTINUE
C
C CALCULATE EITHER THE ABSOLUTE OR RELATIVE RESIDUALS VECTOR
C
      DO 320 I=1,DATPTS
         RESID(I)=CEX(I)-CMOD(I)
         IF(SSE.EQ.2) RESID(I)=RESID(I)/CEX(I)
  320 CONTINUE
      RETURN
      END
C
C***********************************************************************
C
      DOUBLE PRECISION FUNCTION EXER(A,B)
C
C THIS SUBROUTINE IS FROM VAN GENUCHTEN AND ALVES (1982)
C
C PURPOSE: TO CALCULATE EXP(A)*ERFC(B)
C
C DECLARE DUMMY VARIABLES
      DOUBLE PRECISION A, B
C
C DECLARE LOCAL VARIABLES
C
      DOUBLE PRECISION C, X, T, Y
C
      EXER=0.0D0
      IF ((DABS(A).GT.170.).AND.B.LE.0.0) RETURN
      IF (B.NE.0.0) GOTO 100
      EXER=DEXP(A)
      RETURN
  100 C=A-B*B
      IF ((DABS(C).GT.170.).AND.(B.GT.0.0)) RETURN
      IF (C.LT.-170.) GOTO 130
      X=DABS(B)
      IF (X.GT.3.0) GOTO 110
      T=1.0D0/(1.0D0+0.3275911D0*X)
      Y=T*(0.2548296D0-T*(0.2844967D0-T*(1.421414D0-T*(1.453152D0-
     *1.061405D0*T))))
      GOTO 120
  110 Y=0.5641896D0/(X+0.5D0/(X+1.0D0/(X+1.5D0/(X+2.0D0/(X+2.5D0/(X+
     *1.0D0))))))
  120 EXER=Y*DEXP(C)
  130 IF (B.LT.0.0) EXER=2.0*DEXP(A)-EXER
      RETURN
      END
```

```
C
C**********************************************************************
```

Appendix F: FORTRAN Dispersion Program and Output Pages

Best Fit Output for TEST 1

30.4800000 - *length(cm* 84.0000000 – *flow (ml/hr)* 11.40090000000 – *area(cm^2)*
33.6000000000000 – *pore water velocity (cm/hr)* 2.000000000000 – *DH(cm^2/hr)*
1 – *SSE* 18 - *# of datapoints*

0.650000000000000	0.000000000000000E+000
0.760000000000000	2.200000000000000E-002
0.875000000000000	6.330000000000000E-002
0.979000000000000	0.112000000000000
1.07900000000000	0.185500000000000
1.18300000000000	0.260000000000000
1.29000000000000	0.353000000000000
1.38800000000000	0.400000000000000
1.50000000000000	0.510000000000000
1.59200000000000	0.552000000000000
1.70000000000000	0.644000000000000
1.80200000000000	0.695000000000000
1.90300000000000	0.778000000000000
2.01000000000000	0.722000000000000
2.11000000000000	0.778000000000000
2.22000000000000	0.778000000000000
2.35000000000000	0.840000000000000
2.49000000000000	0.840000000000000

THE BEST-FIT PARAMETERS ARE:
VELOCITY = 18.506 POROSITY = 0.398 DH = 48.271

TIME	C/C'(exp)	C/C'(model)	ABS RESIDUAL
0.65	0.0000	0.0147	-.1470E-01
0.76	0.0220	0.0395	-.1748E-01
0.88	0.0633	0.0827	-.1939E-01
0.98	0.1120	0.1360	-.2404E-01
1.08	0.1855	0.1973	-.1177E-01
1.18	0.2600	0.2676	-.7588E-02
1.29	0.3530	0.3431	0.9932E-02
1.39	0.4000	0.4120	-.1201E-01
1.50	0.5100	0.4879	0.2214E-01
1.59	0.5520	0.5464	0.5627E-02
1.70	0.6440	0.6096	0.3436E-01
1.80	0.6950	0.6635	0.3148E-01
1.90	0.7780	0.7111	0.6686E-01
2.01	0.7220	0.7555	-.3352E-01
2.11	0.7780	0.7917	-.1367E-01
2.22	0.7780	0.8260	-.4800E-01
2.35	0.8400	0.8600	-.2000E-01
2.49	0.8400	0.8898	-.4975E-01

THE SUM-OF-SQUARED RESIDUALS IS: 0.1557E-01
THE STANDARD DEVIATION OF THE RESIDUALS IS: 0.3119E-01

Appendix F: FORTRAN Dispersion Program and Output Pages

Best Fit Output for TEST 2

```
 26.6700000000000       78.0000000000000       11.4009000000000
 31.2000000000000       2.17000000000000
       1         17
3.000000000000000E-002  0.000000000000000E+000
0.100000000000000       0.000000000000000E+000
0.430000000000000       8.000000000000000E-002
0.650000000000000       0.180000000000000
0.770000000000000       0.300000000000000
0.880000000000000       0.380000000000000
 1.00000000000000       0.460000000000000
 1.13000000000000       0.530000000000000
 1.25000000000000       0.600000000000000
 1.36000000000000       0.700000000000000
 1.47000000000000       0.750000000000000
 1.58000000000000       0.800000000000000
 1.70000000000000       0.790000000000000
 1.82000000000000       0.890000000000000
 1.95000000000000       0.910000000000000
 2.38000000000000       0.940000000000000
 2.75000000000000        1.00000000000000
    THE BEST-FIT PARAMETERS ARE:
     VELOCITY = 22.320    POROSITY = 0.307    DH = 88.779

     TIME       C/C'(exp)    C/C'(model)    ABS RESIDUAL

     0.03       0.0000       0.0000       -.1896E-28
     0.10       0.0000       0.0000       -.6157E-08
     0.43       0.0800       0.0389       0.4109E-01
     0.65       0.1800       0.1805       -.5109E-03
     0.77       0.3000       0.2807       0.1932E-01
     0.88       0.3800       0.3733       0.6661E-02
     1.00       0.4600       0.4686       -.8614E-02
     1.13       0.5300       0.5609       -.3093E-01
     1.25       0.6000       0.6347       -.3475E-01
     1.36       0.7000       0.6929       0.7073E-02
     1.47       0.7500       0.7427       0.7302E-02
     1.58       0.8000       0.7849       0.1507E-01
     1.70       0.7900       0.8235       -.3348E-01
     1.82       0.8900       0.8553       0.3466E-01
     1.95       0.9100       0.8835       0.2647E-01
     2.38       0.9400       0.9433       -.3319E-02
     2.75       1.0000       0.9695       0.3051E-01

        THE SUM-OF-SQUARED RESIDUALS IS: 0.8640E-02
   THE STANDARD DEVIATION OF THE RESIDUALS IS: 0.2400E-01
```

Appendix F: FORTRAN Dispersion Program and Output Pages

Best Fit Output for TEST 3

```
 26.6700000000000       84.0000000000000       11.4009000000000
 33.6000000000000       2.00000000000000
       1        19
3.000000000000000E-003  0.000000000000000E+000
0.220000000000000       0.000000000000000E+000
0.330000000000000       8.000000000000000E-003
0.470000000000000       7.500000000000000E-002
0.580000000000000       0.152000000000000
0.690000000000000       0.225000000000000
0.780000000000000       0.311000000000000
0.860000000000000       0.369000000000000
0.970000000000000       0.435000000000000
 1.08000000000000       0.488000000000000
 1.15000000000000       0.551000000000000
 1.43000000000000       0.697000000000000
 1.54000000000000       0.745000000000000
 1.74000000000000       0.774000000000000
 1.85000000000000       0.876000000000000
 1.95000000000000       0.897000000000000
 2.03000000000000       0.893000000000000
 2.13000000000000       0.906000000000000
 2.28000000000000       0.997000000000000
    THE BEST-FIT PARAMETERS ARE:
     VELOCITY = 21.910    POROSITY = 0.336    DH = 95.249

     TIME      C/C'(exp)   C/C'(model)   ABS RESIDUAL

     0.00      0.0000      0.0000      0.0000E+00
     0.22      0.0000      0.0006      -.6341E-03
     0.33      0.0080      0.0115      -.3506E-02
     0.47      0.0750      0.0634      0.1162E-01
     0.58      0.1520      0.1335      0.1851E-01
     0.69      0.2250      0.2186      0.6407E-02
     0.78      0.3110      0.2923      0.1867E-01
     0.86      0.3690      0.3574      0.1158E-01
     0.97      0.4350      0.4427      -.7741E-02
     1.08      0.4880      0.5208      -.3278E-01
     1.15      0.5510      0.5661      -.1507E-01
     1.43      0.6970      0.7130      -.1603E-01
     1.54      0.7450      0.7572      -.1216E-01
     1.74      0.7740      0.8213      -.4735E-01
     1.85      0.8760      0.8493      0.2673E-01
     1.95      0.8970      0.8709      0.2610E-01
     2.03      0.8930      0.8860      0.7038E-02
     2.13      0.9060      0.9023      0.3651E-02
     2.28      0.9970      0.9226      0.7438E-01

        THE SUM-OF-SQUARED RESIDUALS IS: 0.1201E-01
   THE STANDARD DEVIATION OF THE RESIDUALS IS: 0.2658E-01
```

Appendix G: Biokinetics Experimental Data

Figure 1

Biokinetics serum bottle preparation data (for cDCE additions)

ρ_{water} (25°C) = 9.97E-01 g/ml Stock Conc= 7.10E-04 mg/µl

Bottle vol= 159.88 ml Bulk Den= 2.19 g/ml

Sample ID	Vol Water (ml)	Soil Wt (g)	Vol Soil (ml)	Vol Gas (ml)	Vol Stock (µl)	Total Mass DCE (µg)	Cin (ppb)	Substrate Added	
COM-1	51.36	11.56009	5.28	103.24	70.40	50.01	973.69	3.13	
COM-2	51.35	11.5319	5.27	103.26	70.40	50.01	973.75	3.13	(ml 99.0%+
COM-3	51.36	11.56949	5.28	103.24	70.40	50.01	973.67	3.13	methane gas)
COM-4	51.35	11.54049	5.27	103.26	70.40	50.01	973.73	3.13	
DO-1	51.36	11.5892	5.29	103.23	70.40	50.01	973.62	--	
DO-2	51.36	11.5603	5.28	103.24	70.40	50.01	973.69	--	
DO-3	51.36	11.5783	5.29	103.23	70.40	50.01	973.65	--	
DO-4	51.35	11.5349	5.27	103.26	70.40	50.01	973.74	--	
HRC-1	51.36	11.5693	5.28	103.24	70.40	50.01	973.67	1.38	
HRC-2	51.36	11.5763	5.29	103.24	70.40	50.01	973.71	1.38	(ml HRC)
HRC-3	51.36	11.5527	5.28	103.25	70.40	50.01	973.70	1.38	
HRC-4	51.35	11.5348	5.27	103.26	70.40	50.01	973.74	1.38	
LAC-1	51.36	11.5552	5.28	103.25	70.40	50.01	973.70	0.40	
LAC-2	51.36	11.6074	5.30	103.22	70.40	50.01	973.58	0.40	(ml sodium
LAC-3	51.36	11.575	5.29	103.24	70.40	50.01	973.65	0.40	lactate)
LAC-4	51.36	11.5513	5.27	103.25	70.40	50.01	973.71	0.40	
MOL-1	51.36	11.5589	5.28	103.25	70.40	50.01	973.69	1.20	
MOL-2	51.36	11.5524	5.28	103.25	70.40	50.01	973.70	1.20	(ml
MOL-3	51.36	11.5519	5.27	103.25	70.40	50.01	973.70	1.20	molasses)
MOL-4	51.36	11.5478	5.27	103.25	70.40	50.01	973.71	1.20	
STER-1	51.37	11.7155	5.35	103.16	70.40	50.01	973.34	--	
STER-2	51.36	11.5579	5.28	103.25	70.40	50.01	973.69	--	
STER-3	51.36	11.5895	5.29	103.23	70.40	50.01	973.62	--	
STER-4	51.37	11.6419	5.32	103.20	70.40	50.01	973.50	--	
UC-1	50.00	--	--	109.88	70.40	50.01	1000.10	--	
UC-2	50.00	--	--	109.88	70.40	50.01	1000.10	--	
UC-3	50.00	--	--	109.88	70.40	50.01	1000.10	--	
UC-4	50.00	--	--	109.88	70.40	50.01	1000.10	--	

Appendix G: Biokinetics Experimental Data

Figure 2

GC With ECD cDCE PEAK AREAS

	Date Sampled																								
	22-Aug	23-Aug	26-Aug	29-Aug	30-Aug	4-Sep	7-Sep	12-Sep	13-Sep	16-Sep	23-Sep	1-Oct	3-Oct	5-Oct	8-Oct	9-Oct	11-Oct	12-Oct	15-Oct	20-Oct	27-Oct	3-Nov	10-Nov	17-Nov	22-Nov	29-Nov	9-Dce
Sample ID	cDCE PEAK AREAS																										
COM-1		3662.4		4343.3			4242.1		4255.9	5148.2	5396.9		4365.9			4286.7		4733.2	4358.2	4293.1							
COM-2		3319.9		4451.5			4590.2		4248	4714	5649.7		4391.7					4563.5	4497								
COM-3	4817.5	5096.3	5110.1		5962.8	5843.6	5747.4	6366.2			7563.4	6367.7					7352.9			7655.9		6708.6		5257.6		6216.5	
COM-4	5304.7	5761.8	5602.3		5357.9	5752.1	5718.6	5928.1			7699.9	8133.4					6787.3			6702.2		5877.2		4621.5		6001	
DO-1		3691.8		4068.4			4452.2		3888.8	4845.3	5518		4561.8			3810.8		4562.5	4599.1	4187.9							
DO-2		3479.9		4634			4450.6		4315.4	4155.9	4897		4572.5					4594.8	4396.9								
DO-3	5385.5	5487.4	5130.6		6389.3	5980.9	5552.6	4837.5			7544.7	8013.5					6650.7			7228.6		6194.5		5480.8		5532.9	
DO-4	5362.2	5579.7	5476.1		6132.5	6115.5	5695.2	5411.8			6615.4	7350.7					6685.3			7227		5755.2		5046.6		5100.8	
HRC-1		3651.7		3706.1			4294.5		4336.9	4731.6	5171.8		4478.3			4371.9		4632.2	4616.8	4451.4							
HRC-2		3535.3		4057.5			4630.3		4190.3	5004	5398.1		4465.3					4522.8	4666.8								
HRC-3	5016.9	5443.1	5513.5		5848.8	6131.3	5642	5465.2			7453.5	7503.8		8055.7	8548.3		7544.4		7716.2	8345	7326		7523		8995.9		
HRC-4	5226.5	5213.4	5781		6503.1	6209.8	6129.1	6148.6			7884.8	8169.7		8602.2		7943.5	7297		1.11E+04	6909.2	7388		7376		6863.6		
LAC-1		3650.4		4470.4			4686.4		4212.8	4680.1	5330.1		4763.1			4669.1		4924.6	4925.2	4589.1							
LAC-2		3534.4		4727.6			4456.9		4035.8	4329.9	4560.3		4400					4631.4	4950.5								
LAC-3	5676.9	5771.6	6730.7		5584.1	6020	6273.3	5958.4			6971.3	7586.7		7938.4	9316.9		7714.5		9821.1	7026.6	7499		7787	8656	8097.9		
LAC-4	5966.4	5687.9	6830.2		5931.2	6342.1	6473.3	5537.6			7145.2	7159.6		7131.47		8467.6	7191.4		9633.1	8308.1	7565			9316.2	8504.2		
MOL-1		3718.2		4884.5			5134.5		4113.8	4677.1	5013.5		4097			4878.1		4559.1	4707.8	4689.7							
MOL-2		3628.7		4827.7			4339.2		4443.1	4522	5040.7		4470.1					4814.6	4884.8	4020.5							
MOL-3	4718.2	5988.4	5527.2		6232.4	6126.6	5392.5	5893.9			6987.9	8234.3		8185.3	8197.7	8645.6	7628.3		1.13E+04	9025.9	6447			8826.3	5107		8069.4
MOL-4	5413.2	5925.1	5217.6		6311.2	6087.5	6330.2	5891.1			7026.7	7934.9		8261.3	9330.6		7354.8	8309.4	1.26E+04	8804.6	7550			8811.8	6320		8153.3
STER-1		3833		4233.1			4606.5		4280.2	4579.6	4884.8		4411.1			3935.2		4490.7	4424.3	4164							
STER-2		2825.8		4825.8			4309.1		5162.9	4512.2	5706.1		4563.5					4713.5	4465.1								
STER-3	5905.97	6252.7	7140.5		5939.1	6307.3	6047.1	5627.7			6791.3	7287		7828.7	6741.1	7197.7	7186.2		7801.2	6943.9		5476.5		7246.6	6485.6		
STER-4	6278.99	5724.5	6592.9		6137.6	6018.7	5643.7	5091.5			6955.1	7379.8		8057.6		7423.3	7192.3		8264.3	7526.8		5110.8		6858.3	6785.5		
UC-1		3055.6		4743.2			4419		4273	5133.6	4730.8		5034.1			3860.7		4911.4	5325.8	4919.7							
UC-2		3096.1		4631			4633.3		4416.7	5233.4	5219		5089.6					5455.1	5091.8								
UC-3	5924.6	6403.9	6209.4		5889.8	5746.4	6181.6	5974.5			7548.1	8062.2					8812.7			8844.1		8515.6		8530.9		8212.8	
UC-4	6136.7	5823.8	6776.6		6026	5652	6126.8	5593.9			6962	7593.4					8420.2			7642.2		7966.7		6954.9		7613.6	
		Cold @ 10 C		Cold @ 19 C			Cold @ 19 C				Cold @ 19		Cold @ 14				Adjust pH to ~7										

Appendix G: Biokinetics Experimental Data

Figure 3

GC With ECD Aqueous cDCE Concentrations

	Time (days)																									
	1	2	5	8	9	14	17	22	23	26	33	41	43	45	48	49	51	52	55	60	67	74	81	88	93	100	110
Sample ID	AQUEOUS cDCE CONCENTRATIONS (mg/L)																										
COM-1		1.252		1.093			1.066		1.070	1.305	1.371		1.099			1.078		1.196	1.097								
COM-2		1.128		1.122			1.158		1.068	1.191	1.438		1.106					1.151	1.134								
COM-3	0.390	0.434	0.436		0.516	0.505	0.496	0.554			0.667	0.554					0.647			0.646		0.560		0.429		0.516	
COM-4	0.434	0.497	0.482		0.459	0.496	0.493	0.513			0.680	0.721					0.594			0.560		0.485		0.372		0.496	
DO-1		1.262		1.020			1.122		0.973	1.226	1.403		1.151			0.953		1.151	1.161								
DO-2		1.186		1.170			1.121		1.086	1.044	1.239		1.154					1.159	1.107								
DO-3	0.441	0.450	0.418		0.531	0.495	0.456	0.391			0.636	0.678					0.555			0.607		0.514		0.449		0.454	
DO-4	0.459	0.480	0.470		0.532	0.531	0.491	0.464			0.578	0.647					0.584			0.607		0.474		0.410		0.415	
HRC-1		1.248		0.925			1.080		1.091	1.196	1.312		1.129			1.101		1.169	1.165								
HRC-2		1.206		1.018			1.169		1.053	1.267	1.371		1.125					1.140	1.178								
HRC-3	0.408	0.446	0.452		0.483	0.508	0.464	0.448			0.627	0.632		0.682	0.726		0.636		0.594	0.708	0.616		0.634		0.767		
HRC-4	0.426	0.425	0.477		0.542	0.515	0.508	0.510			0.666	0.692		0.731		0.672	0.613		0.633	0.578	0.622		0.620		0.574		
LAC-1		1.247		1.127			1.184		1.059	1.182	1.353		1.204			1.179		1.246	1.247								
LAC-2		1.205		1.194			1.123		1.012	1.090	1.150		1.108					1.169	1.253								
LAC-3	0.467	0.476	0.562		0.459	0.498	0.521	0.493			0.584	0.639		0.671	0.796		0.651		0.644	0.589	0.632		0.658	0.736	0.686		
LAC-4	0.493	0.468	0.571		0.490	0.527	0.539	0.455			0.600	0.601		0.598		0.719	0.604		0.656	0.705	0.637			0.795	0.722		
MOL-1		1.272		1.236			1.302		1.032	1.181	1.270		1.028			1.234		1.150	1.189								
MOL-2		1.239		1.221			1.092		1.119	1.140	1.277		1.126					1.217	1.236								
MOL-3	0.381	0.495	0.454		0.517	0.508	0.441	0.487			0.585	0.698		0.693	0.695	0.735	0.643		0.519	0.769	0.537			0.751	0.416		0.683
MOL-4	0.443	0.490	0.426		0.524	0.504	0.526	0.486			0.589	0.671		0.700	0.797		0.619	0.705	0.581	0.749	0.636			0.750	0.525		0.691
STER-1		1.313		1.064			1.163		1.076	1.155	1.236		1.111			0.985		1.132	1.114								
STER-2		0.949		1.220			1.084		1.309	1.138	1.453		1.151					1.191	1.125								
STER-3	0.488	0.519	0.599		0.491	0.524	0.501	0.463			0.568	0.612		0.661	0.563	0.604	0.603		0.601	0.581		0.449		0.609	0.540		
STER-4	0.546	0.494	0.576		0.533	0.521	0.486	0.434			0.610	0.650		0.714		0.654	0.632		0.639	0.634		0.416		0.574	0.594		
UC-1		1.023		1.194			1.109		1.071	1.297	1.191		1.271			0.962		1.238	1.347								
UC-2		1.038		1.165			1.165		1.108	1.323	1.319		1.285					1.381	1.286								
UC-3	0.490	0.534	0.516		0.487	0.474	0.513	0.495			0.637	0.683					0.751			0.754		0.724		0.726		0.697	
UC-4	0.509	0.481	0.567		0.499	0.466	0.509	0.460			0.584	0.641					0.716			0.645		0.675		0.583		0.643	

Appendix G: Biokinetics Experimental Data

Figure 4

GC With FID cDCE Area Peaks

	Date Sampled																				
	30-Aug	7-Sep	12-Sep	13-Sep	16-Sep	23-Sep	1-Oct	3-Oct	8-Oct	9-Oct	11-Oct	12-Oct	15-Oct	20-Oct	27-Oct	3-Nov	10-Nov	17-Nov	22-Nov	23-Nov	29-Nov	09-Dec.
Sample ID	cDCE AREA PEAKS																					
COM-1				4.13E+04	4.24E+04	3.96E+04		3.20E+04		3.36E+04		3.91E+04	2.72E+04									
COM-2					4.18E+04	4.32E+04				3.10E+04		3.22E+04	3.59E+04									
COM-3	6.05E+04					5.54E+04	6.01E+04		6.28E+04		5.81E+04		7.71E+04	5.81E+04		4.49E+04		4.39E+04			4.02E+04	
COM-4	6.05E+04					5.34E+04	5.27E+04		5.78E+04		5.24E+04		5.23E+04	4.78E+04		3.84E+04		3.47E+04			3.04E+04	
DO-1					4.38E+04	4.05E+04				3.16E+04		3.09E+04	2.84E+04									
DO-2					4.14E+04	3.96E+04		3.10E+04				3.38E+04	2.77E+04									
DO-3	6.13E+04	5.98E+04				5.62E+04	5.41E+04		5.47E+04		4.81E+04		5.18E+04	4.55E+04		4.76E+04		3.69E+04			3.45E+04	
DO-4	5.97E+04		6.00E+04			5.62E+04	5.32E+04		5.39E+04			5.02E+04	5.23E+04	4.37E+04		3.69E+04		3.39E+04			3.20E+04	
HRC-1					4.50E+04	3.83E+04		3.35E+04		3.33E+04		3.11E+04	2.98E+04									
HRC-2					4.30E+04	3.69E+04		3.33E+04		3.38E+04		3.23E+04	3.01E+04									
HRC-3	5.85E+04	6.15E+04				5.82E+04		5.98E+04	6.03E+04		5.46E+04			5.47E+04	4.82E+04		5.04E+04		5.49E+04	6.01E+04		
HRC-4	5.79E+04					5.94E+04	5.69E+04		5.95E+04		5.78E+04		6.28E+04	5.57E+04	4.84E+04		4.92E+04		4.62E+04	6.21E+04		
LAC-1					4.42E+04	3.96E+04		3.31E+04		3.36E+04		3.57E+04	3.06E+04									
LAC-2					4.41E+04	4.12E+04		3.13E+04		3.43E+04		3.26E+04	3.12E+04									
LAC-3	6.13E+04					5.98E+04	5.76E+04		6.17E+04		5.62E+04		6.43E+04	5.61E+04	4.90E+04		5.04E+04		4.48E+04	6.38E+04		
LAC-4	6.15E+04					5.56E+04	5.72E+04		6.02E+04			6.22E+04	6.30E+04	5.52E+04	5.50E+04		5.03E+04			6.45E+04		
MOL-1					4.35E+04	4.04E+04		3.51E+04		3.50E+04		3.66E+04	3.23E+04									
MOL-2	4.31E+04				4.30E+04	3.92E+04		3.40E+04		3.42E+04		3.53E+04	4.15E+04									
MOL-3	6.23E+04	6.29E+04				5.87E+04	5.33E+04		6.39E+04		5.61E+04		6.25E+04	5.35E+04	4.90E+04		5.07E+04			6.45E+04		
MOL-4	6.22E+04					6.15E+04	5.56E+04		6.35E+04		5.86E+04		5.92E+04	5.67E+04	4.87E+04		4.93E+04			6.04E+04		
STER-1					4.21E+04	4.03E+04						3.11E+04										
STER-2					4.15E+04	3.92E+04						3.40E+04										
STER-3	6.14E+04	6.10E+04				5.42E+04	5.41E+04		5.47E+04			4.85E+04	5.09E+04	4.55E+04		4.03E+04	4.17E+04			4.94E+04		
STER-4	6.11E+04					5.54E+04	5.44E+04		5.42E+04			5.09E+04	5.25E+04	4.95E+04		4.22E+04	4.19E+04			5.08E+04		
UC-1					4.36E+04	4.27E+04						3.71E+04										
UC-2				4.54E+04		4.36E+04						3.69E+04										
UC-3	6.03E+04					6.10E+04		6.33E+04	6.19E+04			6.04E+04	6.22E+04	6.00E+04		5.14E+04		4.88E+04			4.74E+04	4.43E+04
UC-4	6.05E+04		6.20E+04			5.84E+04		5.98E+04	6.10E+04			5.93E+04	5.36E+04	5.08E+04		4.52E+04		4.18E+04			3.93E+04	4.05E+04

Appendix G: Biokinetics Experimental Data

Figure 5

GC With FID Aqueous Concentrations

	Time (days)																		
	10	9	23	34	42	44	49	52	53	56	61	68	75	82	89	94	95	101	111
Sample ID	**AQUEOUS cDCE CONCENTRATIONS (mg/L)**																		
COM-1																			
COM-2																			
COM-3	0.854			0.783	0.848		0.885	0.845		0.986	0.846		0.655		0.641			0.588	
COM-4	0.853			0.754	0.745		0.817	0.763		0.672	0.697		0.562		0.508			0.447	
DO-1																			
DO-2																			
DO-3	0.865	0.845		0.794	0.764		0.773	0.701		0.665	0.664		0.695		0.540			0.506	
DO-4	0.843		0.846	0.793	0.752		0.762		0.732	0.672	0.638		0.541		0.497			0.469	
HRC-1																			
HRC-2																			
HRC-3	0.825	0.868		0.822		0.843	0.851	0.795			0.796	0.703		0.735			0.875		
HRC-4	0.818			0.838	0.803		0.840	0.841		0.831	0.812	0.706		0.717		0.675	0.903		
LAC-1																			
LAC-2																			
LAC-3	0.865			0.845	0.813		0.871	0.818		0.876	0.817	0.715		0.735		0.654	0.928		
LAC-4	0.868			0.785	0.808		0.850		0.905	0.859	0.804	0.801		0.733			0.938		
MOL-1																			
MOL-2																			
MOL-3	0.879	0.888		0.828	0.753		0.901	0.817		0.801	0.779	0.715		0.739			0.938		
MOL-4	0.878			0.868	0.786		0.895	0.853		0.759	0.826	0.710		0.719			0.879		
STER-1																			
STER-2																			
STER-3	0.867	0.860		0.765	0.764		0.773		0.707	0.654	0.664		0.590	0.609			0.720		
STER-4	0.862			0.782	0.769		0.765		0.741	0.674	0.722		0.617	0.612			0.741		
UC-1																			
UC-2																			
UC-3	0.852			0.862		0.895	0.875		0.881	0.800	0.875		0.751		0.712			0.692	0.648
UC-4	0.855		0.876	0.826		0.845	0.863		0.865	0.691	0.741		0.660		0.612			0.576	0.593

Appendix G: Biokinetics Experimental Data

Figure 6

GC With FID Methane Peak Areas

	Date Sampled																					
	30-Aug	7-Sep	12-Sep	13-Sep	16-Sep	23-Sep	1-Oct	3-Oct	5-Oct	8-Oct	9-Oct	11-Oct	12-Oct	15-Oct	20-Oct	27-Oct	3-Nov	10-Nov	17-Nov	22-Nov	23-Nov	29-Nov	09-Dec.
Sample ID	**PEAK AREAS**																						
COM-1		2.74E+08		2.72E+08	2.71E+08	2.39E+08		2.53E+08			2.56E+08		2.56E+08	2.40E+08	2.41E+08								
COM-2		1.10E+08		1.09E+08	1.10E+08	1.07E+08					1.06E+08		1.06E+08	1.03E+08									
COM-3	2.61E+08	2.67E+08	2.69E+08			2.40E+08	2.52E+08			2.68E+08		2.66E+08		2.67E+08	2.66E+08		2.37E+08		2.25E+08			2.20E+08	
COM-4	2.29E+08	2.34E+08	2.35E+08			2.18E+08	2.09E+08			2.32E+08		2.25E+08		2.25E+08	2.21E+08		2.00E+08		1.90E+08			1.81E+08	
DO-1													5.65E+04	6.41E+04	6.03E+04								
DO-2													1.36E+04	1.20E+04									
DO-3																							
DO-4																							
HRC-1		3.98E+04		3.89E+04	3.66E+04	3.18E+04		3.23E+04			3.35E+04		7.25E+04	7.29E+04	5.10E+04								
HRC-2		4.11E+04		3.62E+04	3.89E+04	2.75E+04		3.25E+04			3.53E+04		5.26E+04	5.22E+04	4.40E+04								
HRC-3	3.47E+04	3.67E+04	4.22E+04			3.32E+04	3.07E+04			3.77E+04		4.31E+04		4.28E+04	3.75E+04	3.41E+04		3.70E+04		3.60E+04	4.56E+04		
HRC-4	3.40E+04	3.83E+04	3.90E+04			3.63E+04	3.27E+04			3.76E+04		3.72E+04		3.93E+04	3.53E+04	3.54E+04		3.44E+04		3.46E+04	4.27E+04		
LAC-1		3.89E+04		4.01E+04	4.58E+04	2.90E+04		3.17E+04			3.51E+04		3.43E+04	3.60E+04	3.16E+04								
LAC-2		6.46E+04		3.53E+04	3.99E+04	3.17E+04		3.07E+04			3.47E+04		3.63E+04	3.88E+04									
LAC-3	8.23E+04	5.60E+04	3.60E+04			3.35E+04	3.06E+04			3.55E+04		4.38E+04		4.18E+04	3.75E+04	3.84E+04		3.76E+04		4.10E+04	5.00E+04		
LAC-4	4.82E+04	4.67E+04	3.69E+04				3.23E+04			3.81E+04			4.05E+04	3.94E+04	3.77E+04	3.69E+04		4.55E+04			5.20E+04		
MOL-1		7.81E+04		4.36E+04	3.76E+04	3.05E+04		3.09E+04			3.62E+04		4.54E+04	4.25E+04	3.94E+04								
MOL-2		3.28E+04		3.90E+04	3.60E+04	2.89E+04		3.16E+04			3.54E+04		3.85E+04	4.15E+04	3.80E+04								
MOL-3	3.42E+04	3.65E+04	3.81E+04			3.04E+04	2.98E+04		3.73E+04	3.86E+04		4.04E+04		3.82E+04	3.50E+04	5.73E+04		5.47E+04			6.27E+04		4.51E+04
MOL-4	3.38E+04	3.72E+04	3.92E+04			3.55E+04	3.37E+04		3.08E+04	3.68E+04		1.56E+05		4.01E+04	1.40E+05	1.49E+05		1.25E+05			1.41E+05		8.71E+04
STER-1																							
STER-2																							
STER-3																							
STER-4																							
UC-1													4.43E+04										
UC-2													2.30E+04										
UC-3																							
UC-4																							

Appendix G: Biokinetics Experimental Data

Figure 7

GC With FID Methane Aqueous Concentrations

	Time (days)																						
	10	18	23	24	27	34	42	44	46	49	50	52	53	56	61	68	75	82	89	94	95	101	111
Sample ID	AQUEOUS METHANE CONCENTRATIONS (umol/L)																						
COM-1		4.43E+02		4.40E+02	4.39E+02	3.87E+02		4.10E+02			4.15E+02		4.14E+02	3.89E+02	3.91E+02								
COM-2		1.79E+02		1.77E+02	1.78E+02	1.73E+02					1.72E+02		1.72E+02	1.67E+02									
COM-3	4.23E+02	4.33E+02	4.36E+02			3.89E+02	4.09E+02			4.35E+02		4.31E+02		4.32E+02	4.31E+02		3.84E+02		3.64E+02			3.56E+02	
COM-4	3.71E+02	3.79E+02	3.81E+02			3.54E+02	3.39E+02			3.75E+02		3.64E+02		3.64E+02	3.58E+02		3.24E+02		3.08E+02			2.94E+02	
DO-1													9.15E-02	1.04E-01	9.76E-02								
DO-2													2.20E-02	1.94E-02									
DO-3																							
DO-4																							
HRC-1		6.44E-02		6.30E-02	5.94E-02	5.15E-02		5.23E-02			5.43E-02		1.17E-01	1.18E-01	8.26E-02								
HRC-2		6.67E-02		5.87E-02	6.30E-02	4.46E-02		5.26E-02			5.72E-02		8.51E-02	8.45E-02	7.12E-02								
HRC-3	5.62E-02	5.94E-02	6.83E-02			5.37E-02	4.98E-02			6.10E-02		6.98E-02		6.94E-02	6.08E-02	5.52E-02		5.99E-02		5.83E-02	7.38E-02		
HRC-4	5.50E-02	6.21E-02	6.31E-02			5.87E-02	5.30E-02			6.10E-02		6.03E-02		6.37E-02	5.72E-02	5.73E-02		5.57E-02		5.60E-02	6.91E-02		
LAC-1		6.31E-02		6.49E-02	7.42E-02	4.70E-02		5.13E-02			5.68E-02		5.56E-02	5.84E-02	5.11E-02								
LAC-2		1.05E-01		5.71E-02	6.46E-02	5.13E-02		4.97E-02			5.61E-02		5.88E-02	6.29E-02									
LAC-3	1.33E-01	9.07E-02	5.83E-02			5.43E-02	4.95E-02			5.76E-02		7.09E-02		6.77E-02	6.08E-02	6.22E-02		6.09E-02		6.64E-02	8.10E-02		
LAC-4	7.80E-02	7.56E-02	5.98E-02				5.23E-02			6.18E-02			6.56E-02	6.38E-02	6.11E-02	5.98E-02		7.37E-02			8.42E-02		
MOL-1		1.26E-01		7.07E-02	6.09E-02	4.93E-02		5.01E-02			5.86E-02		7.35E-02	6.89E-02	6.38E-02								
MOL-2		5.31E-02		6.32E-02	5.83E-02	4.67E-02		5.11E-02			5.73E-02		6.23E-02	6.72E-02	6.15E-02								
MOL-3	5.53E-02	5.91E-02	6.17E-02			4.92E-02	4.83E-02		6.05E-02	6.25E-02		6.54E-02		6.19E-02	5.67E-02	9.28E-02		8.86E-02			1.02E-01		7.31E-02
MOL-4	5.47E-02	6.03E-02	6.34E-02			5.75E-02	5.46E-02		4.98E-02	5.96E-02		2.52E-01		6.50E-02	2.27E-01	2.41E-01		2.02E-01			2.29E-01		1.41E-01
STER-1																							
STER-2																							
STER-3																							
STER-4																							
UC-1													7.17E-02										
UC-2													3.72E-02										
UC-3																							
UC-4																							

Appendix G: Biokinetics Experimental Data

Figure 8

Biokinetics serum bottle preparation data (for PCE additions) and Aqueous PCE Concentrations

ρ_{water} (25°C) = 9.97E-01 g/ml Stock Conc= 6.77E-04 mg/µl

Bottle vol= 159.88 ml Bulk Den= 2.19 g/ml

									Time (days)										
									45	48	49	51	55	60	67	81	88	93	110
Sample ID	Vol Water (ml)	Soil Wt (g)	Vol Soil (ml)	Vol Gas (ml)	Vol Stock (µl)	Total Mass DCE (µg)	Co (mg/L)	Substrate Added (ml)	AQUEOUS PCE CONCENTRATIONS (mg/L)										
HRC-3	51.36	11.5527	5.28	103.25	73.80	49.95	972.59	1.38	0.421	0.441		0.390	0.494	0.434	0.348	0.357		0.407	
HRC-4	51.35	11.5348	5.27	103.26	73.80	49.95	972.63	1.38	0.446		0.448	0.390	0.488	0.456	0.342	0.363		0.301	
LAC-3	51.36	11.575	5.29	103.24	73.80	49.95	972.54	0.40	0.383	0.427		0.355	0.349	0.358	0.354	0.386	0.342	0.302	
LAC-4	51.36	11.5513	5.27	103.25	73.80	49.95	972.59	0.40	0.400		0.435	0.457	0.450	0.412	0.359		0.383	0.386	
MOL-3	51.36	11.5519	5.27	103.25	73.80	49.95	972.59	1.20	0.426	0.337	0.475	0.408	0.421	0.467	0.317		0.361	0.241	0.497
MOL-4	51.36	11.5478	5.27	103.25	73.80	49.95	972.60	1.20	0.373	0.442		0.374	0.478	0.386	0.285		0.289	0.223	0.433
STER-3	51.36	11.5895	5.29	103.23	73.80	49.95	972.51	--	0.455	0.322	0.417	0.406	0.398	0.388	0.287		0.339	0.312	
STER-4	51.37	11.6419	5.32	103.20	73.80	49.95	972.39	--	0.476		0.405	0.429	0.430	0.461	0.297		0.354	0.374	

Appendix G: Biokinetics Experimental Data

Figure 9
GC With ECD PCE Peak Areas

	Date Sampled										
	5-Oct	8-Oct	9-Oct	11-Oct	15-Oct	20-Oct	27-Oct	10-Nov	17-Nov	22-Nov	09-Dec.
Sample ID	PCE PEAK AREAS										
HRC-3	1.48E+05	1.55E+05		1.37E+05	2.03E+05	1.52E+05	1.23E+05	1.26E+05		1.43E+05	
HRC-4	1.56E+05		1.57E+05	1.37E+05	2.01E+05	1.60E+05	1.21E+05	1.28E+05		1.07E+05	
LAC-3	1.35E+05	1.50E+05		1.25E+05	1.45E+05	1.26E+05	1.25E+05	1.36E+05	1.21E+05	1.07E+05	
LAC-4	1.41E+05		1.52E+05	1.60E+05	1.85E+05	1.45E+05	1.27E+05		1.35E+05	1.36E+05	
MOL-3	1.49E+05	1.19E+05	1.66E+05	1.43E+05	1.80E+05	1.63E+05	1.12E+05		1.27E+05	8.66E+04	1.73E+05
MOL-4	1.32E+05	1.55E+05		1.32E+05	2.04E+05	1.36E+05	1.02E+05		1.03E+05	8.03E+04	1.52E+05
STER-3	1.59E+05	1.14E+05	1.46E+05	1.43E+05	1.46E+05	1.37E+05	1.02E+05		1.20E+05	1.11E+05	
STER-4	1.66E+05		1.42E+05	1.51E+05	1.57E+05	1.61E+05	1.05E+05		1.25E+05	1.32E+05	

Appendix G: Biokinetics Experimental Data

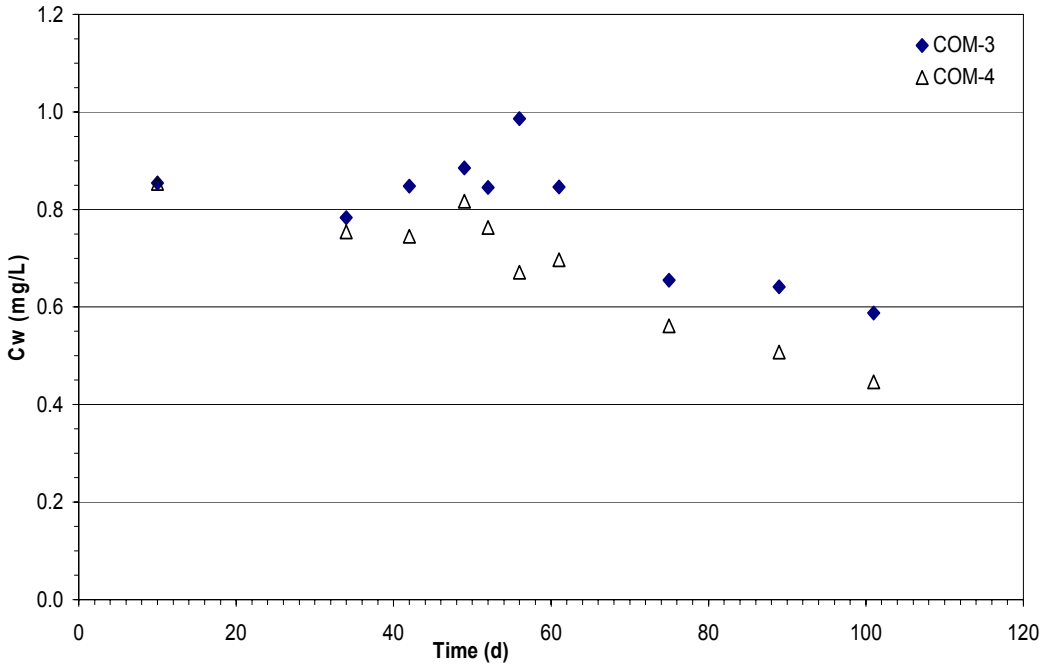

Aqueous cDCE concentration
Aerobic oxidation microcosms at 30°C (COM-3, COM-4)
Each point represents a single GC w/ FID headspace injection sample.

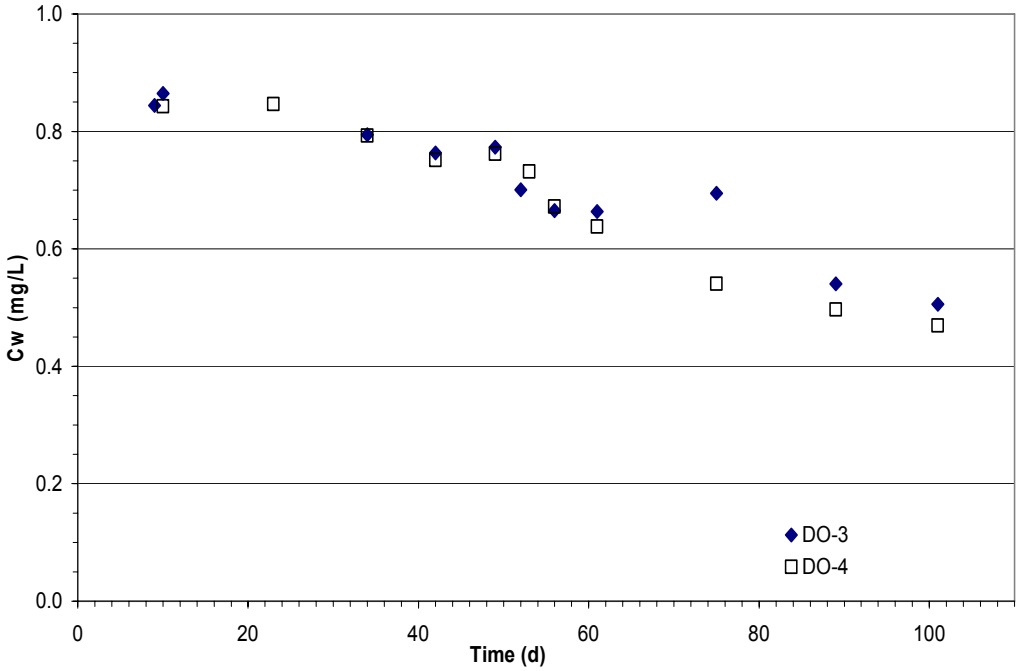

Aqueous cDCE concentration
Aerobic oxidation microcosms at 30°C (DO-3, DO-4)
Each point represents a single GC w/ FID headspace injection sample.

Appendix G: Biokinetics Experimental Data

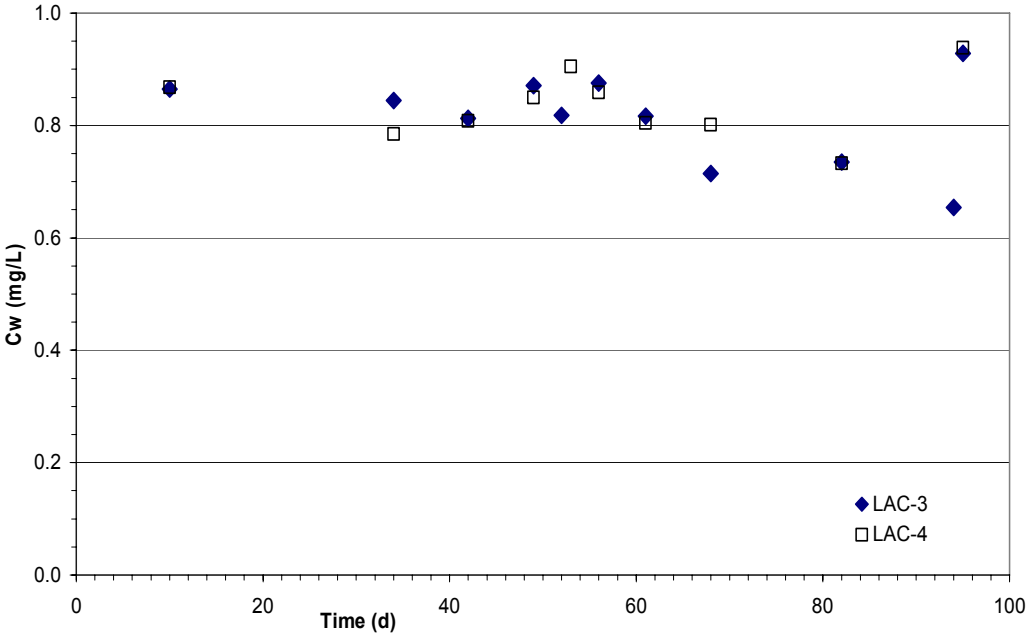

Aqueous cDCE concentration
Anaerobic red. dechl. microcosms at 30°C (LAC-3, LAC-4)
Each point represents a single GC w/ FID headspace injection sample.

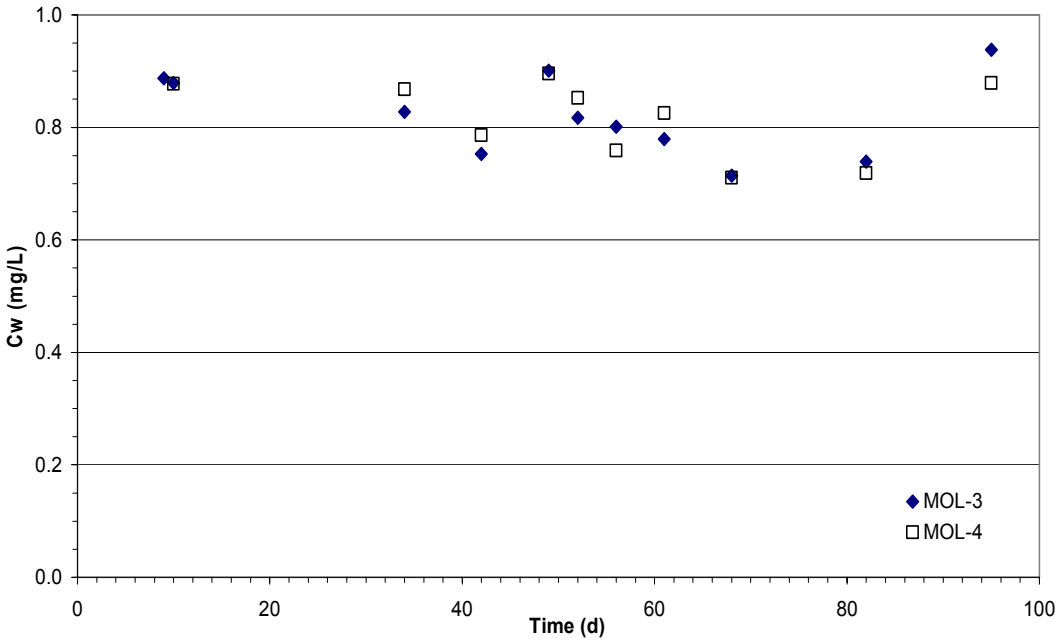

Aqueous cDCE concentration
Anaerobic red. dechl. microcosms at 30°C (MOL-3, MOL-4)
Each point represents a single GC w/ FID headspace injection sample.

Appendix G: Biokinetics Experimental Data

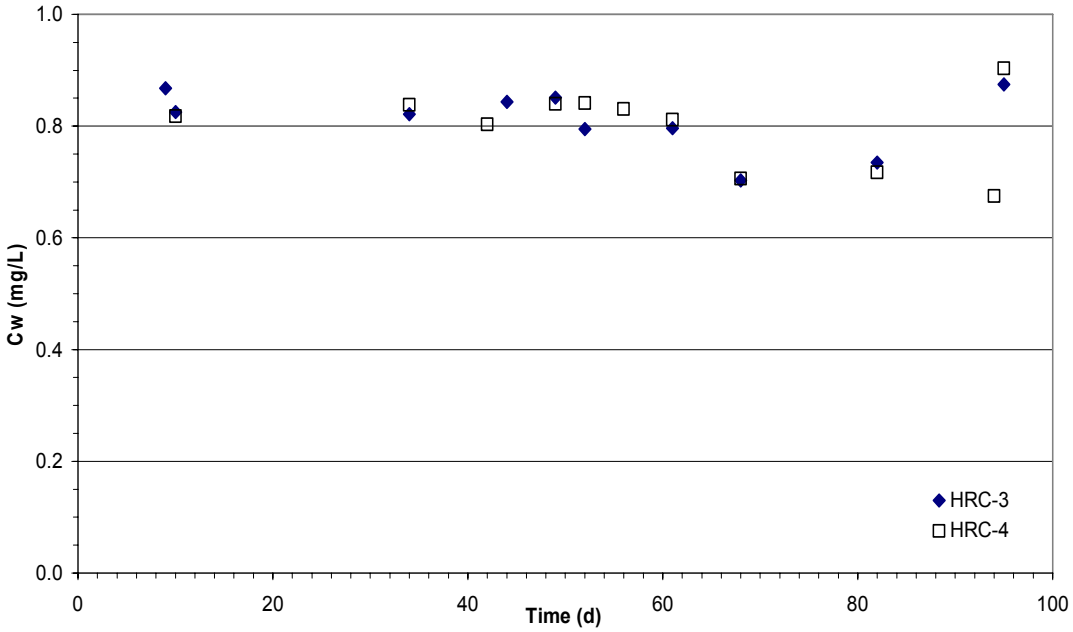

Aqueous cDCE concentration
Anaerobic red. dechl. microcosms at 30°C (HRC-3, HRC-4)
Each point represents a single GC w/ FID headspace injection sample.

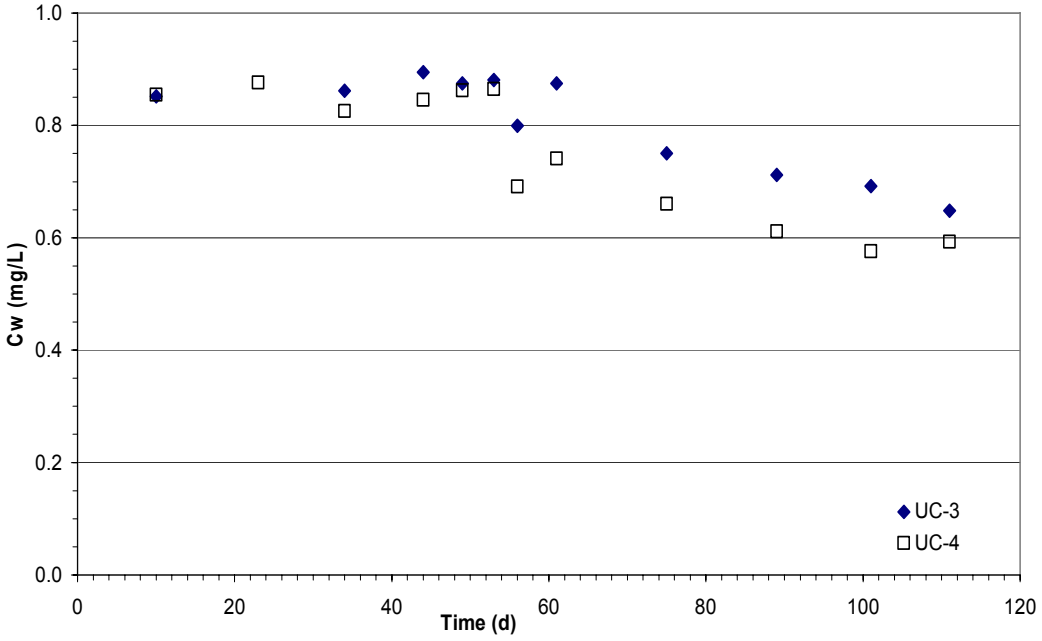

Aqueous cDCE concentration
Uninoculated control microcosms at 30°C (UC-3, UC-4)
Each point represents a single GC w/ FID headspace injection sample.

Appendix G: Biokinetics Experimental Data

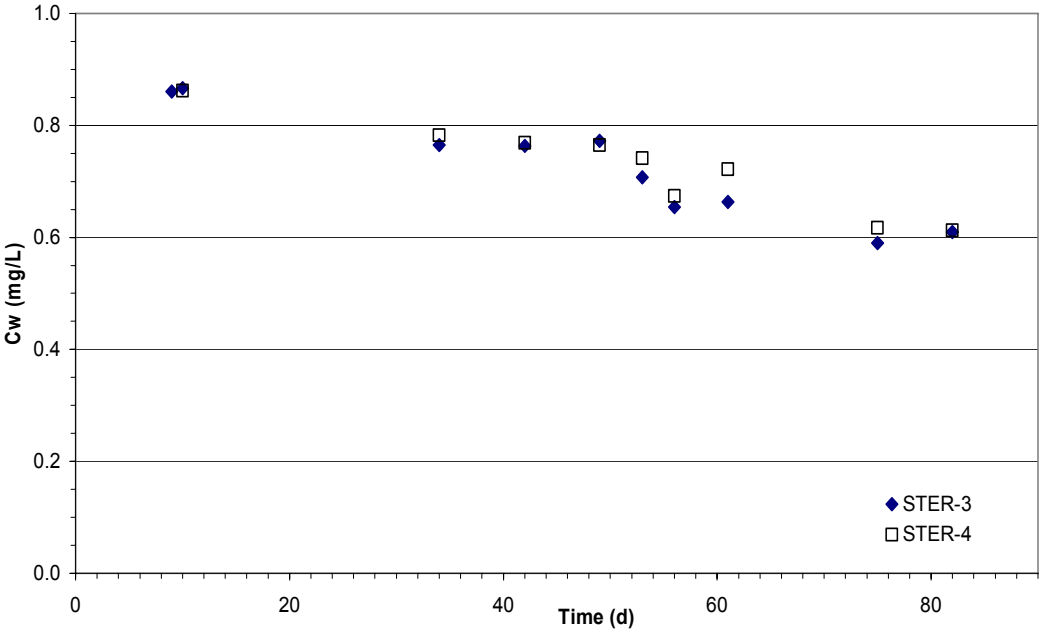

Aqueous cDCE concentration
Sterilized microcosms at 30°C (STER-3, STER-4)
Each point represents a single GC w/ FID headspace injection sample.

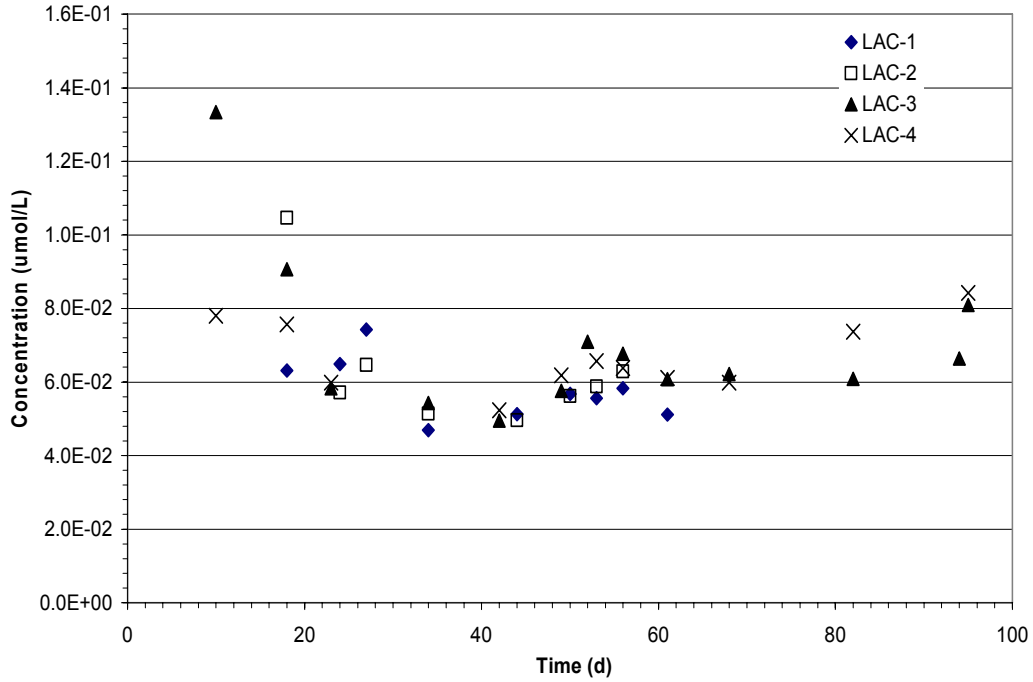

Anaerobic microcosm methane concentrations at 14°C (LAC-1, LAC-2)
And 30°C (LAC-3, LAC-4).

Appendix G: Biokinetics Experimental Data

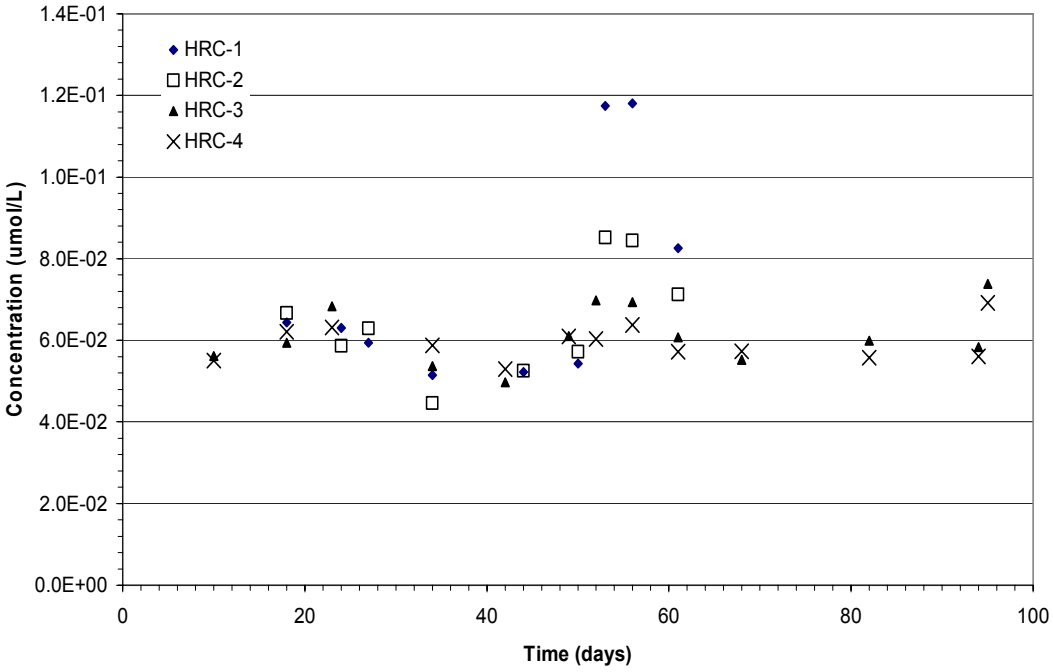

Anaerobic microcosm methane concentrations at 14°C (HRC-1, HRC-2) and 30°C (HRC-3, CHRCOM-4).

Appendix H: Mass-transfer Rate and K_d Experimental Data

Figure 1

cDCE mass-transfer rate experimental data (Test 1)

ρ_{water} (25°C) = 0.9973 g/ml Stock Conc= 0.000718 mg/µl
Bottle vol= 26.2 ml Bulk Den= 2.19 g/ml

Sample ID	Dry Wt (g)	Wet Wt (g)	Vol Water (ml)	Wet+Soil Wt (g)	Vol Soil (ml)	Vol Gas (ml)	+ DCE (g)	Total Stock added (mg)	Vol Stock (µl)	Total Mass DCE (µg)	Cin (ppb)	Time Sampled (hr)	Area Counts (avg)	Cw (mg/L)	Cg (mg/L)	Cg (normalized)	Cw (normalized)
4	30.6024	41.0249	10.45	46.2221	2.37	13.38	46.2326	10.5	13.26	9.52	911.07	4	3260.15	0.80	0.12	0.118	0.786
16	30.6427	40.9195	10.30	46.1171	2.37	13.52	46.1274	10.3	13.01	9.34	906.39	16	3254.55	0.80	0.12	0.117	0.779
24	30.5422	41.1002	10.59	46.2981	2.37	13.24	46.309	10.9	13.77	9.88	933.64	24	3532.45	0.88	0.13	0.129	0.861
48	30.2264	40.4453	10.25	45.6428	2.37	13.58	45.6535	10.7	13.51	9.70	946.92	47.5	2860.2	0.70	0.10	0.100	0.669
72	30.639	41.0462	10.44	46.2336	2.37	13.40	46.2444	10.8	13.64	9.79	938.48	93	3109.35	0.76	0.11	0.112	0.744
96	29.7683	40.0938	10.35	45.2895	2.37	13.47	45.3005	11	13.89	9.97	963.42	136.75	2638.95	0.64	0.10	0.093	0.622
B4	30.7192	41.0255	10.33			15.87	41.0365	11	13.89	9.97	965.22	4	3296.45	0.81	0.12		
B16	30.6599	40.9306	10.30			15.90	40.9411	10.5	13.26	9.52	924.54	16	3080.7	0.76	0.11		
B24	30.4508	40.8078	10.39			15.81	40.8182	10.4	13.13	9.43	908.10	24	3323.5	0.82	0.12		
B48	30.7071	41.122	10.44			15.76	41.1323	10.3	13.01	9.34	894.37	47.5	3043.3	0.75	0.11		
B72	30.601	40.9616	10.39			15.81	40.9726	11	13.89	9.97	960.16	93	3333.1	0.82	0.12		
B96	29.9386	40.2459	10.34			15.86	40.2567	10.8	13.64	9.79	947.57	136.75					

= Sample blank results.

Appendix H: Mass-transfer Rate and K_d Experimental Data

Figure 2

cDCE mass-transfer rate experimental data (Test 2)

ρ_{water} (25°C) = 9.97E-01 g/ml Stock Conc= 7.18E-04 mg/µl

Bottle vol= 26.2 ml Bulk Den= 2.19 g/ml

Sample ID	Dry Wt (g)	Wet Wt (g)	Vol Water (ml)	Water+Soil Wt (g)	Soil Mass (g)	Vol Soil (ml)	Vol Gas (ml)	Sample + DCE (g)	Total Stock added (mg)	Vol Stock (µl)	Total Mass DCE (µg)	Cin (ppb)	Time Sampled (hr)	Area Counts (avg)	Cw (mg/L)	Cg (mg/L)	Cg (normalized)	Cw (normalized)
2-5	30.6189	40.9669	10.38	46.1534	5.1865	2.3683	13.46	46.1644	11	13.89	9.97	961.33	4.5	3406.5	0.84	0.13	0.123	0.820
2-B5	30.5856	40.8711	10.31				15.89	40.8818	10.7	13.51	9.70	940.79	28.5	3669.55	0.91	0.14	0.133	0.887
2-29	30.6517	40.9883	10.36	46.184	5.1957	2.3725	13.46	46.1951	11.1	14.02	10.07	971.14	52	3219.567	0.79	0.12	0.116	0.771
2-B29	30.7323	41.0275	10.32				15.88	41.0375	10	12.63	9.07	878.42	72	3069.4	0.75	0.11	0.110	0.733
2-53	30.245	40.5618	10.34	45.7529	5.1911	2.3704	13.48	45.7635	10.6	13.39	9.61	929.17	102	3074.7	0.76	0.11	0.111	0.738
2-B53	30.6345	40.9651	10.36				15.84	40.9757	10.6	13.39	9.61	927.93	124.5	2992.15	0.73	0.11	0.106	0.709
2-77	30.5165	40.8371	10.35	46.0319	5.1948	2.3721	13.48	46.0429	11	13.89	9.97	963.88	147.5	3223.5	0.79	0.12	0.116	0.775
2-B77	30.333	40.7898	10.49				15.71	40.8008	11	13.89	9.97	951.32	B5	3343.65	0.83	0.12	0.124	0.826
2-101	30.7034	41.1066	10.43	46.304	5.1974	2.3732	13.40	46.3152	11.2	14.14	10.16	973.61	B29	3497.55	0.87	0.13	0.130	0.867
2-B101	29.795	40.0736	10.31				15.89	40.0838	10.2	12.88	9.25	897.43	B53	2966.95	0.73	0.11	0.109	0.729
2-125	30.4437	40.6724	10.26	45.867	5.1946	2.3720	13.57	45.8776	10.6	13.39	9.61	937.17	B77	3045.7	0.75	0.11	0.113	0.756
2-B125	30.6121	40.9503	10.37				15.83	40.9609	10.6	13.39	9.61	927.25	B101	3078.6	0.76	0.11	0.113	0.756
2-149	30.684	41.0657	10.41	46.261	5.1953	2.3723	13.42	46.2724	11.4	14.40	10.34	993.05	B125	3316.5	0.82	0.12	0.123	0.822
2-B149	29.9703	40.2921	10.35				15.85	40.3034	11.3	14.27	10.25	990.05	B149	3481	0.86	0.13	0.130	0.864

= Sample blank results.

Appendix H: Mass-transfer Rate and K_d Experimental Data

Figure 3

Sorption distribution coefficient (K_d) experimental data and calculations

ρ_{water} (25°C) =	9.97E-01	g/ml	Stock Conc	7.18E-04	mg/µl
Bottle vol=	26.2	ml	Bulk Den=	2.19	g/ml
Cis Dens=	1.284	g/ml			

Sample ID	Dry Wt (g)	Wet Wt (g)	Vol Water (ml)	+ Formal. (g)	Formal (g)	Wet+Soil Wt (g)	Mass Soil (g)	Vol Soil (ml)	Vol Gas (ml)	+ DCE (g)	Total Stock added (mg)	Vol Stock (µl)	Total Mass DCE (µg)	Cin (ppb)	Area Counts (avg)	Cw (ug/ml)	Cg (ug/ml)	Cg (normalized)	Cw (normalized)	X (%)
Kd-1	30.014	40.3438	10.36			45.5362	4.04	2.3710	13.47	45.5476	11.4	14.40	10.34	998.04	3307.25	0.82	0.12	0.119	0.796	7.11
Kd-2	30.3648	40.7313	10.39			45.9272	4.05	2.3726	13.43	45.9385	11.3	14.27	10.25	985.78	3314.25	0.82	0.12	0.120	0.800	6.68
Kd-3	30.5987	40.8316	10.26			46.0268	4.05	2.3722	13.57	46.0381	11.3	14.27	10.25	998.65	3203.75	0.79	0.12	0.115	0.764	10.79
Kd-4	30.5222	40.7759	10.28	41.1120	0.3361	46.3062	4.05	2.3718	13.24	46.3177	11.5	14.52	10.43	1014.27	3574.35	0.89	0.13	0.128	0.856	0.05
Kd-5	30.6975	41.0162	10.35	41.3466	0.3304	46.5446	4.05	2.3735	13.18	46.556	11.4	14.40	10.34	999.11	3323.315	0.82	0.12	0.119	0.796	7.08
Kd-6	30.9106	41.133	10.25	41.4301	0.2971	46.6261	4.05	2.3726	13.30	46.6375	11.4	14.40	10.34	1008.52	3663.15	0.91	0.14	0.132	0.878	-2.42
Kd-7	30.617	40.8661	10.28						15.92	40.8778	11.7	14.78	10.61	1032.37	3452.9	0.85	0.13	0.128	0.855	
Kd-8	29.7375	40.1231	10.41						15.79	40.1347	11.6	14.65	10.52	1010.09	Bad Sample (possible leak in septum)					
Kd-9	30.5667	40.8775	10.34						15.86	40.8891	11.6	14.65	10.52	1017.42	3455	0.86	0.13	0.129	0.859	

= Results may have been affected by presence of formaldahyde; are not considered representative of Quantico slate.

Bottle Pairs	*Kd (ml/g)*	*Average Kd (L/kg) from pairs*
K_d1/K_d7	3.18E-01	3.33E-01
K_d1/K_d9	3.47E-01	
K_d2/K_d7	2.94E-01	3.09E-01
K_d2/K_d9	3.24E-01	
K_d3/K_d7	4.79E-01	4.94E-01
K_d3/K_d9	5.10E-01	
Overall Average K_d Estimate:	**3.79E-01**	**L/kg**

Retardation Factor: **$1+(\rho_b/n)K_d$=** 4.59

Appendix I: Slug Test Experimental Data

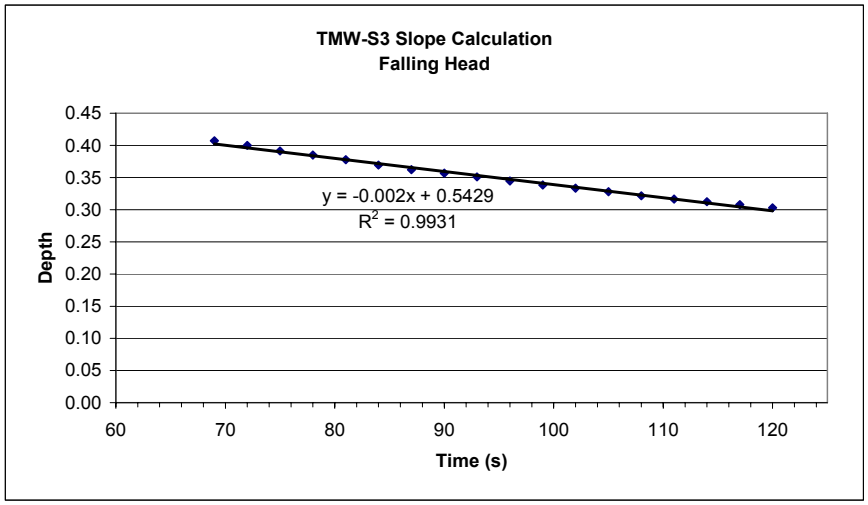

Date	Time	ET (sec)	Chan[2] Pressure Feet H2O	Ho-H(t)	Normalized (H(t)/Ho)	Adjusted t
3/30/2005	9:54:59	96	11.821	0		
3/30/2005	9:55:02	99	11.819	0		
3/30/2005	9:55:05	102	11.826	0		
3/30/2005	9:55:08	105	14.037	2.211	1.000	0
3/30/2005	9:55:11	108	13.363	1.537	0.695	3
3/30/2005	9:55:14	111	13.523	1.697	0.768	6
3/30/2005	9:55:17	114	13.26	1.434	0.649	9
3/30/2005	9:55:20	117	13.288	1.462	0.661	12
3/30/2005	9:55:23	120	13.207	1.381	0.625	15
3/30/2005	9:55:26	123	13.205	1.379	0.624	18
3/30/2005	9:55:29	126	13.118	1.292	0.584	21
3/30/2005	9:55:32	129	13.088	1.262	0.571	24
3/30/2005	9:55:35	132	13.021	1.195	0.540	27
3/30/2005	9:55:38	135	13.031	1.205	0.545	30
3/30/2005	9:55:41	138	12.874	1.048	0.474	33
3/30/2005	9:55:44	141	12.966	1.14	0.516	36
3/30/2005	9:55:47	144	12.9	1.074	0.486	39
3/30/2005	9:55:50	147	12.914	1.088	0.492	42
3/30/2005	9:55:53	150	12.889	1.063	0.481	45
3/30/2005	9:55:56	153	12.863	1.037	0.469	48
3/30/2005	9:55:59	156	12.843	1.017	0.460	51
3/30/2005	9:56:02	159	12.82	0.994	0.450	54
3/30/2005	9:56:05	162	12.799	0.973	0.440	57
3/30/2005	9:56:08	165	12.778	0.952	0.431	60
3/30/2005	9:56:11	168	12.758	0.932	0.422	63
3/30/2005	9:56:14	171	12.739	0.913	0.413	66
3/30/2005	9:56:17	174	12.726	0.9	0.407	69
3/30/2005	9:56:20	177	12.71	0.884	0.400	72
3/30/2005	9:56:23	180	12.691	0.865	0.391	75
3/30/2005	9:56:26	183	12.677	0.851	0.385	78
3/30/2005	9:56:29	186	12.661	0.835	0.378	81
3/30/2005	9:56:32	189	12.643	0.817	0.370	84
3/30/2005	9:56:35	192	12.627	0.801	0.362	87
3/30/2005	9:56:38	195	12.615	0.789	0.357	90
3/30/2005	9:56:41	198	12.602	0.776	0.351	93
3/30/2005	9:56:44	201	12.588	0.762	0.345	96
3/30/2005	9:56:47	204	12.574	0.748	0.338	99
3/30/2005	9:56:50	207	12.563	0.737	0.333	102
3/30/2005	9:56:53	210	12.551	0.725	0.328	105
3/30/2005	9:56:56	213	12.537	0.711	0.322	108
3/30/2005	9:56:59	216	12.526	0.7	0.317	111
3/30/2005	9:57:02	219	12.517	0.691	0.313	114
3/30/2005	9:57:05	222	12.507	0.681	0.308	117
3/30/2005	9:57:08	225	12.496	0.67	0.303	120
3/30/2005	9:57:11	228	12.487	0.661	0.299	123
3/30/2005	9:57:14	231	12.475	0.649	0.294	126
3/30/2005	9:57:17	234	12.466	0.64	0.289	129
3/30/2005	9:57:20	237	12.457	0.631	0.285	132
3/30/2005	9:57:23	240	12.448	0.622	0.281	135
3/30/2005	9:57:26	243	12.441	0.615	0.278	138
3/30/2005	9:57:29	246	12.432	0.606	0.274	141
3/30/2005	9:57:32	249	12.422	0.596	0.270	144
3/30/2005	9:57:35	252	12.416	0.59	0.267	147
3/30/2005	9:57:38	255	12.407	0.581	0.263	150

Conductivity Calculations			
	To=	500	
	b=	15	
	r_c=	1.51E-01	
	rw=	3.33E-01	
rw*=	rw(Kz/Kr)^0.5=	3.33E-01	
	A=	2.91E+00	
	B=	4.64E-01	
	ln(Re/rw*)=	2.41E+00	
	Kr=	3.69E-06	ft/s
	Kr=	3.19E-01	ft/day
	n=	2.29E-01	
	Velocity=	7.79E-01	ft/day

*

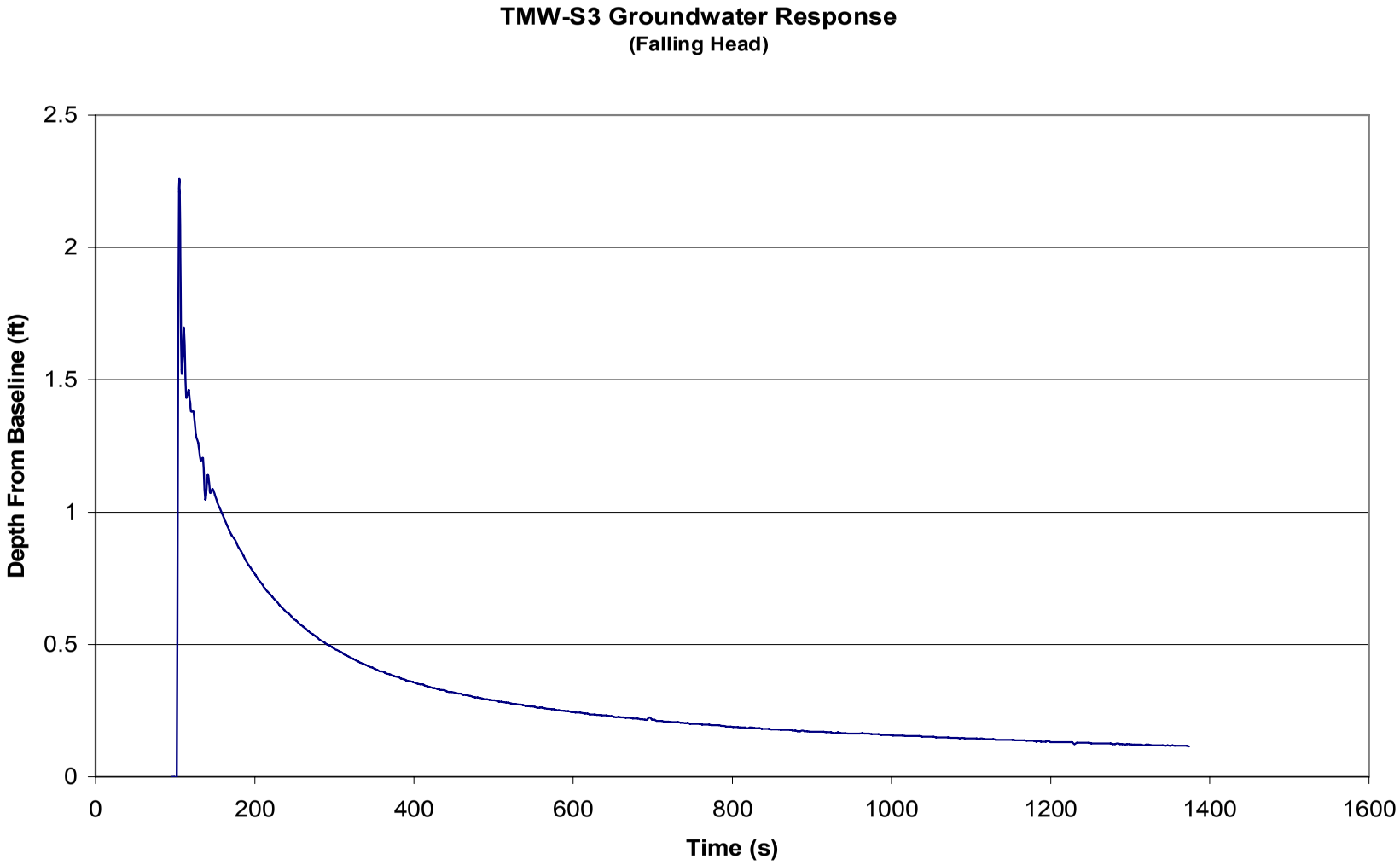
TMW-S3 Groundwater Response
(Falling Head)
Depth From Baseline (ft)
2.5
2
1.5
1
0.5
0
0
200
400
600
800
1000
1200
1400
1600
Time (s)

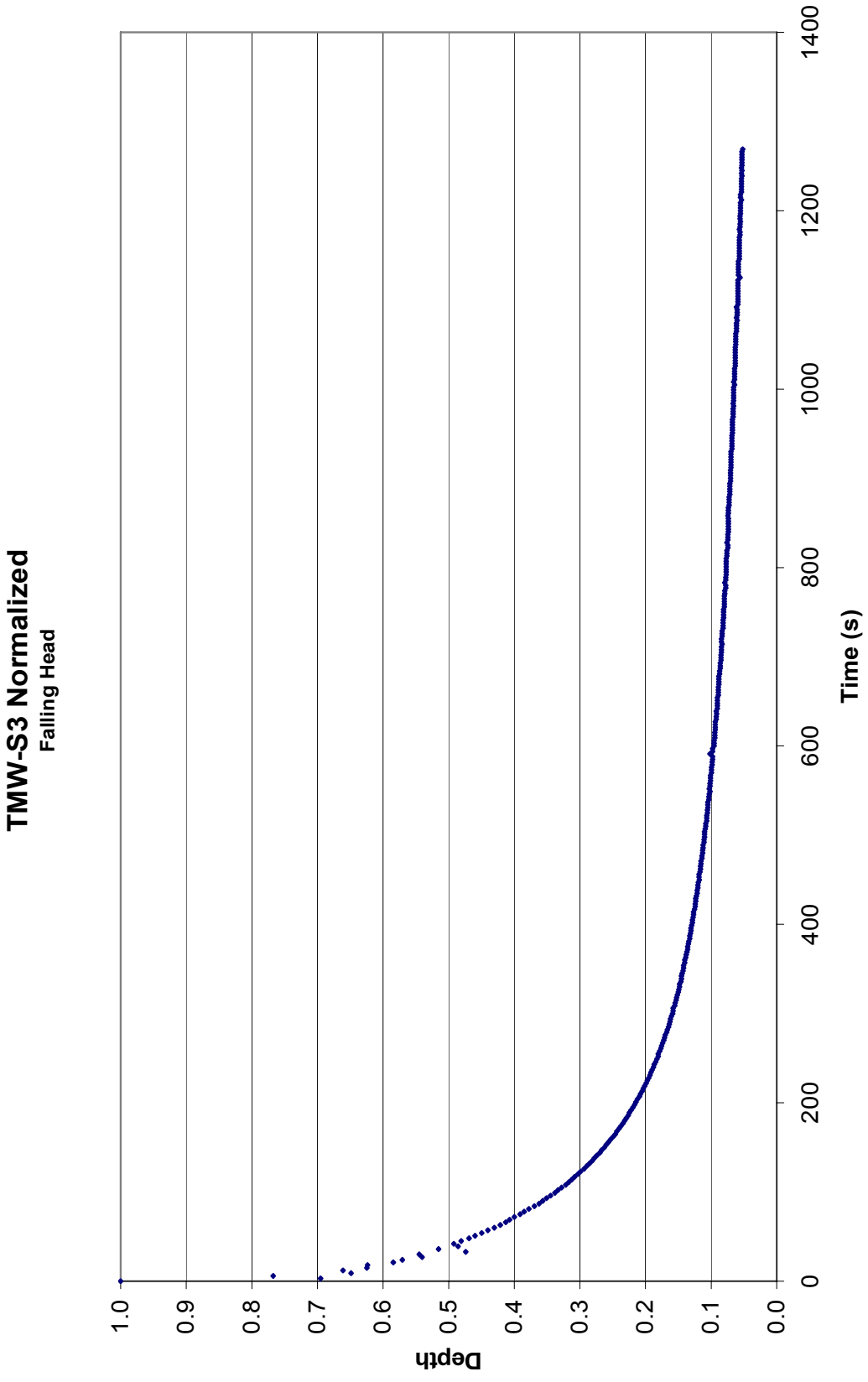
TMW-S3 Normalized
Falling Head
Depth
Time (s)
1.0
0.9
0.8
0.7
0.6
0.5
0.4
0.3
0.2
0.1
0.0
0
200
400
600
800
1000
1200
1400

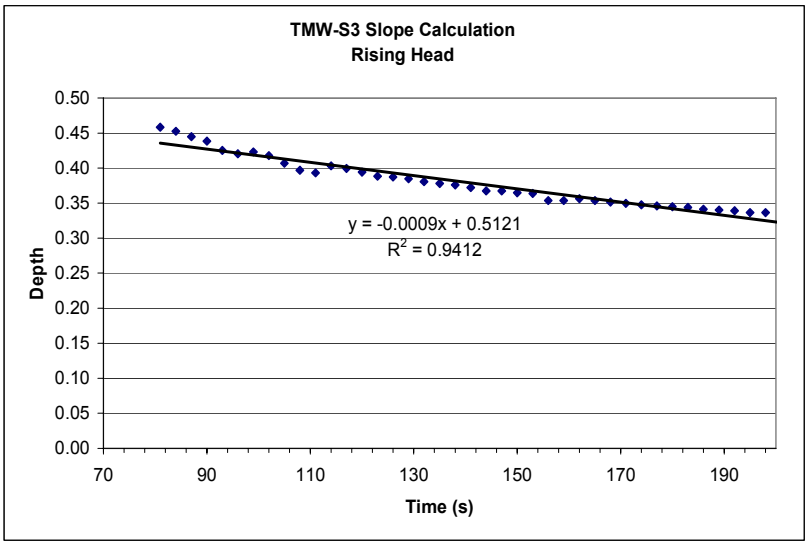

Date	Time	ET (sec)	Chan[2] Pressure Feet H2O		Ho-H(t)	Normalized (H(t)/Ho)	Adjusted t
3/30/2005	10:18:55	0	11.928	0			
3/30/2005	10:18:58	3	11.928	0			
3/30/2005	10:19:01	6	11.831	-0.097	0.097		
3/30/2005	10:19:04	9	10.056	-1.872	1.872	1.000	0
3/30/2005	10:19:07	12	10.262	-1.666	1.666	0.890	3
3/30/2005	10:19:10	15	10.326	-1.602	1.602	0.856	6
3/30/2005	10:19:13	18	10.384	-1.544	1.544	0.825	9
3/30/2005	10:19:16	21	10.435	-1.493	1.493	0.798	12
3/30/2005	10:19:19	24	10.486	-1.442	1.442	0.770	15
3/30/2005	10:19:22	27	10.532	-1.396	1.396	0.746	18
3/30/2005	10:19:25	30	10.573	-1.355	1.355	0.724	21
3/30/2005	10:19:28	33	10.615	-1.313	1.313	0.701	24
3/30/2005	10:19:31	36	10.654	-1.274	1.274	0.681	27
3/30/2005	10:19:34	39	10.689	-1.239	1.239	0.662	30
3/30/2005	10:19:37	42	10.721	-1.207	1.207	0.645	33
3/30/2005	10:19:40	45	10.758	-1.17	1.17	0.625	36
3/30/2005	10:19:43	48	10.786	-1.142	1.142	0.610	39
3/30/2005	10:19:46	51	10.814	-1.114	1.114	0.595	42
3/30/2005	10:19:49	54	10.841	-1.087	1.087	0.581	45
3/30/2005	10:19:52	57	10.869	-1.059	1.059	0.566	48
3/30/2005	10:19:55	60	10.894	-1.034	1.034	0.552	51
3/30/2005	10:19:58	63	10.917	-1.011	1.011	0.540	54
3/30/2005	10:20:01	66	10.936	-0.992	0.992	0.530	57
3/30/2005	10:20:04	69	10.959	-0.969	0.969	0.518	60
3/30/2005	10:20:07	72	10.977	-0.951	0.951	0.508	63
3/30/2005	10:20:10	75	10.996	-0.932	0.932	0.498	66
3/30/2005	10:20:13	78	11.01	-0.918	0.918	0.490	69
3/30/2005	10:20:16	81	11.026	-0.902	0.902	0.482	72
3/30/2005	10:20:19	84	11.042	-0.886	0.886	0.473	75
3/30/2005	10:20:22	87	11.056	-0.872	0.872	0.466	78
3/30/2005	10:20:25	90	11.07	-0.858	0.858	0.458	81
3/30/2005	10:20:28	93	11.081	-0.847	0.847	0.452	84
3/30/2005	10:20:31	96	11.095	-0.833	0.833	0.445	87
3/30/2005	10:20:34	99	11.107	-0.821	0.821	0.439	90
3/30/2005	10:20:37	102	11.132	-0.796	0.796	0.425	93
3/30/2005	10:20:40	105	11.141	-0.787	0.787	0.420	96
3/30/2005	10:20:43	108	11.136	-0.792	0.792	0.423	99
3/30/2005	10:20:46	111	11.146	-0.782	0.782	0.418	102
3/30/2005	10:20:49	114	11.166	-0.762	0.762	0.407	105
3/30/2005	10:20:52	117	11.185	-0.743	0.743	0.397	108
3/30/2005	10:20:55	120	11.192	-0.736	0.736	0.393	111
3/30/2005	10:20:58	123	11.173	-0.755	0.755	0.403	114
3/30/2005	10:21:01	126	11.18	-0.748	0.748	0.400	117
3/30/2005	10:21:04	129	11.19	-0.738	0.738	0.394	120
3/30/2005	10:21:07	132	11.201	-0.727	0.727	0.388	123
3/30/2005	10:21:10	135	11.203	-0.725	0.725	0.387	126
3/30/2005	10:21:13	138	11.208	-0.72	0.72	0.385	129
3/30/2005	10:21:16	141	11.215	-0.713	0.713	0.381	132
3/30/2005	10:21:19	144	11.22	-0.708	0.708	0.378	135
3/30/2005	10:21:22	147	11.224	-0.704	0.704	0.376	138
3/30/2005	10:21:25	150	11.231	-0.697	0.697	0.372	141
3/30/2005	10:21:28	153	11.24	-0.688	0.688	0.368	144
3/30/2005	10:21:31	156	11.24	-0.688	0.688	0.368	147
3/30/2005	10:21:34	159	11.245	-0.683	0.683	0.365	150

Conductivity Calculations

	To=	1111.11111	
	b=	15	
	r_c=	1.65E-01	
	rw=	3.33E-01	
rw*=	rw(Kz/Kr)^0.5=	3.33E-01	
	A=	2.91E+00	
	B=	4.64E-01	
	ln(Re/rw*)=	2.41E+00	
	Kr=	1.98E-06	ft/s
	Kr=	1.71E-01	ft/day
	n=	2.29E-01	
	Velocity=	4.18E-01	ft/day

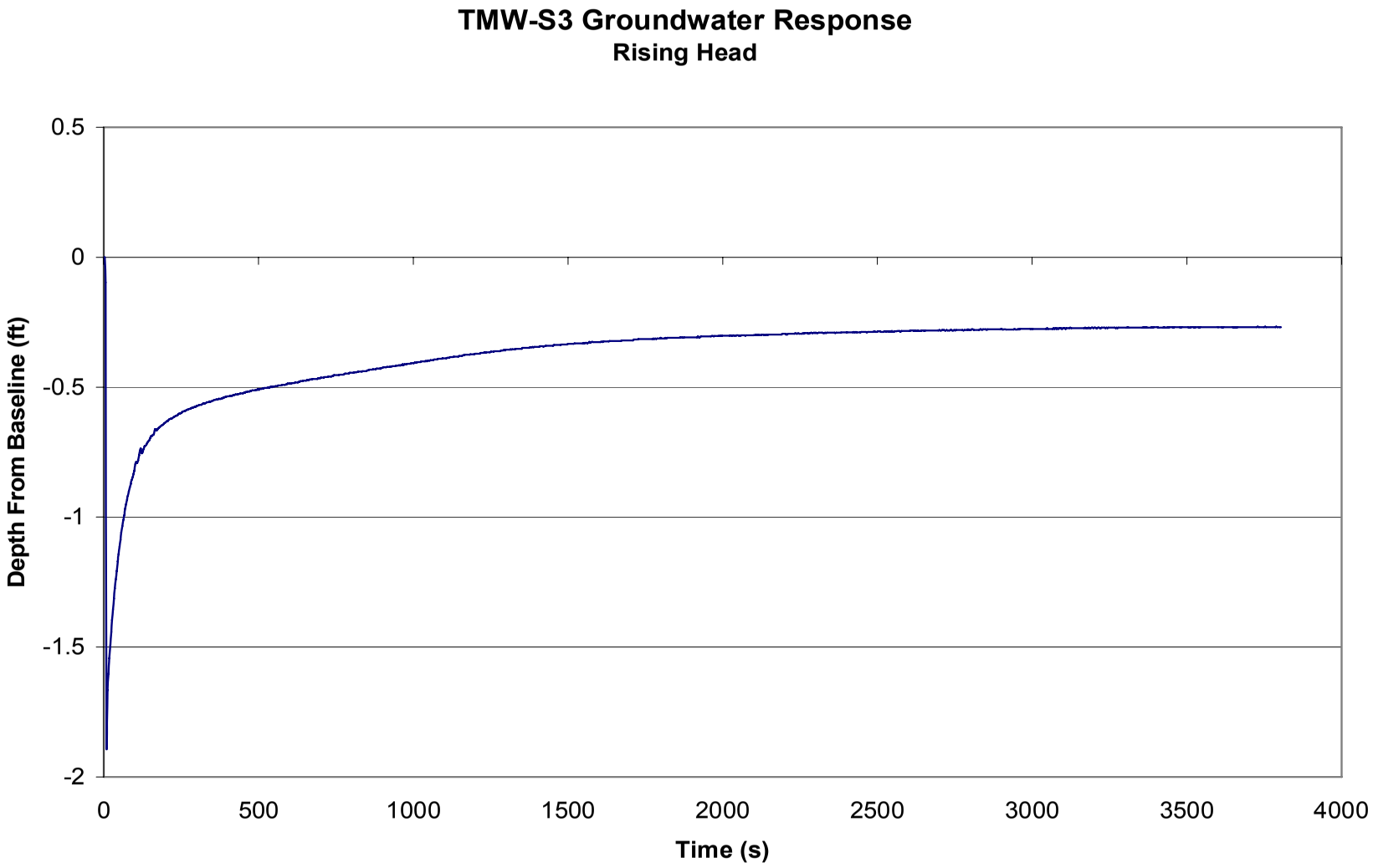
TMW-S3 Groundwater Response
Rising Head
Depth From Baseline (ft)
0.5
0
-0.5
-1
-1.5
-2
0
500
1000
1500
2000
2500
3000
3500
4000
Time (s)

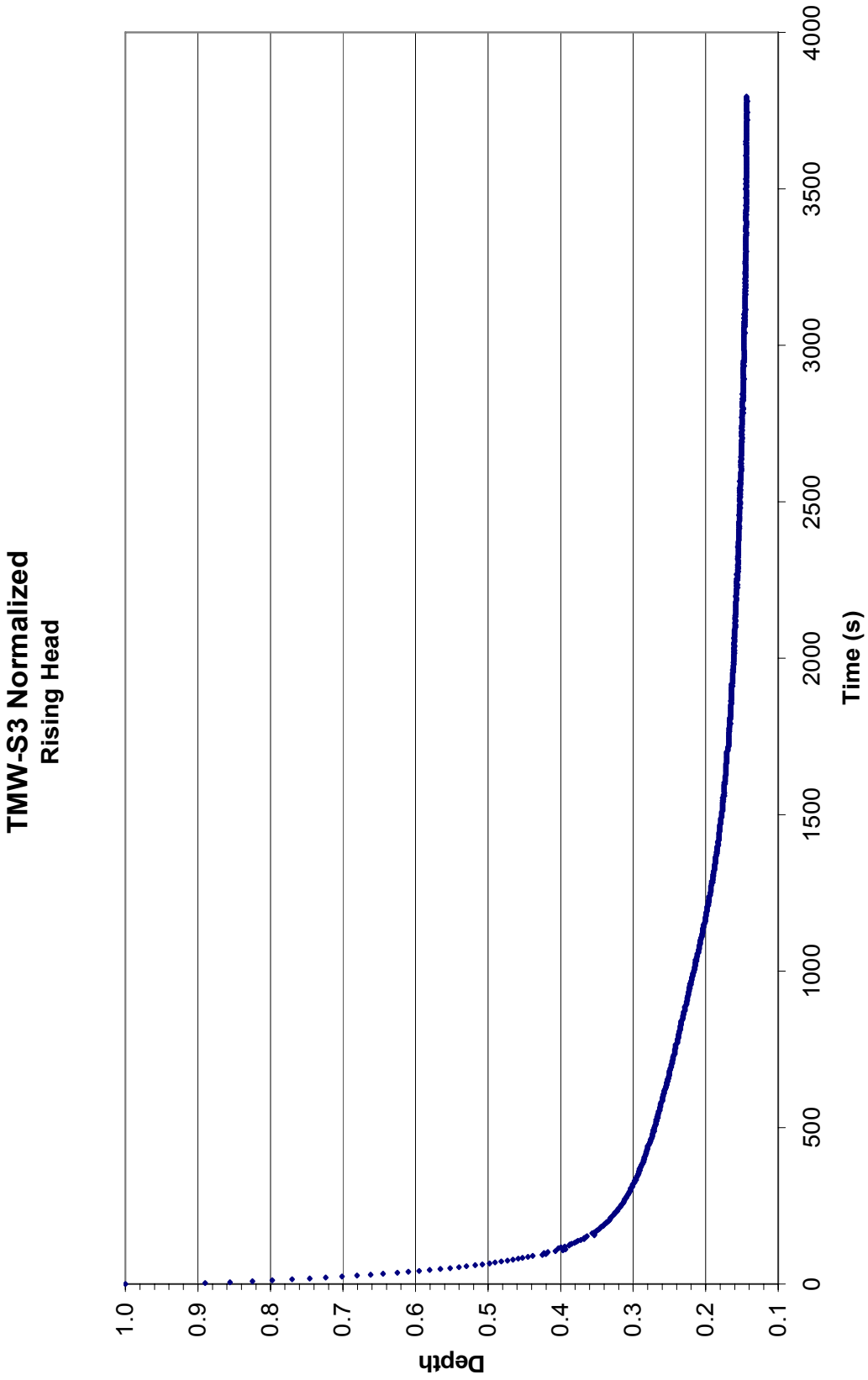
TMW-S3 Normalized
Rising Head
Depth
Time (s)
1.0
0.9
0.8
0.7
0.6
0.5
0.4
0.3
0.2
0.1
0
500
1000
1500
2000
2500
3000
3500
4000

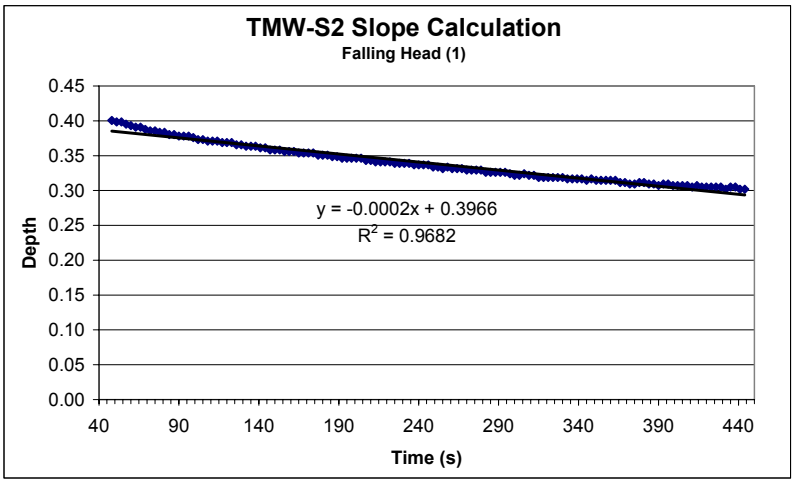

Date	Time	ET (sec)	Chan[2] Pressure Feet H2O	Ho-H(t)	Normalized (H(t)/Ho)	Adjusted t
3/30/2005	12:09:09	99	10.08	0		
3/30/2005	12:09:12	102	10.08	0		
3/30/2005	12:09:15	105	10.08	0		
3/30/2005	12:09:18	108	11.021	0.941	1.000	0
3/30/2005	12:09:21	111	10.538	0.458	0.487	3
3/30/2005	12:09:24	114	10.39	0.31	0.329	6
3/30/2005	12:09:27	117	10.48	0.4	0.425	9
3/30/2005	12:09:30	120	10.478	0.398	0.423	12
3/30/2005	12:09:33	123	10.475	0.395	0.420	15
3/30/2005	12:09:36	126	10.473	0.393	0.418	18
3/30/2005	12:09:39	129	10.471	0.391	0.416	21
3/30/2005	12:09:42	132	10.468	0.388	0.412	24
3/30/2005	12:09:45	135	10.466	0.386	0.410	27
3/30/2005	12:09:48	138	10.466	0.386	0.410	30
3/30/2005	12:09:51	141	10.464	0.384	0.408	33
3/30/2005	12:09:54	144	10.464	0.384	0.408	36
3/30/2005	12:09:57	147	10.462	0.382	0.406	39
3/30/2005	12:10:00	150	10.459	0.379	0.403	42
3/30/2005	12:10:03	153	10.459	0.379	0.403	45
3/30/2005	12:10:06	156	10.457	0.377	0.401	48
3/30/2005	12:10:09	159	10.455	0.375	0.399	51
3/30/2005	12:10:12	162	10.455	0.375	0.399	54
3/30/2005	12:10:15	165	10.452	0.372	0.395	57
3/30/2005	12:10:18	168	10.45	0.37	0.393	60
3/30/2005	12:10:21	171	10.448	0.368	0.391	63
3/30/2005	12:10:24	174	10.448	0.368	0.391	66
3/30/2005	12:10:27	177	10.445	0.365	0.388	69
3/30/2005	12:10:30	180	10.443	0.363	0.386	72
3/30/2005	12:10:33	183	10.443	0.363	0.386	75
3/30/2005	12:10:36	186	10.441	0.361	0.384	78
3/30/2005	12:10:39	189	10.441	0.361	0.384	81
3/30/2005	12:10:42	192	10.438	0.358	0.380	84
3/30/2005	12:10:45	195	10.438	0.358	0.380	87
3/30/2005	12:10:48	198	10.436	0.356	0.378	90
3/30/2005	12:10:51	201	10.436	0.356	0.378	93
3/30/2005	12:10:54	204	10.436	0.356	0.378	96
3/30/2005	12:10:57	207	10.434	0.354	0.376	99
3/30/2005	12:11:00	210	10.431	0.351	0.373	102
3/30/2005	12:11:03	213	10.431	0.351	0.373	105
3/30/2005	12:11:06	216	10.429	0.349	0.371	108
3/30/2005	12:11:09	219	10.429	0.349	0.371	111
3/30/2005	12:11:12	222	10.429	0.349	0.371	114
3/30/2005	12:11:15	225	10.427	0.347	0.369	117
3/30/2005	12:11:18	228	10.427	0.347	0.369	120
3/30/2005	12:11:21	231	10.427	0.347	0.369	123
3/30/2005	12:11:24	234	10.424	0.344	0.366	126
3/30/2005	12:11:27	237	10.424	0.344	0.366	129
3/30/2005	12:11:30	240	10.422	0.342	0.363	132
3/30/2005	12:11:33	243	10.422	0.342	0.363	135
3/30/2005	12:11:36	246	10.422	0.342	0.363	138
3/30/2005	12:11:39	249	10.42	0.34	0.361	141
3/30/2005	12:11:42	252	10.42	0.34	0.361	144
3/30/2005	12:11:45	255	10.417	0.337	0.358	147
3/30/2005	12:11:48	258	10.417	0.337	0.358	150

Conductivity Calculations

	To=	5000	
	b=	15	
	r_c=	2.49E-01	
	rw=	3.33E-01	
rw*=	rw(Kz/Kr)^0.5=	3.33E-01	
	A=	2.91E+00	
	B=	4.64E-01	
	ln(Re/rw*)=	2.45E+00	
	Kr=	1.01E-06	ft/s
	Kr=	8.72E-02	ft/day
	n=	2.29E-01	
	Velocity=	2.13E-01	ft/day

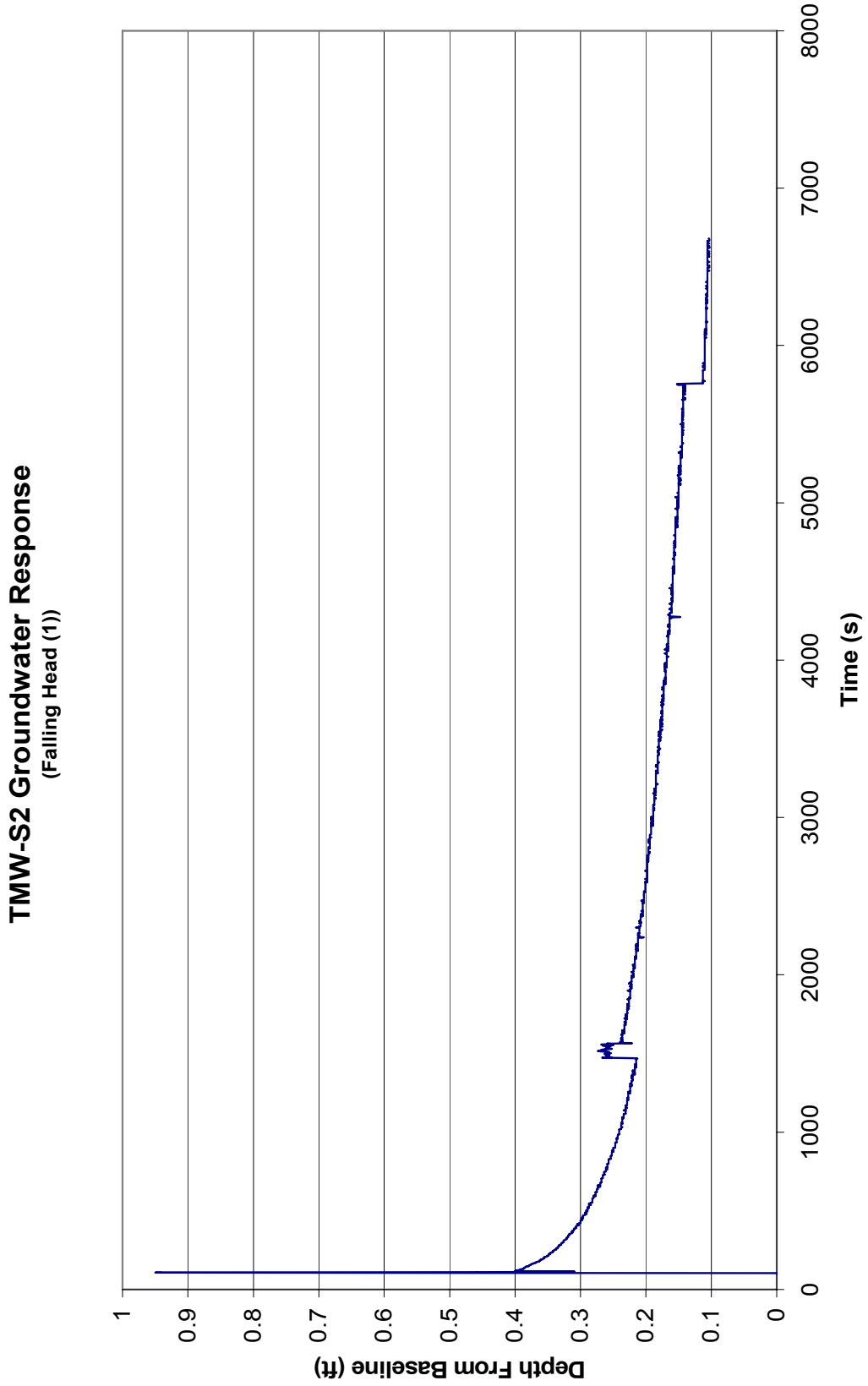
TMW-S2 Groundwater Response
(Falling Head (1))
Depth From Baseline (ft)
1
0.9
0.8
0.7
0.6
0.5
0.4
0.3
0.2
0.1
0
0
1000
2000
3000
4000
5000
6000
7000
8000
Time (s)

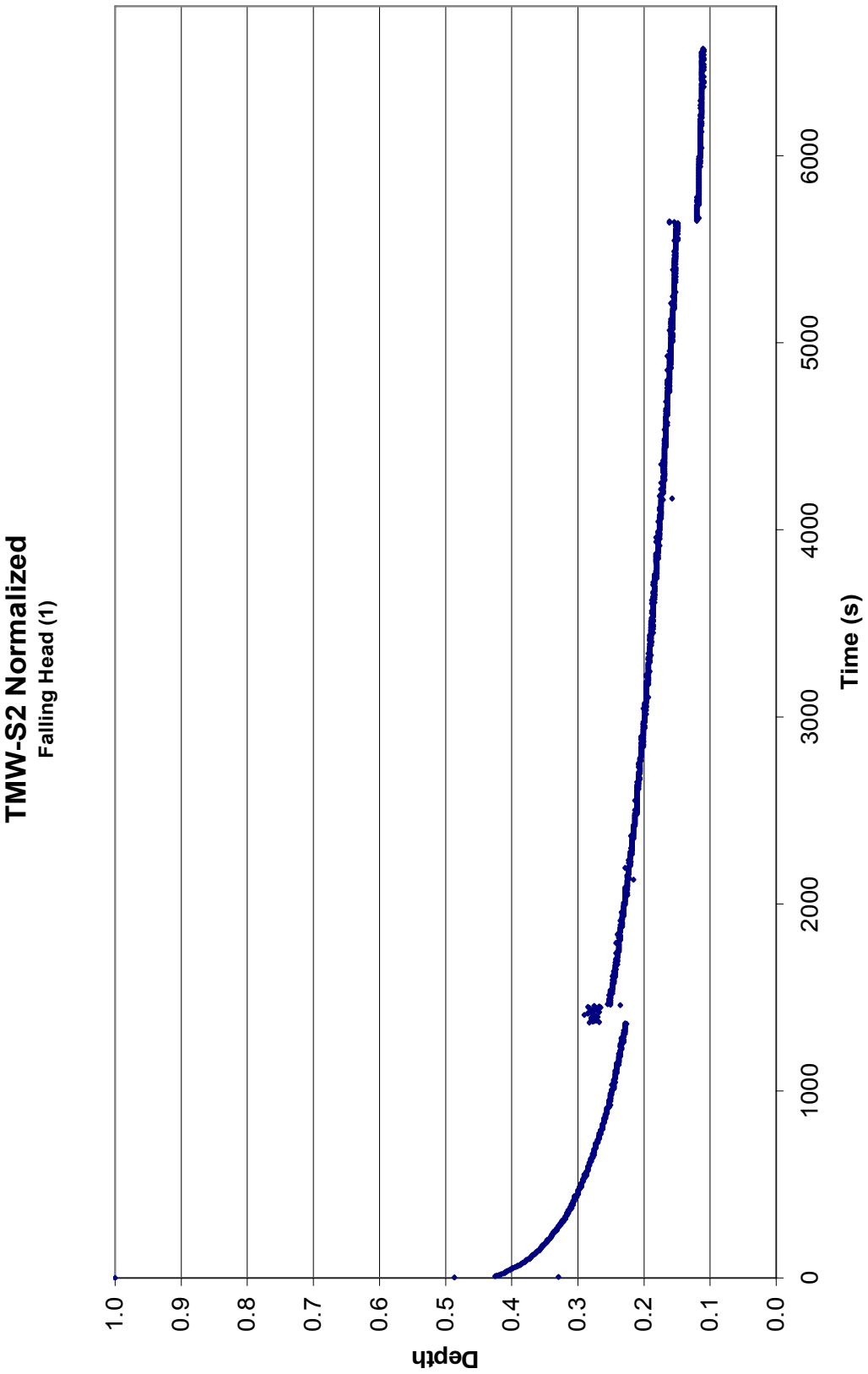
TMW-S2 Normalized
Falling Head (1)
Depth
Time (s)
1.0
0.9
0.8
0.7
0.6
0.5
0.4
0.3
0.2
0.1
0.0
0
1000
2000
3000
4000
5000
6000

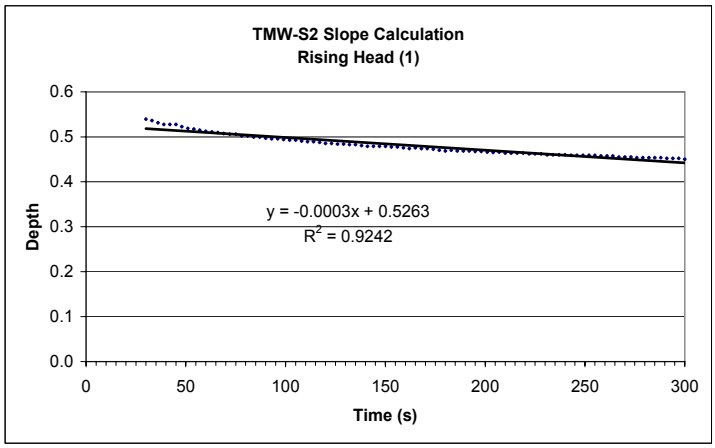

Date	Time	ET (sec)	Chan[2] Pressure Feet H2O		Ho-H(t)	Normalized (H(t)/Ho)	Adjusted t
3/30/2005	14:01:46	0	10.184	0	0	0.000	
3/30/2005	14:01:49	3	10.184	0	0	0.000	
3/30/2005	14:01:52	6	10.184	0	0	0.000	
3/30/2005	14:01:55	9	10.184	0	0	0.000	
3/30/2005	14:01:58	12	10.184	0	0	0.000	
3/30/2005	14:02:01	15	10.184	0	0	0.000	
3/30/2005	14:02:04	18	10.181	-0.003	0	0.000	
3/30/2005	14:02:07	21	10.181	-0.003	0	0.000	
3/30/2005	14:02:10	24	10.184	0	0	0.000	
3/30/2005	14:02:13	27	10.184	0	0	0.000	
3/30/2005	14:02:16	30	10.126	-0.058	0	0.000	
3/30/2005	14:02:19	33	10.445	0.261	0	0.000	
3/30/2005	14:02:22	36	9.065	-1.119	1.38	1.000	0
3/30/2005	14:02:25	39	9.19	-0.994	1.255	0.909	3
3/30/2005	14:02:28	42	9.435	-0.749	1.01	0.732	6
3/30/2005	14:02:31	45	9.564	-0.62	0.881	0.638	9
3/30/2005	14:02:34	48	9.618	-0.566	0.827	0.599	12
3/30/2005	14:02:37	51	9.643	-0.541	0.802	0.581	15
3/30/2005	14:02:40	54	9.662	-0.522	0.783	0.567	18
3/30/2005	14:02:43	57	9.675	-0.509	0.77	0.558	21
3/30/2005	14:02:46	60	9.685	-0.499	0.76	0.551	24
3/30/2005	14:02:49	63	9.694	-0.49	0.751	0.544	27
3/30/2005	14:02:52	66	9.701	-0.483	0.744	0.539	30
3/30/2005	14:02:55	69	9.705	-0.479	0.74	0.536	33
3/30/2005	14:02:58	72	9.712	-0.472	0.733	0.531	36
3/30/2005	14:03:01	75	9.717	-0.467	0.728	0.528	39
3/30/2005	14:03:04	78	9.717	-0.467	0.728	0.528	42
3/30/2005	14:03:07	81	9.717	-0.467	0.728	0.528	45
3/30/2005	14:03:10	84	9.724	-0.46	0.721	0.522	48
3/30/2005	14:03:13	87	9.729	-0.455	0.716	0.519	51
3/30/2005	14:03:16	90	9.731	-0.453	0.714	0.517	54
3/30/2005	14:03:19	93	9.735	-0.449	0.71	0.514	57
3/30/2005	14:03:22	96	9.738	-0.446	0.707	0.512	60
3/30/2005	14:03:25	99	9.74	-0.444	0.705	0.511	63
3/30/2005	14:03:28	102	9.742	-0.442	0.703	0.509	66
3/30/2005	14:03:31	105	9.745	-0.439	0.7	0.507	69
3/30/2005	14:03:34	108	9.747	-0.437	0.698	0.506	72
3/30/2005	14:03:37	111	9.747	-0.437	0.698	0.506	75
3/30/2005	14:03:40	114	9.752	-0.432	0.693	0.502	78
3/30/2005	14:03:43	117	9.752	-0.432	0.693	0.502	81
3/30/2005	14:03:46	120	9.756	-0.428	0.689	0.499	84
3/30/2005	14:03:49	123	9.756	-0.428	0.689	0.499	87
3/30/2005	14:03:52	126	9.759	-0.425	0.686	0.497	90
3/30/2005	14:03:55	129	9.761	-0.423	0.684	0.496	93
3/30/2005	14:03:58	132	9.761	-0.423	0.684	0.496	96
3/30/2005	14:04:01	135	9.763	-0.421	0.682	0.494	99
3/30/2005	14:04:04	138	9.765	-0.419	0.68	0.493	102
3/30/2005	14:04:07	141	9.765	-0.419	0.68	0.493	105
3/30/2005	14:04:10	144	9.768	-0.416	0.677	0.491	108
3/30/2005	14:04:13	147	9.77	-0.414	0.675	0.489	111
3/30/2005	14:04:16	150	9.77	-0.414	0.675	0.489	114
3/30/2005	14:04:19	153	9.772	-0.412	0.673	0.488	117
3/30/2005	14:04:22	156	9.775	-0.409	0.67	0.486	120
3/30/2005	14:04:25	159	9.775	-0.409	0.67	0.486	123
3/30/2005	14:04:28	162	9.777	-0.407	0.668	0.484	126
3/30/2005	14:04:31	165	9.777	-0.407	0.668	0.484	129
3/30/2005	14:04:34	168	9.779	-0.405	0.666	0.483	132
3/30/2005	14:04:37	171	9.779	-0.405	0.666	0.483	135
3/30/2005	14:04:40	174	9.782	-0.402	0.663	0.480	138
3/30/2005	14:04:43	177	9.784	-0.4	0.661	0.479	141
3/30/2005	14:04:46	180	9.784	-0.4	0.661	0.479	144
3/30/2005	14:04:49	183	9.784	-0.4	0.661	0.479	147
3/30/2005	14:04:52	186	9.784	-0.4	0.661	0.479	150

Conductivity Calculations		
To=	3.33E+03	
b=	15	
r_c=	1.75E-01	
rw=	3.33E-01	
rw*= rw(Kz/Kr)^0.5=	3.33E-01	
A=	2.91E+00	
B=	4.64E-01	
ln(Re/rw*)=	2.45E+00	
Kr=	7.49E-07	ft/s
Kr=	6.47E-02	ft/day
n=	2.29E-01	
Velocity=	1.58E-01	ft/day

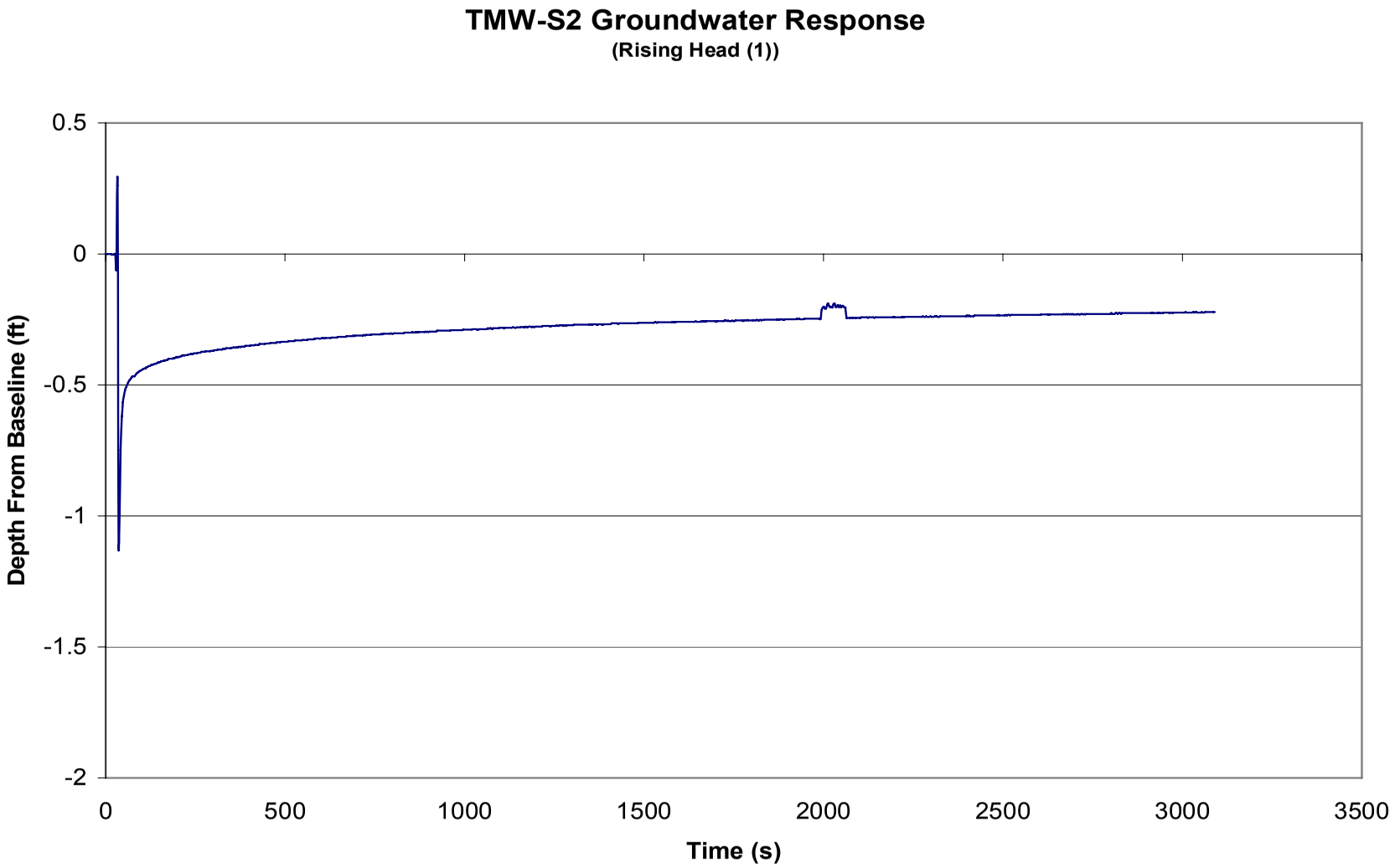
TMW-S2 Groundwater Response
(Rising Head (1))
Depth From Baseline (ft)
0.5
0
-0.5
-1
-1.5
-2
0
500
1000
1500
2000
2500
3000
3500
Time (s)

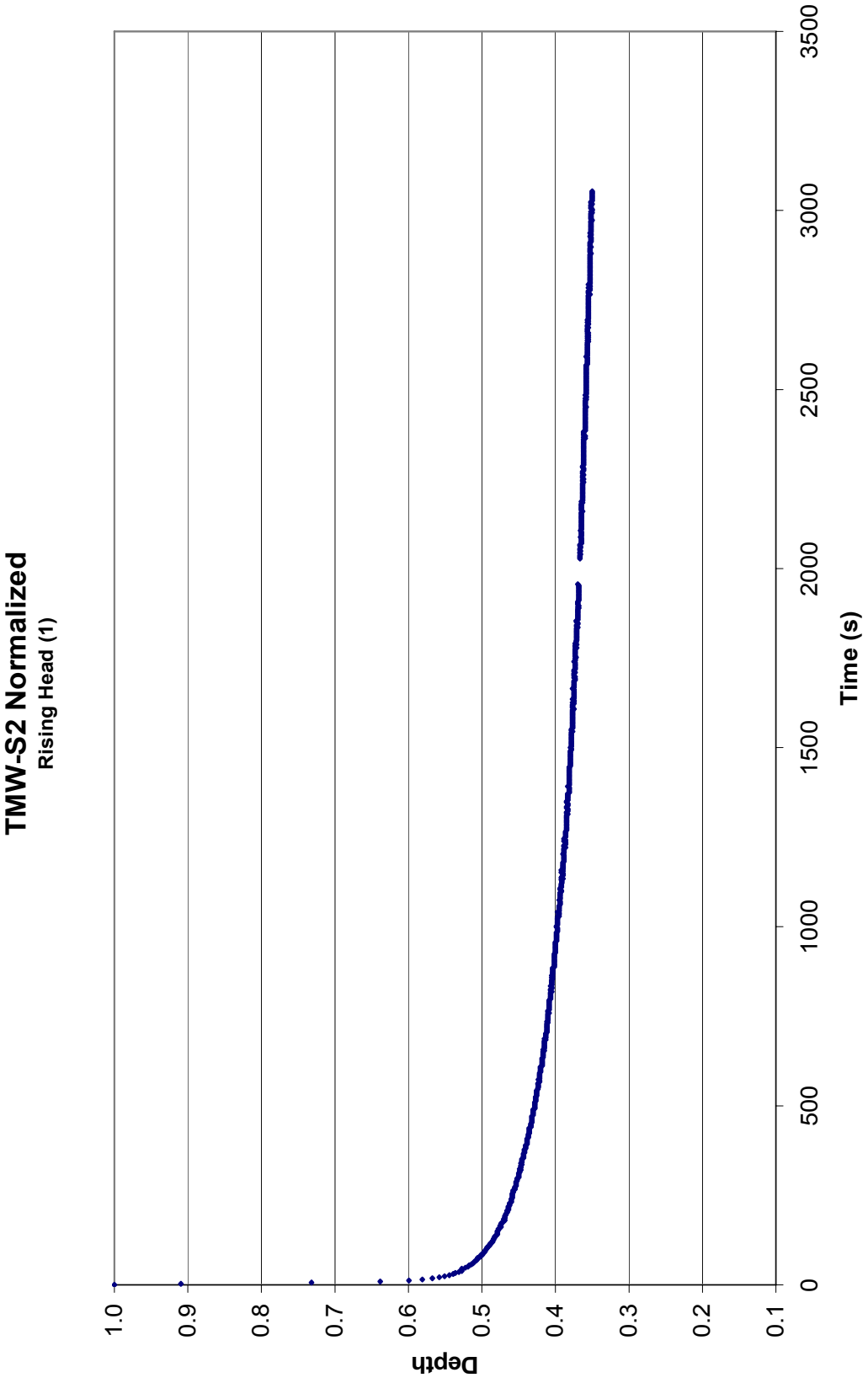
TMW-S2 Normalized
Rising Head (1)
Depth
Time (s)
1.0
0.9
0.8
0.7
0.6
0.5
0.4
0.3
0.2
0.1
0
500
1000
1500
2000
2500
3000
3500

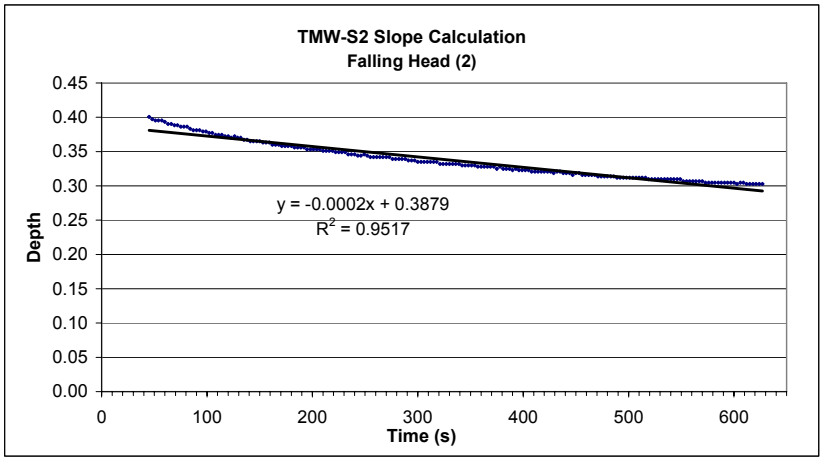

Date	Time	ET (sec)	Chan[2] Pressure Feet H2O	Ho-H(t)	Normalized (H(t)/Ho)	Adjusted t
3/30/2005	14:59:47	0	9.97	0		
3/30/2005	14:59:50	3	9.97	0		
3/30/2005	14:59:53	6	9.97	0		
3/30/2005	14:59:56	9	9.97	0		
3/30/2005	14:59:59	12	9.965	0		
3/30/2005	15:00:02	15	10.959	0.994	1.000	0
3/30/2005	15:00:05	18	10.414	0.449	0.452	3
3/30/2005	15:00:08	21	10.384	0.419	0.422	6
3/30/2005	15:00:11	24	10.381	0.416	0.419	9
3/30/2005	15:00:14	27	10.379	0.414	0.416	12
3/30/2005	15:00:17	30	10.379	0.414	0.416	15
3/30/2005	15:00:20	33	10.377	0.412	0.414	18
3/30/2005	15:00:23	36	10.374	0.409	0.411	21
3/30/2005	15:00:26	39	10.372	0.407	0.409	24
3/30/2005	15:00:29	42	10.37	0.405	0.407	27
3/30/2005	15:00:32	45	10.37	0.405	0.407	30
3/30/2005	15:00:35	48	10.37	0.405	0.407	33
3/30/2005	15:00:38	51	10.365	0.4	0.402	36
3/30/2005	15:00:41	54	10.365	0.4	0.402	39
3/30/2005	15:00:44	57	10.363	0.398	0.400	42
3/30/2005	15:00:47	60	10.363	0.398	0.400	45
3/30/2005	15:00:50	63	10.36	0.395	0.397	48
3/30/2005	15:00:53	66	10.358	0.393	0.395	51
3/30/2005	15:00:56	69	10.358	0.393	0.395	54
3/30/2005	15:00:59	72	10.358	0.393	0.395	57
3/30/2005	15:01:02	75	10.356	0.391	0.393	60
3/30/2005	15:01:05	78	10.353	0.388	0.390	63
3/30/2005	15:01:08	81	10.353	0.388	0.390	66
3/30/2005	15:01:11	84	10.351	0.386	0.388	69
3/30/2005	15:01:14	87	10.351	0.386	0.388	72
3/30/2005	15:01:17	90	10.349	0.384	0.386	75
3/30/2005	15:01:20	93	10.349	0.384	0.386	78
3/30/2005	15:01:23	96	10.349	0.384	0.386	81
3/30/2005	15:01:26	99	10.346	0.381	0.383	84
3/30/2005	15:01:29	102	10.344	0.379	0.381	87
3/30/2005	15:01:32	105	10.344	0.379	0.381	90
3/30/2005	15:01:35	108	10.344	0.379	0.381	93
3/30/2005	15:01:38	111	10.342	0.377	0.379	96
3/30/2005	15:01:41	114	10.342	0.377	0.379	99
3/30/2005	15:01:44	117	10.34	0.375	0.377	102
3/30/2005	15:01:47	120	10.34	0.375	0.377	105
3/30/2005	15:01:50	123	10.337	0.372	0.374	108
3/30/2005	15:01:53	126	10.337	0.372	0.374	111
3/30/2005	15:01:56	129	10.337	0.372	0.374	114
3/30/2005	15:01:59	132	10.335	0.37	0.372	117
3/30/2005	15:02:02	135	10.335	0.37	0.372	120
3/30/2005	15:02:05	138	10.333	0.368	0.370	123
3/30/2005	15:02:08	141	10.335	0.37	0.372	126
3/30/2005	15:02:11	144	10.333	0.368	0.370	129
3/30/2005	15:02:14	147	10.333	0.368	0.370	132
3/30/2005	15:02:17	150	10.33	0.365	0.367	135
3/30/2005	15:02:20	153	10.33	0.365	0.367	138
3/30/2005	15:02:23	156	10.328	0.363	0.365	141
3/30/2005	15:02:26	159	10.328	0.363	0.365	144
3/30/2005	15:02:29	162	10.328	0.363	0.365	147
3/30/2005	15:02:32	165	10.328	0.363	0.365	150

Conductivity Calculations

	To=	5000	
	b=	15	
	r_c=	0.245	
	rw=	3.33E-01	
rw*=	rw(Kz/Kr)^0.5=	3.33E-01	
	A=	2.91E+00	
	B=	4.64E-01	
	ln(Re/rw*)=	2.45E+00	
	Kr=	9.80E-07	ft/s
	Kr=	8.47E-02	ft/day
	n=	2.29E-01	
	Velocity=	2.07E-01	ft/day

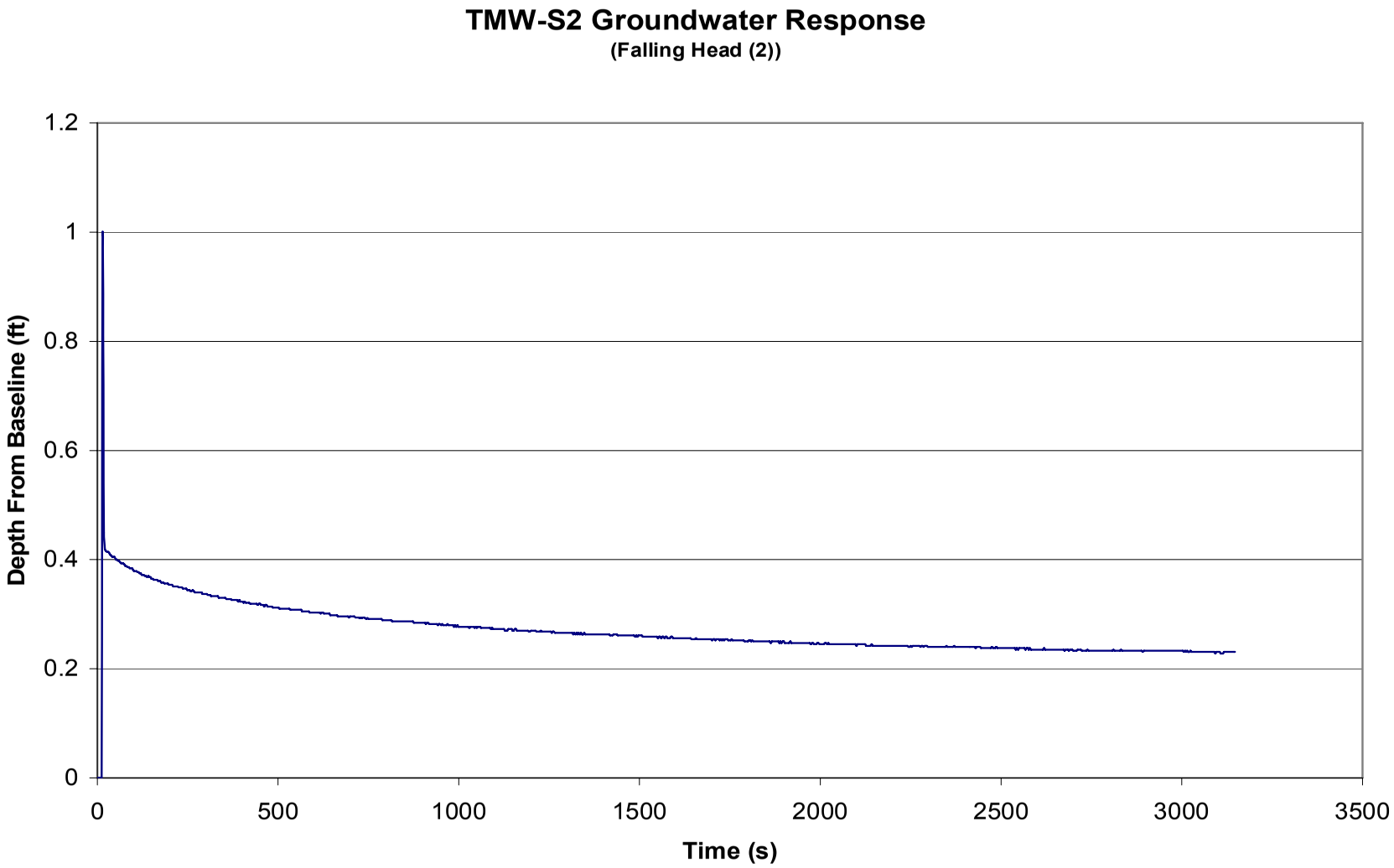
TMW-S2 Groundwater Response
(Falling Head (2))
Depth From Baseline (ft)
1.2
1
0.8
0.6
0.4
0.2
0
0
500
1000
1500
2000
2500
3000
3500
Time (s)

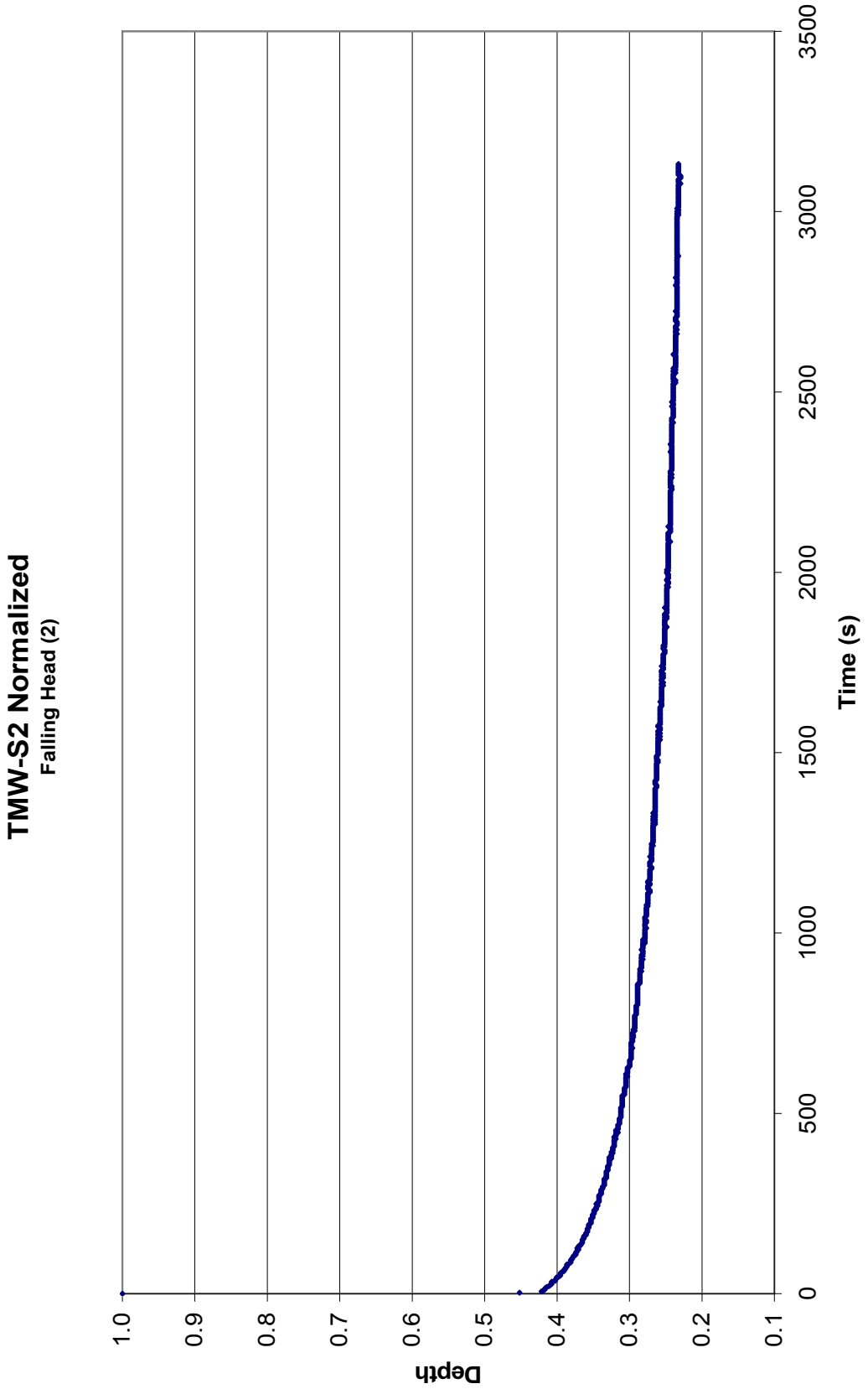
TMW-S2 Normalized
Falling Head (2)
Depth
Time (s)
1.0
0.9
0.8
0.7
0.6
0.5
0.4
0.3
0.2
0.1
0
500
1000
1500
2000
2500
3000
3500

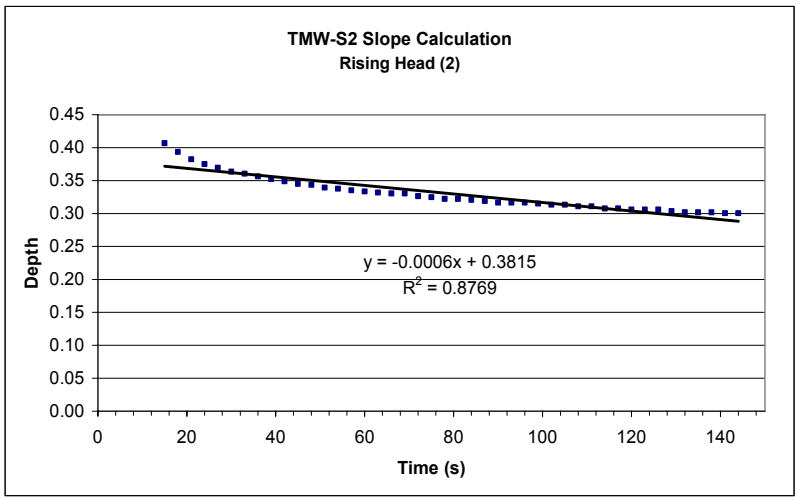

Date	Time	ET (sec)	Chan[2] Pressure Feet H2O		Ho-H(t)	Normalized (H(t)/Ho)	Adjusted t
3/30/2005	15:55:27	0	10.161	0	0		
3/30/2005	15:55:30	3	10.161	0	0		
3/30/2005	15:55:33	6	10.161	0	0		
3/30/2005	15:55:36	9	10.161	0	0		
3/30/2005	15:55:39	12	10.161	0	0		
3/30/2005	15:55:42	15	8.929	-1.232	1.232	1.000	0
3/30/2005	15:55:45	18	9.239	-0.922	0.922	0.748	3
3/30/2005	15:55:48	21	9.452	-0.709	0.709	0.575	6
3/30/2005	15:55:51	24	9.579	-0.582	0.582	0.472	9
3/30/2005	15:55:54	27	9.632	-0.529	0.529	0.429	12
3/30/2005	15:55:57	30	9.66	-0.501	0.501	0.407	15
3/30/2005	15:56:00	33	9.676	-0.485	0.485	0.394	18
3/30/2005	15:56:03	36	9.69	-0.471	0.471	0.382	21
3/30/2005	15:56:06	39	9.699	-0.462	0.462	0.375	24
3/30/2005	15:56:09	42	9.706	-0.455	0.455	0.369	27
3/30/2005	15:56:12	45	9.713	-0.448	0.448	0.364	30
3/30/2005	15:56:15	48	9.717	-0.444	0.444	0.360	33
3/30/2005	15:56:18	51	9.722	-0.439	0.439	0.356	36
3/30/2005	15:56:21	54	9.727	-0.434	0.434	0.352	39
3/30/2005	15:56:24	57	9.731	-0.43	0.43	0.349	42
3/30/2005	15:56:27	60	9.736	-0.425	0.425	0.345	45
3/30/2005	15:56:30	63	9.738	-0.423	0.423	0.343	48
3/30/2005	15:56:33	66	9.743	-0.418	0.418	0.339	51
3/30/2005	15:56:36	69	9.745	-0.416	0.416	0.338	54
3/30/2005	15:56:39	72	9.748	-0.413	0.413	0.335	57
3/30/2005	15:56:42	75	9.75	-0.411	0.411	0.334	60
3/30/2005	15:56:45	78	9.752	-0.409	0.409	0.332	63
3/30/2005	15:56:48	81	9.754	-0.407	0.407	0.330	66
3/30/2005	15:56:51	84	9.754	-0.407	0.407	0.330	69
3/30/2005	15:56:54	87	9.759	-0.402	0.402	0.326	72
3/30/2005	15:56:57	90	9.761	-0.4	0.4	0.325	75
3/30/2005	15:57:00	93	9.764	-0.397	0.397	0.322	78
3/30/2005	15:57:03	96	9.764	-0.397	0.397	0.322	81
3/30/2005	15:57:06	99	9.766	-0.395	0.395	0.321	84
3/30/2005	15:57:09	102	9.768	-0.393	0.393	0.319	87
3/30/2005	15:57:12	105	9.771	-0.39	0.39	0.317	90
3/30/2005	15:57:15	108	9.771	-0.39	0.39	0.317	93
3/30/2005	15:57:18	111	9.771	-0.39	0.39	0.317	96
3/30/2005	15:57:21	114	9.773	-0.388	0.388	0.315	99
3/30/2005	15:57:24	117	9.775	-0.386	0.386	0.313	102
3/30/2005	15:57:27	120	9.775	-0.386	0.386	0.313	105
3/30/2005	15:57:30	123	9.778	-0.383	0.383	0.311	108
3/30/2005	15:57:33	126	9.778	-0.383	0.383	0.311	111
3/30/2005	15:57:36	129	9.782	-0.379	0.379	0.308	114
3/30/2005	15:57:39	132	9.782	-0.379	0.379	0.308	117
3/30/2005	15:57:42	135	9.784	-0.377	0.377	0.306	120
3/30/2005	15:57:45	138	9.784	-0.377	0.377	0.306	123
3/30/2005	15:57:48	141	9.784	-0.377	0.377	0.306	126
3/30/2005	15:57:51	144	9.787	-0.374	0.374	0.304	129
3/30/2005	15:57:54	147	9.789	-0.372	0.372	0.302	132
3/30/2005	15:57:57	150	9.789	-0.372	0.372	0.302	135
3/30/2005	15:58:00	153	9.789	-0.372	0.372	0.302	138
3/30/2005	15:58:03	156	9.791	-0.37	0.37	0.300	141
3/30/2005	15:58:06	159	9.791	-0.37	0.37	0.300	144
3/30/2005	15:58:09	162	9.794	-0.367	0.367	0.298	147
3/30/2005	15:58:12	165	9.794	-0.367	0.367	0.298	150

Conductivity Calculations		
To=	1666.66667	
b=	15	
r_c=	2.22E-01	
rw=	3.33E-01	
rw*= rw(Kz/Kr)^0.5=	3.33E-01	
A=	2.91E+00	
B=	4.64E-01	
ln(Re/rw*)=	2.45E+00	
Kr=	2.41E-06	ft/s
Kr=	2.08E-01	ft/day
n=	2.29E-01	
Velocity=	5.10E-01	ft/day

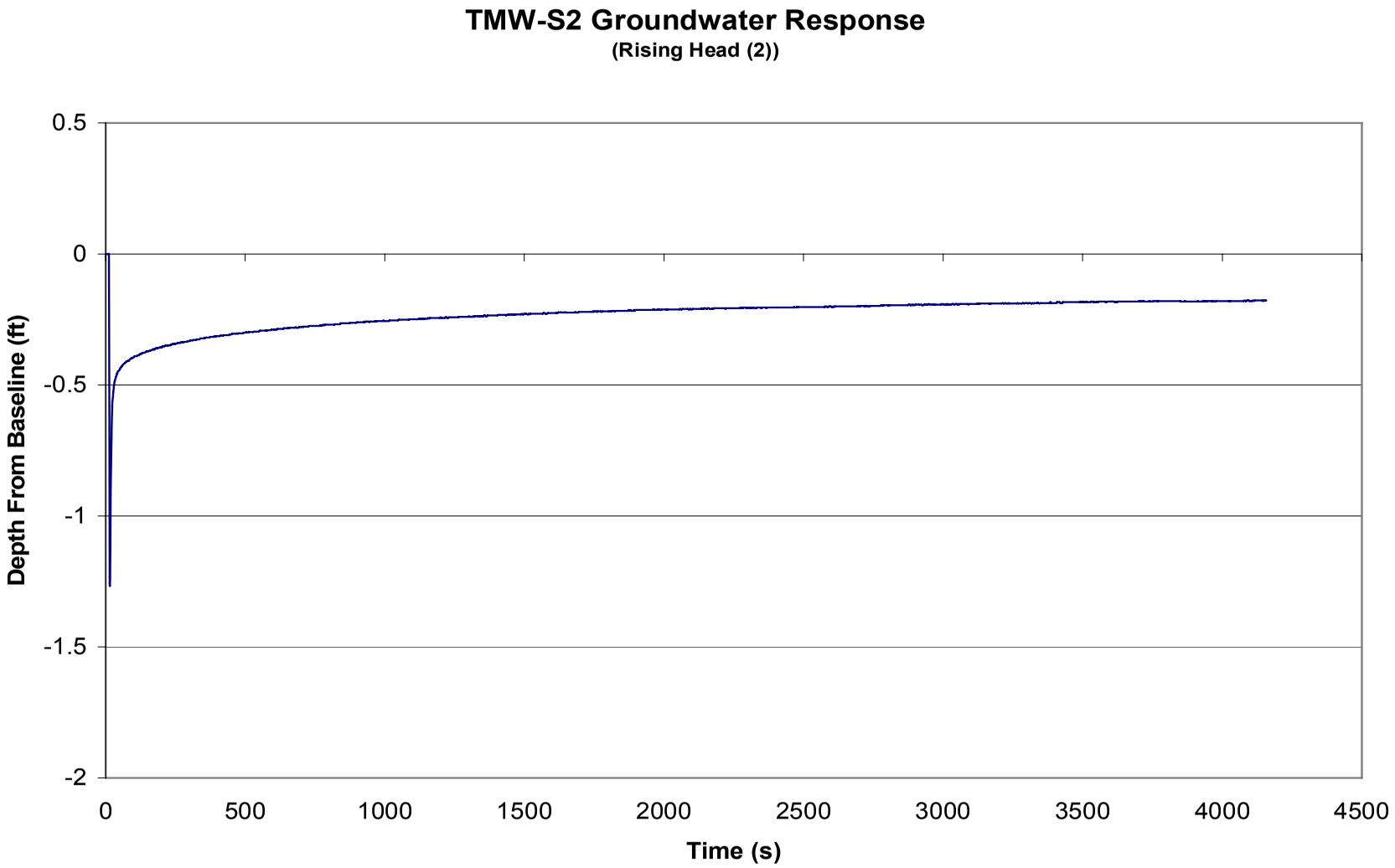
TMW-S2 Groundwater Response
(Rising Head (2))
Depth From Baseline (ft)
0.5
0
-0.5
-1
-1.5
-2
0
500
1000
1500
2000
2500
3000
3500
4000
4500
Time (s)

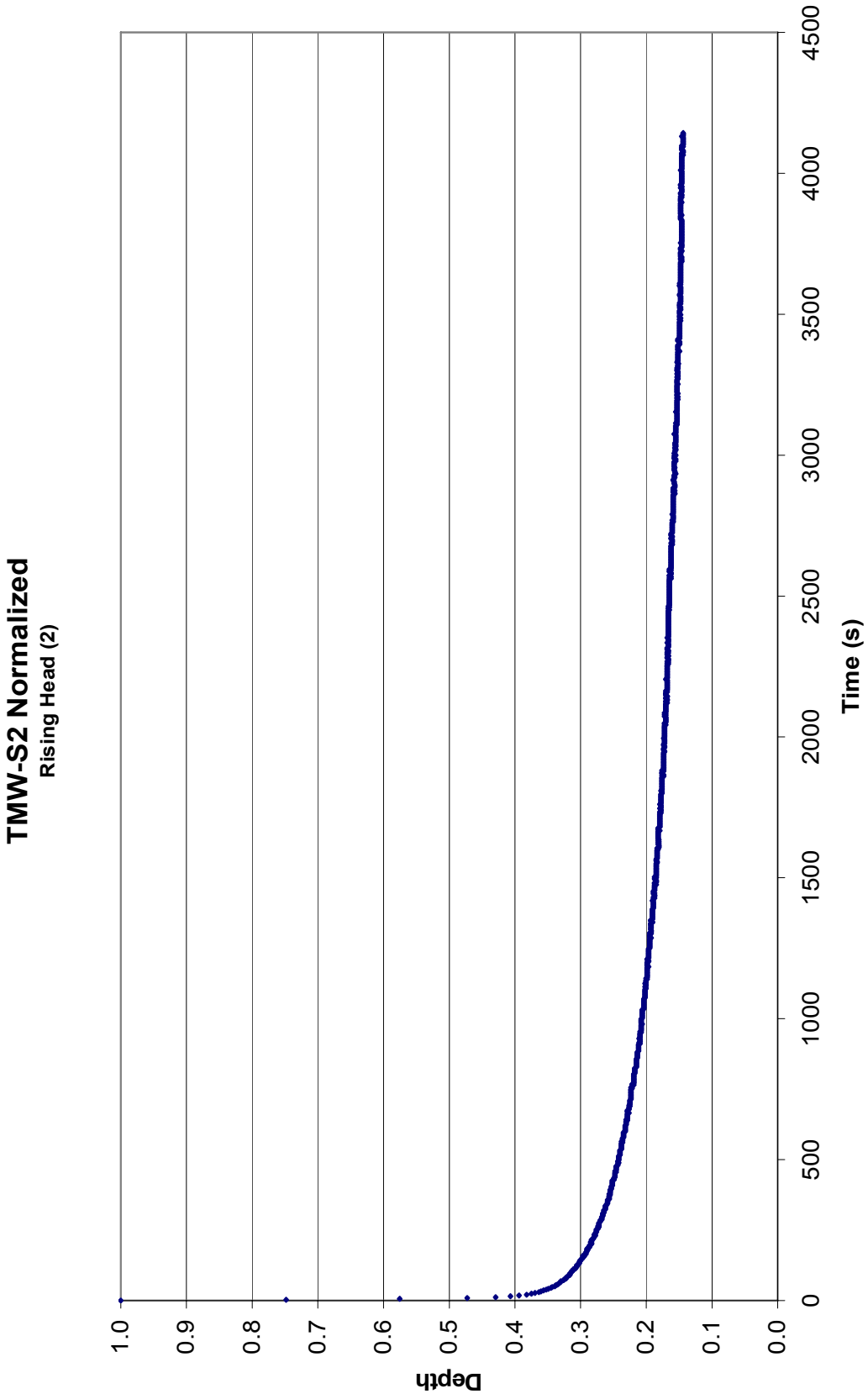
TMW-S2 Normalized
Rising Head (2)
Depth
Time (s)
1.0
0.9
0.8
0.7
0.6
0.5
0.4
0.3
0.2
0.1
0.0
0
500
1000
1500
2000
2500
3000
3500
4000
4500

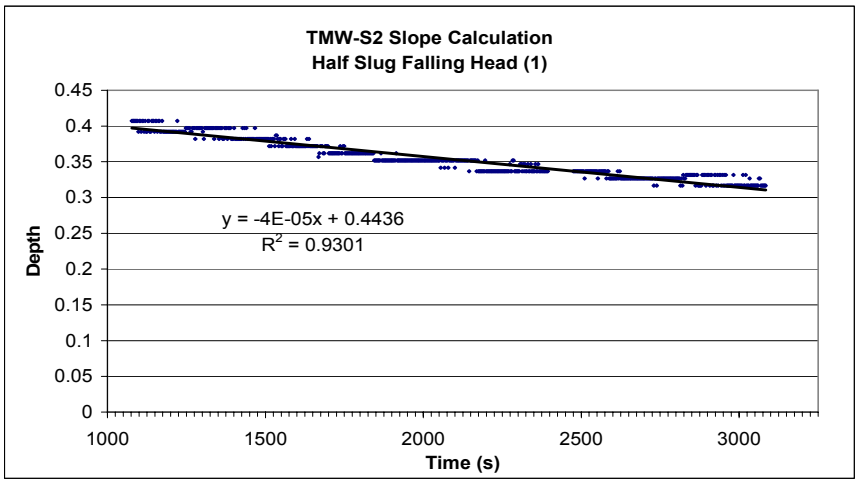

Date	Time	ET (sec)	Chan[2] Pressure Feet H2O	Ho-H(t)	Normalized (H(t)/Ho)	Adjusted t
3/31/2005	8:35:35	0	9.974	0		
3/31/2005	8:35:38	3	9.977	0		
3/31/2005	8:35:41	6	9.979	0		
3/31/2005	8:35:44	9	9.979	0		
3/31/2005	8:35:47	12	10.032	0.053	0.266	0
3/31/2005	8:35:50	15	10.027	0.048	0.241	3
3/31/2005	8:35:53	18	10.053	0.074	0.372	6
3/31/2005	8:35:56	21	10.152	0.173	0.869	9
3/31/2005	8:35:59	24	10.178	0.199	1.000	12
3/31/2005	8:36:02	27	10.161	0.182	0.915	15
3/31/2005	8:36:05	30	10.166	0.187	0.940	18
3/31/2005	8:36:08	33	10.159	0.18	0.905	21
3/31/2005	8:36:11	36	10.164	0.185	0.930	24
3/31/2005	8:36:14	39	10.159	0.18	0.905	27
3/31/2005	8:36:17	42	10.178	0.199	1.000	30
3/31/2005	8:36:20	45	10.164	0.185	0.930	33
3/31/2005	8:36:23	48	10.154	0.175	0.879	36
3/31/2005	8:36:26	51	10.161	0.182	0.915	39
3/31/2005	8:36:29	54	10.161	0.182	0.915	42
3/31/2005	8:36:32	57	10.154	0.175	0.879	45
3/31/2005	8:36:35	60	10.164	0.185	0.930	48
3/31/2005	8:36:38	63	10.154	0.175	0.879	51
3/31/2005	8:36:41	66	10.15	0.171	0.859	54
3/31/2005	8:36:44	69	10.148	0.169	0.849	57
3/31/2005	8:36:47	72	10.157	0.178	0.894	60
3/31/2005	8:36:50	75	10.145	0.166	0.834	63
3/31/2005	8:36:53	78	10.145	0.166	0.834	66
3/31/2005	8:36:56	81	10.15	0.171	0.859	69
3/31/2005	8:36:59	84	10.122	0.143	0.719	72
3/31/2005	8:37:02	87	10.124	0.145	0.729	75
3/31/2005	8:37:05	90	10.122	0.143	0.719	78
3/31/2005	8:37:08	93	10.122	0.143	0.719	81
3/31/2005	8:37:11	96	10.12	0.141	0.709	84
3/31/2005	8:37:14	99	10.12	0.141	0.709	87
3/31/2005	8:37:17	102	10.12	0.141	0.709	90
3/31/2005	8:37:20	105	10.115	0.136	0.683	93
3/31/2005	8:37:23	108	10.115	0.136	0.683	96
3/31/2005	8:37:26	111	10.113	0.134	0.673	99
3/31/2005	8:37:29	114	10.12	0.141	0.709	102
3/31/2005	8:37:32	117	10.113	0.134	0.673	105
3/31/2005	8:37:35	120	10.115	0.136	0.683	108
3/31/2005	8:37:38	123	10.117	0.138	0.693	111
3/31/2005	8:37:41	126	10.115	0.136	0.683	114
3/31/2005	8:37:44	129	10.117	0.138	0.693	117
3/31/2005	8:37:47	132	10.115	0.136	0.683	120
3/31/2005	8:37:50	135	10.12	0.141	0.709	123
3/31/2005	8:37:53	138	10.113	0.134	0.673	126
3/31/2005	8:37:56	141	10.113	0.134	0.673	129
3/31/2005	8:37:59	144	10.113	0.134	0.673	132
3/31/2005	8:38:02	147	10.111	0.132	0.663	135
3/31/2005	8:38:05	150	10.115	0.136	0.683	138
3/31/2005	8:38:08	153	10.11	0.131	0.658	141
3/31/2005	8:38:11	156	10.117	0.138	0.693	144
3/31/2005	8:38:14	159	10.11	0.131	0.658	147
3/31/2005	8:38:17	162	10.111	0.132	0.663	150

Conductivity Calculations

	To=	25000	
	b=	15	
	r_c=	3.75E-01	
	rw=	3.33E-01	
rw*=	rw(Kz/Kr)^0.5=	3.33E-01	
	A=	2.91E+00	
	B=	4.64E-01	
	ln(Re/rw*)=	2.45E+00	
	Kr=	4.59E-07	ft/s
	Kr=	3.96E-02	ft/day
	n=	2.29E-01	
	Velocity=	9.69E-02	ft/day

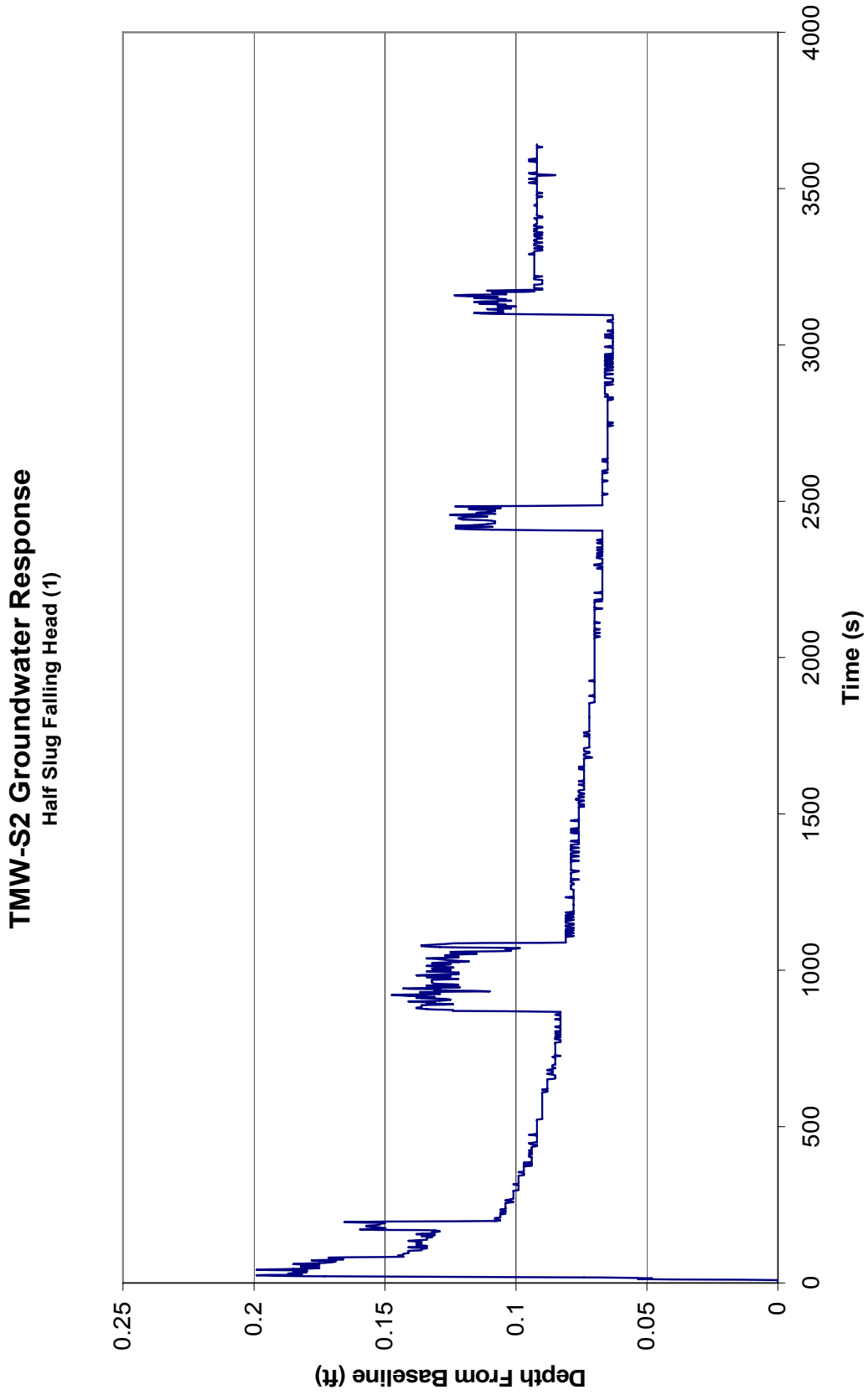
TMW-S2 Groundwater Response
Half Slug Falling Head (1)
Depth From Baseline (ft)
0.25
0.2
0.15
0.1
0.05
0
Time (s)
0
500
1000
1500
2000
2500
3000
3500
4000

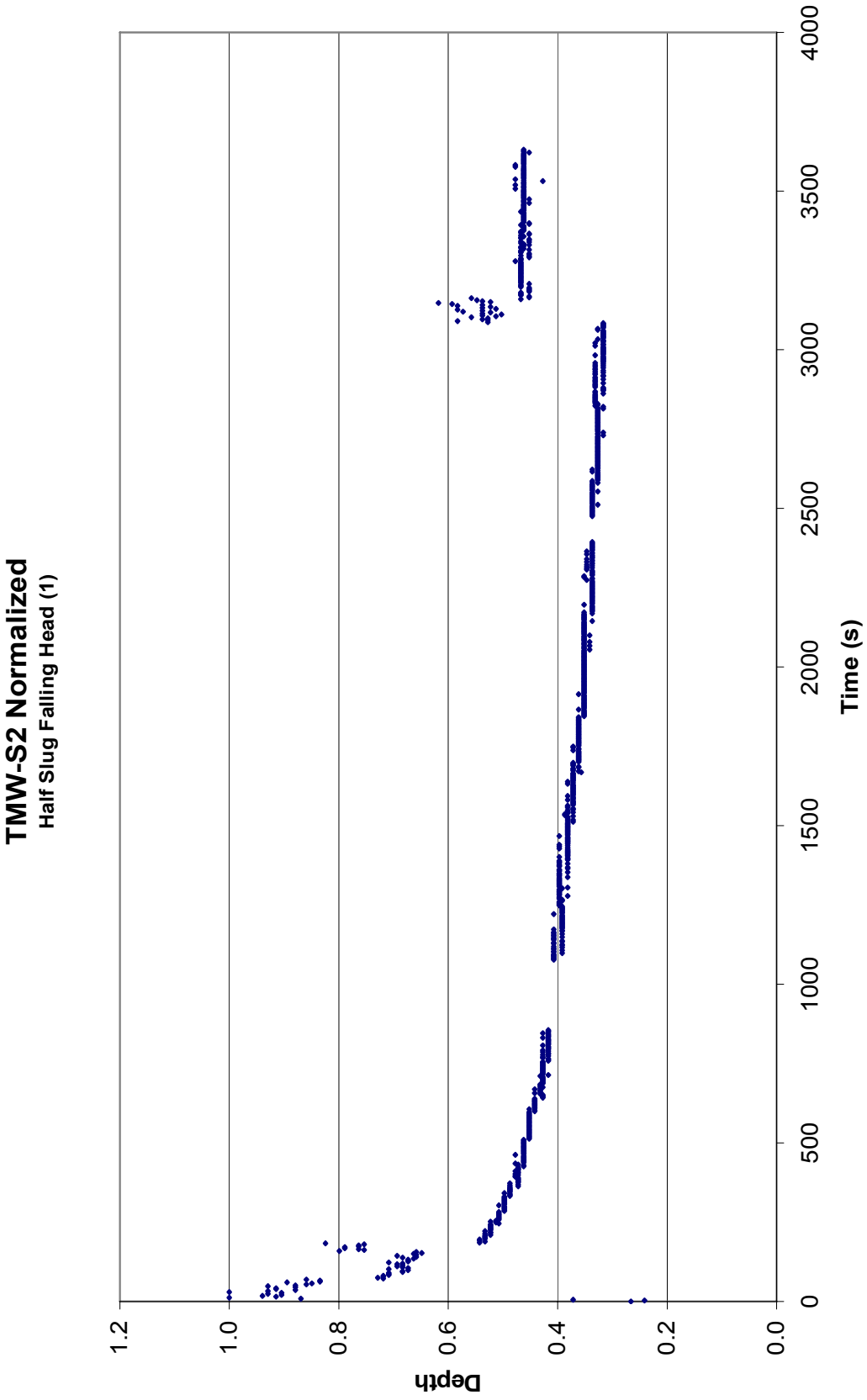
TMW-S2 Normalized
Half Slug Falling Head (1)
Depth
Time (s)
1.2
1.0
0.8
0.6
0.4
0.2
0.0
0
500
1000
1500
2000
2500
3000
3500
4000

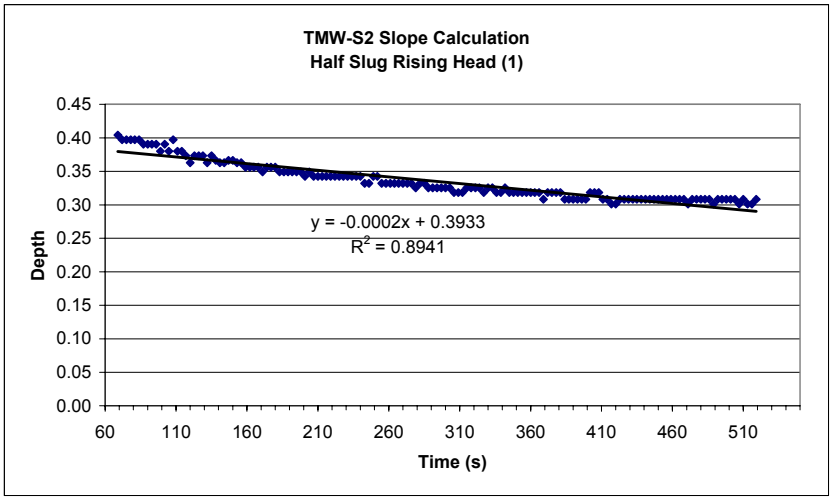

Date	Time	ET (sec)	Chan[2] Pressure Feet H2O		Ho-H(t)	Normalized (H(t)/Ho)	Adjusted t
3/31/2005	9:39:00	0	10.074	0	0		
3/31/2005	9:39:03	3	10.074	0	0		
3/31/2005	9:39:06	6	10.074	0	0		
3/31/2005	9:39:09	9	10.074	0	0		
3/31/2005	9:39:12	12	10.074	0	0		
3/31/2005	9:39:15	15	10.074	0	0		
3/31/2005	9:39:18	18	9.782	-0.292	0.292	1.000	0
3/31/2005	9:39:21	21	9.893	-0.181	0.181	0.620	3
3/31/2005	9:39:24	24	9.916	-0.158	0.158	0.541	6
3/31/2005	9:39:27	27	9.926	-0.148	0.148	0.507	9
3/31/2005	9:39:30	30	9.93	-0.144	0.144	0.493	12
3/31/2005	9:39:33	33	9.935	-0.139	0.139	0.476	15
3/31/2005	9:39:36	36	9.937	-0.137	0.137	0.469	18
3/31/2005	9:39:39	39	9.94	-0.134	0.134	0.459	21
3/31/2005	9:39:42	42	9.942	-0.132	0.132	0.452	24
3/31/2005	9:39:45	45	9.944	-0.13	0.13	0.445	27
3/31/2005	9:39:48	48	9.946	-0.128	0.128	0.438	30
3/31/2005	9:39:51	51	9.944	-0.13	0.13	0.445	33
3/31/2005	9:39:54	54	9.946	-0.128	0.128	0.438	36
3/31/2005	9:39:57	57	9.949	-0.125	0.125	0.428	39
3/31/2005	9:40:00	60	9.949	-0.125	0.125	0.428	42
3/31/2005	9:40:03	63	9.951	-0.123	0.123	0.421	45
3/31/2005	9:40:06	66	9.951	-0.123	0.123	0.421	48
3/31/2005	9:40:09	69	9.951	-0.123	0.123	0.421	51
3/31/2005	9:40:12	72	9.953	-0.121	0.121	0.414	54
3/31/2005	9:40:15	75	9.953	-0.121	0.121	0.414	57
3/31/2005	9:40:18	78	9.953	-0.121	0.121	0.414	60
3/31/2005	9:40:21	81	9.956	-0.118	0.118	0.404	63
3/31/2005	9:40:24	84	9.956	-0.118	0.118	0.404	66
3/31/2005	9:40:27	87	9.956	-0.118	0.118	0.404	69
3/31/2005	9:40:30	90	9.958	-0.116	0.116	0.397	72
3/31/2005	9:40:33	93	9.958	-0.116	0.116	0.397	75
3/31/2005	9:40:36	96	9.958	-0.116	0.116	0.397	78
3/31/2005	9:40:39	99	9.958	-0.116	0.116	0.397	81
3/31/2005	9:40:42	102	9.958	-0.116	0.116	0.397	84
3/31/2005	9:40:45	105	9.96	-0.114	0.114	0.390	87
3/31/2005	9:40:48	108	9.96	-0.114	0.114	0.390	90
3/31/2005	9:40:51	111	9.96	-0.114	0.114	0.390	93
3/31/2005	9:40:54	114	9.96	-0.114	0.114	0.390	96
3/31/2005	9:40:57	117	9.963	-0.111	0.111	0.380	99
3/31/2005	9:41:00	120	9.96	-0.114	0.114	0.390	102
3/31/2005	9:41:03	123	9.963	-0.111	0.111	0.380	105
3/31/2005	9:41:06	126	9.958	-0.116	0.116	0.397	108
3/31/2005	9:41:09	129	9.963	-0.111	0.111	0.380	111
3/31/2005	9:41:12	132	9.963	-0.111	0.111	0.380	114
3/31/2005	9:41:15	135	9.965	-0.109	0.109	0.373	117
3/31/2005	9:41:18	138	9.968	-0.106	0.106	0.363	120
3/31/2005	9:41:21	141	9.965	-0.109	0.109	0.373	123
3/31/2005	9:41:24	144	9.965	-0.109	0.109	0.373	126
3/31/2005	9:41:27	147	9.965	-0.109	0.109	0.373	129
3/31/2005	9:41:30	150	9.968	-0.106	0.106	0.363	132
3/31/2005	9:41:33	153	9.965	-0.109	0.109	0.373	135
3/31/2005	9:41:36	156	9.967	-0.107	0.107	0.366	138
3/31/2005	9:41:39	159	9.968	-0.106	0.106	0.363	141
3/31/2005	9:41:42	162	9.968	-0.106	0.106	0.363	144
3/31/2005	9:41:45	165	9.967	-0.107	0.107	0.366	147
3/31/2005	9:41:48	168	9.967	-0.107	0.107	0.366	150

Conductivity Calculations		
To=	5000	
b=	15	
r_c=	3.20E-01	
rw=	3.33E-01	
rw*= rw(Kz/Kr)^0.5=	3.33E-01	
A=	2.91E+00	
B=	4.64E-01	
ln(Re/rw*)=	2.45E+00	
Kr=	1.67E-06	ft/s
Kr=	1.45E-01	ft/day
n=	2.29E-01	
Velocity=	3.54E-01	ft/day

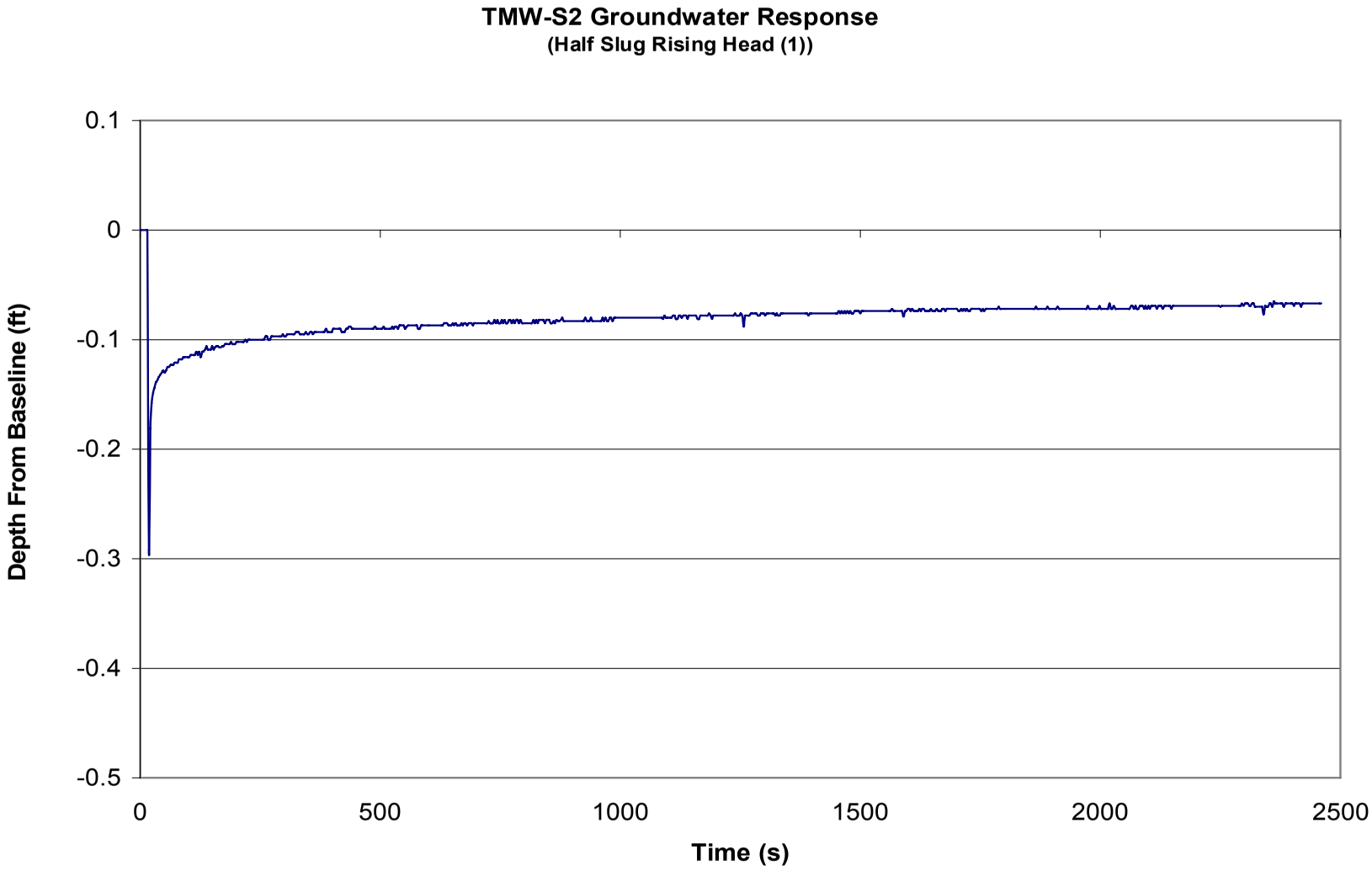
TMW-S2 Groundwater Response
(Half Slug Rising Head (1))
Depth From Baseline (ft)
0.1
0
-0.1
-0.2
-0.3
-0.4
-0.5
0
500
1000
1500
2000
2500
Time (s)

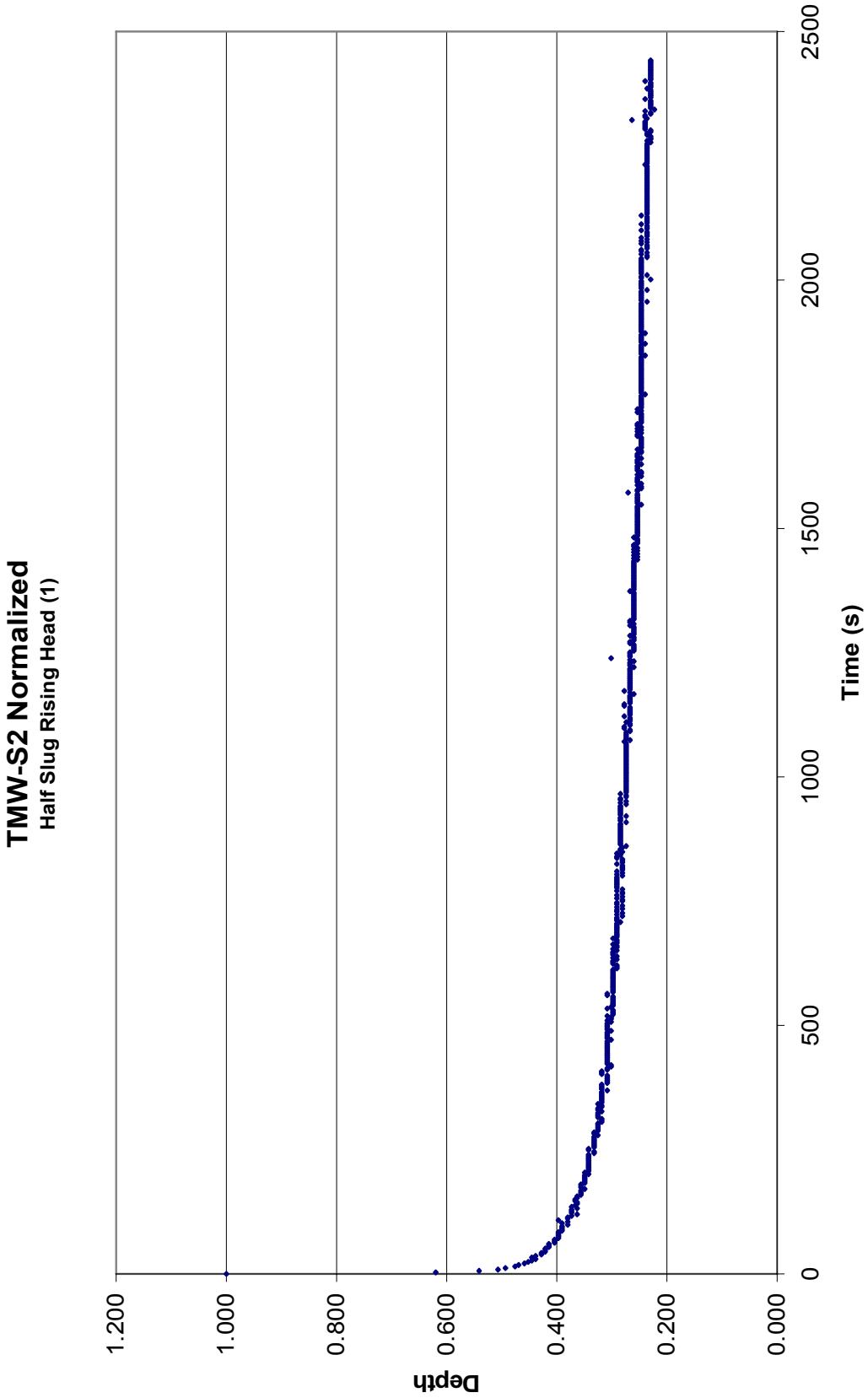
TMW-S2 Normalized
Half Slug Rising Head (1)
Depth
1.200
1.000
0.800
0.600
0.400
0.200
0.000
0
500
1000
1500
2000
2500
Time (s)

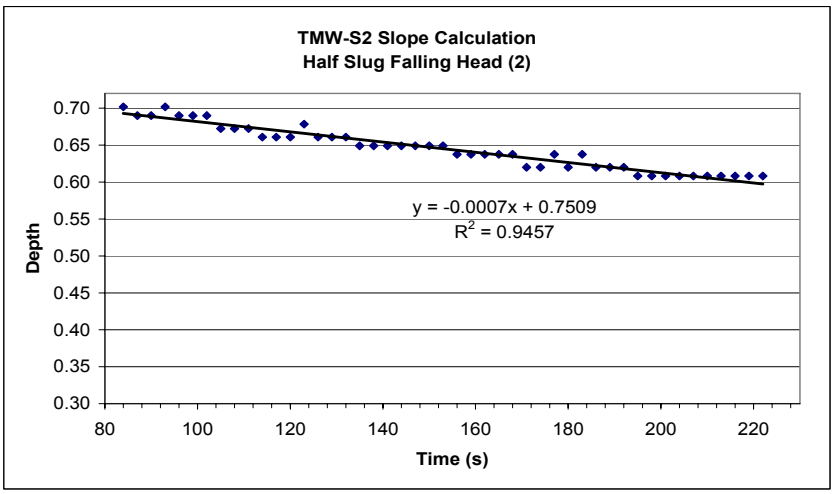

Date	Time	ET (sec)	Chan[2] Pressure Feet H2O	Ho-H(t)	Normalized (H(t)/Ho)	Adjusted t
3/31/2005	10:23:11	0	10.011	0		
3/31/2005	10:23:14	3	10.011	0		
3/31/2005	10:23:17	6	10.011	0		
3/31/2005	10:23:20	9	10.011	0		
3/31/2005	10:23:23	12	10.011	0		
3/31/2005	10:23:26	15	10.011	0		
3/31/2005	10:23:29	18	10.011	0		
3/31/2005	10:23:32	21	10.048	0.037	0.216	0
3/31/2005	10:23:35	24	10.182	0.171	1.000	3
3/31/2005	10:23:38	27	10.157	0.146	0.854	6
3/31/2005	10:23:41	30	10.157	0.146	0.854	9
3/31/2005	10:23:44	33	10.154	0.143	0.836	12
3/31/2005	10:23:47	36	10.15	0.139	0.813	15
3/31/2005	10:23:50	39	10.15	0.139	0.813	18
3/31/2005	10:23:53	42	10.15	0.139	0.813	21
3/31/2005	10:23:56	45	10.148	0.137	0.801	24
3/31/2005	10:23:59	48	10.145	0.134	0.784	27
3/31/2005	10:24:02	51	10.145	0.134	0.784	30
3/31/2005	10:24:05	54	10.143	0.132	0.772	33
3/31/2005	10:24:08	57	10.143	0.132	0.772	36
3/31/2005	10:24:11	60	10.141	0.13	0.760	39
3/31/2005	10:24:14	63	10.141	0.13	0.760	42
3/31/2005	10:24:17	66	10.138	0.127	0.743	45
3/31/2005	10:24:20	69	10.138	0.127	0.743	48
3/31/2005	10:24:23	72	10.138	0.127	0.743	51
3/31/2005	10:24:26	75	10.138	0.127	0.743	54
3/31/2005	10:24:29	78	10.138	0.127	0.743	57
3/31/2005	10:24:32	81	10.136	0.125	0.731	60
3/31/2005	10:24:35	84	10.133	0.122	0.713	63
3/31/2005	10:24:38	87	10.134	0.123	0.719	66
3/31/2005	10:24:41	90	10.136	0.125	0.731	69
3/31/2005	10:24:44	93	10.133	0.122	0.713	72
3/31/2005	10:24:47	96	10.133	0.122	0.713	75
3/31/2005	10:24:50	99	10.131	0.12	0.702	78
3/31/2005	10:24:53	102	10.131	0.12	0.702	81
3/31/2005	10:24:56	105	10.131	0.12	0.702	84
3/31/2005	10:24:59	108	10.129	0.118	0.690	87
3/31/2005	10:25:02	111	10.129	0.118	0.690	90
3/31/2005	10:25:05	114	10.131	0.12	0.702	93
3/31/2005	10:25:08	117	10.129	0.118	0.690	96
3/31/2005	10:25:11	120	10.129	0.118	0.690	99
3/31/2005	10:25:14	123	10.129	0.118	0.690	102
3/31/2005	10:25:17	126	10.126	0.115	0.673	105
3/31/2005	10:25:20	129	10.126	0.115	0.673	108
3/31/2005	10:25:23	132	10.126	0.115	0.673	111
3/31/2005	10:25:26	135	10.124	0.113	0.661	114
3/31/2005	10:25:29	138	10.124	0.113	0.661	117
3/31/2005	10:25:32	141	10.124	0.113	0.661	120
3/31/2005	10:25:35	144	10.127	0.116	0.678	123
3/31/2005	10:25:38	147	10.124	0.113	0.661	126
3/31/2005	10:25:41	150	10.124	0.113	0.661	129
3/31/2005	10:25:44	153	10.124	0.113	0.661	132
3/31/2005	10:25:47	156	10.122	0.111	0.649	135
3/31/2005	10:25:50	159	10.122	0.111	0.649	138
3/31/2005	10:25:53	162	10.122	0.111	0.649	141
3/31/2005	10:25:56	165	10.122	0.111	0.649	144
3/31/2005	10:25:59	168	10.122	0.111	0.649	147
3/31/2005	10:26:02	171	10.122	0.111	0.649	150

Conductivity Calculations			
	To=	1428.57143	
	b=	15	
	r_c=	3.11E-01	
	rw=	3.33E-01	
rw*=	rw(Kz/Kr)^0.5=	3.33E-01	
	A=	2.91E+00	
	B=	4.64E-01	
	ln(Re/rw*)=	2.45E+00	
	Kr=	5.51E-06	ft/s
	Kr=	4.76E-01	ft/day
	n=	2.29E-01	
	Velocity=	1.16E+00	ft/day

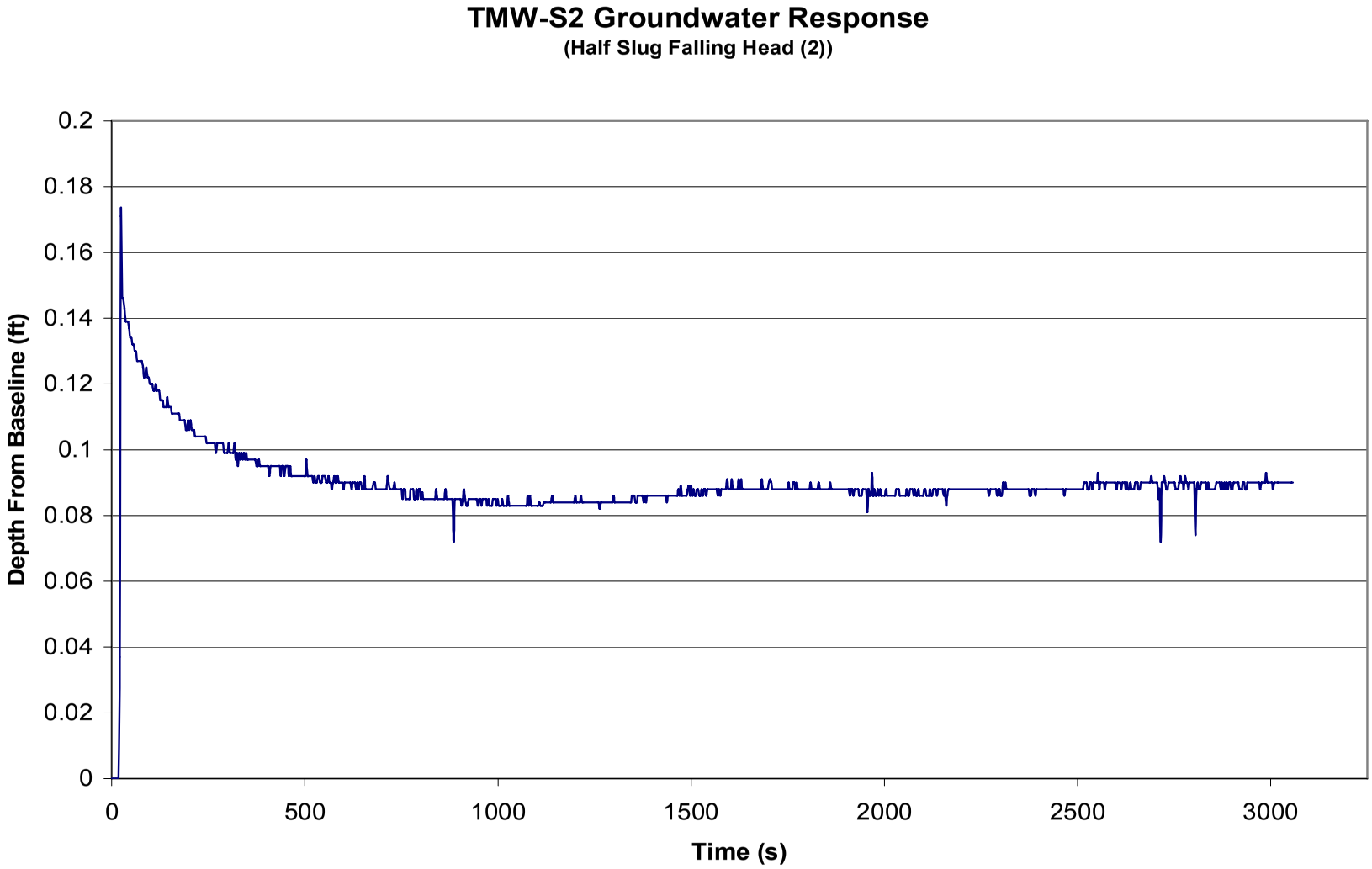
TMW-S2 Groundwater Response
(Half Slug Falling Head (2))
Depth From Baseline (ft)
0.2
0.18
0.16
0.14
0.12
0.1
0.08
0.06
0.04
0.02
0
0
500
1000
1500
2000
2500
3000
Time (s)

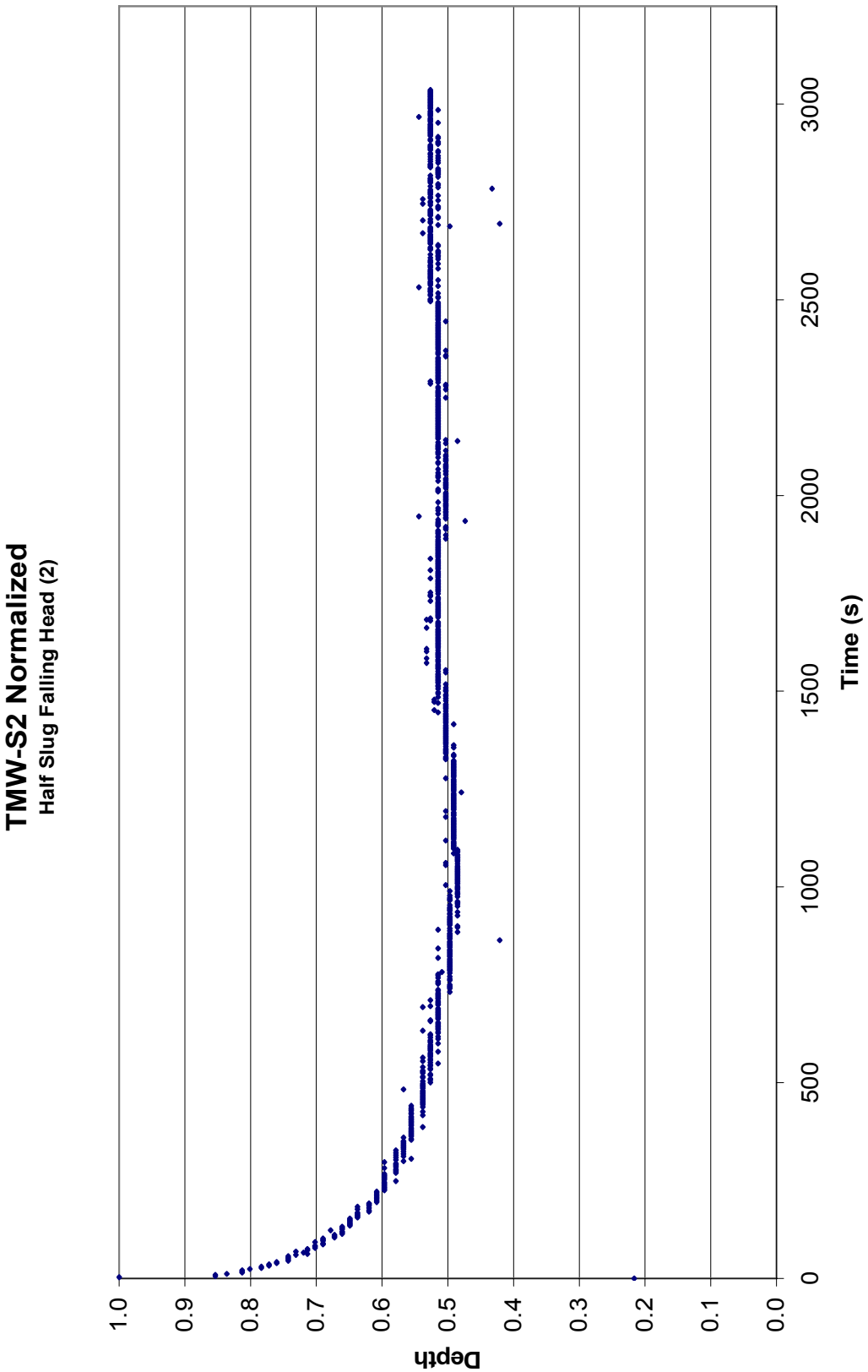
TMW-S2 Normalized
Half Slug Falling Head (2)
Depth
Time (s)
1.0
0.9
0.8
0.7
0.6
0.5
0.4
0.3
0.2
0.1
0.0
0
500
1000
1500
2000
2500
3000

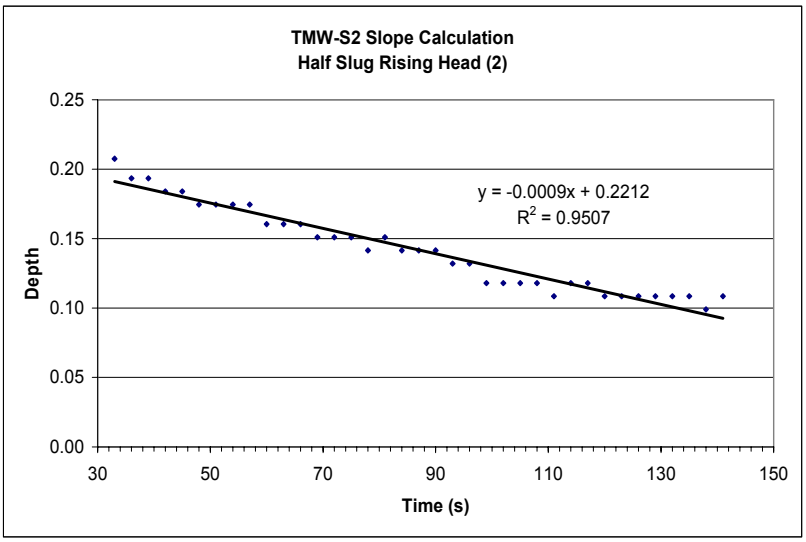

Date	Time	ET (sec)	Chan[2] Pressure Feet H2O		Ho-H(t)	Normalized (H(t)/Ho)	Adjusted t
3/31/2005	11:16:38	0	10.009	-0.002	0		
3/31/2005	11:16:41	3	10.011	0	0		
3/31/2005	11:16:44	6	9.799	-0.212	0.212	1.000	0
3/31/2005	11:16:47	9	9.93	-0.081	0.081	0.382	3
3/31/2005	11:16:50	12	9.946	-0.065	0.065	0.307	6
3/31/2005	11:16:53	15	9.953	-0.058	0.058	0.274	9
3/31/2005	11:16:56	18	9.956	-0.055	0.055	0.259	12
3/31/2005	11:16:59	21	9.958	-0.053	0.053	0.250	15
3/31/2005	11:17:02	24	9.96	-0.051	0.051	0.241	18
3/31/2005	11:17:05	27	9.963	-0.048	0.048	0.226	21
3/31/2005	11:17:08	30	9.965	-0.046	0.046	0.217	24
3/31/2005	11:17:11	33	9.97	-0.041	0.041	0.193	27
3/31/2005	11:17:14	36	9.967	-0.044	0.044	0.208	30
3/31/2005	11:17:17	39	9.967	-0.044	0.044	0.208	33
3/31/2005	11:17:20	42	9.97	-0.041	0.041	0.193	36
3/31/2005	11:17:23	45	9.97	-0.041	0.041	0.193	39
3/31/2005	11:17:26	48	9.972	-0.039	0.039	0.184	42
3/31/2005	11:17:29	51	9.972	-0.039	0.039	0.184	45
3/31/2005	11:17:32	54	9.974	-0.037	0.037	0.175	48
3/31/2005	11:17:35	57	9.974	-0.037	0.037	0.175	51
3/31/2005	11:17:38	60	9.974	-0.037	0.037	0.175	54
3/31/2005	11:17:41	63	9.974	-0.037	0.037	0.175	57
3/31/2005	11:17:44	66	9.977	-0.034	0.034	0.160	60
3/31/2005	11:17:47	69	9.977	-0.034	0.034	0.160	63
3/31/2005	11:17:50	72	9.977	-0.034	0.034	0.160	66
3/31/2005	11:17:53	75	9.979	-0.032	0.032	0.151	69
3/31/2005	11:17:56	78	9.979	-0.032	0.032	0.151	72
3/31/2005	11:17:59	81	9.979	-0.032	0.032	0.151	75
3/31/2005	11:18:02	84	9.981	-0.03	0.03	0.142	78
3/31/2005	11:18:05	87	9.979	-0.032	0.032	0.151	81
3/31/2005	11:18:08	90	9.981	-0.03	0.03	0.142	84
3/31/2005	11:18:11	93	9.981	-0.03	0.03	0.142	87
3/31/2005	11:18:14	96	9.981	-0.03	0.03	0.142	90
3/31/2005	11:18:17	99	9.983	-0.028	0.028	0.132	93
3/31/2005	11:18:20	102	9.983	-0.028	0.028	0.132	96
3/31/2005	11:18:23	105	9.986	-0.025	0.025	0.118	99
3/31/2005	11:18:26	108	9.986	-0.025	0.025	0.118	102
3/31/2005	11:18:29	111	9.986	-0.025	0.025	0.118	105
3/31/2005	11:18:32	114	9.986	-0.025	0.025	0.118	108
3/31/2005	11:18:35	117	9.988	-0.023	0.023	0.108	111
3/31/2005	11:18:38	120	9.986	-0.025	0.025	0.118	114
3/31/2005	11:18:41	123	9.986	-0.025	0.025	0.118	117
3/31/2005	11:18:44	126	9.988	-0.023	0.023	0.108	120
3/31/2005	11:18:47	129	9.988	-0.023	0.023	0.108	123
3/31/2005	11:18:50	132	9.988	-0.023	0.023	0.108	126
3/31/2005	11:18:53	135	9.988	-0.023	0.023	0.108	129
3/31/2005	11:18:56	138	9.988	-0.023	0.023	0.108	132
3/31/2005	11:18:59	141	9.988	-0.023	0.023	0.108	135
3/31/2005	11:19:02	144	9.99	-0.021	0.021	0.099	138
3/31/2005	11:19:05	147	9.988	-0.023	0.023	0.108	141
3/31/2005	11:19:08	150	9.99	-0.021	0.021	0.099	144
3/31/2005	11:19:11	153	9.99	-0.021	0.021	0.099	147
3/31/2005	11:19:14	156	9.992	-0.019	0.019	0.090	150

Conductivity Calculations

	To=	1.1E+03	
	b=	15	
	r_c=	5.27E-01	
	rw=	3.33E-01	
rw*=	rw(Kz/Kr)^0.5=	3.33E-01	
	A=	2.91E+00	
	B=	4.64E-01	
	ln(Re/rw*)=	2.45E+00	
	Kr=	2.04E-05	ft/s
	Kr=	1.76E+00	ft/day
	n=	2.29E-01	
	Velocity=	4.31E+00	ft/day

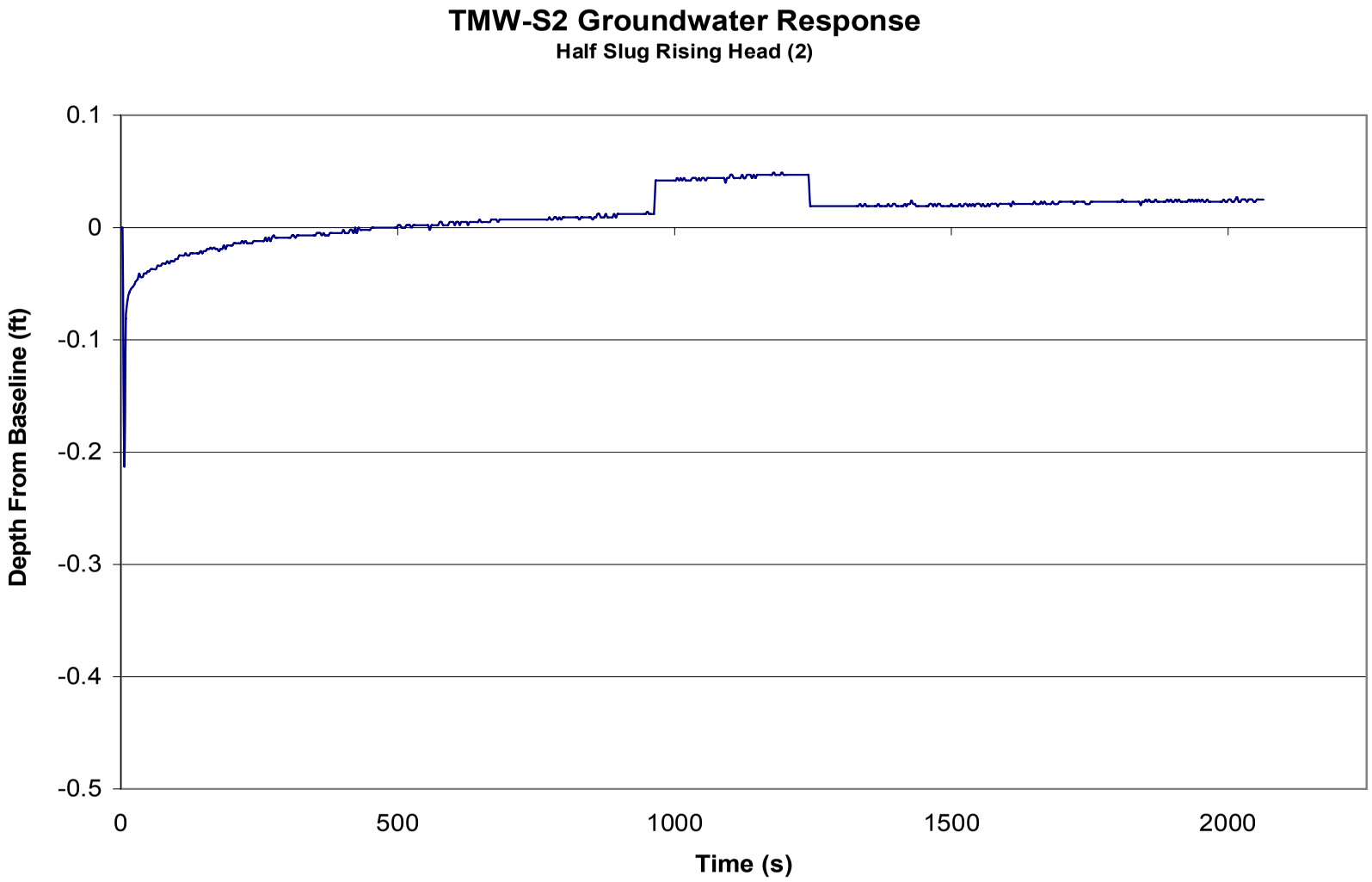
TMW-S2 Groundwater Response
Half Slug Rising Head (2)
Depth From Baseline (ft)
0.1
0
-0.1
-0.2
-0.3
-0.4
-0.5
0
500
1000
1500
2000
Time (s)

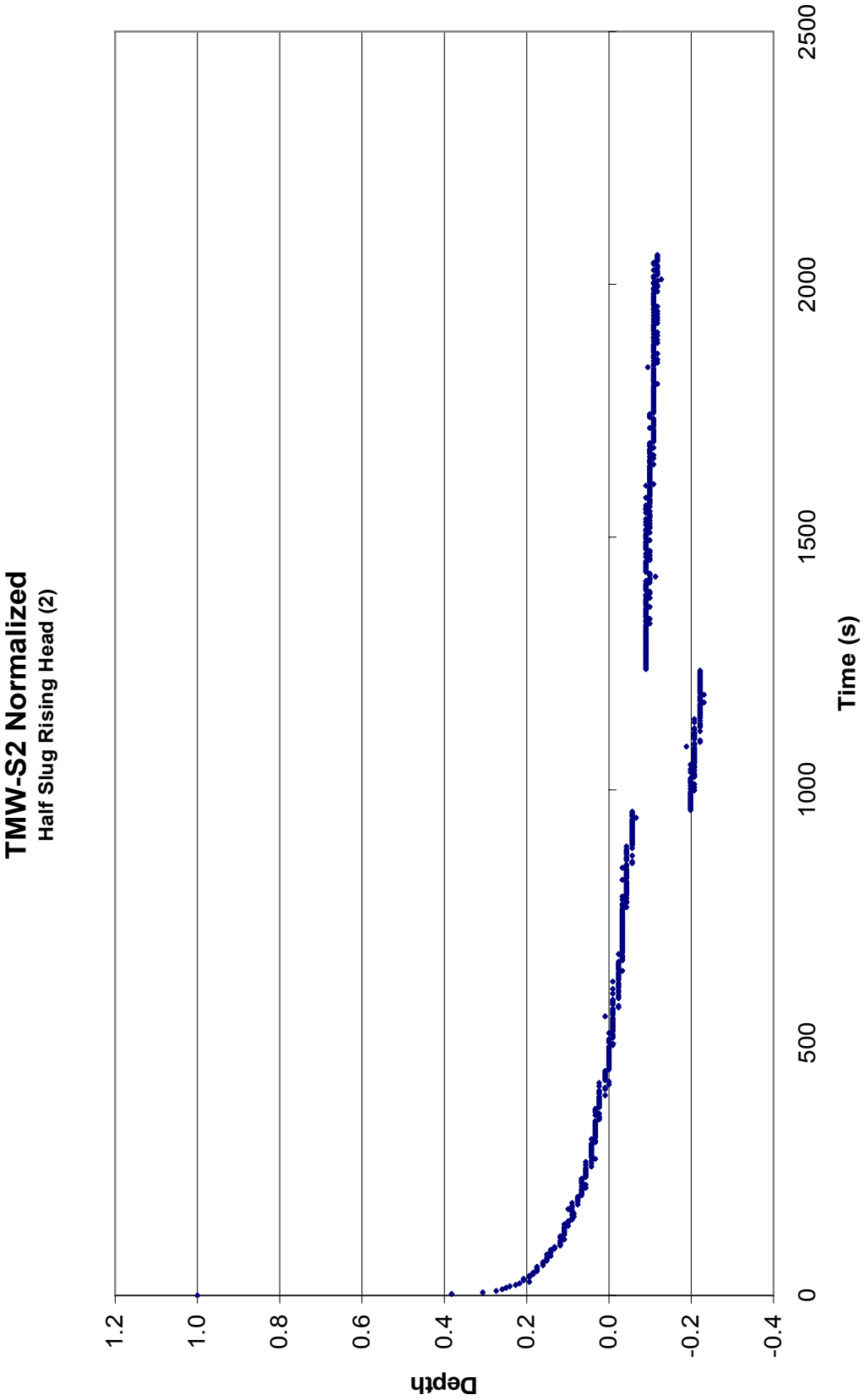
TMW-S2 Normalized
Half Slug Rising Head (2)
Depth
Time (s)
1.2
1.0
0.8
0.6
0.4
0.2
0.0
-0.2
-0.4
0
500
1000
1500
2000
2500

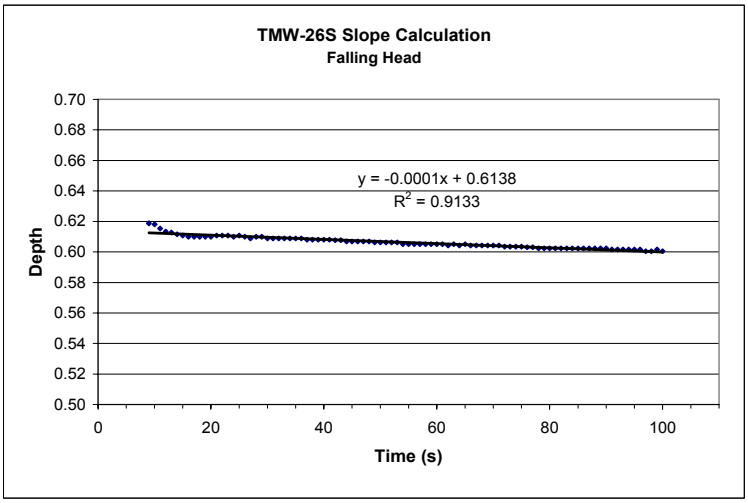

Date	Time	ET (sec)	Chan[2] Pressure Feet H2O	Ho-H(t)	Normalized (H(t)/Ho)	Adjusted t
4/13/2005	7:56:40	30	8.57	0		
4/13/2005	7:56:41	31	8.57	0		
4/13/2005	7:56:42	32	8.568	0		
4/13/2005	7:56:43	33	8.573	0		
4/13/2005	7:56:44	34	8.587	0		
4/13/2005	7:56:45	35	11.119	2.549	0.974	0
4/13/2005	7:56:46	36	11.188	2.618	1.000	1
4/13/2005	7:56:47	37	9.966	1.396	0.533	2
4/13/2005	7:56:48	38	10.278	1.708	0.652	3
4/13/2005	7:56:49	39	10.153	1.583	0.605	4
4/13/2005	7:56:50	40	10.216	1.646	0.629	5
4/13/2005	7:56:51	41	10.172	1.602	0.612	6
4/13/2005	7:56:52	42	10.197	1.627	0.621	7
4/13/2005	7:56:53	43	10.195	1.625	0.621	8
4/13/2005	7:56:54	44	10.19	1.62	0.619	9
4/13/2005	7:56:55	45	10.188	1.618	0.618	10
4/13/2005	7:56:56	46	10.181	1.611	0.615	11
4/13/2005	7:56:57	47	10.176	1.606	0.613	12
4/13/2005	7:56:58	48	10.174	1.604	0.613	13
4/13/2005	7:56:59	49	10.171	1.601	0.612	14
4/13/2005	7:57:00	50	10.169	1.599	0.611	15
4/13/2005	7:57:01	51	10.167	1.597	0.610	16
4/13/2005	7:57:02	52	10.167	1.597	0.610	17
4/13/2005	7:57:03	53	10.167	1.597	0.610	18
4/13/2005	7:57:04	54	10.167	1.597	0.610	19
4/13/2005	7:57:05	55	10.167	1.597	0.610	20
4/13/2005	7:57:06	56	10.169	1.599	0.611	21
4/13/2005	7:57:07	57	10.169	1.599	0.611	22
4/13/2005	7:57:08	58	10.169	1.599	0.611	23
4/13/2005	7:57:09	59	10.167	1.597	0.610	24
4/13/2005	7:57:10	60	10.169	1.599	0.611	25
4/13/2005	7:57:11	61	10.167	1.597	0.610	26
4/13/2005	7:57:12	62	10.164	1.594	0.609	27
4/13/2005	7:57:13	63	10.167	1.597	0.610	28
4/13/2005	7:57:14	64	10.167	1.597	0.610	29
4/13/2005	7:57:15	65	10.164	1.594	0.609	30
4/13/2005	7:57:16	66	10.164	1.594	0.609	31
4/13/2005	7:57:17	67	10.164	1.594	0.609	32
4/13/2005	7:57:18	68	10.164	1.594	0.609	33
4/13/2005	7:57:19	69	10.164	1.594	0.609	34
4/13/2005	7:57:20	70	10.164	1.594	0.609	35
4/13/2005	7:57:21	71	10.164	1.594	0.609	36
4/13/2005	7:57:22	72	10.162	1.592	0.608	37
4/13/2005	7:57:23	73	10.162	1.592	0.608	38
4/13/2005	7:57:24	74	10.162	1.592	0.608	39
4/13/2005	7:57:25	75	10.162	1.592	0.608	40
4/13/2005	7:57:26	76	10.162	1.592	0.608	41
4/13/2005	7:57:27	77	10.161	1.591	0.608	42
4/13/2005	7:57:28	78	10.161	1.591	0.608	43
4/13/2005	7:57:29	79	10.159	1.589	0.607	44
4/13/2005	7:57:30	80	10.159	1.589	0.607	45
4/13/2005	7:57:31	81	10.159	1.589	0.607	46
4/13/2005	7:57:32	82	10.159	1.589	0.607	47
4/13/2005	7:57:33	83	10.159	1.589	0.607	48
4/13/2005	7:57:34	84	10.157	1.587	0.606	49
4/13/2005	7:57:35	85	10.157	1.587	0.606	50

Conductivity Calculations

	To=	10000	
	b=	2.5	
	r_c=	1.19E-01	
	rw=	3.33E-01	
rw*=	rw(Kz/Kr)^0.5=	3.33E-01	
	A=	1.73E+00	
	B=	2.76E-01	
	ln(Re/rw*)=	1.33E+00	
	Kr=	3.75E-07	ft/s
	Kr=	3.24E-02	ft/day
	n=	2.29E-01	
	Velocity=	7.92E-02	ft/day

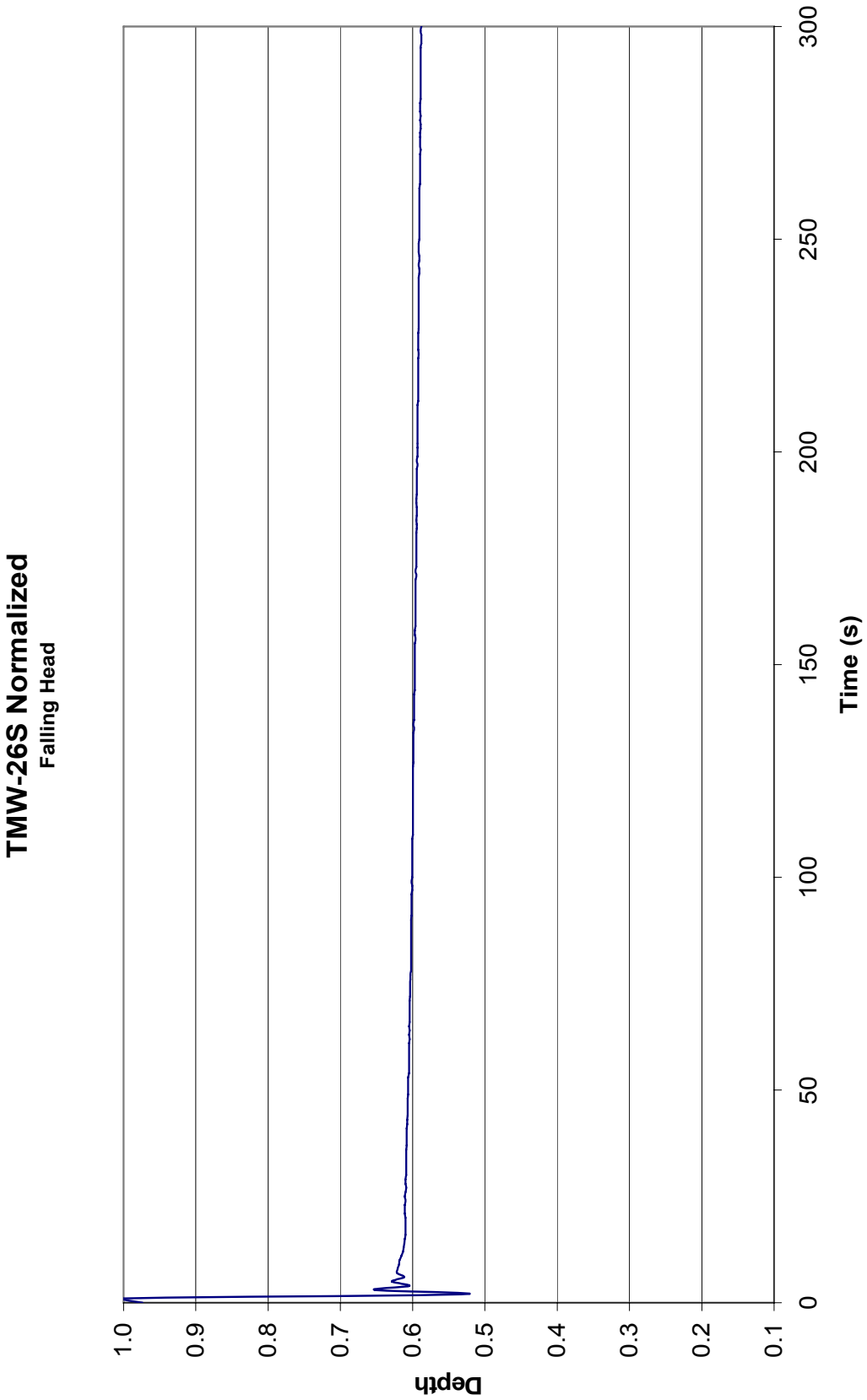
TMW-26S Normalized
Falling Head
Depth
Time (s)
1.0
0.9
0.8
0.7
0.6
0.5
0.4
0.3
0.2
0.1
0
50
100
150
200
250
300

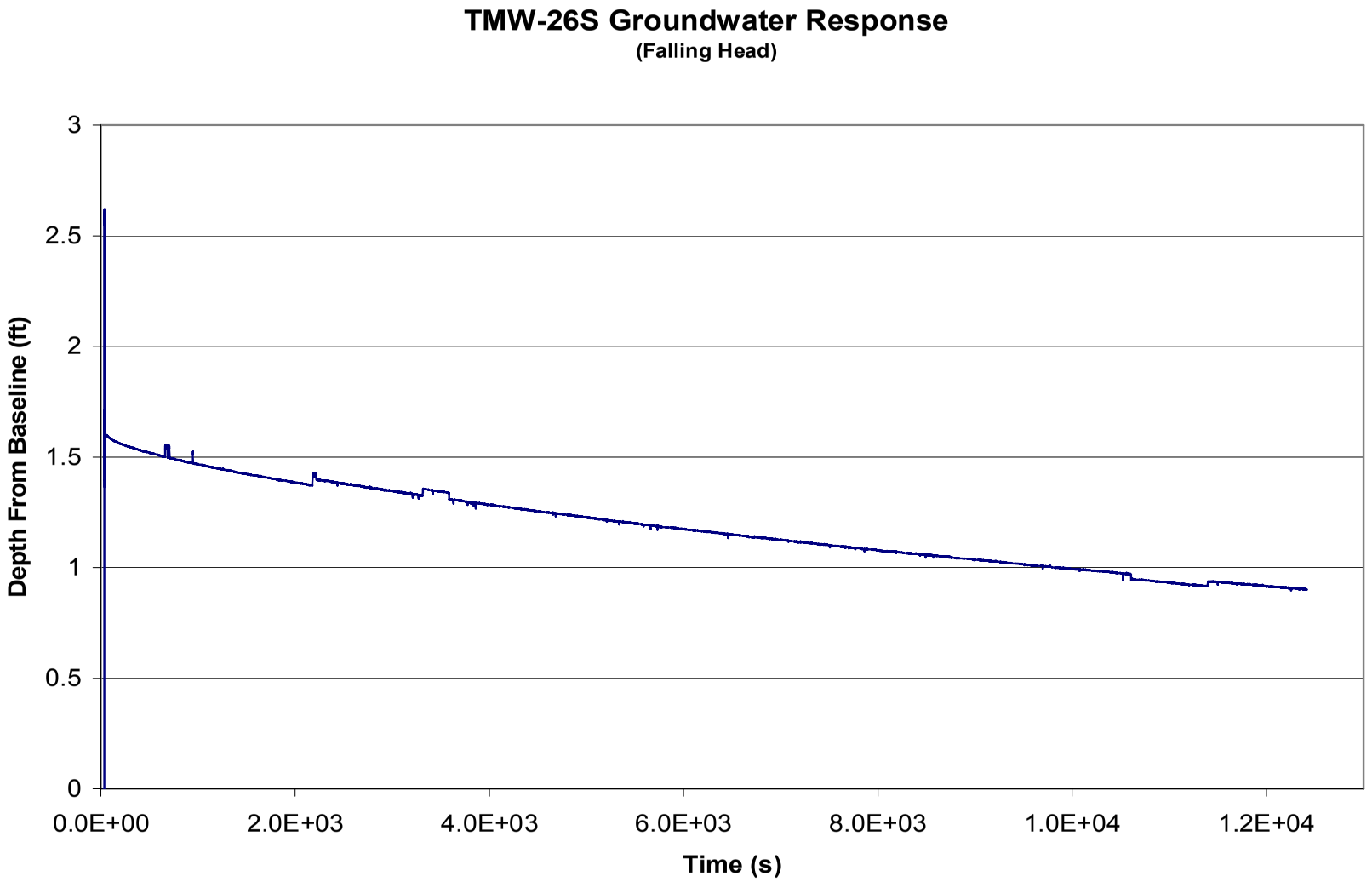
TMW-26S Groundwater Response
(Falling Head)
Depth From Baseline (ft)
3
2.5
2
1.5
1
0.5
0
0.0E+00
2.0E+03
4.0E+03
6.0E+03
8.0E+03
1.0E+04
1.2E+04
Time (s)

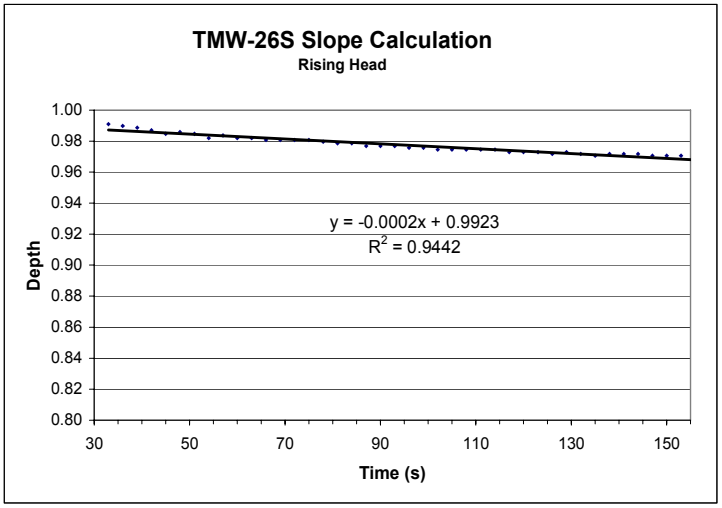

Date	Time	ET (sec)	Chan[2] Pressure Feet H2O	Ho-H(t)	Normalized (H(t)/Ho)	Adjusted t
4/13/2005	11:23:28	0	9.47	0		
4/13/2005	11:23:31	3	9.467	-0.003		
4/13/2005	11:23:34	6	9.467	-0.003	0	
4/13/2005	11:23:37	9	9.359	-0.111	0	
4/13/2005	11:23:40	12	7.808	-1.662	1.659	0.937 0
4/13/2005	11:23:43	15	7.745	-1.725	1.722	0.973 3
4/13/2005	11:23:46	18	7.711	-1.759	1.756	0.992 6
4/13/2005	11:23:49	21	7.697	-1.773	1.77	1.000 9
4/13/2005	11:23:52	24	7.697	-1.773	1.77	1.000 12
4/13/2005	11:23:55	27	7.697	-1.773	1.77	1.000 15
4/13/2005	11:23:58	30	7.699	-1.771	1.768	0.999 18
4/13/2005	11:24:01	33	7.704	-1.766	1.763	0.996 21
4/13/2005	11:24:04	36	7.706	-1.764	1.761	0.995 24
4/13/2005	11:24:07	39	7.71	-1.76	1.757	0.993 27
4/13/2005	11:24:10	42	7.71	-1.76	1.757	0.993 30
4/13/2005	11:24:13	45	7.713	-1.757	1.754	0.991 33
4/13/2005	11:24:16	48	7.715	-1.755	1.752	0.990 36
4/13/2005	11:24:19	51	7.717	-1.753	1.75	0.989 39
4/13/2005	11:24:22	54	7.72	-1.75	1.747	0.987 42
4/13/2005	11:24:25	57	7.724	-1.746	1.743	0.985 45
4/13/2005	11:24:28	60	7.722	-1.748	1.745	0.986 48
4/13/2005	11:24:31	63	7.724	-1.746	1.743	0.985 51
4/13/2005	11:24:34	66	7.729	-1.741	1.738	0.982 54
4/13/2005	11:24:37	69	7.726	-1.744	1.741	0.984 57
4/13/2005	11:24:40	72	7.729	-1.741	1.738	0.982 60
4/13/2005	11:24:43	75	7.729	-1.741	1.738	0.982 63
4/13/2005	11:24:46	78	7.731	-1.739	1.736	0.981 66
4/13/2005	11:24:49	81	7.731	-1.739	1.736	0.981 69
4/13/2005	11:24:52	84	7.731	-1.739	1.736	0.981 72
4/13/2005	11:24:55	87	7.731	-1.739	1.736	0.981 75
4/13/2005	11:24:58	90	7.733	-1.737	1.734	0.980 78
4/13/2005	11:25:01	93	7.735	-1.735	1.732	0.979 81
4/13/2005	11:25:04	96	7.735	-1.735	1.732	0.979 84
4/13/2005	11:25:07	99	7.738	-1.732	1.729	0.977 87
4/13/2005	11:25:10	102	7.738	-1.732	1.729	0.977 90
4/13/2005	11:25:13	105	7.738	-1.732	1.729	0.977 93
4/13/2005	11:25:16	108	7.74	-1.73	1.727	0.976 96
4/13/2005	11:25:19	111	7.74	-1.73	1.727	0.976 99
4/13/2005	11:25:22	114	7.742	-1.728	1.725	0.975 102
4/13/2005	11:25:25	117	7.742	-1.728	1.725	0.975 105
4/13/2005	11:25:28	120	7.742	-1.728	1.725	0.975 108
4/13/2005	11:25:31	123	7.742	-1.728	1.725	0.975 111
4/13/2005	11:25:34	126	7.742	-1.728	1.725	0.975 114
4/13/2005	11:25:37	129	7.745	-1.725	1.722	0.973 117
4/13/2005	11:25:40	132	7.745	-1.725	1.722	0.973 120
4/13/2005	11:25:43	135	7.745	-1.725	1.722	0.973 123
4/13/2005	11:25:46	138	7.747	-1.723	1.72	0.972 126
4/13/2005	11:25:49	141	7.745	-1.725	1.722	0.973 129
4/13/2005	11:25:52	144	7.747	-1.723	1.72	0.972 132
4/13/2005	11:25:55	147	7.749	-1.721	1.718	0.971 135
4/13/2005	11:25:58	150	7.747	-1.723	1.72	0.972 138
4/13/2005	11:26:01	153	7.747	-1.723	1.72	0.972 141
4/13/2005	11:26:04	156	7.747	-1.723	1.72	0.972 144
4/13/2005	11:26:07	159	7.749	-1.721	1.718	0.971 147
4/13/2005	11:26:10	162	7.749	-1.721	1.718	0.971 150

Conductivity Calculations

	To=	5000	
	b=	2.5	
	r_c=	0.114	
	rw=	0.333	
rw*=	rw(Kz/Kr)^0.5=	0.333	
	A=	1.733	
	B=	0.276	
	ln(Re/rw*)=	1.326	
	Kr=	6.89E-07	ft/s
	Kr=	5.96E-02	ft/day
	n=	0.229	
	Velocity=	1.46E-01	ft/day

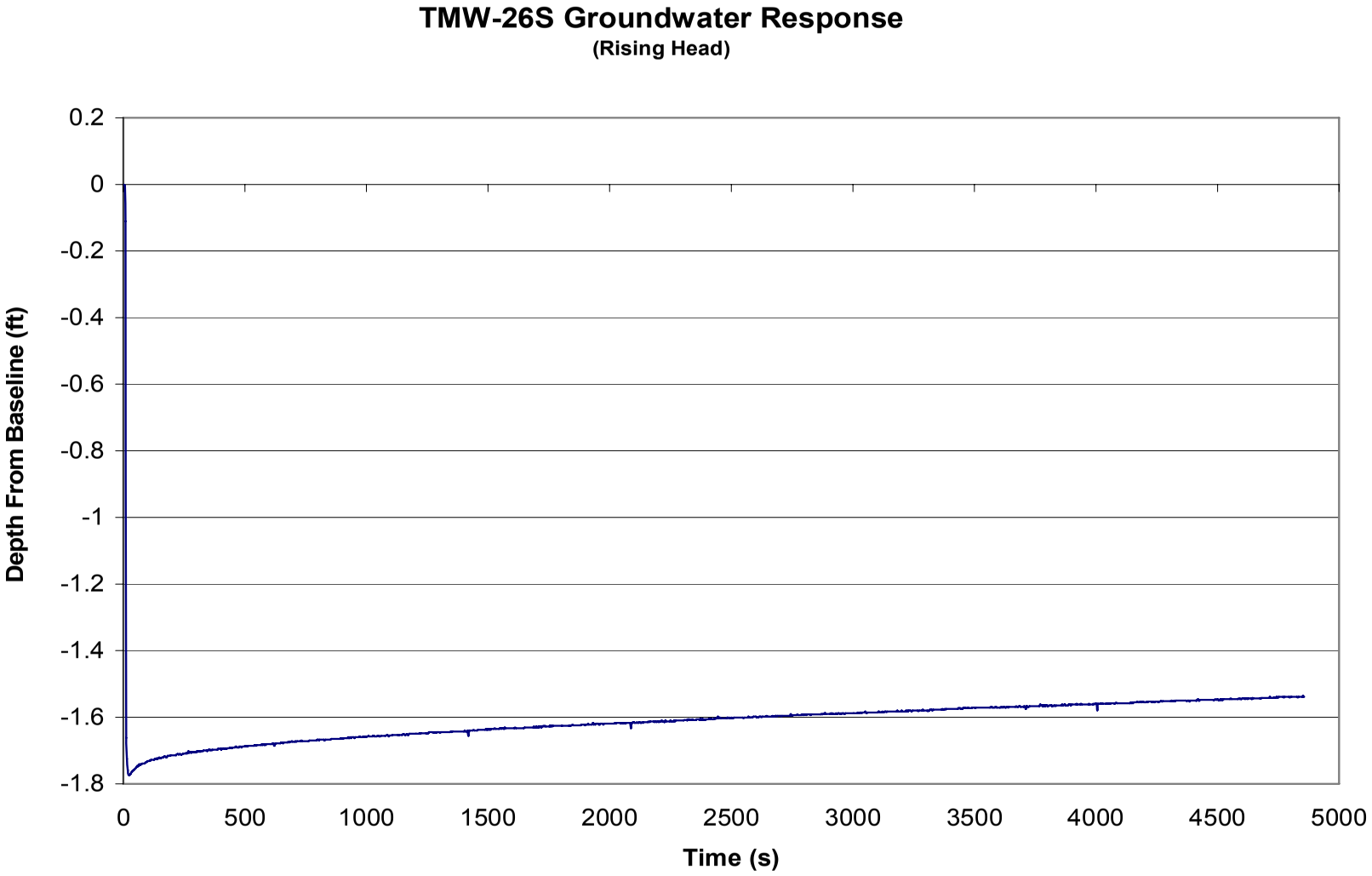
TMW-26S Groundwater Response
(Rising Head)
Depth From Baseline (ft)
0.2
0
-0.2
-0.4
-0.6
-0.8
-1
-1.2
-1.4
-1.6
-1.8
0
500
1000
1500
2000
2500
3000
3500
4000
4500
5000
Time (s)

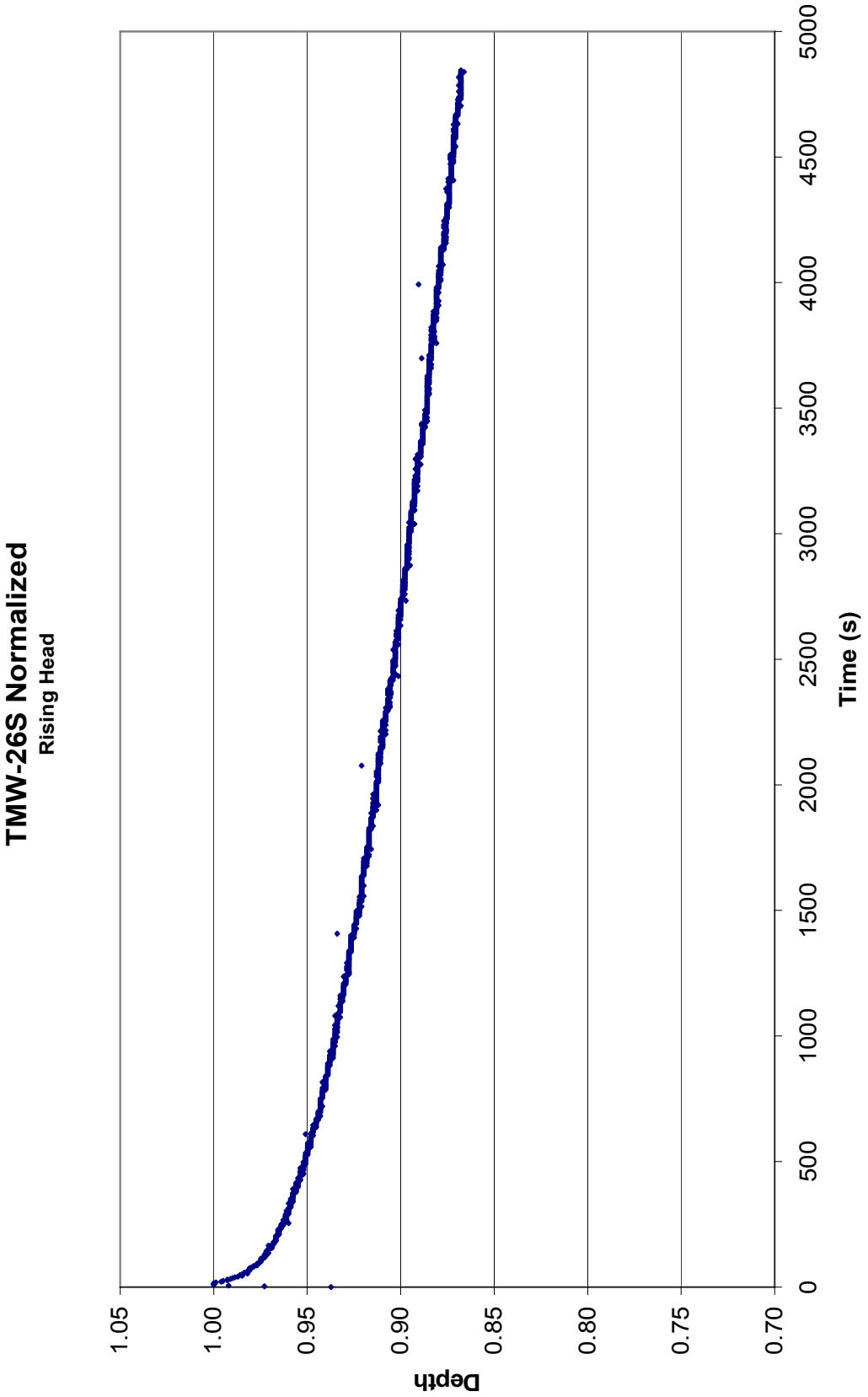
TMW-26S Normalized
Rising Head
Depth
Time (s)
1.05
1.00
0.95
0.90
0.85
0.80
0.75
0.70
0
500
1000
1500
2000
2500
3000
3500
4000
4500
5000

Appendix J: Calibration Data

Figure 1

cDCE calibration experimental data for GC with an ECD (14°C)

ρ_{water} (25°C) = 9.97E-01 g/ml Stock Conc= 7.18E-04 mg/µl

Bottle vol= 26.2 ml Hc= 0.15

Sample #	Dry Wt. (g)	Wet Wt. (g)	Wet - Dry wt. (ml)	Vol Water (ml)	Vol Gas (ml)	Wt. w/ DCE stock (g)	Total Stock added (mg)	Vol Stock (µl)	Total Mass as cDCE (mg)	Conc. (µg/L)	M_{Tgas} (µg)	Cg (µg/ml)	Cw (µg/ml)	Peak Area
1	30.41	43.32	12.91	12.95	13.25	43.32	0.70	0.88	6.35E-04	49.03	0.08	6.38E-03	4.25E-02	408.2467
2	30.67	43.67	13.00	13.03	13.17	43.67	1.40	1.77	1.27E-03	97.40	0.17	1.27E-02	8.46E-02	537.0433
3	30.18	43.07	12.90	12.93	13.27	43.08	2.50	3.16	2.27E-03	175.31	0.30	2.28E-02	1.52E-01	834.7433
4	30.90	43.83	12.92	12.96	13.24	43.83	6.40	8.08	5.80E-03	447.87	0.77	5.83E-02	3.88E-01	1561.527
5	30.45	43.44	12.98	13.02	13.18	43.45	16.10	20.33	1.46E-02	1121.31	1.92	1.46E-01	9.73E-01	3903.977
6	30.75	43.60	12.85	12.88	13.32	43.62	21.00	26.52	1.90E-02	1477.90	2.56	1.92E-01	1.28E+00	5087.287
7	30.65	43.43	12.78	12.81	13.39	43.46	29.10	36.75	0.03	2059.85	3.58	2.67E-01	1.78E+00	6829.357
8	29.98	42.96	12.98	13.02	13.18	43.00	34.50	43.57	0.03	2403.40	4.13	3.13E-01	2.09E+00	8264.267

Appendix J: Calibration Data

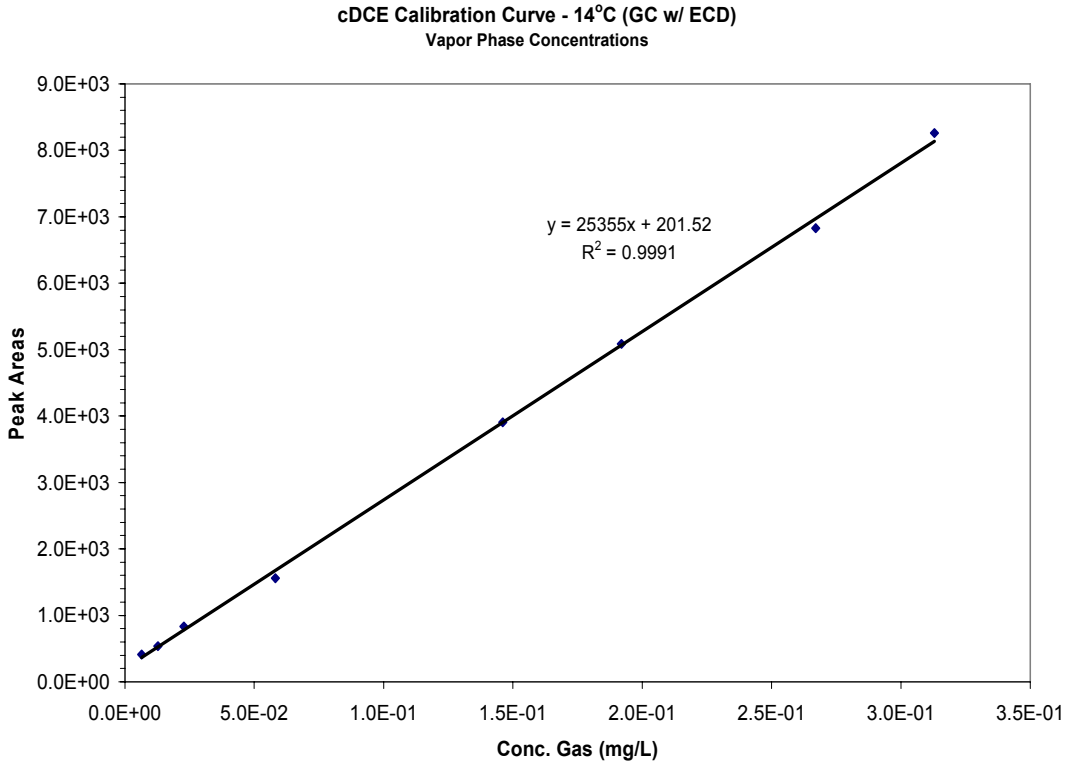

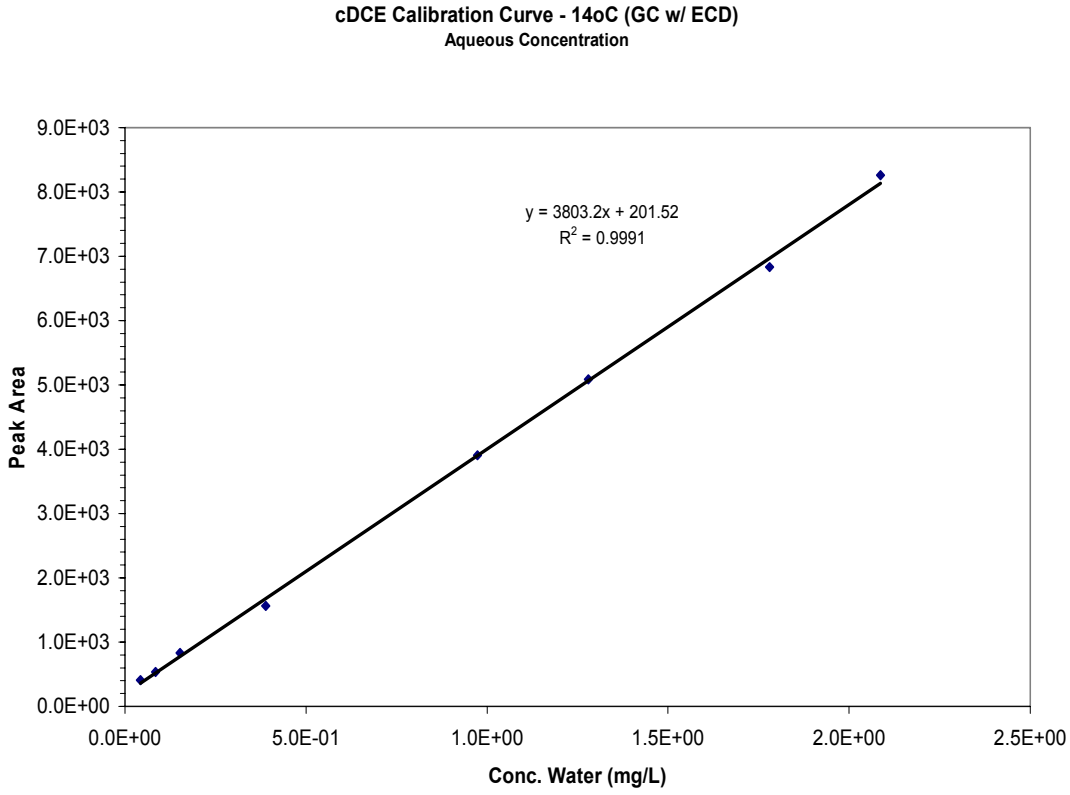

Appendix J: Calibration Data

Figure 2

cDCE Calibration Data and Calculations

30°C on GC With ECD

ρ_{water} (25°C) = 9.97E-01 g/ml Stock Conc= 7.18E-04 mg/µl

Bottle vol= 26.2 ml H'= 0.191

Sample #	Dry Wt. (g)	Wet Wt. (g)	Diff (ml)	Vol Water (ml)	Vol Gas (ml)	Wt. w/ DCE stock (g)	Total Stock added (mg)	Vol Stock (µl)	Total Mass DCE (mg)	Conc (µg/L)	Mg (µg)	Cg (mg/L)	Cw (mg/L)	Area
1	30.68	43.66	12.98	13.02	13.18	43.67	0.90	1.14	8.16E-04	62.69	0.13	1.00E-02	5.25E-02	1099.9
2	30.72	43.59	12.87	12.91	13.29	43.59	3.20	4.04	2.90E-03	224.81	0.48	3.59E-02	1.88E-01	2300.967
3	29.96	42.93	12.97	13.00	13.20	42.93	7.30	9.22	6.62E-03	509.17	1.08	8.15E-02	4.26E-01	5176.7
4	30.58	43.31	12.73	12.77	13.43	43.33	15.90	20.08	1.44E-02	1129.27	2.41	1.80E-01	9.40E-01	10444
5	30.72	43.71	13.00	13.03	13.17	43.74	20.80	26.27	1.89E-02	1447.34	3.05	2.32E-01	1.21E+00	13281.5

Appendix J: Calibration Data

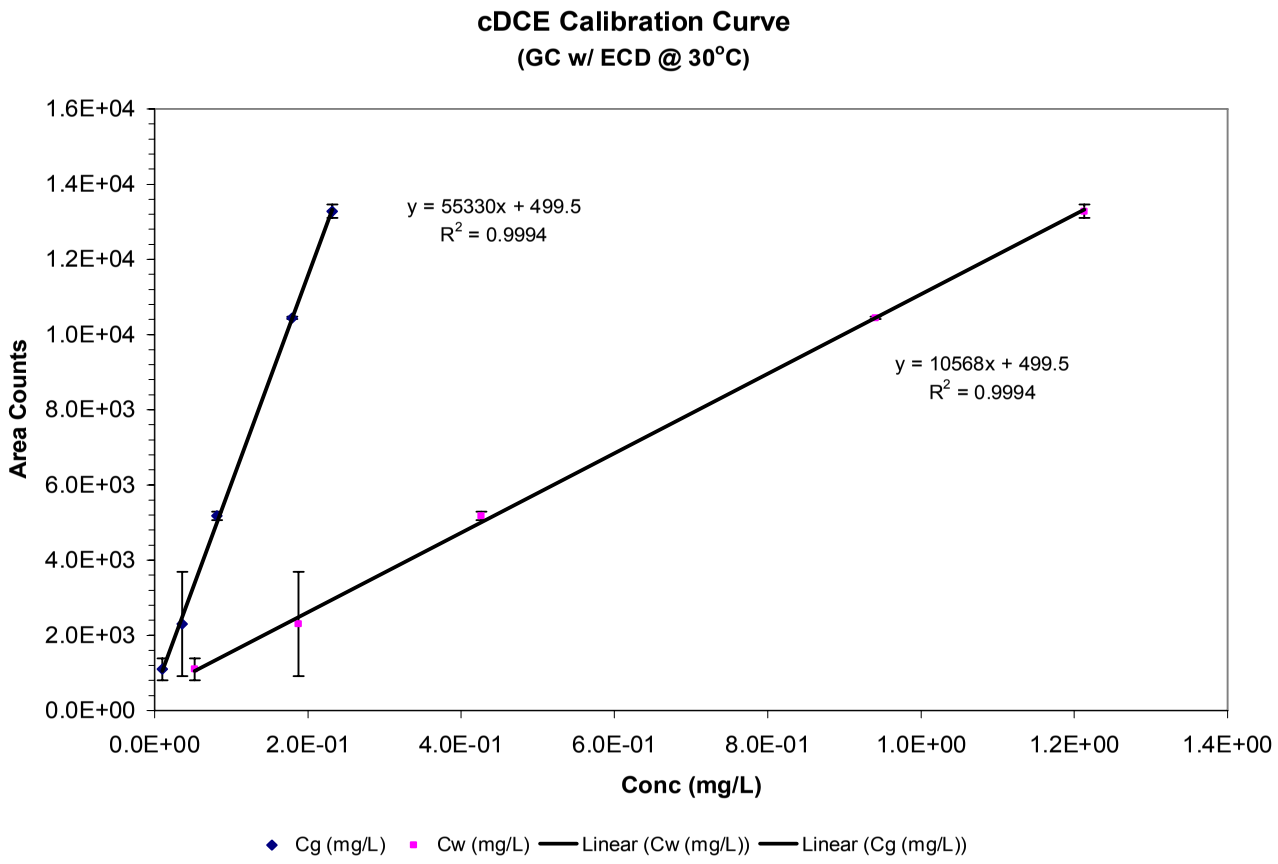

Appendix J: Calibration Data

Figure 3

cDCE Calibration Data and Calculations

30°C on GC With FID

ρ_{water} (25°C) = 9.97E-01 g/ml Stock Conc= 7.18E-04 mg/µl

Bottle vol= 26.2 ml Hc= 0.191

Sample #	Dry Wt. (g)	Wet Wt. (g)	Diff (ml)	Vol Water (ml)	Vol Gas (ml)	Wt. w/ DCE stock (g)	Total Stock added (mg)	Vol Stock (µl)	Total Mass DCE (mg)	Conc (µg/L)	Mg (µg)	Cg (mg/L)	Cw (mg/L)	Area
1	30.68	43.66	12.98	13.02	13.18	43.67	0.90	1.14	8.16E-04	62.69	0.13	1.00E-02	5.25E-02	3973.60
2	30.72	43.59	12.87	12.91	13.29	43.59	3.20	4.04	2.90E-03	224.81	0.48	3.59E-02	1.88E-01	14926.20
3	29.96	42.93	12.97	13.00	13.20	42.93	7.30	9.22	6.62E-03	509.17	1.08	8.15E-02	4.26E-01	32272.30
4	30.58	43.31	12.73	12.77	13.43	43.33	15.90	20.08	1.44E-02	1129.27	2.41	1.80E-01	9.40E-01	74227.60
5	30.72	43.71	13.00	13.03	13.17	43.74	20.80	26.27	1.89E-02	1447.34	3.05	2.32E-01	1.21E+00	96661.27

Appendix J: Calibration Data

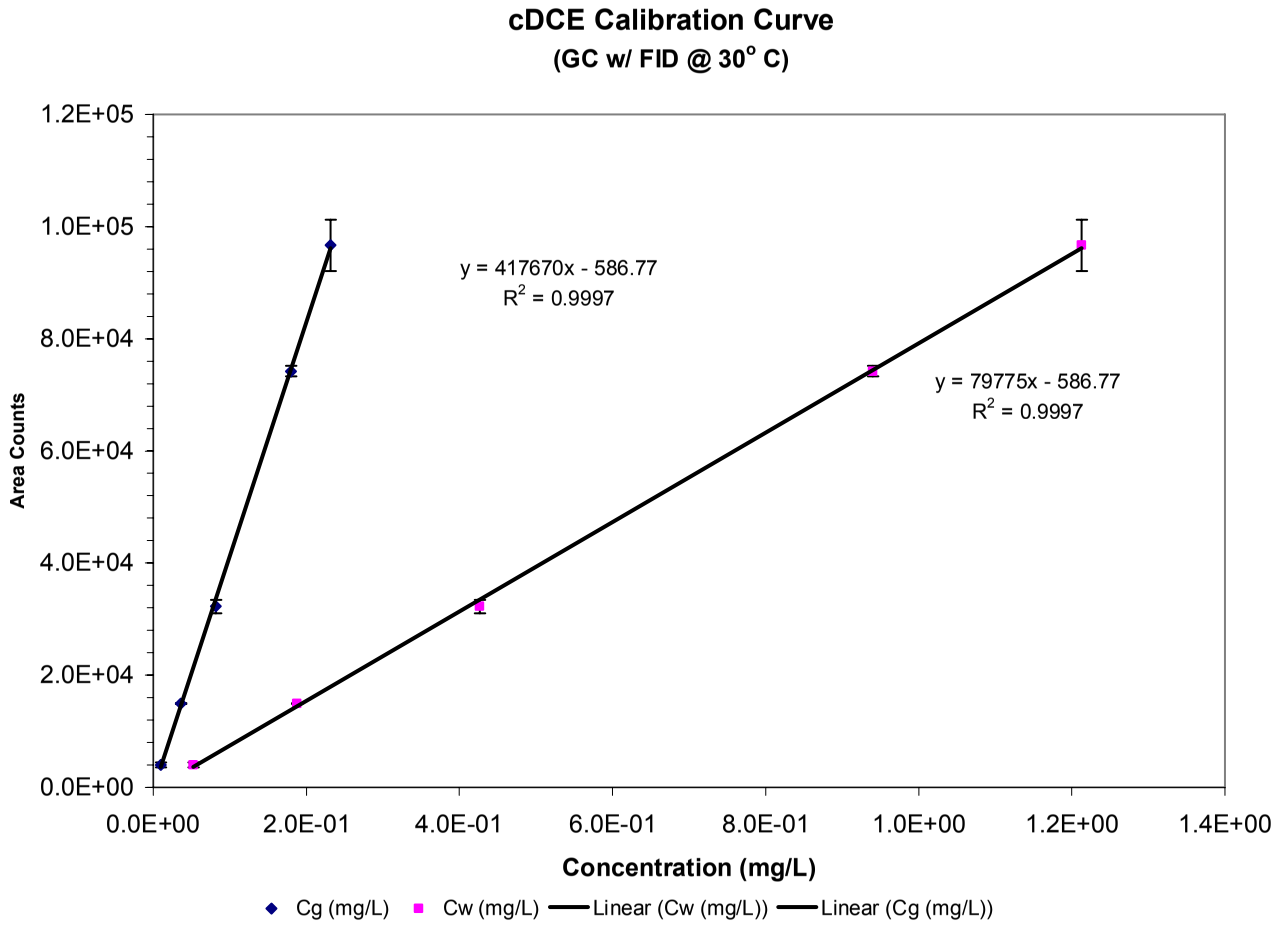

Appendix J: Calibration Data

Figure 1

cDCE calibration experimental data for GC with an ECD (14°C)

ρ_{water} (25°C) = 9.97E-01 g/ml Stock Conc= 7.18E-04 mg/µl

Bottle vol= 26.2 ml Hc= 0.15

Sample #	Dry Wt. (g)	Wet Wt. (g)	Wet - Dry wt. (ml)	Vol Water (ml)	Vol Gas (ml)	Wt. w/ DCE stock (g)	Total Stock added (mg)	Vol Stock (µl)	Total Mass as cDCE (mg)	Conc. (µg/L)	M_{Tgas} (µg)	Cg (µg/ml)	Cw (µg/ml)	Peak Area
1	30.41	43.32	12.91	12.95	13.25	43.32	0.70	0.88	6.35E-04	49.03	0.08	6.38E-03	4.25E-02	408.2467
2	30.67	43.67	13.00	13.03	13.17	43.67	1.40	1.77	1.27E-03	97.40	0.17	1.27E-02	8.46E-02	537.0433
3	30.18	43.07	12.90	12.93	13.27	43.08	2.50	3.16	2.27E-03	175.31	0.30	2.28E-02	1.52E-01	834.7433
4	30.90	43.83	12.92	12.96	13.24	43.83	6.40	8.08	5.80E-03	447.87	0.77	5.83E-02	3.88E-01	1561.527
5	30.45	43.44	12.98	13.02	13.18	43.45	16.10	20.33	1.46E-02	1121.31	1.92	1.46E-01	9.73E-01	3903.977
6	30.75	43.60	12.85	12.88	13.32	43.62	21.00	26.52	1.90E-02	1477.90	2.56	1.92E-01	1.28E+00	5087.287
7	30.65	43.43	12.78	12.81	13.39	43.46	29.10	36.75	0.03	2059.85	3.58	2.67E-01	1.78E+00	6829.357
8	29.98	42.96	12.98	13.02	13.18	43.00	34.50	43.57	0.03	2403.40	4.13	3.13E-01	2.09E+00	8264.267

Appendix J: Calibration Data

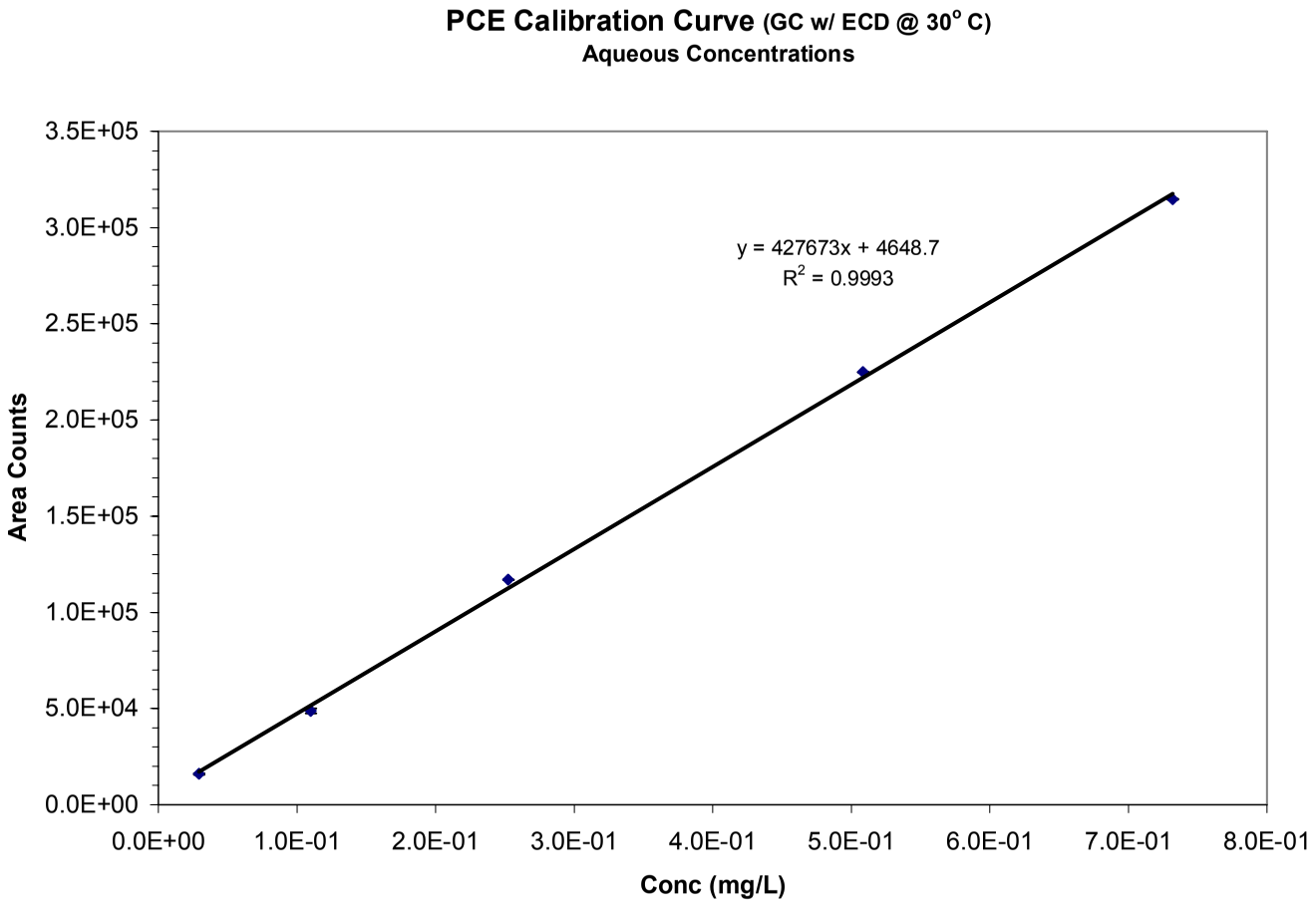

Appendix J: Calibration Data

Figure 5
Methane Calibration Data and Calculations

T = 293 **K** H' (20° C)= 26.93 **PV=nRT**
R = 0.08205 **L-atm/K-mol**
P = 1 atm
V = Volume
n = moles

Gas Phase Methane Mass (umol)	Peak Area
0	**5867.32**
0.05	2.07E+06
0.25	1.24E+07
1.00	5.10E+07
4.00	1.77E+08
10.00	4.91E+08
24.00	1.09E+09

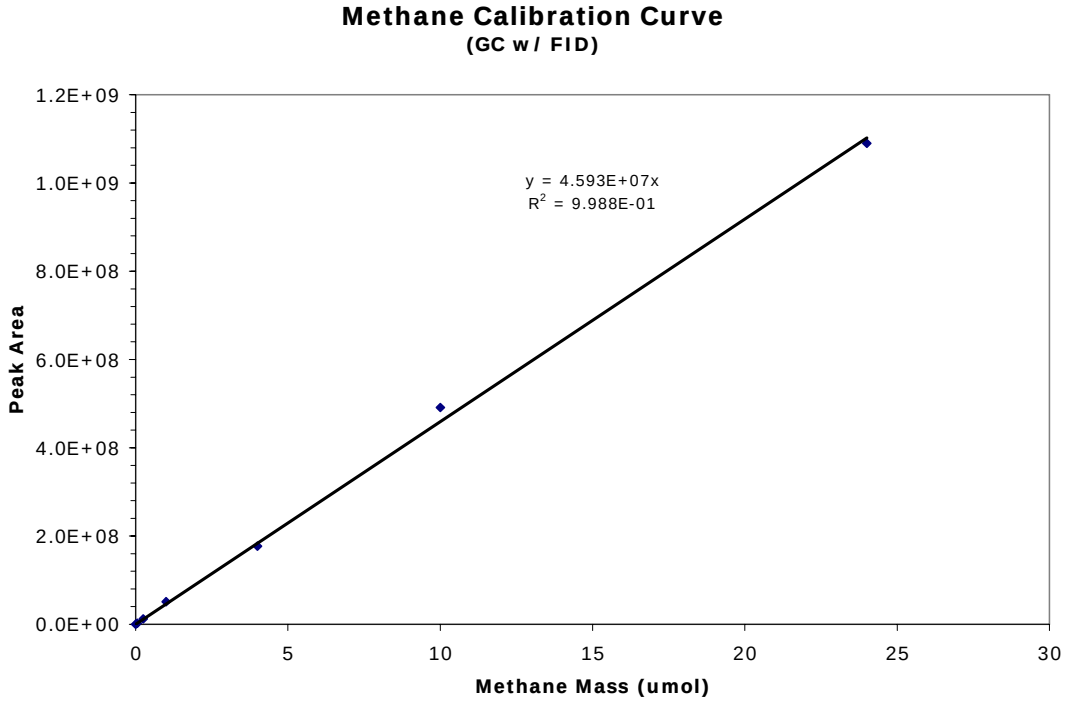

Appendix K: Laboratory and Field Tracer Experimental Data

Laboratory Tracer Results

Including Best Fit Model Esimates (Cmodel)

Orion Electrode Results

Trial

mV	Time	hr	C	Corrected	C/Co
195	0	0.00	0.31	0	0
20	34.3	0.57	148.50	148.19	0.29775
4	52.75	0.88	261.00	260.69	0.523789
-1	60.5	1.01	311.30	310.99	0.624854
-7	67	1.12	384.50	384.19	0.771931
-6	72.5	1.21	371.20	370.89	0.745208
-10	82.1	1.37	427.40	427.09	0.858127
-13	89.5	1.49	475.00	474.69	0.953767
-9	97	1.62	412.60	412.29	0.828391
-10	104	1.73	427.40	427.09	0.858127
-10	109	1.82	427.40	427.09	0.858127
-10	116.5	1.94	427.40	427.09	0.858127
-11	166	2.77	442.70	442.39	0.888869

Test 1

						Cmodel
168	0	0.00	2.35	0	0	0
168	5.75	0.10	2.35	0	0	0
151	14	0.23	4.14	0	0	0
147	20.5	0.34	4.72	0	0	0
148	26.75	0.45	4.57	0	0	0
147	33	0.55	4.72	0	0	0
147	39	0.65	4.72	0	0	0.0147
141	45.75	0.76	5.76	1.039478	0.021611	0.0395
132	52.5	0.88	7.77	3.043032	0.063265	0.0827
124	58.75	0.98	10.12	5.401938	0.112306	0.136
115	64.75	1.08	13.64	8.92241	0.185497	0.1973
108	71	1.18	17.21	12.48709	0.259607	0.2676
101	77.3	1.29	21.71	16.98303	0.353078	0.3431
98	83.25	1.39	23.98	19.25315	0.400273	0.412
92	89.75	1.50	29.25	24.53049	0.509989	0.4879
90	95.5	1.59	31.26	26.53616	0.551687	0.5464
86	102	1.70	35.69	30.96945	0.643855	0.6096
84	108.1	1.80	38.14	33.41658	0.694731	0.6635
81	114.2	1.90	42.13	37.40544	0.77766	0.7111
83	120.5	2.01	39.42	34.70237	0.721463	0.7555
81	126.5	2.11	42.13	37.40544	0.77766	0.7917
81	133	2.22	42.13	37.40544	0.77766	0.826
79	140.75	2.35	45.02	40.29384	0.83771	0.86
79	149.1	2.49	45.02	40.29384	0.83771	0.8898

Cole Parmer Electrode Results

Test 2

mV	Time	hr	C	Corrected	C/Co	Cmodel
184.6	0	0.00	0.50	0.00	0.00	0
184.6	6	0.10	0.50	0.00	0.00	0
180.4	26	0.43	3.16	2.66	0.08	0.0398
162.4	39	0.65	6.97	6.47	0.18	0.1805
152.1	46	0.77	10.95	10.45	0.30	0.2807
146.6	53	0.88	13.94	13.44	0.38	0.3733
142.2	60	1.00	16.91	16.41	0.46	0.4686
139.1	68	1.13	19.37	18.87	0.53	0.5609
136.4	75	1.25	21.81	21.31	0.60	0.6347
133.1	81.5	1.36	25.21	24.71	0.70	0.6929
131.5	88	1.47	27.04	26.54	0.75	0.7427
130.2	95	1.58	28.63	28.13	0.80	0.7849
130.4	102	1.70	28.38	27.88	0.79	0.8235
127.8	109	1.82	31.81	31.31	0.89	0.8553
127.1	117	1.95	32.81	32.31	0.91	0.8835
126.6	143	2.38	33.53	33.03	0.93	0.9433
124.4	165	2.75	36.93	36.43	1.03	0.9695

Test 3

						Cmodel
208.6	0	0.00	0.50	0.00	0.00	0
204.5	13	0.22	0.50	0.00	0.00	0
180.9	20	0.33	0.85	0.35	0.01	0.0115
148.6	28	0.47	3.91	3.41	0.07	0.0634
135	35	0.58	7.43	6.93	0.15	0.1335
127.2	41.5	0.69	10.73	10.23	0.22	0.2186
120.6	46.5	0.78	14.65	14.15	0.31	0.2923
117.1	51.5	0.86	17.28	16.78	0.37	0.3574
113.7	58	0.97	20.28	19.78	0.43	0.4427
111.3	64.5	1.08	22.71	22.21	0.49	0.5208
108.8	69	1.15	25.55	25.05	0.55	0.5661
103.9	86	1.43	32.19	31.69	0.70	0.713
102.5	92.5	1.54	34.39	33.89	0.74	0.7572
103.3	98.5	1.64	33.12	32.62	0.72	0.8213
101.7	104.5	1.74	35.71	35.21	0.77	0.8493
99.1	111	1.85	40.37	39.87	0.88	0.8709
98.6	117	1.95	41.33	40.83	0.90	0.886
98.7	122	2.03	41.14	40.64	0.89	0.9023

Appendix K: Laboratory and Field Tracer Experimental Data

Field tracer study results and initial injection data

Wells sampled with corresponding sample depths in parenthesis

TMW-S3 (25')			*TMW-S3 (30')*			*TMW-26S (29')*			*TMW-26D (47')*		
Time (day)	mV	C	Time (day)	mV	C	Time (day)	mV	C	Time (day)	mV	C
7	>180	0.5	7	>180	0.5	7	169.5	1.02	29	179.6	0.50
11	>181	0.5	11	>181	0.5	11	149.8	1.85			
13	>182	0.5	13	>182	0.5	13	149.3	2.09			
			14	>183	0.5	14	133	4.45			
			17	170.2	0.74	17	158.5	1.27			
			20	168	0.82	20	141.1	2.83			
			23	167.1	0.79	23	93.3	24.60			
			26	160.3	0.65	26	155.3	0.84			
			29	180.1	0.50	29	170.2	0.50			

Inject 2nd round on 6/29/05 (day=0)

NIP-2

Inject 42 ml of 100g/L Br- stock into well to achieve uniform concentration of 400 ppm in 10.5 L water column

Depth	mV	C (ppm)
30	3.5	1425.04
25	46.6	216.48

SIP-2

Inject 29 ml of 100g/L Br- stock into well to achieve uniform concentration of 400 ppm in 7.2 L water column

Depth	mV	C (ppm)
30	24.5	568.94
25	41.4	271.74

References

Aichberger, H., Hasinger, M., Braun, R., Loibner, A.P., 2005. Potential of preliminary test methods to predict biodegradation performance of petroleum hydrocarbons in soil. Biodegradation. 16: 115-125.

Alexander, M., 2000. Aging, bioavailability, and overestimation of risk from environmental pollutants. Environmental Science & Technology. 34(20): 4259-4265.

American Society for Testing Materials, 1991. (Field procedure) for instantaneous change in head (slug tests) for determining hydraulic properties of aquifers. Designation: D 4044-91.

American Society for Testing Materials, 2003. Standard test method for 24-hour batch-type measurement of volatile organic sorption by soils and sediments. Designation: D 5285-03.

Ashworth, R.A., Howe, G.B., Mullins, M.E., Rogers, T.N., 1988. Air water partitioning coefficients of organics in dilute aqueous-solutions. Journal of Hazardous Materials. 18(1): 25-36.

Aulenta, F., Bianchi, A., Majone, M., Papini, M.P., Potalivo, M., Tandoi, V., 2005. Assessment of natural or enhanced in situ bioremediation at a chlorinated solvent-contaminated aquifer in Italy: a microcosm study. Environmental International. 31: 185-190.

Ball, W.P., and Roberts, P.V., 1991. Long-term sorption of halogenated organic-chemicals by aquifer material. 2. Intraparticle diffusion. Environmental Science & Technology. 25(7): 1237-1249.

Battelle Environmental Restoration Division. 2003. Draft Final Corrective Action Plan for Groundwater at the Russell Road Landfill, Marine Corps Base Quantico, Quantico, Virginia. Prepared for Engineering Field Activity Chesapeake Naval Facilities Engineering Command, Washington, D.C.

Baveye, P., and Valocchi, A., 1989. An evaluation of mathematical models of the transport of biologically reacting solutes in saturated soils and aquifers. Water Resources Research, 25(6): 1413-1421.

Bosma, T.N.P., Middeldorp, P.J.M., Schraa, G., Zehnder, A.J.B., 1997. Mass transfer limitations of biotransformation: Quantifying bioavailability. Environmental Science & Technology. 31(1): 248-252.

Bouwer, E.J., 1994. Bioremediation of chlorinated solvents using alternate electron acceptors. In: Handbook of Bioremediation. Lewis Publishers, Inc., Boca Raton, FL.

Bouwer H., Rice, R.C., 1976. A slug test for determining hydraulic conductivity of unconfined aquifers with completely or partially penetrating wells. Water Resources Research. 12(3)423-428.

Bradley, P.M., and Chapelle, F.H., 1998. Effect of contaminant concentration on aerobic microbial mineralization of DCE and VC in stream-bed sediments. Environmental Science & Technology. 32(5): 553-557.

Bradley, P.M., and Chapelle, F.H., 2000. Aerobic microbial mineralization of dichloroethene as sole carbon substrate. Environmental Science & Technology. 34(1): 221-223.

Brockman, F.J., Murray, C.J., 1997. Microbiological heterogeneity in the terrestrial subsurface and approaches for is description. In: P.S. Amy and D.L. Haldeman (Editor*), The Microbiology of the Terrestrial Deep Subsurface*. Lewis Publishers, Boca Raton, FL.

Brusseau, M.L., Hu, M.Q., Wang, J.M., Maier, R.M., 1999. Biodegradation during contaminant transport in porous media. 2. The influence of physicochemical factors. Environmental Science & Technology. 33(1): 96-103.

Bulter, J.J., 1997. *The Design, Performance, and analysis of Slug Tests*. Lewis Publishers, Washington, DC.

Coleman, N.V., Mattes, T.E., Gossett, J.M., Spain, J.C., 2002. Biodegradation of *cis*-dichloroethene as the sole carbon source by a β-proteobacterium. Applied and Environmental Microbiology. 68(6): 2726-2730.

Cookson, J.T., 1995. *Bioremediation Engineering, Design and Application*. McGraw-Hill, Inc., Washington, D.C.

Cupples, A.M., Spormann, A.M., McCarty, P.L., 2003. Growth of a *Dehalococcoides*-like microorganism on vinyl chloride and *cis*-dichloroethene as electron acceptors as determined by competitive PCR. Applied and Environmental Microbiology. 69(2): 953-959.

Davis, C., Cort, T., Dai, D., Illangasekare, T.H., Munakata-Marr, J., 2003. Effects of heterogeneity and experimental scale on the biodegradation of diesel. Biodegradation. 14: 373-384.

Davis, S.N., Thompson, G.M., Bentley, H.W., Stiles, G., 1980. Groundwater tracers – A short review, *Groundwater*, 18 (1): 14-23.

DeWulf, J., van Langenhove, H., 1999. Sediment/water and octanol/water equilibrium partitioning of volatile organic compounds: Temperature dependence in the 2 – 25^{o}C range. Water Research. 33(10): 2424-2436.

DiStefano, T.D., Baral, R., Duran, M., Speece, R.E., 2001. A comparison of complex electron donors for anaerobic dechlorination of PCE. Bioremediation Journal. 5(2): 131-143.

Duhamel, M., Wehr, S.D., Yu, L., Rizvi, H., Seepersad, D., Dworatzek, S., Cox, E.E., Edwards, E.A., 2002. Comparison of anaerobic dechlorinating enrichment cultures maintained on tetrachloroethene, trichloroethene, *cis*-dichloroethene, and vinyl chloride. Water Research. 36: 4193-4202.

Ellis, D.E., Lutz, E.J., Odom, J.M., Buchanan, R.J., Bartlett, C.L., Lee, M.D., Harkness, M.R., Deweerd, K.A., 2000. Bioaugmentation for accelerated in situ anaerobic bioremediation. Environmental Science & Technology. 34(11): 2254-2260.

Ferguson, J.F., Pietari, J.M.H., 2000. Anaerobic transformations and bioremediation of chlorinated solvents. Environmental Pollution. 107(2): 209-215.

Fitts, C.R., 2002. *Groundwater Science*, Academic Press, San Diego, CA.

Freedman, D.L., Danko, A.S., Verce, M.F., 2001. Substrate interactions during aerobic biodegradation of methane, ethene, vinyl chloride and 1,2-dichloroethenes. Water Science and Technology. 43(5): 333-340.

Freedman, D.L., Gossett, J.M., 1989. Biological reductive dechlorination of tetrachloroethylene and trichloroethylene to ethylene under methanogenic conditions. Applied and Environmental Microbiology. 55: 2144-2151.

Freeze, R.A., and Cherry, J.A., 1979. *Groundwater*. Prentice Hall Publishers, Englewood Cliffs, NJ.

Friedman, G.M., Sanders, J.E., Kopaska-Merkel, D.C., 1992. *Principles of Sedimentary Deposits, Stratigraphy and Sedimentology*. Macmillan Publishing Company, New York, NY.

Garbarini, D.R., and Lion, L.W., 1985. Evaluation of sorptive partitioning of nonionic pollutants in closed systems by headspace analysis. Environmental Science & Technology. 19(11): 1122-1128.

Gelhar, L.W., Welty, C., Rehfeldt, K.R., 1992. A critical review of data on field-scale dispersion in aquifers. Water Resources Research. 28(7): 1955-1974.

Ghiorse, W.C., Wilson, J.T., 1988. Microbial ecology of the terrestrial subsurface. Advances in Applied Microbiology. 33: 107-172.

Goltz, M.N., Bouwer, E.J., Huang, J., 2001. Transport issues and bioremediation modeling for the *in situ* aerobic co-metabolism of chlorinated solvents. Biodegradation. 12: 127-140.

Gossett, J.M., 1987. Measurements of Henry's law constants for C_1 and C_2 chlorinated hydrocarbons. Environmental Science & Technology. 21(2): 202-208.

Häggblom, M.M., M.D. Rivera, and L.Y. Young. 1993. Influence of alternative electron acceptors on the anaerobic biodegradability of chlorinated phenols and benzoic acids. Applied and Environmental Microbiology. 59: 1162-1167.

Harkness, M.R., Bracco, A.A., Brennan, M.J., Deweerd, K.A., Spivack, J.L., 1999. Use of bioaugmentation to stimulate complete reductive dechlorination of trichloroethene in Dover soil columns. Environmental Science & Technology. 33(7): 1100-1109.

He, J., Ritalahti, K.M., Koenigsberg, S.S., Löffler, F.E., 2003. Detoxification of vinyl chloride to ethene coupled to growth of an anaerobic bacterium. Nature. 424: 62-65.

Harms, H., Bosma, T.N.P., 1997. Mass transfer limitation of microbial growth and pollutant degradation. Journal of Industrial Microbiology and Biotechnology. 18: 97-105.

Harvey, R.W., Garabedian, S.P., 1991. Use of colloid filtration theory in modeling movement of bacteria through a contaminated sandy aquifer. Environmental Science & Technology. 25(1): 178-185.

Haws, N.W., Ball, W.P., Bouwer, E.J., 2006. Modeling and interpreting bioavailability of organic contaminant mixtures in subsurface environments. Journal of Contaminant Hydrology. 82: 255-292.

Hinchee, R.E, 1995. Bioremediation of Chlorinated Solvents. Hinchee, R.E., and Leeson, A., Semprini, L. (Editors). Battelle Press, Columbus, OH.

Hunkeler, D., Aravena, R., Cox, E., 2002. Carbon isotopes as a tool to evaluate the origin and fate of vinyl chloride: Laboratory experiments and modeling of isotope evaluation. Environmental Science & Technology. 36(15): 3378-3384.

Hvorslev, M.J., 1951. Time lag and soil permeability in ground-water observations. United States Corps of Engineers Waterways Experiments Station Bulletin 36, Vicksburg, MS.

Hyder, Z., Butler, J.J., 1995. Slug tests in unconfined formations: An assessment of the Bouwer and Rice technique. Groundwater. 33(1): 16-22.

Hyder, Z., Butler, J.J., McElwee, C.D., Liu, W., 1994. Slug tests in partially penetrating wells. Water Resources Research. 30(11): 2945-2957.

Johnson, M.A., 2004. A quantitative framework for understanding the complex interactions of competing interfacial processes and in-situ biodegradation. Masters Thesis, The University of Maryland, College Park, MD.

Jones, R.E., Beeman, R.E., Suflita, J.M., 1989. Anaerobic metabolic processes in the deep terrestrial subsurface. Geomicrobiology Journal. 7(1-2): 117-130.

Karapanagioti, H.K., Gossard, C.M., Strevett, K.A., Kolar, R.L., Sabatini, D.A., 2001. Model coupling intraparticle diffusion/sorption, nonlinear sorption, and biodegradation processes. Journal of Contaminant Hydrology. 48: 1-21.

Klier, N.J., West, R.J., Donberg, P.A., 1999. Aerobic biodegradation of dichloroethylenes in surface and subsurface soils. Chemosphere. 38(5): 1175-1188.

Klute, A., 1986. *Methods of Soil Analysis*, 2nd Edition. American Society of Agronomy: Soil Science Society of America, Madison, WI.

Knapp, R.B., Faison, B.D., 1997. A bioengineering system for i*n situ* bioremediation of contaminated groundwater. Journal of Industrial Microbiology and Biotechnology. 18: 189-197.

Korom, S.F., 2000. An Adsorption Isotherm for Bromide, *Water Res. Res.,* 36 (7): 1969-1974.

LeBlanc, D.R., Garabedian, S.P., Hess, K.M., Gelhar, L.W., Quadri, R.D., Stollenwerk, K.G., Wood, W.W., 1991. Large-scale natural gradient tracer test in sand and gravel, Cape Cod, Massachusetts. 1. Experimental design and observed tracer movement. Water Resources Research. 27(5): 895-910.

Lapidus, L., and Amundson, N.R., 1952. The rate determining steps in radial adsorption analysis. Journal of Physical Chemistry. 56(3): 373-383.

Lee, M.D., Odom, J.M., Buchanan, R.J., 1998. New perspectives on microbial dehalogenation of chlorinated solvents: Insights from the field. Annual Review of Microbiology. 52: 423-52.

Lenczewski, M., P. Jardine, L. McKay, and A. Layton. 2003. Natural attenuation of trichloroethylene in fractured shale bedrock. Journal of Contaminant Hydrology. 64: 151-168.

Linsley, R.K., Franzini, J.B., Tchobanoglous, G., Freyberg, D.L., 1992. Water Resources Engineering, 4th Edition. McGraw-Hill, New York, NY.

Lorah, M.M., Olsen, L.D., Smith, B.L., Johnson, M.A., Fleck, W.B., 1997. Natural attenuation of chlorinated volatile organic compounds in a freshwater tidal wetland, Aberdeen Proving Ground, Maryland. Prepared for: U.S. Geological Survey. Water-Resources Investigations Report 97-4171.

Major, D.W., McMaster, M.L., Cox, E.E., Edwards, E.A., Dwaratzek, S.M., Hendrickson, E.R., Starr, M.G., Payne, J., Buonamici, L.W., 2002. Field demonstration of successful bioaugmentation to achieve dechlorination of tetrachloroethene to ethene. Environmental Science & Technology. 36(23): 5106-5116.

Masters, G.M., 1998. *Introduction to Environmental Engineering and Science*, 2nd Edition. Prentice Hall, Upper Saddle River, NJ.

Maymó-Gatell, X., Chien, Y., Gossett, J.M., Zinder, S.H., 1997. Isolation of a bacterium that reductively dechlorinates tetrachloroethene to ethene. Science. 276: 1568-1571.

Maymó-Gatell, X., Nijenhuis, I., Zinder, S.H., 2001. Reductive dechlorination of *cis*-1,2-dichloroethene and vinyl chloride by "*Dehalococcoides ethenogenes*". Environmental Science & Technology. 35(3): 516-521.

McCarty, P.L., Semprini, L., 1993. Engineering and hydrogeological problems associated with i*n situ* treatment. Hydrological Sciences. 38(4): 261-272.

McMahon, P.B., and F.H. Chapelle. 1991. Microbial production of organic acids in aquitard sediments and its role in aquifer geochemistry. Nature (London). 349: 233-235.

Miller, M.E., Alexander, M., 1991. Kinetics of bacterial-degradation of benzylamene in a montmorillonite suspension. Environmental Science & Technology. 25(2): 240-245.

Molz, F.J., and Widdowson, M.A., 1988. Internal inconsistencies in dispersion-dominated models that incorporate chemical and microbial kinetics. Water Resources Research. 22(8): 1207-1216.

Morkin, M., Devlin, J.F., Barker, J.F., Butler, B.J., 2000. In situ sequential treatment of a mixed contaminant plume. Journal of Contaminant Hydrology. 45: 283-603.

Murphy, E.M., T.R. Ginn, A. Chilakapati, C.T. Resch, J.L. Phillips, T.W. Wietsma, and C.M. Spadoni. 1997. The influence of physical heterogeneity on microbial degradation and distribution in porous media. Water Resources Research. 33: 1087-1103.

Murray, W., Dooley, M., Koenigsberg, S., 2001. Enhanced bioremediation of chlorinated solvents. p. 171- 178. Proceedings of the Sixth International In Situ and On-Site Bioremediation Symposium, Sponsored by Battelle. San Diego, CA.

National Research Council. 1993. In Situ Bioremediation: When Does It Work? National Academy Press, Washington, D.C.

North, R.W., Burkett, S.E., Sincock, M.J., 2001. Effective enhancement of biological degradation of tetrachloroethene (PCE) in ground water. p. 163-170. Proceedings of the Sixth International In Situ and On-Site Bioremediation Symposium, Sponsored by Battelle. San Diego, CA.

Odencrantz, J.E., Valocchi, A.J., Rittman, B.E., 1990. Modeling two-dimensional solute transport with different biodegradation kinetics. NWWA/API Petroleum Hydrocarbon Conference; Houston, TX; Oct. 31 – Nov. 2, 1990.

Orndorff, Z.W., Daniels, W.L., 2004, Evaluation of acid-producing sulfidic materials in Virginia highway corridors. Environmental Geology. 46: 209-216.

Oya, S., Valocchi, A.J., 1997. Characterization of traveling waves and analytical estimation of pollutant removal in one-dimensional subsurface bioremediation modeling. Water Resources Research. 33(5): 1117-1127.

Oya, S., and A.J. Valocchi. 1998. Transport and biodegradation of solutes in stratified aquifers under enhanced in situ bioremediation conditions. Water Resources Research. 34:3323-3334.

Parker, J.C., and van Genuchten, 1984. Determining transport parameters from laboratory and field tracer experiments. Virginia Agricultural Experiment Station. Bulletin 84-3.

Puls, R.W., Barcelona, M.J., 1996. Low-flow (minimal drawdown) ground-water sampling procedures. Ground Water Issue. Prepared for: US EPA, Office of Research and Development, Office of Solid Waste and Emergency Response. EPA/540/S-95/504.

Ramaswami, A. and R.G. Luthy. 1997. Measuring and modeling physicochemical limitations to bioavailability and biodegradation. In: C.J. Hurst, et al. (Editors), Manual of Environmental Microbiology. ASM Press: Washington, DC, p. 721-729.

Regenesis Bioremediation Products, Inc., 2003. Final Report Treatability Study, Russell Road Landfill. Prepared by: Applied Power Concepts, Inc., Anaheim, CA.

Regenesis Hydrogen Release Compound (HRC) Brochure, 2006. Prepared by Regenesis, San Clemente California. Available at: www.regenesis.com.

Rittmann, B.E., McCarty, P.L., 2001. *Environmental Biotechnology: Principles and Applications*. McGraw-Hill, Boston, MA.

Seagren, E.A., B.E. Rittmann, and A.J. Valocchi. 1993. Quantitative evaluation of flushing and biodegradation for enhancing in situ dissolution of nonaqueous-phase liquids. Journal of Contaminant Hydrology. 12: 103-132.

Seagren, E.A., B.E. Rittmann, and A.J. Valocchi. 1994. Quantitative evaluation of the enhancement of NAPL-pool dissolution by flushing and biodegradation. Environmental Science and Technology. 28: 833-839.

Semprini, L., Roberts, P.V., Hopkins, G.D., McCarty, P.L., 1990. A field evaluation of in-situ biodegradation of chlorinated ethenes: Part 2, results of biostimulation and biotransformation experiments. Groundwater. 28(5): 715-727.

Shimotori, T., Arnold, W.A, 2002, Henry's law constants of chlorinated ethylenes in aqueous alcohol solutions: Measurement, estimation, and thermodynamic analysis. Journal of Chemical and Engineering Data. 47(2): 183-190.

Smith, R.L., Garabedian, S.P., Brooks, M.H., 1996. Comparison of denitrification activity measurements in groundwater using cores and natural-gradient tracer tests. Environmental Science & Technology. 30(12): 3448-3456.

Smith, R.L., Howes, B.L., Garabedian, S.P., 1991. In situ measurement of methane oxidation in groundwater by using natural-gradient tracer tests. Applied And Environmental Microbiology. 57(7): 1997-2004.

Sturman, P.J., Stewart, P.S., Cunningham, A.B., Bouwer, E.J., Wolfram, J.H., 1995. Engineering scale-up of in situ bioremediation processes: A review. Journal of Contaminant Hydrology. 19: 171-203.

Schwarzenbach, R.P., Gschwend, P.M., Imboden, D.M., 2003. *Environmental Organic Chemistry*. Second Edition. John Wiley and Sons, Inc., Hoboken, NJ.

Szecsody, J.E., Brockman, F.J., Wood, B.D., Streile, G.P., and Truex, M.J. 1994. Transport and biodegradation of quinoline in horizontally stratified porous media. Journal of Contaminant Hydrology. 15: 277-304.

Tetra Tech NUS, Inc. 2002. Engineering Feasibility Study Workplan for Corrective Action, Russell Road Landfill for Marine Corps Base Quantico, Virginia. Prepared for: Engineering Field Activity Chesapeake Naval Facilities Engineering Command, Washington, D.C.

Toride, N., Leij, F.J., van Genuchten, M.T., 1993. A comprehensive set of analytical solutions for nonequilibrium solute transport with first-order decay and zero-order production. Water Resources Research. 29(7): 2167-2182.

U.S. Environmental Protection Agency, 1998. Technical protocol for evaluating natural attenuation of chlorinated solvents in groundwater. Office of Research and Development. EPA/600/R-98/128.

U.S. Environmental Protection Agency, 2000. Engineered approaches to in situ bioremediation of chlorinated solvent: Fundamentals and field applications. Office of Solid Waste and Emergency Response, Technology Innovation Office. EPA 542-R-00-008.

United State Environmental Protection Agency, 2003, www.epa.gov/safewater/mcl.html#mcls

United State Environmental Protection Agency, 2006a, http://www.epa.gov/safewater/dwh/t-voc/12-dich2.html

United State Environmental Protection Agency, 2006b, http://www.epa.gov/safewater/standard/setting.html

United State Environmental Protection Agency, 2006c, http://www.epa.gov/safewater/dwh/t-voc/11-dichl.html

United State Environmental Protection Agency, 2006d, http://www.epa.gov/safewater/dwh/t-voc/vinylchl.html

van Genuchten, M.T. and P.J. Wierenga. 1976. Mass transfer studies in sorbing porous media I. Analytical solutions. Soil Science Society of America Journal. 40: 473-480.

Van Loosdrecht, M.C.M, Lyklema, J., Jorde, W., Zehnder, A.J.B., 1990. Influence of interfaces on microbial activity. Microbiological Reviews. 54(1): 75-87.

Vogel, M.T., Criddle, C.S., McCarty, P.L., 1987. Transformations of halogenated aliphatic compounds. Environmental Science & Technology. 21(8): 722-736.

Washington, J.W., 1996. Gas partitioning of dissolved volatile organic compounds in the vadose zone: Principles, temperature effects and literature review. Ground Water. 34(4): 709-718.

Weber, W.J., McGinley, P.M., Katz, L.E., 1991. Sorption phenomena in subsurface systems – Concepts, models, and effects on contaminant fate and transport. Water Research. 25(5): 499-528.

Weiner, R.W., Seagren, E., Arnosti, C., Quintero, E., 1999. Bacterial survival in biofilms: Probes for exopolysaccharride and its hydrolysis and measurement of interphase mass fluxes. In: R. Doyle (Editor), *Methods in Enzymology*, Vol. 310, Academic Press, San Diego, CA. p. 403-426.

Wood, B.D., C.N. Dawson, J.E. Szecsody, and G.P. Streile. 1994. Modeling contaminant transport and biodegradation in a layered porous media system. Water Resources Research. 30: 1833-1845.

Wu, W., Nye, J., Jain, M.K., Hickey, R.F., 1998. Anaerobic dechlorination of trichloroethylene (TCE) to ethylene using complex organic materials. Water Research. 32(5): 1445-1454.

Zlotnik, V., 1994. Interpretation of slug and packer tests in anisotropic aquifers. Ground Water. 32(5): 761-766.